Investigations into the protective effects of the Multiple Myeloma Bone Marrow Microenvironment

Rachel E. Piddock

A thesis presented for the Degree of Doctor of Philosophy

Date of Submission: 28th March 2018

Norwich Medical School, University of East Anglia

Declaration

The work contained in this thesis is my own original work, unless due reference is made to other authors. It has not previously been submitted at any university, including the University of East Anglia.

This thesis is approximately 43,000 words in length.

Parts of this research have been published, prior to submission, and is referenced below:

Piddock RE, Loughran N, Marlein CR, Robinson SD, Edwards DR, et al. PI3Kdelta and PI3Kgamma isoforms have distinct functions in regulating pro-tumoural signalling in the multiple myeloma microenvironment. Blood Cancer J. 2017;7(3):e539.

Piddock RE, Marlein CR, Abdul-Aziz A, Shafat MS, Auger MJ, Bowles KM, et al. Myeloma-derived macrophage inhibitory factor regulates bone marrow stromal cell-derived IL-6 via c-MYC. Journal of Hematology & Oncology. 2018;11(1):66.

Acknowledgements

Firstly, I would like to thank my supervisors Dr Stuart Rushworth and Professor Kristian Bowles for their guidance and patience. Special thanks to Dr Rushworth for all of your help both in the lab and with my writing, your support through the past few years has been invaluable. It has been a long slog, but with a little humour and a lot of drinking, we got there. I still never got my pun title.

Many thanks to my funding body, the Norwich Research Park DTP programme for their support and to UEA for hosting my PhD.

Thanks to my fellow students Chris Marlein, Manar Shafat and Amina Abdul-Aziz for their friendship and company in the trenches – I already miss not working with you guys, we all made a really great team. Chris, you made those long days in the DMU not only bearable, but fun – apologies, but you are my best friend now.

To the women who supported me – Kasia, Meena, Elena and Nicole – without your strength and encouragement I would have never even tried. Thank you all for believing in me, even when I couldn't believe in myself. Long may we all continue to be nasty women. To Dr Melanie Febrer, your backing and glowing recommendation has started my career as a researcher and the generosity you have shown me will not be forgotten.

Finally, I would like to thank my parents Simon and Jill for their endless love and support – I am sorry I only call home if there is a crisis. I will never be able to describe how much you both mean to me and how grateful I am for everything you have done for me.

This thesis is dedicated to the memory of my mother.

"Let us prepare to grapple with the ineffable itself, and see if we may not eff it after all."

- *Douglas Adams*

Abstract

Multiple Myeloma (MM) is the second most common haematological cancer in the Western World, accounting for approximately 10% of all newly diagnosed blood cancers each year. Despite the recent advancements in its treatment, MM remains incurable. This is partly due to the protective niche in which it inhabits – the bone marrow microenvironment (BMM). MM cells have been shown to `re-program' other cell populations within this milieu to produce the growth factors needed for its own development. These factors initiate pro-survival pathways within MM cells, including the phosphatidylinositol 3-kinase (PI3K) pathway. The PI3K catalytic isoforms p110δ and p110γ are known to be specifically enriched by the haematopoietic system, providing a highly precise therapeutic target.

In this thesis, the PI3K pathway was shown to be activated in response to both the BMM and IL-6 alone. Both p110δ/p110γ were found to be highly expressed in MM and were implicated in MM growth, survival and migration. p110γ only knockdown within human MM cell lines caused a significant reduction in MM adhesion to fibronectin. *In vivo,* xenograft models showed that knockdown of either of these isoforms in the human MM cell line U266 increased overall survival (OS), as did dual inhibition of p110δ and p110γ (via the drug IPI-145).

Cytokine array analysis of MM primary cells revealed extremely high levels of extracellular Macrophage Migratory Inhibitory Factor (MIF), a known stimulator of the PI3K pathway. Knockdown of MM cell MIF resulted in significantly increased OS and reduced tumour burden in secondary sites. MIF was found to stimulate the production of IL-6/8 from bone marrow stromal cells, and c-Myc was implicated in the regulation of this process.

Taken together, the data presented here demonstrates that PI3K signalling is beneficial to MM disease progression. MM-derived MIF increases the availability of IL-6 within the BMM, causing activation of the PI3K pathway. Therapies targeting the PI3K isoforms or MIF (alongside conventional MM therapeutics) could therefore benefit MM patient treatment, and warrants clinical investigation.

Table of Contents

List of Abbreviations

Akt	see PKB
AML	Acute Myeloid Leukaemia
ASCT	Autologous Stem Cell Transplantation
ATP	Adenosine Tri-Phosphate
BAD	Bcl-2-associated death
BCL2	B-Cell Lymphoma 2 gene
BLI	Bioluminescent imaging
BM	Bone Marrow
BMM	Bone Marrow Microenvironment
BM-MSC	Bone Marrow Mesenchymal Stem Cell
BMP	Bone Morphogenic Protein
BMSC	Bone Marrow Stromal Cell
BRCA1/2	Breast Cancer Associated gene 1/2
C/EBPa	CCAAT/Enhancer Binding Protein a
CAM-DR	Cell Adhesion Mediated - Drug Resistance
CCND1/2	Cyclin D 1/2 gene
CD	Cluster of differentiation
c-Myc	Cellular Myelocytomatosis transcription factor
CRAB	Calcium, Renal insufficiency, Anaemia and/or Bone lesions
CTG	Cell Titre Glo
CXCR4	C-X-C chemokine receptor type 4
DMEM	Dulbecco's Modified Eagle's Medium
DNA	Deoxyribonucleic Acid
ECM	Extra-Cellular Matrix
ELISA	Enzyme-linked immunosorbent assay
ERK	Extracellular signal-regulated kinase
FACS	Fluorescent activated cell sorting
FBS	Foetal Bovine Serum
FDA	Food and Drug Administration
FLC	Free Light-Chain

Fn	Fibronectin
FOXO	Forkhead box class O
GAPDH	Glyceraldehyde 3-phosphate dehydrogenase
GPCR	G-Protein Coupled Receptor
GTP	Guanosine Triphosphate
GWAS	Genome-Wide Association Studies
HSC	Haematopoietic Stem Cell
Ig	Immunoglobulin
IgH	Immunoglobulin Heavy chain
IkBa	Nuclear factor of kappa light polypeptide gene enhancer in B-cells inhibitor a
IL	Interleukin
IMWG	International Myeloma Working Group
IP	Intraperitoneal
IV	Intravenous
JAG1	Jagged 1
JAK	Janus Kinase
KD	Knockdown
KRAS	Kirsten Rat Sarcoma virus
MA	Marrow Adipocytes
MAPK	Mitogen-activated protein kinase
MEK	Mitogen-activated protein kinase kinase (also known as MAPKK)
MGUS	Monoclonal Gammopathy of Undetermined Significance
MIF	Macrophage migratory Inhibitory Factor
MM	Multiple Myeloma
mTOR	Mammalian Target Of Rapamycin
NF-kB	Nuclear Factor kappa-light-chain-enhancer of activated B cells
NICE	National Institute for health and Care guidance
NRAS	Neuroblastoma Rat Sarcoma viral oncogene homolog
NSG	Non-obese diabetic, severe combined immunodeficiency, Il2rg knockout
OS	Overall Survival
PBMS	Peripheral Blood Mononuclear cells

PBS	Phosphate Buffered Saline
PC	Plasma Cell
PCR	Polymerase Chain Reaction
PI	Proteasome Inhibitor(s)
PI3K	Phosphoinositide 3-kinase
PIP2	Phosphatidylinositol-4,5-bisphosphate
PIP3	Phosphatidylinositol-3,4,5-triphosphate
PKB	Protein kinase B (also known as AKT)
PTEN	Phosphatase and tensin homolog
RAF	Rapidly Accelerated Fibrosarcoma
RBC	Red Blood Cell
RIPA	Radio Immunoprecipitation Assay buffer
RISC	RNA-induced silencing complex
RNA	Ribonucleic Acid
RNAi	RNA interference
RPMI	Roswell Park Memorial Institute
RTK	Receptor Tyrosine Kinase
RT-qPCR	Reverse Transcription - quantitative PCR
SCF	Stem Cell Factor
s.d	Standard Deviation
SDF-1	Stromal Derived Factor 1
SDS-PAGE	SDS-polyacrylamide gel electrophoresis
shRNA	Short hairpin RNA
SMM	Smouldering Multiple Myeloma
SNP	Single Nucleotide Polymorphism
SSC	Skeletal Stem Cell - see BM-MSC
STAT	Signal transducer and activator of transcription
TGFb	Transforming Growth Factor b
WM	Waldenström's macroglobulinemia
Wnt	Wingless-type mouse mammary tumour virus integration site

List of Figures

List of Tables

1 – Introduction

1.1 – Multiple Myeloma (MM)

1.1.1 – General Introduction

Multiple Myeloma (MM) is a devastating and currently incurable type of blood cancer. Specifically, it is a cancer of the plasma cell (PC), the terminal differentiation stage of a B-Lymphocyte cell (see Figure 1.1.1). These cancerous PCs (or MM cells) can no longer produce working antibodies, instead yielding monoclonal or light chain (Bence Jones protein) only immunoglobulins (Igs), most commonly referred to as 'paraproteins'. Paraproteins may be detectable via protein electrophoresis of the patient's blood serum or urine – higher levels of which can be indicative of a more advanced disease stage [1].

Accumulation of MM cells within the body can lead to many complications. As the disease develops, so too do the plasmacytomas and lytic lesions [2], causing bone pain and pathological fracture [3]. Decreased number of functional PCs results in immunodeficiency, whilst the ever increasing protein level damages the kidneys - typically resulting in a fatal infection (most commonly pneumonia) or kidney failure respectively [4, 5].

MM is the second most commonly diagnosed blood cancer in the Western world with approximately 5,700 new cases in the UK annually and a 5-year survival rate of 51.6% [6]. Despite the recent advances in the treatment of MM, average life expectancy following diagnosis is still only 4 years [6]. Although current therapeutics are effective at reducing the bulk of the disease burden significantly, drug-resistant cells will always remain harboured within the bone marrow (BM). Here they are protected in an environment that is rich in the cytokines and chemokines that are critical to MM growth and metastasis [7, 8]. Indeed, MM cells have been shown to initiate the production of these soluble factors in the cells of the bone marrow microenvironment (BMM) [9-11], effectively adapting other cells within the milieu to benefit their own survival. Adhesion to the extracellular matrix (ECM) or BMM cells can also initiate cyto-protective signalling cascades within the MM cell further protecting and nurturing the cancer, as well as contributing to malignant cell drug resistance [12].

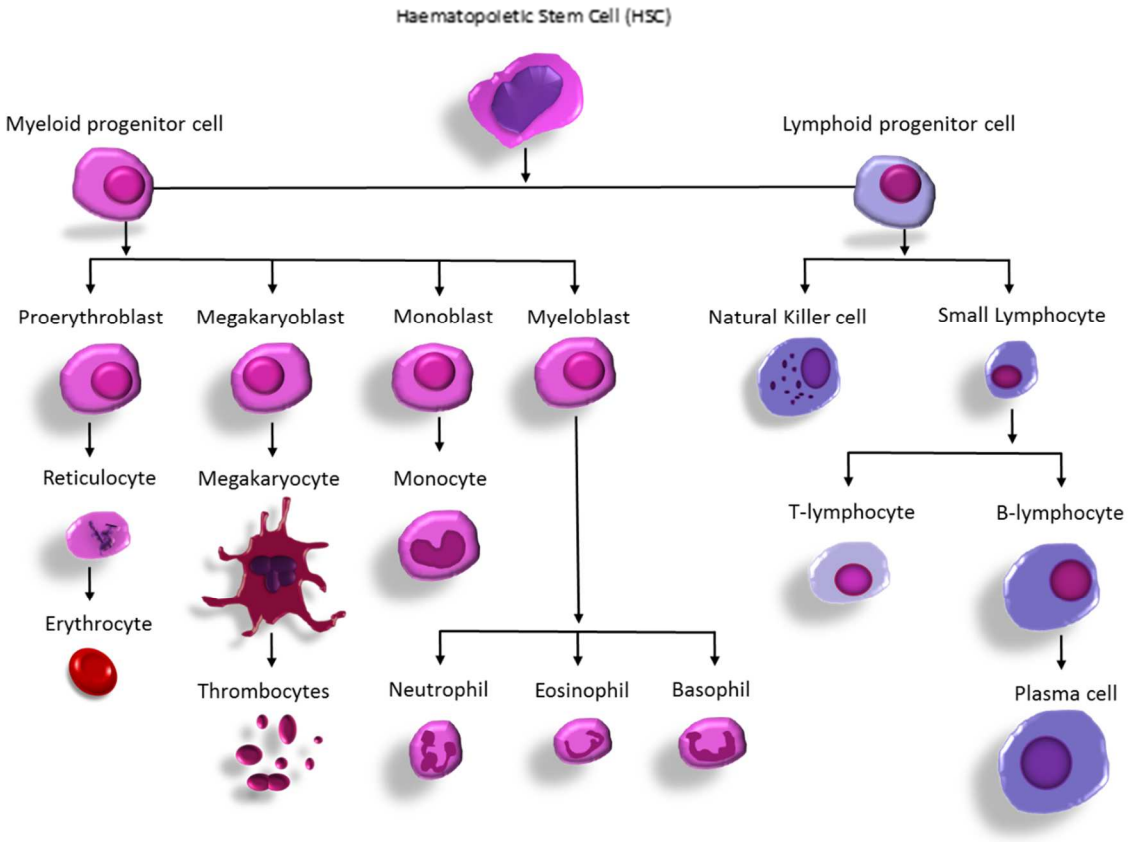

Figure 1.1.1 – Blood cell lineage.
Simplified schematic of typical human haematopoiesis. Haem Multiple Myeloma is a cancer of the plasma cell (shown bottom right of the figure).

The characterisation and obstruction of the symbiotic relationship between the tumour cell and its microenvironment is the next critical stage in cancer research in general, and this remains true in the treatment of MM. Complimentary therapies that negate the BMM's protection could increase the efficacy of treatments already routinely used in the clinic – reducing symptoms, increasing duration until patient relapse, and, ultimately, extending survival time.

1.1.2 – The Plasma Cell Immunoglobulin (Ig)

A typical plasma cell produces and secretes thousands of Ig molecules over its lifetime (Figure 1.1.2), initiating the destruction of specific antigens. The Ig created by plasma cells are classified by isotype, and there are five main groups in placental mammals: IgA, IgD, IgE, IgG and IgM. Isotype categorisation is based on the sequence of the Ig heavy chain (IgH), and can be further classified by determination of the light chain (κ or λ) (see Table 1.1.1).

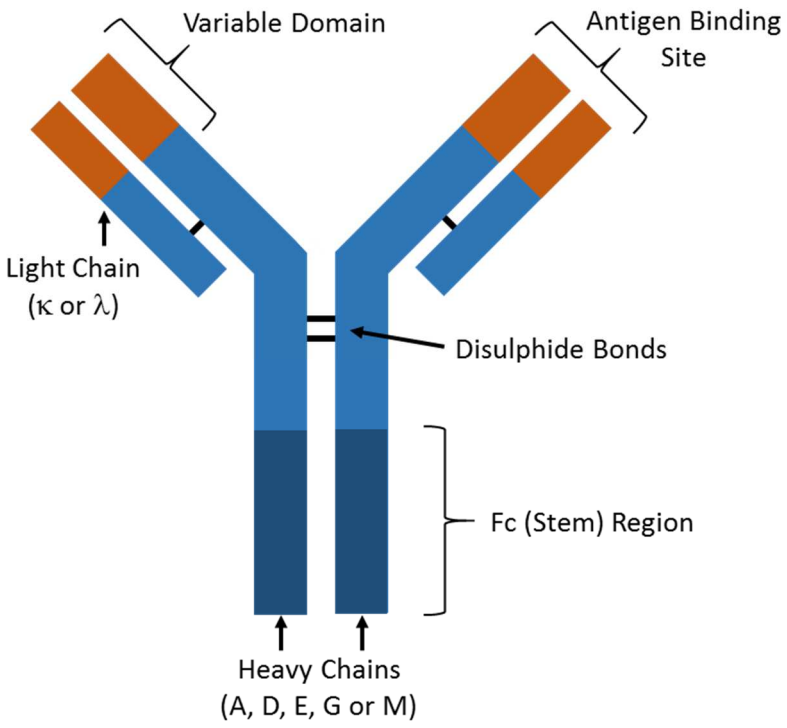

Figure 1.1.2 – Structure of a typical Immunoglobulin (Ig).
Igs are present on the surface of both typical and malignant plasma cells and can be measured in the urine or blood of patients.

Of all these subtypes, IgG (both κ and λ) is the most common in MM – accounting for approximately 52% of all diagnosed cases [13]. IgA is identified in approximately 21% of patients with all other subtypes totalling 27% of diagnosed cases (see Table 1.1.1). Ig / paraprotein isotype has been shown to correlate with the prognosis of disease and overall patient survival – with IgG patients, for example, surviving on average 1.6 times longer than IgA patients (median survival of IgG patients was 61.8 months vs. 38.5 months seen in IgA patients)[13]. The IgD sub-type, although rarer, is more aggressive still with average survival reduced to just 21 months [14].

IgM MM and Waldenström's macroglobulinemia (WM) are malignancies both characterised by an IgM monoclonal gammopathy [15]. WM is a type of non-Hodgkin lymphoma and effects not only the plasma cells (as in MM) but the B-Cells as well [16]. However, where MM will classically present with lytic bone lesions and end organ damage, WM does not. IgM (as well as IgE and non-secretory) MM though has been shown to have higher instances of t(11;14) translocations, a feature not associated with WM [17]. This abnormality therefore has the potential be utilised as a differentiator between the diseases before organ damage occurs.

IgE is so rare that only a handful of cases have been reported since it was first defined in 1967 [18] - so statistically few conclusions can be drawn on the nature of this sub-type. In Light-Chain MM, the malignant plasma cells can only produce the Light-Chain portion of the antibody and therefore diagnosis relies more heavily on the serum free light chain (FLC) assay to determine the ratio of κ : λ Ig Light Chains. In healthy subjects, there will be a presence of free light chains in the blood at low levels, with a κ : λ ratio of between 0.26 to 1.65. Anything outside this range is considered abnormal and in the case of MM may indicate monoclonal expansion. Non-secretory MM is where the malignant plasma cells produce or secrete little or no Ig at all, and therefore can be highly difficult to diagnose or to monitor disease progression [19].

Heavy Chain	Light Chain	% of patients
IgG	κ	34
	λ	18
IgA	κ	13
	λ	8
IgD	κ	1
	λ	1
IgM	κ	0.3
	λ	0.2
IgE	κ	None identified
	λ	None identified
None	κ	9
	λ	7
Bi-clonal (Two different heavy chains present)		2
Non-secretory		7

Table 1.1.1 –Table showing Immunoglobulin distribution in MM patients.
Table adapted from data obtained by The Mayo Clinic, 2003, of 1027 patients with MM [13].

1.1.3 – The clinical stages of MM

Approximately one third of all MM patients have been previously diagnosed with either monoclonal gammopathy of undetermined significance (MGUS) or smouldering multiple myeloma (SMM) prior to developing MM, although virtually all MM cases are thought to be preceded by one of these two conditions [20, 21]. All three of these disorders affect the plasma cells specifically, with the distinction between MGUS/SMM and MM fundamentally relying on the quantity of abnormal plasma cells within the bone marrow and the presence of tissue damage (see Table 1.1.2). Oncogenic studies have found no genetic mutations that are unique to a particular stage of malignancy [22], although a t(11;14)(q13;q32) translocation (and subsequent up-regulation of cyclin D1) is most frequently observed in symptomatic MM and is thought to be an early oncogeneic event [23]. Despite the fact that immunophenotypic analyses can discriminate between typical PCs and malignant cells [24, 25], there are currently no known markers that are completely unique to any one of these conditions. This essentially demonstrates that these malignancies can be classed as a spectrum of disease, ranging from MGUS to advanced MM and accumulating genetic insults along the way.

1.1.3.1 – Monoclonal Gammopathy of Undetermined Significance (MGUS)

MGUS is one of the most common plasma cell disorders, occurring in 1% of over 50 year olds [26] and 3% of over 70 year olds [27]. It is defined by the presence of paraprotein in patients, without the symptoms of MM (such as bone lesions) or other related disorders. Both genetic [28, 29] and environmental factors [30, 31] have been shown to affect MGUS prevalence, however the actual risk of progression from MGUS to MM is low (less than 1% of patients per year [32, 33]). Just as with MM, MGUS incidence increases with age [29] and can also vary with race [34] (see Section 1.1.4). It can be classified based on the monoclonal Ig that is expanded, with IgA MGUS more likely to become malignant in comparison to the other isotypes [35-37]. The speed at which MGUS progresses to MM is highly variable between patients, with some patients rapidly progressing to MM while others take decades (or not at all in some cases). The risk of progression is effected by several factors, including the Ig type, the FLC ratio and the initial level of monoclonal immunoglobulin [33].

1.1.3.2 – Smouldering MM (SMM)

Smouldering MM (SMM), also known as a-symptomatic MM or indolent MM - has the same diagnostic criteria as MM, with the exception of no patient symptoms or tissue damage (see Table 1.1.2). 'Tissue damage' refers to the fulfilment of one or more of the CRAB criteria: Elevated serum **C**alcium, **R**enal insufficiency, **A**naemia, and/or **B**one lesions. It is instead defined by paraprotein levels $\geq$ 30g/l or $\geq$10% monoclonal plasma cells within the bone marrow [38] and there is currently no treatment regimen for patients at this stage of disease. Instead, the disease is closely monitored for progression and treated at the first signs of tissue damage, when it can become classified as symptomatic MM. Although intervention at the precursor stage has not yet been approved, a recent study has shown that treatment of high-risk smouldering MM can significantly decrease disease progression time. In a study by Mateos *et al.*, it was shown that treating this high-risk group with Lenalidomide plus Dexamethasone increased 3-year progression free survival from 30% in the control group to 77% [39]. There are currently several active clinical trials [40-49] studying pharmacological intervention in SMM, however it remains to be seen if the benefits of early treatment outweigh the physical and emotional costs to the patients.

1.1.3.3 – Symptomatic MM

Once the CRAB criteria (mentioned above) have been met, patients have officially progressed from MGUS/SMM to symptomatic MM. The immune dysfunction that is characteristic of this disease means that infection remains the major cause of morbidity [50]. Indeed, a Swedish population based study of MM patients revealed that they had an 7 fold increased risk of developing any infection in comparison to matched controls [51], with risk of viral infections increasing by 10 fold. Other identifying characteristics of MM include bone pain and pathological fractures, with 90% of MM patients exhibiting features of bone disease at some stage of the disease [52]. MM bone disease is driven by a disruption in the production of both osteoblasts [53, 54] and an increase in osteoclast creation [55-57] which creates an environment of bone weakness and, ultimately, destruction. This bone damage can also cause hypercalcemia which in turn leads to renal failure in up to half of all patients [58].

Critical to the diagnosis of MM is the presence of MM cells that have infiltrated the bone marrow and for a diagnosis of MM this must exceed 10%. These malignant cells are identified by first performing a bone marrow biopsy, which is immunohistochemically stained and analysed via microscopy. Throughout MM disease progression, malignant cells are dependent on their environment with circulating plasma cells only present in a more aggressive disease type (or indeed in Plasma cell leukaemia [59]) and is indicative of a poor prognosis for the patient.

		MGUS	Smouldering Myeloma	Symptomatic Myeloma
1	Serum Paraprotein	Ig < 30g/l	Ig ≥ 30g/l, Or IgA > 10g/l	Ig ≥ 30g/l, Or IgA > 10g/l
2	Ig Light Chain	n/a	>1g/24h	>1g/24h
3	BM clonal plasma cells	<10%	≥10%	≥10%
4	Related tissue damage	None	None	CRAB criteria fulfilled[1]

Table 1.1.2 – Diagnostic criteria for varying plasma cell disorders.
Data obtained from criteria set by the IMWG, [1] CRAB criteria defined in report [60].
In IgA MM, only >10g/l serum paraprotein is required for classification, due to aggressive nature of this subtype. The only measureable difference between Smouldering MM and Symptomatic MM is the presence of related tissue damage.

1.1.4 – Epidemiology

1.1.4.1 – Age and Gender

Blood cancers account for approximately 10% of all newly diagnosed cancers in the Western world, of which Myeloma is the second most commonly diagnosed (see Figure 1.1.4 for a breakdown of commonly diagnosed cancers).

Primarily a disease of the elderly, MM has a median age of onset at approximately 73 years in the UK [61]. The incidence of MM has a strong positive correlation with increasing age, which is evident when looking at the breakdown of instances recorded in the UK between 2012 and 2014 (see Figure 1.1.3), and there are very few cases diagnosed before the age of 40. These data are comparable to the numbers recorded in other Western populations. The USA and Australia, for example, have slightly lower median ages of diagnosis of 69 years [6] and 71 years respectively [62]. As the average life expectancy continues to increase in these countries, so too will the incidence of MM. These rates will seem to further increase with improvements in clinical testing and better disease monitoring.

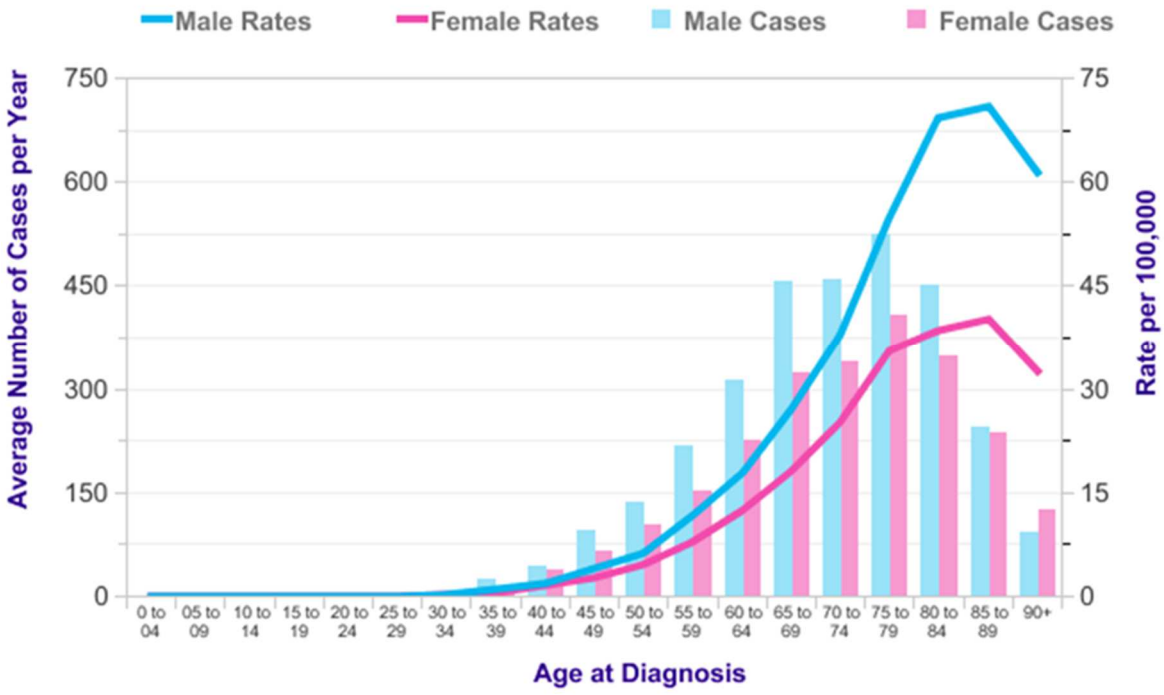

Figure 1.1.3 – MM age-specific incidence rates, UK, 2012-2014.
Source: Cancer Research UK, cruk.org/cancerstats, Accessed Oct 2017.

Gender too is known to highly influence the incidence of certain cancers, and MM is no exception to this with a diagnosis of MM 40-50% more common in men than women (depending on age group assessed) [61]. The only age group for which this is not true is the 85+ group – most likely due to the higher number of women within this age group in general. Although it is universally accepted that the incidence is significantly higher in males, the reasons behind this are unclear – although the frequency of some genetic aberrations were identified in a study by Boyd *et al.* in 2011 [63]. They found that the incidence of IgH translations was significantly higher in women (50% of women vs. 38% of men) and hyperdiploidy prevalence higher in men (50% of women vs. 62% of men) – factors which could possibly influence further genetic events.

Despite the significant gender differences observed in many different diseases [64-66], clinical trials are still overwhelmingly populated by Caucasian males. In a study by Geller *et al.* in 2011 [67] it was found that women only accounted for 37% of patients enrolled in clinical studies (with 15% of studies having lower than 20% women) and that 75% of studies did not report outcomes by gender at all. This is likely to influence the development of therapeutics and unfortunately may cause effective medicines to be disregarded prematurely.

A

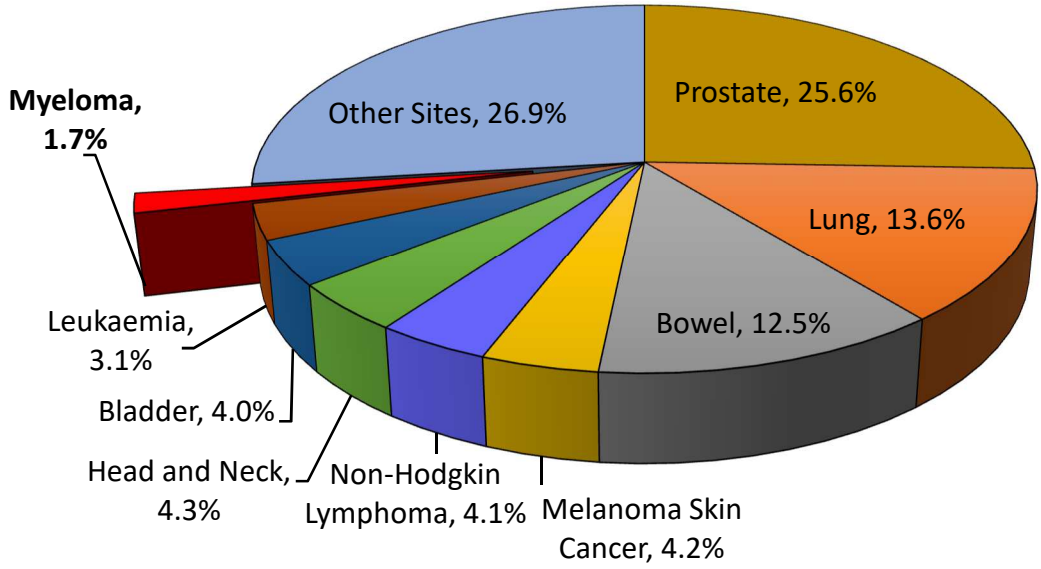

B

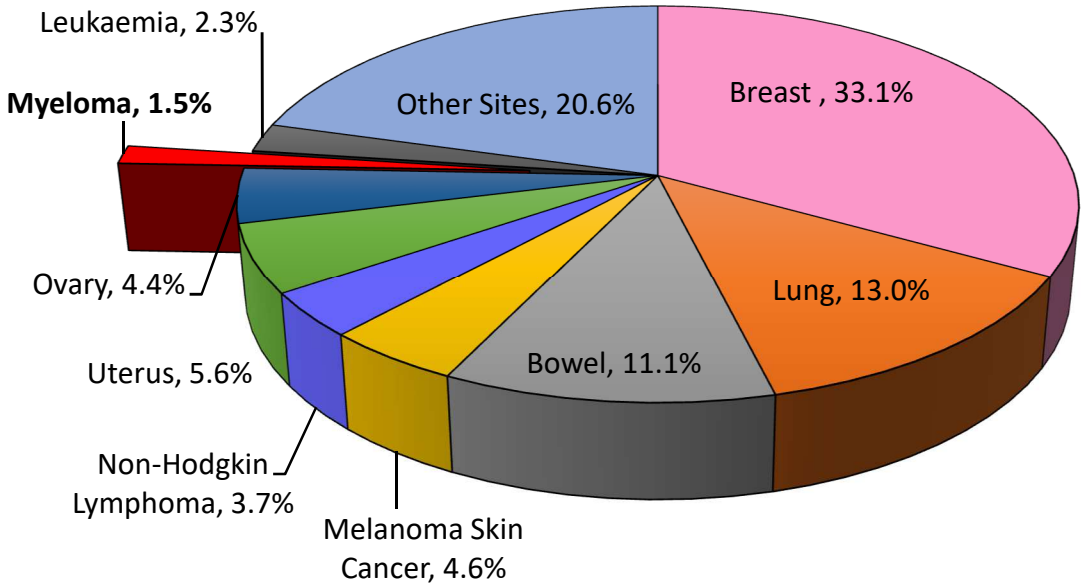

Figure 1.1.4 – Newly diagnosed cancers by type in the UK (2014)
Most frequently diagnosed cancers in Males (A) and Females (B). Raw data obtained from Cancer Research UK, cruk.org/cancerstats, accessed Oct 2017.

1.1.4.2 – Nationality and Race

An aging population can be highly indicative of a strong economic country and an accessible healthcare system and it is pertinent to remember this when looking at the global prevalence of MM. When analysing data, both MM and MGUS occurrence seem to be significantly higher in North America, Australia and Europe but low in the traditionally weaker economic countries of Africa. However, these rates are more likely to reflect poor data ascertainment, the lack of access to a good standard of health care, and overall lower life expectancy. For example, although MM incidence appears to be lower in African countries, the average life expectancies of men in Chad, the Central African Republic and Sierra Leone are only 51.7 years, 50.9 years and 49.3 years respectively. Therefore, the chance of developing MM is much lower as the population is much younger as a whole. In the USA those of African descent are actually more than twice as likely to be diagnosed with MM [6] in comparison to those of European lineage. This increase remains significant upon normalisation for economic factors [68], suggesting there is an underlying biological reason for this difference. Similar studies have also highlighted the increased incidence in those of African descent, with the average age of onset also lower by approximately 4 years [68].

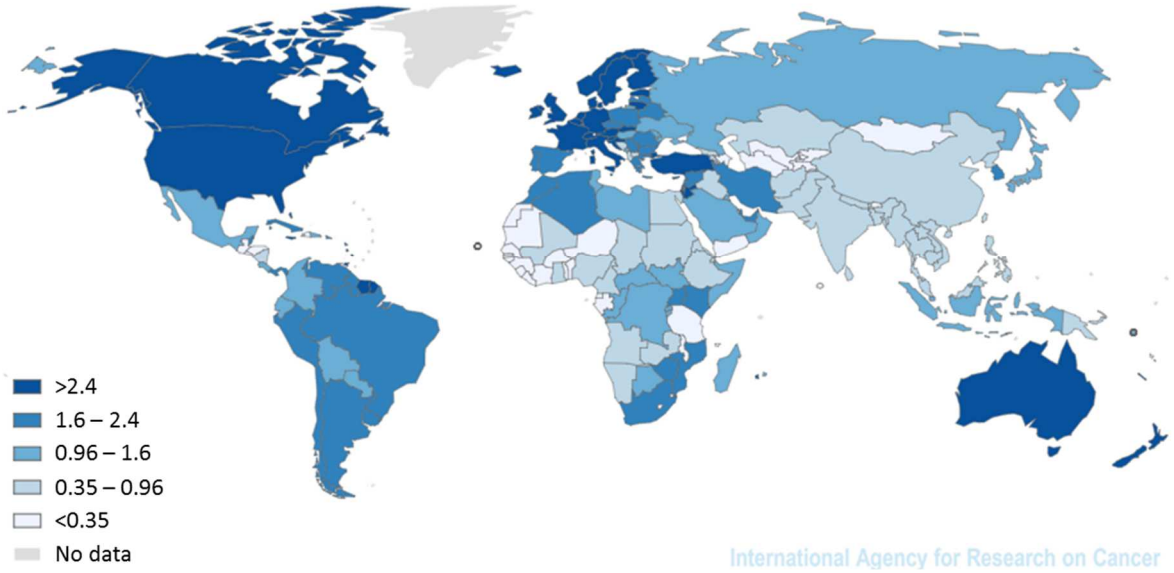

Figure 1.1.5 – Global Age-standardised rate of MM incidence per 100,000.
Countries with higher life expectancies and stronger economies appear to have higher incidence of MM. Source: GLOBOCAN 2012 [69]

Asian populations currently have the lowest recorded incidence of MM of all the studied ethnicities (just 0.8% of newly diagnosed cancers) [69], however the occurrence of MM seems to be increasing in some Asian nations [70-72]. This has been attributed to the rapid industrialisation of some of these countries, resulting in an increase of wealth and consequently a longer life expectancy. All of the racial trends described are consistent across genders, however the reasons behind racial differences in MM are still not clear. IgH translocations have been shown to be 12% lower in African American populations [73], but no significant difference in high-risk disease were found. A recent study by Greenberg *et al.* [74] showed differences in the cytogenetic profile between White and Black populations, however the cytogenetic subtypes studied were only present in a subset of patients (63.4% Black and 34.6% White).

As mentioned previously, clinical trials in the UK and the USA are predominantly filled by Caucasian males, and minorities are far less likely to be enrolled in general [75, 76] (most likely due to socio-economic factors). Better representation of both women and minority populations needs to be addressed if new effective treatments are to be developed for all.

1.1.4.3 – Other factors

Socio-economic status can have a large influence on the quality of medical treatment received and this has been shown to reduce overall life expectancy more than both obesity and high blood pressure [77]. For those that do not have access to universal healthcare (in the USA for example), uninsured adults have a 25% higher risk of mortality compared to those with private insurance [78], a figure which has been largely unchanged since the 1980s [79]. This has been shown to disproportionately affect younger MM patients (under 65) in the USA [80] – with 4-year survival rate declining alongside privilege (71.1%, 63.2%, 53.4%, and 46.5% respectively, for patients with 0, 1, 2, or 3 adverse sociodemographic factors). Early detection and monitoring of MGUS/MM has proved to be critical, and without access to routine blood tests and other forms of screening, poorer communities are far less likely to get the treatment they need in a timely manner.

There has also been a familial element identified in MM, with several studies which show that people who have first degree relatives who have developed MGUS/MM are more likely to develop the malignancy themselves [29, 81, 82]. This, linked with the distribution of disease in different races and sexes, would imply a genetic susceptibility to MM. Indeed, there has been evidence that there is increased risk of MM in carriers of both the mutated BRCA1 or BRCA2 genes in Ashkenazi Jewish populations [83]. More recently, Genome-wide association studies (GWASs) have been performed in the attempt to identify risk variants for MM. In a study by Broderick *et al.*, 1675 MM patients of European origin were genotyped and compared to 5903 healthy control individuals [84] and they found two SNPs that were associated with the risk of MM: rs4487645 (7p15.3) and rs1052501 (3p22.1). rs4487645 is particularly interesting as in the region to which it maps, the CDCA7L (cell division cycle-associated 7-like) gene also is present. CDCA7L has been shown to interact with MYC (a proto-oncogene that is critical in many growth promoting pathways [85]) through differential IRF4 binding, resulting in increased MM cell proliferation and reduced patient survival [86]. The following year, this group added four further variants that could confer MM risk, providing more evidence for the genetic contribution to this malignancy [87].

Obesity too has been associated with increased risk of MM, however there are other factors that may be influencing these data sets. African-Americans, for example, have a higher prevalence of extreme obesity in the USA [88] which could account for the higher rates of MM – however, higher rates of extreme obesity was also observed in all women vs. men, regardless of ethnicity.

In summary, there are many factors that could influence an individual's probability of a MM diagnosis. Based on the current literature, the most at risk group comprises of elderly males (>70 years) of African descent.

1.1.5 – Treatment of Myeloma and its limitations

The first well documented cases of Multiple Myeloma were first described by Solly in 1844 [89] and later by Macintyre in 1850 [90]. Both of these cases reported fatigue and bone pain caused by multiple fractures in their patients, and attempts to treat the disease ranged from an 'infusion of orange peel' to 'sea air and sea bathing'. Strangely, neither of these treatments proved effective and it was over 100 years later in 1958 that the first working treatment for MM was found.

1.1.5.1 – Early treatments

Melphalan was first synthesised in the early 1950s by Bergel and Stock [91]. It is a type of nitrogen mustard alkylating agent that was found to have beneficial effects in MM patients by Blokhin *et al.* in 1958 [92]. Melphalan works as an alkylating agent, inhibiting both RNA transcription and protein synthesis, causing cell growth arrest and apoptosis. This initial study was followed by several others [93-96], and melphalan soon became a routine treatment for MM – improving the condition of approximately 50% of Myeloma patients.

In the 1960s, the corticosteroid prednisone was found to decrease serum Ig and increase the Red Blood Cell (RBC) count in MM patients [97, 98]. However, there was no significant increase in survival when compared to a control group. It was not until it was used in combination with melphalan that the benefits became truly apparent. A randomised trial conducted by Alexanian *et al.* in 1969 [99] showed that the melphalan with prednisone increased overall survival by 6 months when compared to melphalan alone. Over the following decades other therapeutic agents were trialled (such as cyclophosphamide and vincristine [100]) but, despite promising responses, overall survival was not significantly increased [101]. The treatment regimen of melphalan-prednisone was used as the core therapy for decades.

1.1.5.2 – The past 20 years

It was not until nearly 3 decades after the establishment of melphalan and prednisone that another effective drug for the treatment of MM was developed. Originally marketed as a sedative and a treatment for morning sickness in the 1950's, thalidomide (an immunomodulatory drug) was shown to have severe teratogenic properties [102]. Throughout the late 1960's to the 1980's there was increasing evidence for the use of thalidomide in several diseases – including leprosy [103, 104], Behçet's syndrome [105] and HIV related complications [106] – and was later shown to have significant anti-angiogenic properties [107]. Based on these findings (and the increased awareness of the role of angiogenesis in MM), Singhal *et al.* produced a paper in 1999 showing the effects of thalidomide in MM patients [108]. They showed that 78% of patients showed a reduced level of paraprotein after two months, with decreased plasma cell infiltration into the bone marrow and patients reported a reduction of bone pain. In the subsequent years, thalidomide became an established therapeutic for the treatment of MM, most frequently used alongside melphalan and prednisone (mentioned previously).

Whilst thalidomide was being clinically investigated, another potential cancer treatment was being developed – proteasome inhibitors (PI). The ubiquitin-proteasome pathway is the primary pathway for intracellular protein degradation [109], and as such plays a critical role in cell cycle control and tumour growth. The proteasome also plays a vital role in the activation of the transcription factor NF-κB (see Figure 1.1.6), via degradation of IκBα, NF-κB's inhibitory protein [110]. Stabilisation of IκBα (and subsequent NF-κB inhibition) causes dividing cells to become more susceptible to apoptosis [111], as well as interfering with cell adhesion [112] and reducing angiogenesis [113]. Therefore, PI have the potential to arrest tumour metastasis and make malignant cells more susceptible to other therapeutics available.

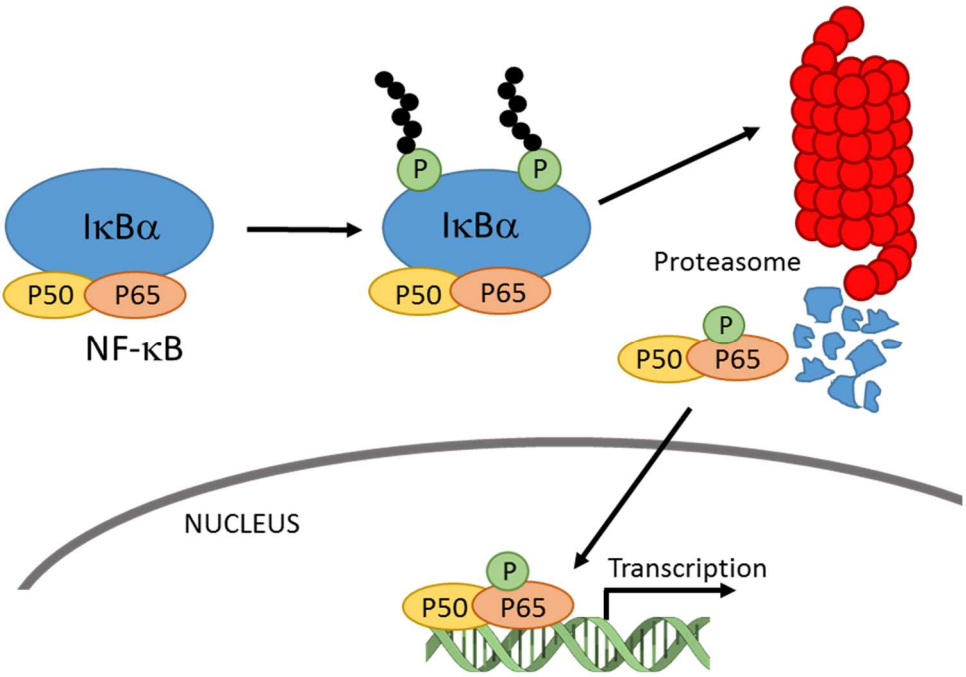

Figure 1.1.6 – The role of the proteasome in NF-κB translocation.
Under typical conditions, NF-κB (p50/p65 heterodimer) is sequestered by IκB in the cytoplasm. Activated IκB is then ubiquitinated and subsequently degraded by the proteasome. This leaves NF-κB to translocate to the nucleus where it activates a variety of NF-κB target genes. PI cause a build-up of damaged proteins in the cell as well as preventing NF-κB target gene activation. Canonical pathway shown.

The first PI that was specific enough for clinical use was a boronic acid derived compound, Bortezomib (trade name of Velcade). The NF-κB transcription factor is known to be aberrantly activated in MM [12], and Phase 2 trials of this drug in MM patients showed promising results. For example, a study by Richardson *et al.* in 2003 [114] showed that 35% of patients had a complete, partial or minimal response to bortezomib alone, some of who had been previously refractory to treatment. Addition of bortezomib to standard melphalan with prednisone treatment was shown to work synergistically with standard treatment, with time to progression increasing from a median of 16.6 months in the control group to 24.0 months in the bortezomib group [115] – and this soon became the established regimen for the first line treatment of MM, approved by the FDA in 2003.

Due to the success of bortezomib, other PIs were soon being developed and trialled in the treatment of MM, as well as other cancers. Ixazomib [116], Marizomib [117] and Carfilzomib [117], for example, have all completed clinical trials in varying stages and are yielding positive results – increasing progression free survival time and overall survival. The National Institute for health and Care guidance (NICE) guidelines now allow Carfilzomib as an option for treating relapsed myeloma, and other PI are likely to continue this trend in the future.

1.1.5.3 – The future of MM treatment

Currently, in the UK, NICE recommend a combination of dexamethasone (a corticosteroid) alongside thalidomide and bortezomib [118] as the first line treatment for MM (following an autologous stem cell transplantation if eligible). Autologous stem cell transplantation (ASCT is the process by which a fraction of the patients Haematopoietic Stem Cells (HSCs, see section 1.2.1.1) are collected, prior to high dose chemotherapy can be toxic to this cell population. Following this, the HSCs are returned to the patient intravenously and return to the BM where they can re-engraft. Unfortunately, the majority of patients with MM are not eligible for ASCT under NICE guidelines due to advanced age, frailty and renal impairment.

Relapsed patients will be given bortezomib monotherapy, with subsequent therapies of lenalidomide (a thalidomide derivative) and dexamethasone, as appropriate. The 5 year survival rate of MM patients has nearly doubled since melphalan/prednisone became the first established treatment regimen (26.3% in 1975 vs. 52.7% in 2009 [6]) and the detection and monitoring of this disease has improved substantially. However, despite the wide array of therapeutics that are now available for the treatment of MM, all patients will eventually relapse or become refractory to treatment. This is due, in part, to a sub-set of MM cells that are resistant to therapeutics and are encouraged to proliferate and grow by the environment in which they develop. These cells are harboured in the BMM, and until the protective effects of this sanctuary are removed, the efficacy of current treatments will continue to be limited.

1.2 – The Bone Marrow Microenvironment

1.2.1 – Overview

Bone marrow is a spongy, flexible tissue that occupies the cavities of bones. It is comprised of both yellow marrow and red marrow (which is also known as myeloid tissue). Platelets, RBCs and the majority of leukocytes are produced in the red marrow whereas the yellow marrow has a much larger proportion of adipocytes. In adults, the bone marrow is the primary site of haematopoiesis and it is comprised of blood vessels and a plethora of cell types that either are directly involved in this process or that support it. The 'support' system is known collectively as the bone marrow stroma and works to create and maintain an environment in which haematopoiesis can occur and be maintained [119]. Haematopoiesis begins with haematopoietic stem cells (HSCs, also known as Haemocytoblasts), which are the multipotent cells that reside within the haematopoietic niche. These cells are capable of self-renewal, as well as differentiation into either myeloid progenitor cells or lymphoid progenitor cells (which then differentiate further, see Figure 1.1.1).

Bone Marrow Stromal Cells (BMSCs), on the other hand, give rise to cells specifically of the skeletal lineage [120] – that is cells that comprise the cartilage, bone, and marrow adipocytes. The definition and terminology used to describe these particular pluripotent cells has been thoroughly debated, and the terms 'Bone Marrow Mesenchymal Stem Cell' (BM-MSC) and 'Skeletal Stem Cell' (SSC) have been used interchangeably in literature. Although both the haematopoietic and stromal systems have distinct lineages, they are thought to work symbiotically.

1.2.1.1 – Haematopoietic Stem Cells (HSC)

In the wake of World War II, a proportion of the citizens of Horoshima and Nagasaki that survived the initial atomic bomb explosion experienced low radiation exposure and subsequently perished. Patients were found to no longer produce sufficient leukocytes to ward off infection, or adequate platelets needed for blood clotting. Mouse experiments could replicate this compromised haematopoietic system, but showed that the shielding of an individual bone or the spleen could prevent this failure [121]. It was later revealed that fully irradiated mice which were injected with suspensions of cells from the bone marrow also avoided haematopoietic failure [122] and that this could be directly attributed to the bone marrow cells themselves regenerating the haematopoietic system (rather than a secondary effect causing repair of radiation damage) [123, 124].

Thanks to work by Till and McCulloch [125], we now know that the rejuvenation of haematopoiesis seen in these experiments was due to one population of cells, the haematopoietic stem cells (HSC). HSC are defined by their ability to differentiate into any blood cell lineage as well as their ability for self-renewal (which is required for the maintenance of the population). Under normal conditions approximately 75% of HSC are quiescent, with the remaining HSC in varying stages of the cell cycle [126]. Moreover, a study by Sugiyama *et al.* in 2006 showed that SDF-1/CXCR4 signalling is critical in the maintenance of this quiescent HSC pool [127]. They demonstrated how a deletion of CXCR4 in mice resulted in a significant reduction of HSC numbers as well as increased sensitivity to myelotoxic injury (using the anti-metabolite 5-fluorouracil, which only affects cycling haematopoietic cells) without the impaired expansion of mature progenitors. However, HSC are also highly responsive to changes in the environment and can be driven to self-renew under stress conditions [128, 129], showing their dynamic adaptability.

HSC are an incredibly rare population, constituting approximately 0.005-0.01% of all bone marrow cells [130], and their isolation and identification is incredibly difficult. Morphologically similar to lymphocytes, HSC must be identified by the cell surface markers that they express (however no single marker can specifically identify an HSC). Cell surface markers and cluster of differentiation (CD) antigens are identified by flow cytometry with Fluorescence-activated cell sorting (FACS) allowing this population to be isolated. Currently, human HSC are recognised using the following markers: $CD34^+$, $CD59^+$,

$CD90^{+}$, $CD38^{low/-}$, $c\text{-}Kit^{-/low}$, and are negative for mature cell lineage markers (although most HSC are primarily identified by CD34+ selection despite this marker encompassing cells at various stages of maturation) [131-133].

1.2.1.2 – Mesenchymal Bone Marrow Stromal Cells (BMSCs)

The characterisation of BMSCs has always been a challenge, not least due to the rarity of the cell population - approximately 1 in 10,000 to 50,000. BMSCs are the source of all the cells that form the bone marrow environment itself, most notably marrow adipocytes, chondrocytes and osteocytes (see Figure 1.2.1).

The concept of a BMSCs first originated in the 1960s, where studies showed that BM cell suspensions could produce their own ossicles *in vivo* – essentially mimicking the architecture of the BM [134, 135]. These cells were discernible for their ability to adhere to tissue culture plastic and their fibroblast-like appearance. Subsequent work by Friedenstein and colleagues showed that these cells were clonogenic, multipotent progenitors - the lineage of which was independent from HSC [136, 137]. It was not until 2006, however, that the true "stem cell" nature of these cells was completed, when they were shown to self-renew [138, 139].

When placed under different niche conditions, BMSCs have been shown to display remarkable plasticity in terms of their differentiation pathway, forming adipocytic, osteocytic and chondrocytic cell lines, and their full potential in medical applications is yet to be realised. As well as differentiating into cells of the mesodermal lineage, BMSCs have been shown to have the potential to form cells of other embryonic lineages. For example, a study by Orlic *et al.* in 2001 showed the how dead myocardium could be restored by the transplantation of Lin^{-} $c\text{-}kit^{+}$ BM cells into the contracting wall bordering the infarct [140]. Other studies have demonstrated how BMSCS can overcome their 'mesenchymal' fate, and under specific conditions *in vitro* can differentiate into neural cells [141, 142], providing options for the treatment of a plethora of neurological diseases and spinal injuries [143].

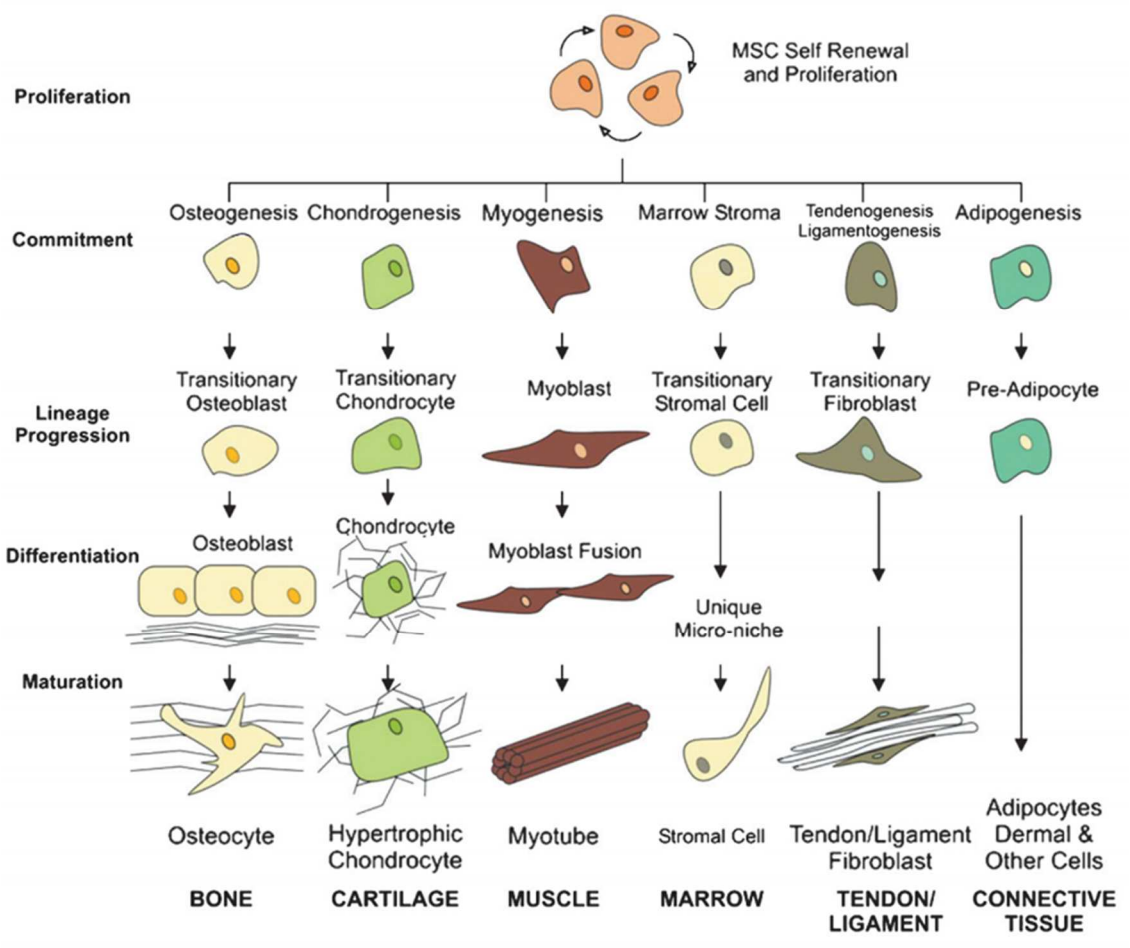

Figure 1.2.1 – The potential of Mesenchymal BMSCs.
The mesenchymal BMSC has the potential to differentiate into several cell types. Although most commonly committing to osteoblastic, adipocytic and chondrocytic lineages, mesenchymal BMSCs can also form muscle cells. Image taken from Firth and Yuan, 2012 [144]

1.2.1.2.1 – Osteocytes and Marrow Adipocytes

Bone homeostasis is maintained by the continuous cycle of bone remodelling within the microenvironment - synthesis (via osteoblasts and subsequently osteocytes) and absorption (via osteoclasts). Imbalances in this axis can result in either net loss, as seen in diseases such as rheumatoid arthritis, Osteoporosis and MM. Alternatively, net gain can cause conditions such as osteopetrosis, which causes the bones to become harder and denser. Although osteoclasts (bone destroying cells) are often grouped with osteoblasts and osteocytes in literature, they are actually derived from macrophage lineage [145], and by extension HSC. Marrow adipocytes (MA), however, are derived from mesenchymal BMSCs and comprise approximately 15% of the bone marrow in young adults. The proportion of MA in the bone marrow has been shown to increase every year (up to 60% by the age of 65) [146]. Recently, MA have been shown to synthesis stem cell factor (SCF), promoting the regeneration of HSC after irradiation [147]. The lineage commitment of BMSCS into osteoblasts / osteocytes is known to be in delicate balance with marrow adipocyte differentiation, and is influenced by key transcription factors and signalling pathways.

Wnt signalling, for example, has been shown to have a critical role in BMSCS differentiation. The activation of this large group of glycoproteins, specifically Wnt10b, has been shown to inhibit adipogenic differentiation by maintaining cells in a pre-adipoctye state via inhibition of the transcription factor CCAAT/enhancer binding protein α (C/EBPα) and proliferator-activated receptor γ (PPARγ) [148, 149]. In agreement with this, inhibition of Wnt signalling pathways has been shown to promote osteoblast maturation and subsequent bone formation [150] and the proportion of marrow adipocytes has been shown to be inversely correlated with bone quality [147].

The transforming growth factor β (TGFβ) superfamily have also been heavily implicated in BMSCS differentiation, with different members of this family provoking a variety of responses. Bone morphogenic proteins (BMPs) are a subset of TGFβ ligands and BMP4 has been shown to promote the adipocyte lineage in C3H10T1/2 (murine mesenchymal) cells [151]. BMP2 (in combination with Rosiglitazone, a thiazolidinedione) can also induce adipogenic differentiation [152] – however the effects of BMP2 have been shown to be dose dependent, with higher doses

stimulating production of osteocyte and chondrocyte lineages [153]. Like the TGBβ family, the Notch signalling pathway has also demonstrated a dual role in BMSCS differentiation. Blocking of Notch signalling has been shown to inhibit osteoblast production by supressing the Wnt/β-catenin pathway [154], however Notch signalling has also been shown to promote adipogenic differentiation via the PI3K pathway [154]. Indeed, Notch signalling in combination with TGF-β have also been shown to stimulate myeogenesis [155] via Notch ligand Jagged 1 (JAG1), highlighting the complex network of signalling that is interwoven in BMSCS differentiation.

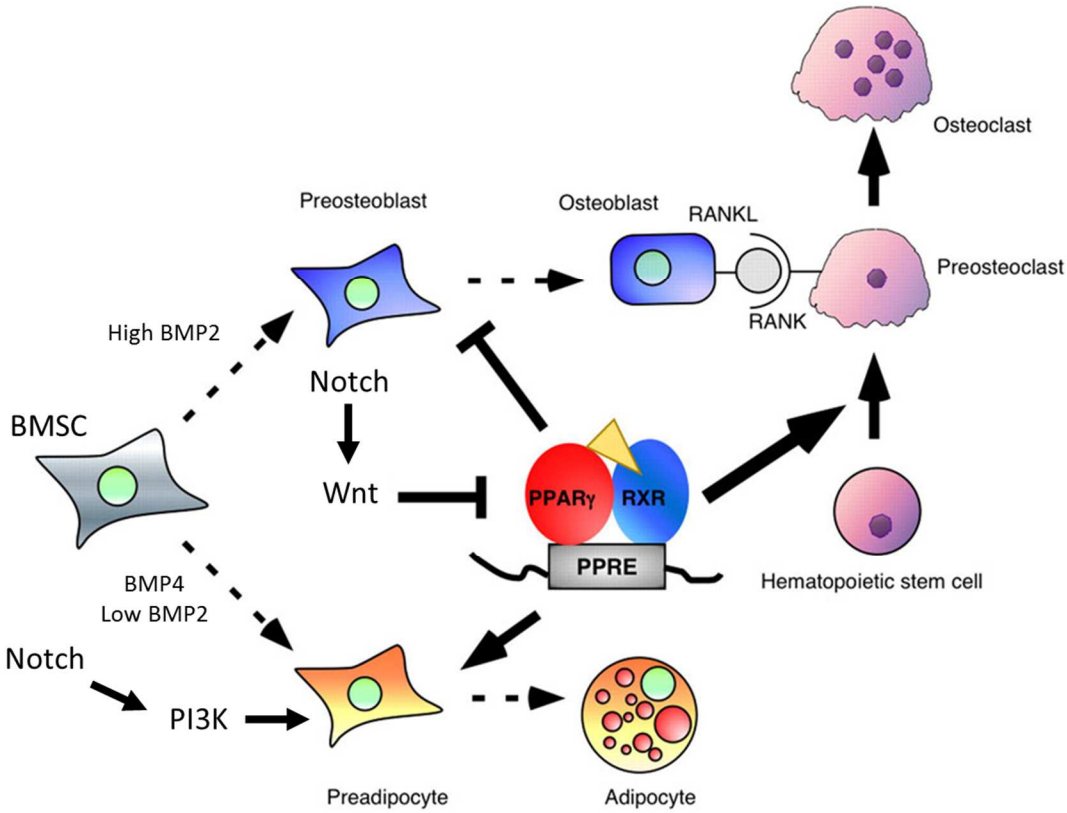

Figure 1.2.2 – Factors effecting BMSC differentiation.
Schematic showing several ways in which BMSC differentiation can be effected by signalling. Figure adapted from Katada and Kato, 2008 [156].

1.2.1.2.2 – Chrondrogenic cells

Chondrocytes are the cells that form cartilage, a tissue that in adults lacks the ability for self-repair [157] (most notably demonstrated in conditions such as osteoarthritis), and account for 1-5% of total cartilage tissue [158]. These cells are metabolically active and can synthesise a large volume of ECM components including collagen, proteoglycans and glycoproteins. *In vitro*, chondrocyte differentiation can be triggered using a medium containing ascorbate-2-phosphate, insulin, transferrin, dexamethasone, sodium pyruvate and TGFβ [159, 160]. The molecular events that regulate chondrocyte differentiation *in vivo* are still largely unknown, however some signalling molecules have been identified. Sox9 for example is a transcription factor that has been shown to critical in the establishment of chondrocytes and loss of Sox9 has been shown to cause defective cartilage primordia and premature mineralisation of many skeletal elements [161].

1.2.2 – Signalling pathways in the Cancer BMM

The cells located within the BMM are constantly secreting growth factors and cytokines, regulated by autocrine/paracrine loops and cell-cell adhesion or adhesion to the extracellular matrix. These interactions activate varying signalling cascades within the cells – controlling everything from cell differentiation to apoptosis. Many of these common signalling pathways can be hijacked by tumour cells – becoming de-regulated or constitutively activated within the malignant cell, benefitting disease progression.

1.2.2.1 – MAPK/ERK pathway

The MAPK/ERK pathway (also known as the Raf/MEK/ERK pathway) is pivotal in several fundamental cellular processes, including differentiation [162], proliferation [163] and apoptosis [164]. The primary route of MAPK signalling is via the activation of receptor tyrosine kinases (RTKs) that are embedded in the cell's surface membrane. Stimulated RTKs prompt Ras-GTPase activation and subsequent Raf kinase recruitment. Raf kinases can then phosphorylate ERK (either at the plasma membrane, Gogli apparatus or endosomes) which is then available to stimulate a wide selection of both cytosolic and nuclear targets. The net effect of MAPK/ERK activation is cellular proliferation and growth.

Abnormalities in all levels of the MAPK/ERK signalling cascade have been heavily implicated in many different types of cancer [165-167]. RAS mutations, for example, are highly frequent in pancreatic cancer [168], occurring in over 90% of all cases. There are three variations of Ras proteins (H-Ras, K-Ras and N-Ras) and of these, K-Ras mutations are the most frequently observed in oncogenesis [169, 170]. RAS mutations can cause Ras GTPase to become constitutively active – continuously binding GTP and activating the MAPK/ERK pathway leading to uncontrollable growth (as this pathway has been linked to the regulation of several key transcription factors, including c-Myc [171]).

In MM, mutations in the MAPK pathway occur in over 50% of all newly diagnosed cases [172]. A study by Bezieau *et al.* [173] found that although mutations in N-RAS and/or K-RAS2 are highly frequent in MM (approximately 55% at diagnosis or 81% at time of relapse), the frequency of this mutation in MGUS is significantly lower (12.5%). This could indicate a role for these mutations in the advancement of MM. Inhibition of MAPK has

been shown to increase the efficacy of PI-induced cell death [174], however the blockage of this pathway alone is not always sufficient to induce MM cell death *in vivo.* In most cases, the BMM is capable of stimulating compensatory pathways within the malignant cell. For example, Chatterjee *et al.* showed that in co-cultures of MM and BMSCS inhibition of both the MAPK and signal transducers and activators of transcription 3 (STAT3) pathways was required to induce apoptosis in MM cells [175].

1.2.2.2 – JAK/STAT pathway

The Janus kinase (JAK) family consists of JAK1-3 and Tyk2 and can be activated by many of the cytokines found within the BMM – including IL-6 [176], IL-10 [177, 178], IL-12 [179] and interferon α (IFNα) [180]. Upon activation, the non-receptor tyrosine kinase JAK can subsequently phosphorylate Signal Transducer and Activator of Transcription (STAT) proteins, which are latent transcription factors. Phosphorylated STAT can translocate to the nucleus (via the importin α-5 / Ran nuclear import pathway) where it initiates the transcription of many key genes that are involved in the cell cycle maintenance and survival (such as MYC [181, 182], CCND1/2 [183-185] and BCL2[186]).

Due to the crucial role of JAK/STAT signalling in cell growth and survival, abnormalities that cause the up-regulation in this pathway are indicative of poor outcome in cancer. This pathway has shown to play a role in several solid malignancies including colon cancer [187, 188], prostate cancer [189] and gastric cancer [190]. However, it is with haematological malignancies that this pathway is more traditionally associated. The JAK/STAT pathway plays a critical role in the haematopoietic system, and this has been demonstrated using varying *in vivo* knockout models. For example, a study by Witthuhn *et al.* in 1993 [191] showed that the mice lacking Jak2 expression die *in utero* due to fatal anaemia, and Buckley *et al.* demonstrated that Jak3 deficiency causes T-cell and B-cell loss (due to the absence of IL-7 receptor signalling). Genetic alterations to the JAK/STAT pathway are prevalent in blood cancers with JAK2 mutations the most frequently observed in diseases such as Hodgkin lymphoma [192, 193] and chronic myeloproliferative disorders [194].

With the cytokine IL-6 known to play a crucial role in MM disease progression (as well as its ability to stimulate the JAK/STAT pathway) it stands to reason that this pathway would be over-expressed in Myeloma. Indeed, this was found to be the case in MM cell lines including MDN [176] and U266 [195], and inhibition of JAK has been shown to have devastating effects on MM cells – even when cultured with BMSCS [196]. Phase 1b clinical trials of the drug OPB-111077 (a STAT inhibitor) are currently recruiting for acute myeloid leukaemia (AML) (NCT03197714) and solid tumours (NCT02250170), however its effects on MM still need to be investigated.

1.2.2.3 – NF-κB

The NF-κB transcription factor family (schematic shown in Figure 1.1.6) is known to regulate the transcription of over 100 cyto-protective genes within a cell and it consists of the following transcription factors: NF-κB1/p105, NF-κB2/p100 (which can produce p50 and p52 respectively, following proteolytic activity), RelA/p65, RelB and c-Rel. NF-κB mutations in solid tumours are extremely rare, but there more frequently found in haematological malignancies. For example, rearrangement (and subsequent amplification) of c-Rel are regularly detected in non-Hodgkin B-cell lymphomas and diffuse large cell lymphoma [197, 198]. NF-κB2/p52 chromosomal rearrangements or deletions (at position 10q24) can generate constitutively active p52 protein which has been linked to B-cell and T-cell lymphoma development and maintenance [199-201]. A study by Chapman *et al*. in 2011 that detailed the initial genome sequencing in MM found common mutations in 11 members of the NF-κB signalling pathway [22], confirming the findings made by earlier studies [202, 203].

However, direct mutations to the genes that control the NF-κB transcription factors are not the only way that these proteins can become aberrantly activated. Cross-talk from other oncogenic pathways [204-206] are also known to play a contributing role to the activation of these transcription factors.

1.2.2.4 – PI3K pathway

The PI3K pathway has been associated with many types of cancer – both solid [207-209] and haematological [210, 211]. Aberrant activation of this pathway can occur either by overexpression of the PI3K isoforms (such as the high frequency of PI3KCA mutations seen in breast and ovarian cancers [212, 213]) or by mutations in its negative regulator, Phosphatase and Tensin Homolog (PTEN) [214, 215]. In MM, although no common mutations in the PI3K pathway genes have been described, this pathway is constitutively activated. Inhibition of this pathway is therefore a potential therapeutic target for MM, and this will be explored in detail in Section 1.4.

1.3 – The Myeloma Microenvironment

Under typical conditions, a sub-set of plasma cells home to the bone marrow where they locate and adhere to a niche which is key in aiding their survival (and transition into long-lived plasma cells). Long-lived plasma cells can, as the name suggests, survive a much longer time that those plasma cells located in the spleen (3-4 weeks in the bone marrow versus 3 days in the spleen) [216]. Much in the same way, MM cells are critically dependent on their microenvironment for their longevity. The BMM shields and nurtures the MM cells, with removal of these malignant cells into *ex vivo* culture swiftly resulting in their death. Although malignant plasma cells have been detected in the peripheral blood of patients [217, 218], this is primarily at later stages of the disease when accumulating genetic alterations have produced a more independent clonal population. An overview of common ways the BMM can protect the MM cell is shown in Figure 1.3.1.

1.3.1 – MM-BMSC adhesion

The adhesion of MM cells to either the ECM (such as vitronectin, laminin, collagen or fibronectin) or other cells within the milieu has long been known to infer drug resistance within the MM cell (cell adhesion mediated drug resistance, CAM-DR) [219, 220]. MM cells can express a wide array of adhesion receptors, including CD29, CD44, CD49d (also known as VLA-4), CD54, CD138 and CD184 as well as variable expression of CD49e (VLA-5), CD11a and CD18 [221, 222].

VLA-4 has been implicated in MM-BMSC adhesion, interacting with vascular cell adhesion molecule 1 (VCAM1) / integrin β1 (ITGB1) and intracellular adhesion molecule 1 (ICAM1) / integrin β2 (ITGB2). This has been shown to cause the activation of both the MAPK and NF-κB pathways in both the MM cell and the BMSC [220, 223]. Interestingly, Hatano *et al.* showed that exposure to the proteasome inhibitor Bortezomib has been shown to reduce MM VLA-4 expression on MM cells, thereby reducing MM cell CAM-DR and sensitising the malignancy to common MM therapeutics such as dexamethasone [224].

MM-BMSC adhesion has also been shown to cause the release of the MM critical cytokine IL-6 [225] from the BMSCs, which causes both MAPK [226] and JAK/STAT [176] pathway activation within the malignant cells. Overexpression of the JAK/STAT pathway results in the upregulation of Bcl-xl and Mcl-1, known anti-apoptotic proteins [227, 228]. MM cells also

cause the BMSCs to produce stroma-modulating growth factors which stimulate angiogenesis [229, 230] and create a pro-inflammatory environment.

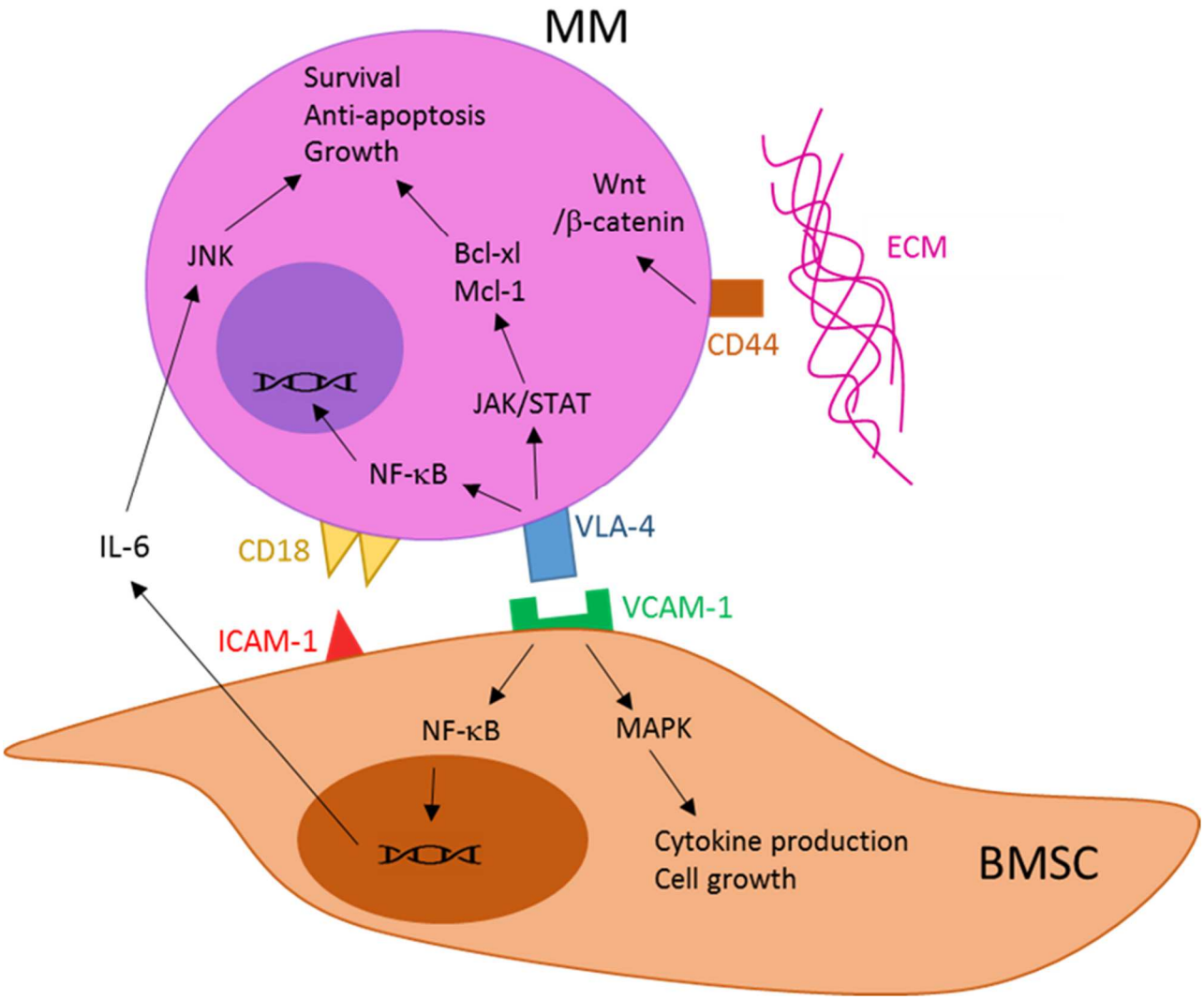

Figure 1.3.1 – Role of the BMSC in MM pathogenesis.
MM cells are critically dependent on their microenvironment, and adhesion of MM cells to either the BMSC or the different components of the ECM can stimulate pro-survival signals in the MM cell, some of which are shown above. MM cell shown in pink, BMSC shown in brown.

1.3.2 – MM and Osteoclasts

One of the clearest signs of MM disease is the appearance of lytic bone lesions within the patient – the severity of which increases with tumour burden. These symptoms are caused by a surge in osteoclast production that is initiated by the MM cells.

Receptor activator of nuclear factor κB (RANK) is known to be expressed on the surface of osteoclast lineage cells and its ligand, RANKL, is commonly expressed on BMSC. The interactions between these proteins has been shown to play a key role in the activation and development of osteoclasts [231, 232]. After homing to the BM, MM cells can stimulate an increase in RANKL from the BMSC, whilst simultaneously reducing levels of osteoprotegerin (a decoy receptor for RANKL) [9]. This results in a gain of osteoclast activity and differentiation – leading to a net loss of bone that is detectable via radiography (as seen in Figure 1.3.2).

IL-6 also has been implicated in the in the formation of osteoclasts, and has been shown to work in a RANKL independent manner [233, 234]. IL-6 serum levels are known to be abnormally high in MM patients, and levels increase alongside tumour burden [235]. This high concentration of IL-6 therefore also causes osteoclast populations to flourish, resulting in the net bone absorption that is synonymous with MM disease progression.

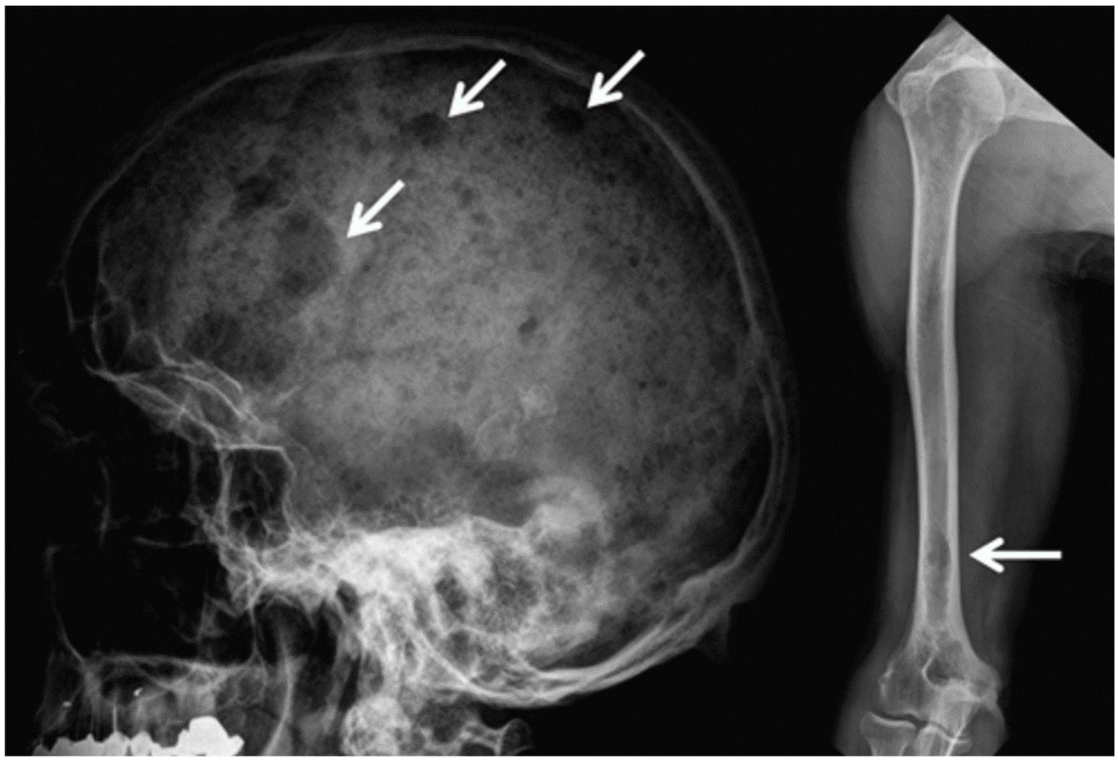

Figure 1.3.2 – Radiographs showing osteolytic regions in the skull and humorous.
Osteolytic lesions (shown with white arrows) are caused by an overproduction and activation of osteoclasts, initiated by the MM cells. Image taken from Walker *et al.* [236].

1.3.3 – MM and Endothelial cells

In a tumorous environment, the cells that form the inner surface of blood or lymphatic vessels (the endothelial cells) can differ greatly from those found in a healthy environment. Highly increased levels of angiogenesis mean that these vessels are growing rapidly, to accommodate the rapidly proliferating malignant cells [237]. Because of this rapid expansion, these cells are often abnormally shaped and are more likely to be permeable (due to a discontinuous basement membrane) [238].

This is also the case in MM where endothelial cells have been shown to form thin, branching vessels [239]. As with solid tumours, angiogenesis is stimulated – this time due to increased levels of cytokines such as VEGF and matrix metalloproteinases (MMPs) that are secreted from the malignant plasma cells [8, 240, 241]. Osteopontin too (a protein secreted by osteoclasts) is known to be pro-angiogenic [242] and helps form a brutal cycle of angiogenesis and bone destruction.

1.4 – The PI3K pathway overview

Phosphoinositide 3-kinases (PI3K) are a family of intra-cellular lipid kinases that are ubiquitously involved in common cellular functions, including cell growth [243, 244] and survival [245, 246]. Activation of PI3K occurs downstream of both RTKs and G-protein coupled receptors (GPCRs) in response to various growth factors, cytokines and hormones. Once PI3K has been phosphorylated, Phosphatidylinositol-4,5-bisphosphate (PIP_2) can be converted to Phosphatidylinositol-3,4,5-triphosphate (PIP_3) at the plasma membrane. PIP_3 can bind to proteins that contain pleckstrin homology domains, including 3-phosphoinositide-dependent protein kinase 1 (PDK1). Once bound, PDK1 is activated and can then phosphorylate Akt [247] (with dual phosphorylation at both its Serine 473 (Ser473) and Threonine 308 (Thr308) residues needed for full activation). Following phosphorylation, Akt is available to activate a large range of substrates – and therefore influences a wide array of cellular processes. An overview of the PI3K pathway is shown in Figure 1.4.1.

In a study by Datta *et al.,* PI3K/Akt activation was shown to contribute to cell survival via the phosphorylation of Bcl-2-associated death (BAD) promoter [248] – as only non-phosphorylated BAD is able form a heterodimer with BCL-xl or Bcl-2 [249], thereby causing the suppression of apoptosis. Alternatively, PI3K / Akt activation can induce cell death via apoptosis. Under typical conditions, Caspase-9 is also to prevent apoptosis, however with Akt phosphorylation inhibiting the cascade of caspase activation, further cell death is observed [250]. Another inhibitor of apoptosis, the forkhead box class O (FoxO) transcription factor family, is negatively regulated by active Akt. Non-phosphorylated FoxO is able to translocate to the nucleus and subsequently activate of a large set of genes that promote cell cycle arrest (such as the CDKN1A and CDKN1B genes [251-253]), apoptosis (via activation of the BCL2L11 gene [254]) and drug resistance [255]. However, upon phosphorylation via Akt, FoxO is confined to the cytoplasm where it is degraded by the ubiquitin-proteasome pathway.

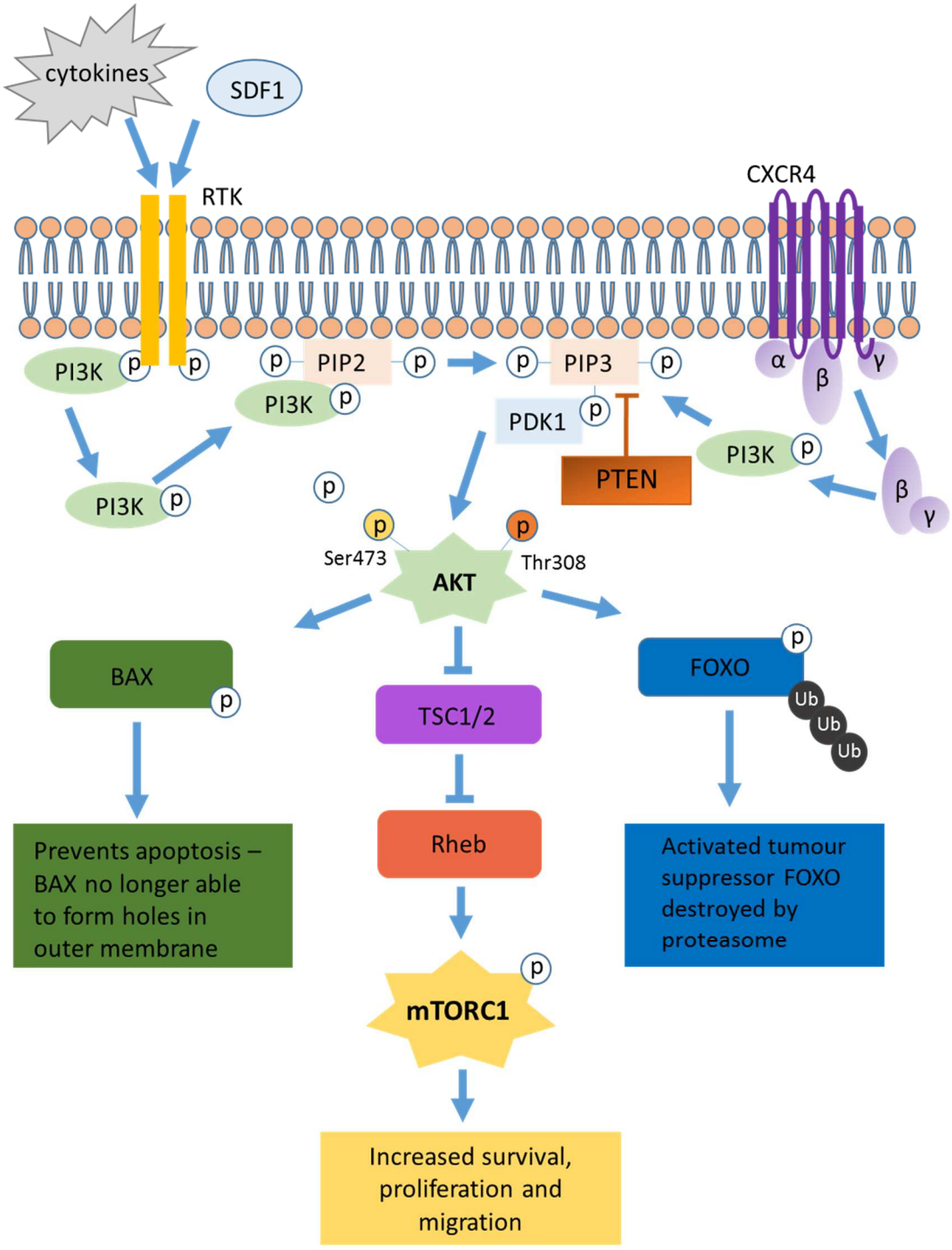

Figure 1.4.1 – Schematic showing PI3K pathway stimulation.
Adapted from Piddock *et al.* [256].

Mammalian target of rapamycin (mTOR) is also a well-defined target of Akt, and the Akt/mTOR pathway has been implicated in many processes – from skeletal muscle hypertrophy [257] to glucose metabolism [258]. Upon activation, it is known to positively regulate cell metabolism and growth [259] and limit autophagy (via

phosphorylation of Ulk1 [260]). Overall, the stimulation of PI3K and its downstream targets results in a net increase in cellular proliferation, growth and migration – known hallmarks of cancer metastasis.

1.4.1 – PI3K and cancer

Under typical conditions, PIP_3 is moderated and returned to its inactive state by the negative regulator, phosphatase and tensin homolog (PTEN). However, in some tumour types, a mutation in the PTEN gene causes it to lose functionality – instigating a continual activation of the PI3K pathway upon stimulation. This mutation has been seen in many cancers, including prostate, breast and glioblastomas [214] – however PTEN mutations are uncommon in MM. Activating mutations in upstream regulators (such as the FLT3 mutation seen in AML [261]), are also absent from the majority of MM patients. The a-typical activation of this pathway is therefore more likely to be attributed to the microenvironmental stimuli received as well as the differential expression seen in the PI3K class I catalytic subunits.

There are three classes of PI3Ks, which have differing structures and functions (see Table 1.4.1), of which class I is the most well defined. Class I PI3Ks comprise of a regulatory subunit and one of four catalytic subunits (p110α/β/γ/δ). They are most commonly activated by Receptor Tyrosine Kinases (RTKs), however the G-protein coupled receptor (GPCR) subunit Gβγ has been shown to bind directly to the PI3K subunits p110β and p110γ, thereby bypassing the need for RTK activation [262, 263].

1.4.1.1 – p110α

p110α is expressed ubiquitously in mammalian tissues, and has been shown to contribute to insulin-like growth factor-1 (IGF-1) stimulation of Akt. It has also long been associated with a variety of cancers, with breast cancer one of the most highly connected [264-266]. Somatic activation of the gene that codes for p110α production (PIK3CA increased copy number / 3q26.3 amplification) has been found in a subset of primary breast [265], endometrial [267, 268] and colon [269, 270] tumorous tissues, and this mutation correlates with the loss of PTEN function and is a marker of poor prognosis. However, the inhibition of this isoform alone has

been shown to be insufficient to reverse the effects of PI3KCA mutations, with p110β compensating for the inhibition by producing vast amounts of PIP_3 and maintaining partial PI3K activation [271].

Despite the frequency of p110α activation in solid tumours, mutations in haematological malignancies are extremely rare [272, 273], and are therefore is not a potential target for MM.

1.4.1.2 – p110β

p110β has been shown to be activated by both RTKs and GPCRs [263], and is most frequently associated with platelet aggregation [274]. p110β signalling has been shown to be essential for the progression of prostate cancer [275], and can maintain PI3K signalling in PTEN-deficient cancer sub-types [276].

However, in blood cancers activating mutations or increased p110β expression are infrequent [277]. A study by Sahin *et al.* in 2014 [278] showed that p110β was highly expressed in a selection of MM cell lines and that knockdown of PIK3CB *in vivo* showed lower rates of tumour growth – however the levels of p110β expression in primary MM samples was not analysed in this investigation.

1.4.1.3 – p110γ

The PI3K enzyme p110γ is often put in its own sub-class (class I_B), as it lacks a p85 binding domain - instead binding to the regulatory units p101 or p84/87 [279]. This isoform is present only in mammals, and is expressed primarily by leukocytes. It has a crucial role in the production of PIP_3 via GPCR activation [280], and subsequently macrophage motility, and has been shown to be critically involved in inflammation [281]. PI3KCG mutations have previously been associated with lung cancer [282] and idiopathic pulmonary fibrosis – where inhibition of p110γ resulted in a reduction in malignant cell proliferation [283].

1.4.1.4 – p110δ

p110δ is expressed only in leukocytes [284] and, alongside p110α, plays a vital role in B-Cell development [285]. It has been linked to several immune disorders, including inflammatory bowel disease and PI3Kδ syndrome (caused by gain of function mutations in the PIK3CD gene). p110δ has also been shown to have an oncogenic role in several blood cancers including chronic lymphocytic leukaemia (CLL), acute lymphoblastic leukaemia (ALL), AML and MM [211, 286, 287] and the pharmacological inhibition of this subunit has beneficial effects in the treatment of both non-Hodgkin's lymphoma and CLL [288]. Inhibition of p110δ has been shown to have a conservative effect on MM cell monocultures too, inhibiting proliferation [289] and inducing cytotoxicity [290].

Class	Protein	Gene
I – Catalytic	p110α	PIK3CA
	p110β	PIK3CB
	p110γ	PIK3CG
	p110δ	PIK3CD
I – Regulatory	p85α, p55α, p50α	PIK3R1
	p85β	PIK3R2
	p55γ	PIK3R3
	p101	PIK3R5
	p84/87	PIK3R6
II – Catalytic	PI3K-C2α	PIK3C2A
	PI3K-C2β	PIK3C2B
	PI3K-C2γ	PIK3C2G
III – Catalytic	Vps34	PIK3C3
III – Regulatory	Vps15	PIK3R4

Table 1.4.1 – Table of PI3K catalytic and regulatory subunit isoforms.
Class I PI3K isoforms are most commonly linked with oncogenesis.

1.5 – Hypotheses and objectives

MM is a debilitating and currently incurable disease due, in part, to the pro-oncogenic stimuli it receives from other cells within the BMM. MM-BMSC interactions have been shown to benefit the disease, causing the activation of signalling cascades that encourage proliferation, growth and drug resistance. Targeting these interactions provides us with an opportunity to not only learn more about the mechanisms of the disease, but to potentially increase the efficacy and tolerability of current therapeutics.

This project aims to increase the current understanding of PI3K signalling within the MM microenvironment, and to provide novel insight into future therapeutic targets in MM.

Objectives:

1. Investigate if PI3K p110δ and p110γ signalling within the malignant cell benefits MM disease progression.
2. Determine if these PI3K isoforms are activated by the BMM and if they can be inhibited within this environment.
3. Explore if MM cell signalling can re-model the BMM to benefit its survival.

2 – Materials and Methods

2.1 – Materials

2.1.1 – Buffers

The composition of the common buffers made for use in this thesis are detailed below, written in alphabetical order. Solutions were made in deionised and sterilised water, unless otherwise specified.

10X PBS (pH 6.8)
NaCl - 1.37 M
KCl - 27 mM
Na2HPO4 - 119 mM
KH2PO4 - 39 mM

Blocking Solution
Skimmed Milk Powder - 5%
Or BSA - 5%
Suspended in TBST, protein used is dependent on antibody

MACS Buffer (pH 7.2)
BSA - 0.5%
EDTA - 2 mM
In sterile, filtered PBS

RIPA Buffer
Nonidet P-40 - 1%
Sodium deoxydelate - 0.5%
SDS - 0.1%
In sterile, filtered PBS

Tris-Buffered Saline Solution (TBST)
Tris (pH 7.5) - 20mM
NaCl - 150mM
Tween 20 - 0.1%

Western Blot Running Buffer
Tris-HCl - 25 mM
Glycine - 190 mM
SDS - 0.1%

Western Blot Transfer Buffer
Tris-HCl - 25 mM
Glycine - 190 mM
Methanol - 20%

2.1.2 – Reagents and cytokines

PI3K inhibitors (CAL-101, CZC24832 and IPI-145) and MIF inhibitor (ISO-1) were purchased from Selleck Chemicals (Houston, TX, USA). Recombinant human Interleukin-6 (IL-6) and Stromal cell Derived Factor-1 (SDF-1) were purchased from Miltenyi Biotec (Auburn, CA, USA). Recombinant human Macrophage Migratory Inhibitory Factor (MIF) was obtained from R&D Systems (Wiesbaden, Germany) respectively.

All other reagents were obtained from Sigma-Aldrich (Dorset, UK), unless otherwise indicated in the text.

2.1.3 – Antibodies

Antibody	Isotype	MW (kDa)	Product #	Supplier
Akt (Pan)	Rabbit	60	4691	Cell Signaling Technology (Cambridge, MA, USA)
p110α	Rabbit	110	4249	
p110β	Rabbit	110	3011	
p110γ	Rabbit	110	5405	
p44/42 MAPK (Pan)	Rabbit	42/44	4695	
Phospho-Akt (Ser473)	Rabbit	60	4060	
Phospho-p44/p42 MAPK	Rabbit	42/44	4370	
p110δ	Rabbit	110	MAB2687	R&D Systems (Oxford, UK)
β-Actin	Mouse	42	A1978	Sigma-Aldrich (Dorset, UK)

Table 2.1.1 – Antibodies used in Western Blots

	Clone	Order Number	Supplier
CD138-PE	REA104	130-102-580	Miltenyi Biotec (Paris, France)
CD90-FITC	REA879	130-095-403	
CD45-PerCP	30F11	130-095-182	
CD38-FITC	REA616	130-109-254	

Table 2.1.2 – Antibodies used in Flow Cytometry

2.1.4 – PCR Primers

Oligo Name		Supplier Number	Sequence (5'-3')
GAPDH	Forward	SY170306937-069	CTTTTGCGTCGCCAG
	Reverse	SY170306937-070	TTGATGGCAACAATATCCAC
PIK3CD	Forward	SY150410444-024	CTTTCTGGGGAATTTCAAGAC
	Reverse	SY150410444-025	GAACCGTTCAAATTTCTCAC
PIK3CG	Forward	SY150410444-026	TCAGGACATCTGTGTTAAGG
	Reverse	SY150410444-029	GCATCCCGGATATATTCAATG
β-Actin	Forward	SY151136674-054	GACGACATGGAGAAAATCTG
	Reverse	SY151136673-053	ATGATCTGGGTCATCTTCTC
IL8	Forward	SY150107089-035	GTTTTTGAAGAGGGCTGAG
	Reverse	SY150107089-036	TTTGCTTGAAGTTTCACTGG
IL6	Forward	SY141004293-022	GCAGAAAAAGGCAAAGAATC
	Reverse	SY141004293-023	CTACATTTGCCGAAGAGC

Table 2.1.3 –Sequences of PCR primers used.
All primers were obtained from Sigma-Aldrich (Dorset, UK).

2.2 – Cell Culture

2.2.1 – Cell lines

The Myeloma cell lines (MM.1S, MM.1R, RPMI-8226, U266, LP-1 and H929) were all obtained from the European Collection of Cell Cultures, where they are authenticated by DNA fingerprinting. All cell lines were cultured in Roswell Park Memorial Institute (RPMI) 1640 medium (Gibco, Life Technologies), which was supplemented with 1% penicillin and streptomycin antibiotic solution (containing 50 units/mL penicillin and 50 µg/mL streptomycin) as well as 10% heat inactivated foetal bovine serum (FBS).

Cell suspensions were kept between 2.5 x 10^5 and 5.0 x 10^5 cells per mL to ensure optimal growth and fed every 2-3 days on average (as recommended by the supplier). Cells were maintained in a controlled atmosphere in a HERAcell 150 CO_2 incubator, at 5% CO_2 and at a temperature of 37°C. After 6 weeks, cell lines were discarded and new aliquots previously stored at -80°C were put into culture to ensure cell authenticity.

2.2.2 – Patient derived samples

Primary BMSC and MM cells were obtained from the patients' bone marrow following informed consent, in accordance with the Declaration of Helsinki and under approval from the Health Research Authority (07/H0310/146) – the authority formally known as the United Kingdom National Research Ethics Service. Primary cells were isolated from heparinised bone marrow (obtained at the Norfolk and Norwich University Hospital), by Histopaque density gradient centrifugation (see Section 2.2.4) and flasked in Dulbecco's Modified Eagle's Medium (DMEM), containing 20% FBS and 1% pen-strep, in T-75 flasks. All cells were maintained in a controlled atmosphere in a HERAcell 150 CO_2 incubator, at 5% CO_2 at 37°C. Due to poor recovery rates of MM cells following -80°C storage, primary MM cells collected were not subject to cryopreservation/thawing in my study.

After 24hrs, all non-adherent cells were removed and primary Myeloma cells were purified from supernatant using magnetic-activated cell sorting with CD138+ MicroBeads (see Section 2.2.5) and re-suspended in DMEM until use. Remaining adherent cells were classified as bone marrow stromal cells (BMSCs) and were grown in DMEM (with 20% FBS and 1% pen-strep) to 60-80% confluency after which they were routinely passaged and expanded for 6-8 weeks.

2.2.3 – Cell passage

All adherent cells used were cultured in T-75 flasks and passaged when confluency reached 60-80%. Briefly, to passage cells medium was removed from cells and discarded. Cells were rinsed with sterile Phosphate Buffered Saline (PBS) and treated with 2 mL of Trypsin at 37°C for 5 minutes. Flasks were agitated and 3 mL of PBS were added to aid in the detachment of cells. Cells were centrifuged at 300 x g for 5 minutes after which supernatant was discarded and cells were re-suspended in appropriate volume of medium and re-seeded into fresh T-75 flasks or tissue culture plates, as appropriate.

2.2.4 – Histopaque density gradient separation

To separate the peripheral blood mononuclear cells (PBMCs) from other components in the patient BM sample (such as serum and red blood cells), the patient sample was subject to Histopaque density gradient separation.

Histopaque is a solution comprising of polysucrose and sodium diatrizoate and is used as the medium for density gradient separation – where cells/particles of different densities in a suspension will travel through the medium at different rates. 20mls of primary sample was layered on to the surface of 10mls Histopaque-1077 (density = 1.077 g/mL) in a 50mL falcon tube. The falcon tube containing the Histopaque and the patient sample was then centrifuged for 20 minutes at 300 x g (with the no brake setting applied on the centrifuge), resulting in distinct layers detailed in Figure 2.2.1.

Peripheral blood mononuclear cell (PBMC) layer was collected using a Pasteur pipette, with great care taken not to disturb the Histopaque layer located underneath. Once collected, the PBMC layer was centrifuged at 300 x g for 10 minutes after which the supernatant was discarded. Cell pellet was then subject to a red cell lysis (using red cell lysis buffer, Sigma-Aldrich) and washed twice in sterile PBS. Cells were then re-suspended and stored in DMEM media containing 20% FBS and 1% pen-strep (conditions detailed in Section 2.2.2) in T-75 flasks. MM cells were purified after 24 hours in culture (see Section 2.2.5).

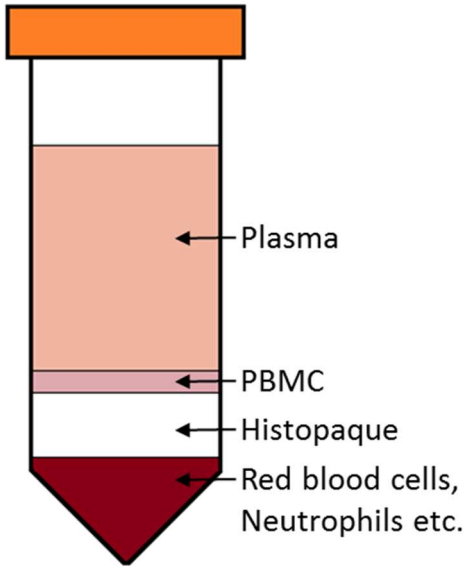

Figure 2.2.1 – Layers achieved in Histopaque density gradient separation.
PBMC layer is removed and purified using CD138+ magnetic bead selection.

2.2.5 – Microbead selection

As the PBMC layer obtained in the previous section only contains a fraction of MM cells, all non-adherent cells obtained in primary samples were subject to purification using Manual Cell Separation (MACS) columns and CD138 microbeads (Miltenyi Biotec, UK) following density gradient separation. This was done to positively select for the desired cell type. CD138 is routinely used as a marker for MM cells, and is expressed on both normal and malignant plasma cells [291].

MACS microbeads are superparamagnetic particles, and a high gradient magnetic field is used to retain any labelled cells. All materials used in this purification were kept at 4°C in a refrigerator during the process wherever possible. A schematic of this protocol is shown in Figure 2.2.2.

2.2.5.1 – Magnetic Labelling

Cell suspensions were pelleted via centrifuge for 10 minutes at 300 x g and resulting supernatant was discarded. Cell pellets were then washed with sterile filtered PBS, and centrifuged to re-form the pellet. Pellet was then re-suspended in 80µL degassed MACS buffer (composition of buffer is detailed in Section 2.1) and 20µL of CD138 Microbeads were added (all volumes detailed are per 2 x 10^7 total cells).

After a 15 minute incubation at 2-8°C with CD138 Microbeads, 2mLs of MACS buffer was added and cells were centrifuged again (300 x g for 10 minutes) and supernatant was removed (washing off any unbound CD138 microbeads). Cells were then re-suspended in 500µL of MACS buffer.

2.2.5.2 – Magnetic Separation, MS column

MS column was placed into magnetic field of MACS separator, was rinsed with 500µL MACS buffer (to remove a hydrophilic coating from the column), and elution was thrown away. Magnetically labelled cells were then added to the column, the column was rinsed another 3 times with MACS buffer (3 x 500µL) and elution was once again discarded (as it contained only unlabelled cells at this point). MACS column was then removed from MACS separator (and subsequently the magnetic

field) and was placed onto a 15mL falcon tube for collection. 1mL of MACS buffer was then immediately applied to the column and was forced through upon the application of a plunger. This 1mL contained the desired $CD138^+$ cells.

Cell population was then cultured in DMEM media + 20% FCS and 1% pen-strep for a maximum of 24 hours.

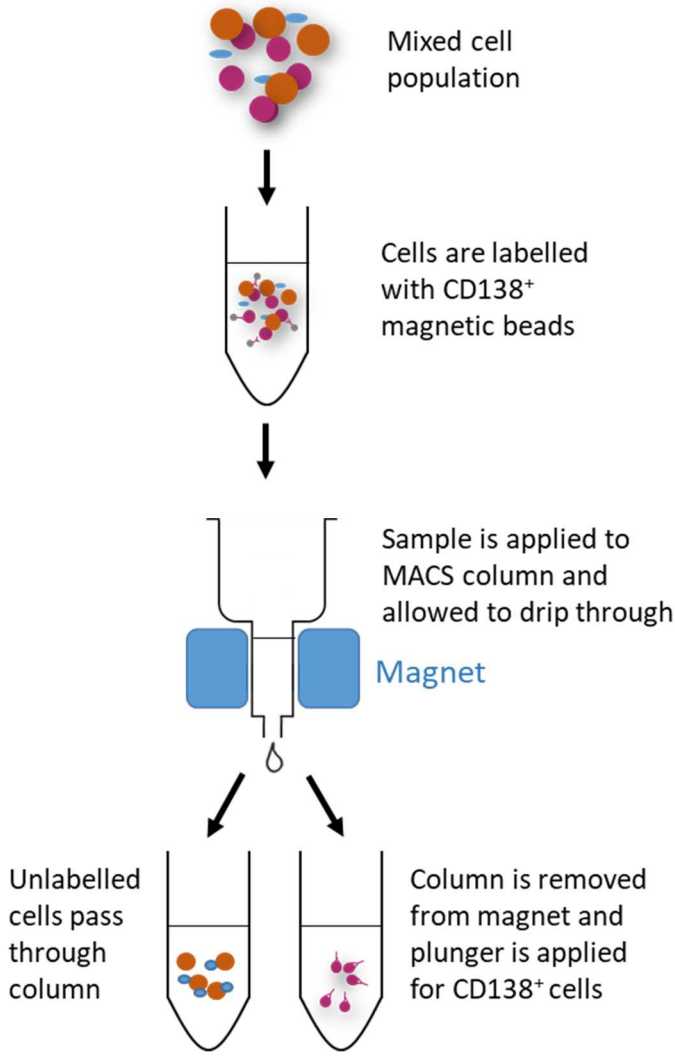

Figure 2.2.2 – Schematic of MACS column $CD138^+$ magnetic bead separation. Plasma cells are magnetically labelled with CD138 Microbeads and cell suspension is separated using a magnet and a MACs column.

2.3 – Trypan Blue Exclusion

Trypan Blue is an azo dye that is used to determine the number of viable cells that is present in a cell suspension [292]. Viable, or intact, cells possess complete membranes that prevent this dye from staining the cell's cytoplasm. Cells which are no longer viable allow the dye to stain the cytoplasm blue.

In all cases, 10µl of test sample was mixed with 10µl of Trypan Blue and viable / non-viable cells were counted using a light microscope and a haemocytometer.

2.4 – Viability Assay

Cell viability was measured using a Cell Titre Glo™ (CTG) assay (Promega, Southampton, UK). CTG is a luciferase based assay, which quantifies the amount of Adenosine Tri-Phosphate (ATP) present within a cell suspension. The amount of ATP has been shown to be directly proportional with the amount of cells present within a culture [293].

Cells were seeded at 5 x 10^4 cells in 100µl (in quintuplicate) in 96-well opaque plates and incubated for varying time periods (24-72h depending on the experiment), with or without test conditions. In all cases, equal quantities (50µl) of cell suspension and CTG were combined on an opaque-walled multi-well plate and mixed to induce cell lysis. Samples were left to incubate for 5 minutes, after which luminescence was measured. Output of luminescence units was recorded and analysed as a percentage, relative to the control.

2.5 – Apoptosis Assay (PI – Annexin V staining)

Flow cytometry was used to measure apoptosis (programmed cell death) using the CyFlow Cube 6 flow cytometer (Sysmex, Milton Keynes, UK). After initiation of apoptosis phosphatidylserine (PS) has been shown to translocate to the extracellular membrane, becoming an available target for Annexin V binding. Recombinant Annexin V conjugated with a green fluorescent FITC dye was used in this assay to make it detectable via flow cytometry. Propidium Iodide (PI) is a red fluorescent dye which binds to dsDNA and is membrane impermeable (and is therefore can only able to stain cells that are no longer viable). PI-Annexin V analysis was performed using the Annexin V apoptosis detection kit as per the manufacturer's instructions. PI-Annexin V was used in conjunction with Trypan Blue exclusion (section 2.3) and CTG analysis (section 2.5) to confirm cell death and viability.

Briefly, cells were spun down and re-suspended in 100µl PBS. 5µl of FITC Annexin V and 1µl of Propidium Iodide (PI) at 100 µg/ml were then added to each sample and incubated away from direct light and at room temperature for 15 minutes. After this incubation, 400µl of 1X annexin-binding buffer was added (5X buffer contains 50mM hepes, 700Mm NaCl, 12.5mM $CaCl_2$ and was at pH 7.4) and stained cells were analysed by flow cytometry (on channels FL1 for Annexin V and FL3 for PI). Population forms 3 groups – live cells, dead cells and apoptotic cells (see Figure 2.5.1). A minimum of 10,000 events was recorded in each case.

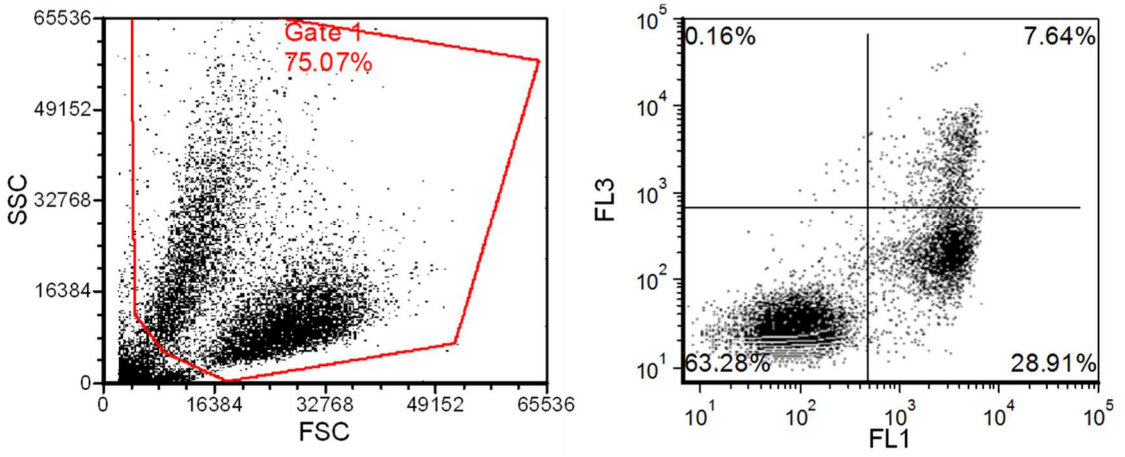

Figure 2.5.1 – Representative gating strategy for Apoptosis assay.
FL1 measures Annexin V (FITC) and FL3 measures PI. Double negative cells are alive, double positive cells are dead and cells positive for Annexin V alone are positive for phosphatidylserine (indicating the intermediate stage of apoptosis).

2.6 – Western Immunoblotting

2.6.1 – Sample preparation

Whole cell lysates were extracted using radio immunoprecipitation assay buffer method (RIPA). RIPA buffer was supplemented with protease and phosphatase inhibitor cocktail tablets (Roche) to aid in the prevention of protein degradation and phosphorylation.

Briefly, 50µl RIPA buffer was added to cell pellets of samples, causing cell lysis and protein solubilisation. Samples were then incubated on ice for 15 minutes and were centrifuged at 4°C for 15minutes at 15000 x g. Supernatant containing protein was removed and kept on ice or alternatively stored at -20°C until use. Prior to running, 5x western blot loading dye (bromophenol blue based) was added to each sample and all samples were heat denatured at 100°C for 5 minutes.

2.6.2 – SDS-PAGE

SDS-polyacrylamide gel electrophoresis (SDS-PAGE) was performed on samples, using a 12% polyacrylamide gel. This process is generally used to separate proteins based on their relative molecular mass – with smaller molecules migrating faster than larger ones.

Gels were made to the specifications shown in Table 2.6.1. Once gels had set (process takes a minimum of 1 hour) they were loaded onto gel cassettes that were submerged in Running Buffer. 10µl of each sample (containing loading dye) was loaded into individual wells on the gel using specialised loading pipette tips, with one well containing 10µL of a protein ladder (Precision Plus Protein All Blue pre-stained standards, Bio-rad).

Gels were subject to a voltage of 200V for 1 hour. Electro-transfer was performed using the wet transfer method onto polyvinyladine fluoride (PVDF) membranes that had been activated in methanol. Transfer was run at 100V for 45 minutes in Transfer Buffer with an ice pack used to counteract heat generated. Once completed, PVDF membrane (now containing protein) was then blocked for 1 hour in 5% BSA or non-skimmed milk (depending on antibody guidelines from manufacturers). Blocking is performed to prevent the non-specific binding of detection antibodies.

Once blocking step was complete, PVDF membranes were incubated in diluted primary antibody at 4°C overnight. The following morning, membranes were washed 3 times (at 10 minute intervals) in TBST buffer after which they were incubated for 1 hour in secondary antibodies (specific to the primary antibody used and conjugated with horseradish peroxidase) that are used for chemiluminescent detection.

For probing of membrane, anti-p110δ antibody was purchased from R&D systems (Oxford, UK). Anti-phosphorylated and pan AKT (Ser473), p44/42 MAPK (Thr202/Tyr202) and anti-p110α/β/γ antibodies were purchased from Cell Signaling Technology (Cambridge, MA, USA). All other antibodies used were purchased from Miltenyi Biotec (Auburn, CA, USA).

2.6.3 – Chemiluminescent detection

Membranes were activated using 1mL of enhanced chemiluminescence (ECL) reagent (GE healthcare, UK) after which excess reagent was removed and membranes were covered in plastic wrap. They were then imaged for 5-15 minutes (antibody depending) to collect the best luminescence signal possible. Light images were also taken to aid in protein identification. Membranes were imaged (following activation) on a Chemdoc-It2 Imager (UVP, CA, USA).

	5% Stacker Gel (per mL)	12% Gel (per mL)
H2O	675µL	330µL
30% Acrylamide-Bis, BioRad	180µL	400µL
1.0M Tris (pH 6.8)	125µL	-
1.5M Tris (pH 8.8)	-	250µL
10% SDS	10µL	10µL
10% Ammonium persulphate	10µL	10µL
TEMED	0.5µL	0.5µL

Table 2.6.1 – SDS-PAGE Gel composition.
Quantities listed are per mL of gel made, average gel contained 6mL of standard 12% gel and 1mL of stacker gel.

2.7 – Cell Adhesion Assay

BMSC were seeded in 96-well tissue culture plates at 2 x 10^4 cells in 200µl of DMEM media and left to adhere and grow for 24 hours (until confluent). In cases where Fibronectin (Fn) was used, 50µl was added to each well of a 96-well tissue culture plate (at 10µg / mL in sterile H_2O) and incubated for 4 hours at room temperature, or overnight at 4°C. In all cases, supernatant was removed prior to the addition of MM cells.

MM cells were fluorescently labelled with 2.5 µM Calcein AM fluorescent dye for 1 hour at 37°C and 5% CO_2. Cells were then washed with PBS and re-suspended in fresh media. 2 x 10^5 MM-Calcein cells were seeded into each prepared BMSC or Fn well (in 100µl volume) for the indicated time points. After incubations, non-adherent Calcein-labelled cells were removed by gently washing wells with PBS. Adherent cell signal was quantified using a FLUOstar Omega multi-well plate reader (BMG Labtech, UK). Calcein dye emission was read at 520nM wavelength and raw values were normalised to control samples.

2.8 – Cell Migration Assay

All migration assays were performed in triplicate on transwell permeable tissue culture plates with 4.0µM pores (Neuroprobe, Gaithersburg, MD, USA). 5 x 10^4 MM cells were used for each well. MM cells were pelleted and re-suspended in serum-free media for 3 hours. Lower chamber of assay (see Figure 2.8.1) contained 30µl of BMSC conditioned media or serum-free media supplemented with 100ng/mL of stromal cell derived factor 1 (SDF-1). MM cells were applied to the upper chamber and allowed to migrate for 4hours. After this incubation, viable cells in the lower chamber were quantified via Trypan Blue exclusion (see Section 2.3).

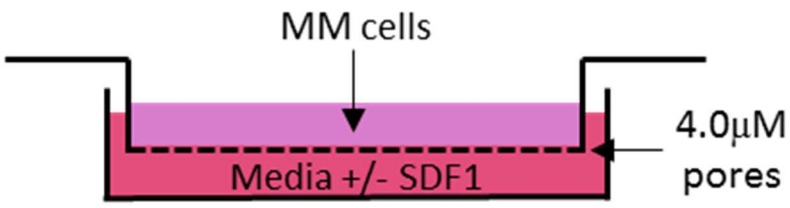

Figure 2.8.1 – Schematic showing structure of transwell system.
Suspended cells were applied to transwell insert (top section) and media with / without SDF-1 was applied to bottom well. In cases where BMSCs were used, these were grown in the bottom well compartment.

2.9 – Gene expression analysis

2.9.1 – RNA extraction

Total RNA was extracted from cells using the ReliaPrep™ RNA Cell Miniprep System (Promega, Southampton, UK). Briefly, cell suspensions are pelleted, supernatant is discarded and cells are lysed using 250µl of BL+TG lysis buffer and manual agitation. Following this step, 85µl of isopropanol is added and samples are mixed thoroughly by vortexing for 10 seconds.

RNA lysates are bound to a ReliaPrep™ minicolumn membrane by centrifugation. Membrane is washed by the addition of 500µl wash solution (EtOH based) and effluent is discarded after wash. All sample embedded membranes are subject to a DNAse I incubation by the application of 30µl DNAse I mix for 15 minutes at room temperature (mix contains 24µl Yellow Core Buffer, 3µl 0.09M $MnCl_2$ and 3µl DNAse1 enzyme per reaction). DNase I is applied to digest contaminating DNA, and the bound RNA is purified. Membranes are washed again and 30µl of sterile nucleotide free H_2O (Roche, UK) is used to elute the RNA from the membrane. RNA was either used immediately or stored at -20°C for future use.

2.9.2 – RNA quantification

RNA was quantified using a Nanodrop 2000 Spectrophotometer (ThermoScientific, UK). Spectrophotometer was blanked using sterile nucleotide free H_2O (the elution medium) before the measurement of any RNA. Quality was analysed using 260 / 230 and 260 / 280 absorbance ratios. Measurements between the ranges of 2.0-2.2 (for 260 / 230 ratio) and 1.9-2.1 (for 260 / 280 ratio) were indicative of “pure” RNA (i.e. not contaminated by RNA extraction reagents). Any samples found to be outside either of these ranges were discarded. Ranges were taken from Thermo Scientific T042 – Technical Bulletin.

2.9.3 – cDNA synthesis

Samples underwent reverse transcription (RT) using the pPCRBIO cDNA synthesis kit (PCR Biosystems, London, UK). As per the manufacturer's instructions, 2µl of 5x cDNA synthesis mix and 0.5µl of 20x RTase was used in each 10µl reaction. Equal concentration of RNA was loaded into each reaction (based on Nanodrop readings) and volume was made up to 10µl using sterile nucleotide free H_2O. Samples were incubated on a Thermocycler (Bio-Rad, UK) at 42°C for 30 minutes, followed by a denaturation at 85°C for 10 minutes and a holding temperature of 4°C. Following RT, cDNA was diluted 1:5 using sterile nucleotide free H_2O and stored at -20°C.

2.9.4 – qRT-PCR

Quantitative real time PCR (qRT-PCR) was performed) on the Roche LC480 LightCycler using the following program settings:

Pre-amplification	– 1 cycle	- 2 min at 95°C
Amplification	– 40 cycles	- 15 sec at 95°C, 10 sec at 60°C, 10 sec at 72°C
Melt Curve analysis	– 1 cycle	- 60–95°C, heating rate of 0.1°C per second

Each reaction contained 4µl SyGreen mix (PCR Biosystems, UK), 4µl diluted cDNA template, 1µl reverse and forward primer mix (at 10 µM, for specific primer sequences see Table 2.9.1) and 1µl of PCR grade water. Samples were run on a 384 well lightcycler plate (Roche, UK) in triplicate to account for pipetting error.

Melt curve analysis was performed with each run to assess if the assays produced specific products – if more than one peak was produced this could be indicative of gDNA contamination (in an RNA sample), primer-dimers that could affect the assay or potential splice variants.

Sequences of the gene-specific primers used in the qPCR step are detailed in Table 2.9.1. Output was analysed using the ΔΔCt method detailed by Livak and Schmittgen [294], with GAPDH and β-Actin used as housekeeping genes as appropriate.

2.10 – Lentiviral RNAi

RNA interference (RNAi) is a process by which double stranded RNA (dsRNA) is used to silence gene expression. Using a viral vector, short hairpin RNAs (shRNAs) can be incorporated into the target cell's nucleus, where they are transcribed and subsequently processed by Drosha and exported into the cytoplasm. In the cytoplasm, they are cleaved by Dicer and TRBP/PACT and the hairpin is removed, creating small interfering RNA (siRNA) which can then be loaded onto the RNA-induced silencing (RISC) complex. The sense strand is cleaved by the enzyme Argonaute 2 (Ago2), and the antisense strand guides the RISC to the corresponding mRNA which is cleaved in the same manner – silencing the gene.

2.10.1 – Lentivirus production

2.10.1.1 – Plasmid preparation

Escherichia coli (*E. coli*) glycerol stocks for pLKO.1-amp vectors containing shRNA sequences of interest were purchased from Sigma-Aldrich (from the MISSION® shRNA library), see Table 2.10.1 for details (Figure 2.10.1 shows pLKO.1-amp empty vector map). Luria Bertani (LB) agar plates containing 50 µg/mL ampicillin (due to presence of ampicillin resistant gene in desired bacteria) were streaked with gene specific MISSION® *E. coli* glycerol stock and incubated, face-down, overnight at 37°C to grow. Single colonies were picked the following day and were incubated in 5 mL of sterile LB broth with 50 µg/mL of ampicillin for 16 hours, on a shaking platform at 240 RPM at 37°C.

Following bacterial growth, colonies were centrifuged at high speed for 10 minutes and supernatant was discarded. Plasmid DNA was then purified using the NucleoSpin® Plasmid kit (Macherey-Nagel), as per the manufacturer's instructions.

Briefly, pelleted bacteria are re-suspended in re-suspension buffer and plasmid DNA is liberated from the *E.coli* cells via SDS / alkaline lysis. This solution is then neutralised using neutralisation buffer causing plasmid DNA to bind to the silica membrane of the NucleoSpin Plasmid EasyPure Column. A centrifugation step removes any cell debris as well as precipitated protein and genomic DNA. Bound plasmid DNA can then be eluted.

Plasmid concentration was measured using the Nanodrop Spectrophotometer (Thermo Fisher Scientific), and purity was confirmed by analysis of 260/230 and 260/280 ratios. Purified plasmid DNA was stored at -20°C until needed.

Gene of interest	TRC#	Sequence
CMYC	TRCN0000039640	CCGGCAGTTGAAACACAAACTTG AACTCGAGTTCAAGTTTGTGTTTC AACTGTTTTTG
MIF	TRCN0000056818	CCGGGACAGGGTCTACATCAACT ATCTCGAGATAGTTGATGTAGACC CTGTCTTTTTG
PIK3CD	TRCN0000033275	CCGGCCACAACGTGTCCAAAGAC AACTCGAGTTGTCTTTGGACACGT TGTGGTTTTTG
PIK3GD	TRCN0000033283	CCGGCCTGTGGAAGAAGATTGCC AACTCGAGTTGGCAATCTTCTTCC ACAGGTTTTTG

Table 2.10.1 – pLKO.1-amp vectors containing shRNA sequences of interest.
All primers were obtained from Sigma-Aldrich (Dorset, UK).

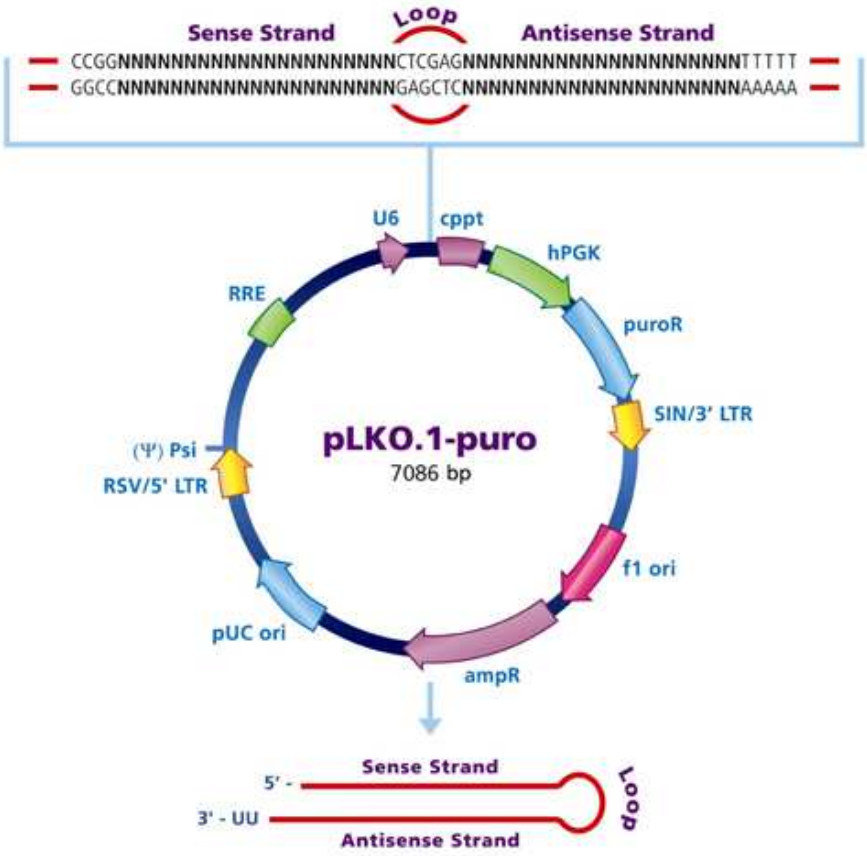

Figure 2.10.1 – Schematic showing pLKO.1-amp empty vector map.
Image taken from Sigma-Aldrich website (accessed 10.11.17), from where *E. coli* glycerol stocks were purchased.

2.10.1.1 – Plasmid precipitation

A minimum plasmid DNA concentration of 180ng was required to proceed with lentiviral production. If this was not achieved from the growth of a single colony, plasmid DNA samples could be pooled and precipitated to increase the DNA concentration.

To achieve this, sodium acetate (3M, pH 5.2) was added to pooled plasmid DNA at a ratio of 1:10. Three times the total volume of ice-cold Ethanol was then added and sample was stored at -20°C for a minimum of 4 hours. Supernatant was then discarded and pellet was re-suspended in 1mL of 75% Ethanol, after which it was centrifuged at high speed for 15 min at 4°C. Ethanol was removed and pellet is left to air dry for a minimum of 15 minutes (until all Ethanol had evaporated). Pellet was then re-suspended in 20µL of sterile H_2O and measured via Nanodrop as before.

2.10.1.2 – Transfection of packaging cells

Human embryonic kidney (HEK) 293T packaging cells were grown in DMEM media with 10% FCS, 0.01% L-Glutamine, and no pen-strep in 5% CO_2 at 37°C. Cells were split 1:4 when confluent and passaged a minimum of 5 times. 24 hours before transfection, cells were split to ensure approximately 70% confluency the following day. Vesicular stomatitis virus glycoprotein (VSV-G) and cytomegalovirus promoter (pCMV) were used as envelope proteins and packaging protein promoter, respectively.

Prior to transfection, media was changed on packaging cell plates. 1 µg of pCMV and 1 µg VSV-G were combined with 1.5µg of plasmid DNA in a total volume of 15 µl TE buffer. DNA mix was then combined with the transfection vehicle (optimum media with Fugene-6 - Promega, WI, USA) and added, dropwise, to packaging cell plate. After a 24 hour incubation, media was removed, discarded, and replaced with fresh media. At 48, 72 and 96 hours media was collected and replaced, each aliquot was frozen at -80°C until needed. 100 µL from each time point was frozen separately in an Eppendorf tube for lentivirus quantification assay.

2.10.2 – Lentivirus titre

2.10.2.1 – Viral RNA isolation

Viral RNA was isolated from aliquot of media collected in section 2.9.1.2, using the Nucleospin® Dx Virus kit (Macherey-Nagel).

50µl aliquots of media collected at 48, 72 and 96 hours were pooled and 600µl of lysis buffer RAV1 was added. Samples were vortexed thoroughly and incubated for 5 minutes at 70°C. A further 600µl of 100% Ethanol was then added and lysates were loaded onto a NucleoSpin® Dx Virus Column and centrifuged at 8000 x g for 1 minute. The empty column was then placed onto a new collection tube and 500µl wash buffer (RAW buffer) was added. Samples were centrifuged again at 8000 x g for 1 minute after which effluent was discarded.

Samples contained on column membranes were then washed twice again using buffer RAV3 and membranes were dried by centrifuging the columns for 3 minutes at 11000 x g. RNA was eluted in 50µl RNAse free H_2O (preheated to 70°C). Once RNA had been eluted, contaminating plasmid DNA was removed using DNAse and incubated at 37°C for 20 minutes.

2.10.2.2 – qRT-PCR Amplification of Lentiviral Genomic RNA

The Lenti-X qRT-PCR titration kit (Clontech) was then used to determine RNA genome copy number. Master reaction mix (detailed in Table 2.10.2) was prepared on ice with the RT enzyme mix added last. 10% excess of master mix was made in each titration to account for pipetting inaccuracies. 10 fold serial dilutions (using EASY dilution buffer) of Lenti-X RNA control template (standard 1 contained 5 x 10^7 copies / mL) were used to create a standard curve. Viral RNA samples were also subject to 10-fold serial dilution, to a total of 4 different concentrations per sample.

Reagent	Volume / well (µl)
RNase-Free Water	6.0
Quant-X Buffer (2X)	10.0
Lenti-X forward Primer (10µM)	0.4
Lenti-X reverse Primer (10µM)	0.4
ROX Reference Dye (LMP)	0.4
Quant-X Enzyme	0.4
RT Enzyme Mix	0.4
Total	18.0

Table 2.10.2 – Master Reaction Mix for Lentiviral Titration qRT-PCR.

2µl per well of control template, sample dilutions and negative control (in duplicate) were added to a 96-well Lightcycler plate (Roche) containing 18µl of master reaction mix. Plate was sealed and run on a Roche Lightcycler LC480 using the following program:

RT Reaction	- 1 cycle	- 5 min at 42°C, 10 sec at 95°
Amplification	- 40 cycles	- 5 sec at 95°C, 30 sec at 60°C
Melt Curve	- 1 cycle	- 15 sec at 95°C, 30 sec at 60°C

2.10.2.3 – Lentiviral Titration Analysis

Standard curve was made using generated C_t values and Roche Lightcycler software and was used to determine raw sample copy number. Actual copies per mL was calculated using the following equation:

$$\text{Copies / mL} = 1000 * \frac{(\text{DNAse dilution factor}) * (\text{Raw copy number}) * (\text{Elution volume})}{(\text{Purified sample volume}) * (\text{Sample volume})}$$

For example, a raw copy number of 1 x 10^7 copies would give the following copies/mL:

$$\text{Copies/mL} = \frac{1000 * (2) * (1 \times 10^7) * (50)}{(150) * (2)}$$

$$= 3.33 \times 10^9$$

Once an acceptable concentration was determined (>1x10^8 copies/mL), remaining supernatant containing lentiviral particles was concentrated (typically 30-40 fold) using Ultra-15 centrifugal Filter Devices (Amicon®).

Media containing lentiviral particles was loaded into pre-cooled Filter Tubes in a tissue culture hood, 10mL at a time. They were then spun on a balanced centrifuge (set to -4°C) at top speed until only 500µL of undiluted lentivirus remained in top chamber (this took approximately 20 minutes). Remaining lentivirus was then added to the same tube and spun again with the same conditions.

New copy number per µl was calculated based on remaining volume of lentivirus. All viruses produced were stored at -80°C and aliquoted into small volumes, to prevent freeze-thaw damage.

2.10.3 – Transduction of target cells

Prior to transduction, target cells were re-suspended in antibiotic free media at a concentration of 5 x 10^5 cells / mL and polybrene (hexadimethrine bromide) was added (10µg/mL). Cell suspensions were transduced at a Multiplicity of Infection (MOI) of 15 and 30 in 100µl volume. After 24hours, replicates were combined and fed with fresh media. Adherent cells were subject to varying levels of MOI, in 12 or 24 well plates.

Gene knockdown (KD) was confirmed at 96 hours using RT-qPCR, relative to the housekeeping genes β-Actin and GAPDH.

2.11 – Cytokine specific ELISA

2.11.1 – ELISA method

Enzyme-linked immunosorbent assays (ELISA) are designed to detect and quantify specific extracellular proteins. The MIF cytokine sandwich ELISA used (measuring antigen between capture and detection antibody) was purchased from R&D biosystems and Human / Murine IL-6 and Human IL-8 ELISA Ready-SET-Go kits were purchased from eBiosystems. MIF ELISA 96 well plates were coated with 100µl per well coating solution and incubated overnight at 4°C, prior to commencing the main ELISA protocol.

All 96 well plates were coated with 100µl of the recommended concentration of capture antibody overnight at 4°C. Wells were then washed 3 times with 300µl wash buffer (containing 0.1% Tween in filtered PBS) and blocked with 300µl of reagent diluent at room temperature for one hour. Following another wash step, selected samples and standards were added in duplicate to the plate and incubated overnight at 4 °C to ensure maximum signal intensity.

The next day after washing the wells again with wash buffer, 100µl of detection antibody solution was added and incubated at room temperature for 2 hours. The wells were then washed again. Conjugated secondary antibody solution was then added and left for 1 hour at room temperature. Streptavidin - Horse radish peroxidase (HRP) was used for detection – 100µl was added to each well and incubated for 20 minutes. All wells were washed as before.

For detection, substrates A and B were combined in equal volume and 100µl of this solution was added to each well. The plate was incubated for 15 minutes (away from any direct light) and colour-change reaction was halted using 50µl of 2N H_2SO_4 (also known as stop solution).

2.11.2 – ELISA

All plates were subject to measurement of absorbance at 450nm and 570nm (for wavelength correction) using the FLUOstar Omega plate reader. Wavelength correction adjusted results to account for any optical imperfections in the plate. All measurements occurred within 10 min of assay completion. Cytokine standards provided with each kit were used to produce standard curves and determine unknown concentrations. Standard curves were generated by plotting the log of mean absorbance for each standard against the log of its known concentration (to produce linearized data).

2.12 – Human Cytokine Arrays

Using the same principle as sandwich ELISA, the Proteome Profiler™ Human XL Cytokine Array Kit (R&D systems - Minneapolis, MN) can analyse a large range of cytokines simultaneously. These nitrocellulose membranes are pre-embedded with capture antibody spots that bind to specific target proteins present in the sample. Captured proteins can be detected with biotinylated detection antibodies and visualised using chemiluminescent detection reagents. Signal produced is proportional to the amount of protein bound. All cytokines available for analyses are detailed in Appendices A and B.

MM and BMSC were incubated for 24 hours in mono- or co-culture, supernatants (1.5mL) were then collected. Array membranes were blocked using 2 mL of Buffer 6 on a rocking platform for 1 hour. Membranes were then incubated (on a rocking platform) in sample supernatants overnight at 2-8°C. After this incubation, membranes were washed for 10 minutes with wash buffer, three times. Membranes were then incubated in detection antibody cocktail buffer (1.5mLs) for 1 hour at room temperature. Following another set of washes, membranes were incubated in 2mL of streptavidin-HRP for 30 minutes on a rocking platform. Membranes were washed again.

Excess buffer was removed from the membranes by blotting the lower corner on paper towel then 1mL of chemiluminescent reagent mix was spread evenly only to membrane and incubated for 1 minute. Membranes were then imaged using a Chemdoc-It2 Imager (UVP, CA, USA). Intensities of samples on the membrane (pixel density) were then quantified using HL++ image software (Western Vision Software, UT, USA). Raw output was given as mean pixel density. Assays were normalised to the pixel density of the reference spots (positions A1-2, A23-24 and J1-2) for consistency between membranes.

2.13 – In Vivo

Non-obese diabetic (NOD) severe combined immunodeficiency (SCID) Il2rg knockout (NOD.Cg-Prkdcscid Il2rgtm1WjI/SzJ, NSG) mice were purchased from the Jackson Laboratory (Bar Harbour, ME, USA) and were housed in a containment level 3 laboratory at the University of East Anglia (pathogen free conditions) and bred. All animal experiments were performed in accordance with UK Home Office regulations under Project Licence: 70/8722 (Dr Robinson) and Project Licence: 70/8814 (Prof. Kristian Bowles). All animal work was performed by myself under UK Home Office Personal Licence (ICC440663, R Piddock) with the assistance of C Marlein (Norwich Medical School, UEA, UK - IBB43C002) and S Rushworth (Norwich Medical School, UEA, UK - ICD3874DB), using 6-8 week old mice.

NSG mice are severely immunocompromised, and as such are ideal candidate for an MM xenograft model as they allow the bone marrow engraftment of primary human cells. These mice lack mature T cells, B cells and functional Natural Killer (NK) cells as well as being deficient in cytokine signalling. No irradiation was needed to allow MM engraftment in this model, meaning that the animals were in good health at the start of experimentation.

All procedures (detailed below) were carried out following the relevant training, and all mice were humanely sacrificed at end point in accordance with the Animals (Scientific Procedures) Act, 1986.

2.13.1 – Modified cells

MM.1S and U266 cell lines had been previously lentivirally modified with a pCDH-luciferase-T2A-mCherry construct (a kind gift from Professor Dr. Irmela Jeremias, Helmholtz Zentrum München, Germany) prior to any other lentiviral modification (see section 2.10). These cells had been positively selected using a BD FACS ARIA II cell sorter (BD Biosciences, Switzerland).

2.13.2 – Intravenous (IV) Injections

To cause vein dilation (to aid in injections), mice were incubated at 37°C for up to 10 minutes prior to injection. They were then restrained using a benchtop restrainer and injected using a 37G needle in the lateral tail vein after which they were allowed time to recover and returned to their original cage. Cell concentrations of either 1 x 10^6 or 0.5 x 10^6 (experiment dependent) MM cells suspended in 200µl sterile filtered PBS were used. Disease was monitored with daily visual checks and frequent bioluminescent imaging (BLI).

2.13.3 – Intraperitoneal (IP) Injections

Mice were manually restrained and injected with a 27G needle via the peritoneum with a maximum 200µl of either D-Luciferin, (15mg/mL suspended in sterile water with a final dosing of 150 mg/kg), JQ1 (50mg/kg suspended in PBS + 10% DMSO) or a vehicle control, depending on the particular experiment. In cases where daily IP injections were required, alternating flanks of mouse were used to minimise irritation to area.

2.13.4 – Blood Sampling

As with IV injections, mice were incubated at 37°C in a small animal warming chamber for up to 10 minutes. After this they were and restrained in a bench top restrainer and a 27G butterfly needle was inserted into the lateral tail vein. Up to 200µl of blood was collected from vein into Eppendorf tubes containing 25µl of Monosodium Citrate (an anti-coagulant). Following collection, samples were centrifuged at high speed and serum (approximately 50µl) was collected and frozen at -25°C until needed.

2.13.5 – Bioluminescent Imaging (BLI)

After IP injection with 150 mg/kg D-Luciferin, mice underwent an incubation period of 15 minutes to allow for a maximum luciferase signal plateau. Oxyluciferin production is detailed in Figure 2.13.1. During the incubation time mice were anaesthetised in a chamber using isoflurane at a flow rate of 3%. At 15 minutes, mice were imaged (30s luminescence exposure, followed by an x-ray and light image) using an In-Vivo Xtreme II imager (Bruker, Coventry, UK) in which anaesthesia coµd be maintained by means of a nose cone. Following imaging, mice were recovered in their original cages, unless tumour burden had exceeded limits. In cases where tumour burden was deemed too severe, mice were sacrificed whilst unconscious. After completion of an experiment, luminescence images were scaled appropriately using Bruker In-Vivo Xtreme II software. Using ImageJ software, luminescence images were then merged with x-ray images and false colour was applied. Representative images are shown in Figure 2.13.2.

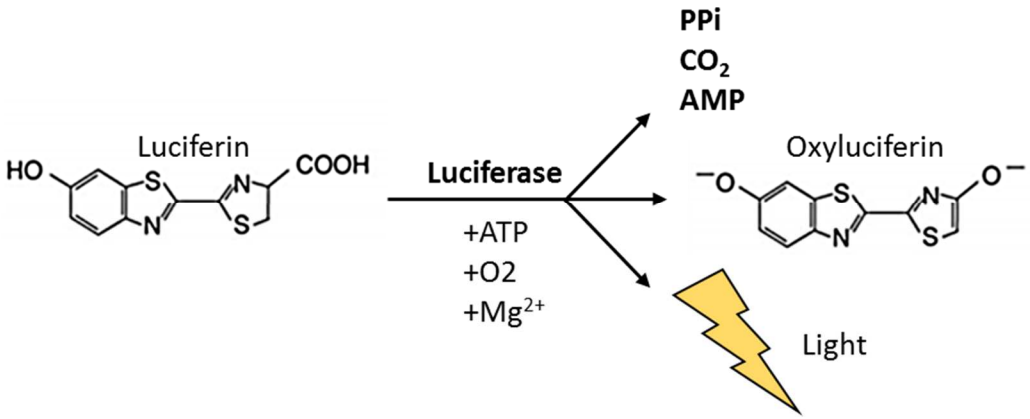

Figure 2.13.1 – Schematic showing the mechanism of Luciferase.
Luciferase labelled tumour cells are injected into mice are detectable via BLI following the injection of Luciferin. Light is detectable emitted at 560 nm.

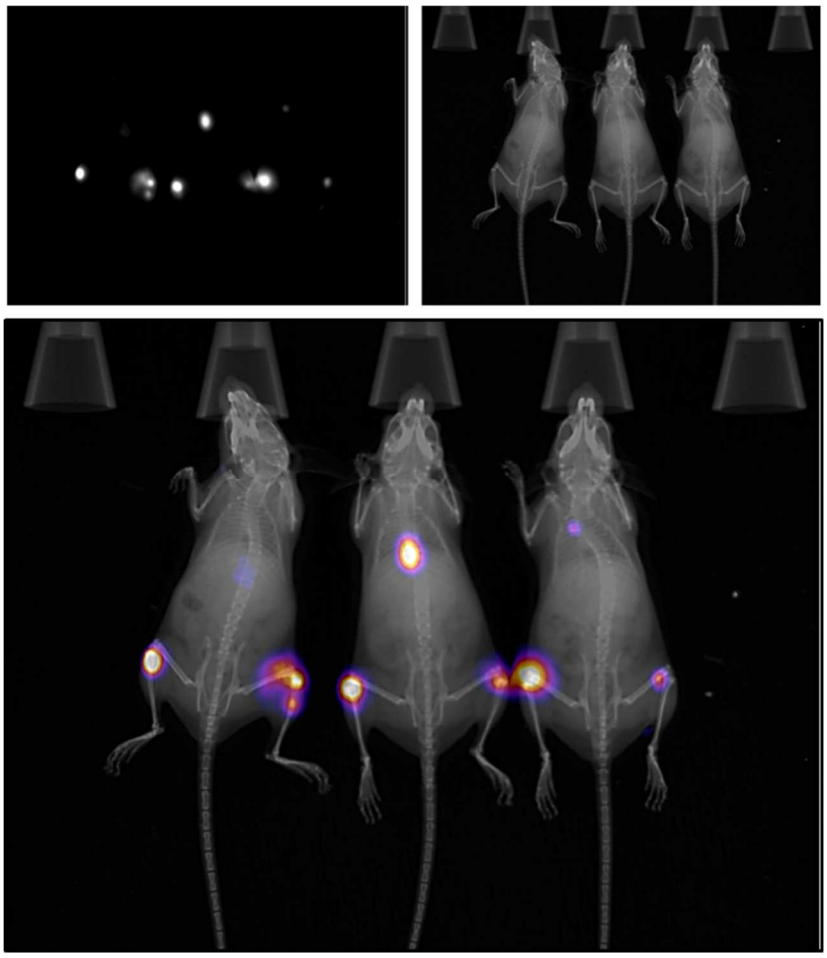

Figure 2.13.2 – *In vivo* image processing.
Luminescence (top left) and X-ray (top right) images are merged to produce composite image (bottom). Images processed using Bruker MI software, false colour was applied using ImageJ software.

2.13.6 – Murine sample collection

At end point, mice were humanely sacrificed in accordance with institute guidelines (by rising CO_2 gradient and neck dislocation to confirm). To dissect, spleens were first removed and femurs and tibiae were then stripped of soft tissues. Bone caps were then removed and individual bones were placed in 0.5ml Eppendorf tubes that had been perforated to allow expulsion of bone marrow. These perforated tubes were placed within 1.5ml Eppendorf tubes and centrifuged at high speed for 15 seconds.

Bone marrow cells present in the lower tube following centrifugation were pooled for each animal and washed / re-suspended twice with PBS. These cells were then analysed for CD38 (FITC) and CD45 (PerCP) using flow cytometry to confirm human MM cell engraftment (see Figure 2.13.3). Cells were gated to exclude non-viable cells and debris.

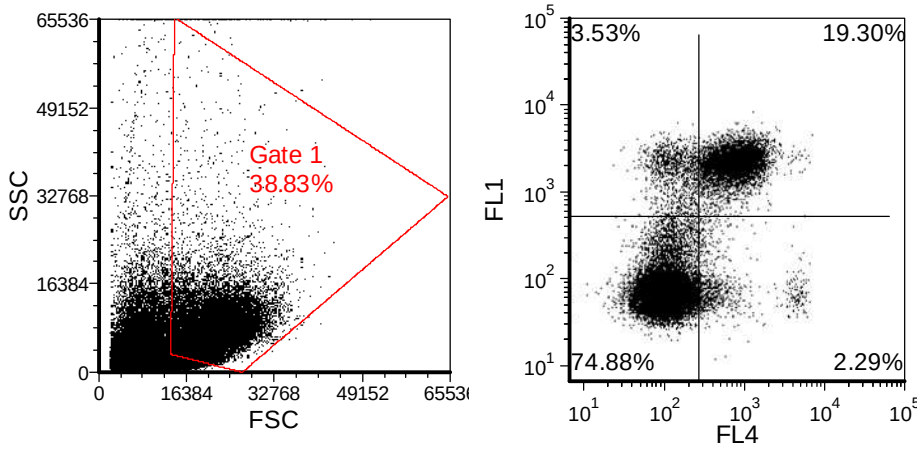

Figure 2.13.3 – Representative gating strategy for engraftment analysis.
Live cells are gated and then CD38 (APC, FL4) and CD45 (FITC, FL1) expression is analysed using FCS express 5 software.

2.14 – Statistical analysis

For Western Blot experiments, all images shown are representative of at least three independent experiments. Kaplan-Meier survival curves were all analysed using the Mantel-Cox regression test (also known as the Log-rank test). The Mann-Whitney U test was used for all other analyses (unless stated otherwise), with error bars showing the standard deviation (s.d) of the mean. All statistical analyses were conducted using GraphPad Prism 7 software. '*', '**', '***' correspond to p values less than 0.05, 0.01 and 0.001 respectively.

3 – PI3K signalling in MM

3.1 – Introduction

Aberrant activation of the PI3K pathway has long been associated with tumorigenesis in both solid and haematological malignancies. Mutations in PI3K (or indeed PTEN) are not frequently associated with MM, however PI3K signalling has shown to be highly activated in these tumorous cells. Although pan-PI3K inhibition has been shown to be effective at slowing MM metastasis [295], the off target effects would make this a non-viable option for the majority of MM patients.

The PI3K isoforms p110δ and p110γ are known to be specifically enriched by the haematopoietic system and have been shown to play a critical role in the development of several blood cancers [296-298]. The non-ubiquitous nature of these isoforms means that targeted therapies should be highly tolerable in MM sufferers.

In this section, I investigate the role of the p110δ/p110γ PI3K isoforms in MM disease metastasis. I focused on MM cell survival, adhesion and migration using both pharmacological inhibition and isoform specific lentiviral knockdown.

3.2 – Results

3.2.1 – p110δ and p110γ subunits are expressed in MM cell lines and primary MM samples.

Before investigating the effect of inhibiting p110δ or p110γ subunits in MM, the expression of both of these isoforms in MM cells needed to be verified. To do this I used Western Blotting (see Section 2.6) to measure total protein in both MM cell lines (Figure 3.2.1) and MM primary samples (Figure 3.2.2), with housekeeping protein β-Actin measured as a loading control. Further details on MM cell lines and MM primary samples are available in sections 2.2.1 and 2.2.2 respectively.

In all MM cell lines used, both isoforms were expressed strongly, with only RPMI-8226 showing slightly lower levels of p110γ. p110δ levels also had some variation, with MM.1r and RPMI-8226 showing elevated expression in comparison to the other cell lines tested.

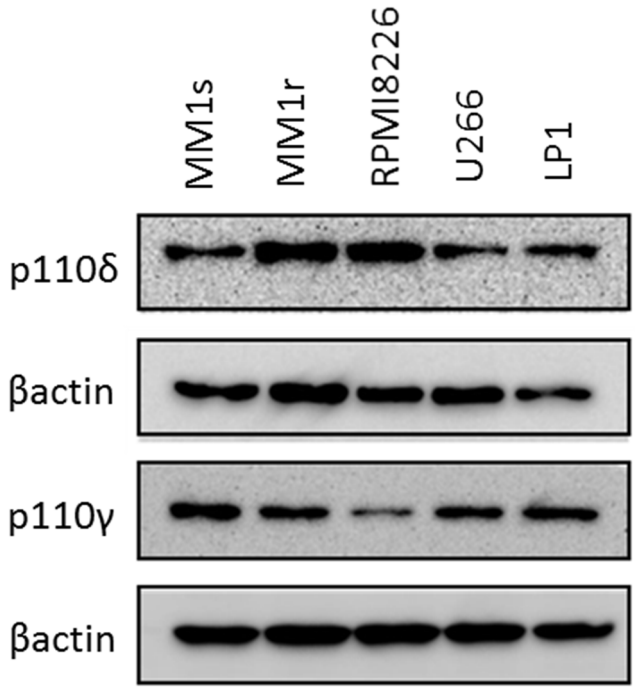

Figure 3.2.1 – p110δ and p110γ are highly expressed in common MM cell lines.
p110δ/γ total protein was measured by Western Blot in all available MM cell lines, blots were also probed with β-Actin to show sample loading. Image shown is representative of 3 independent experiments.

MM primary samples (n = 6) too all showed expression of p110δ and p110γ. However, the levels of expression were lower than that seen in the MM cell lines, which is typical of cells that are more dependent on their microenvironment. There was also arguably more variability in expression between samples with one of the samples showing a much higher level of expression, highlighting the highly diverse nature of the disease. An extra protein band at a higher molecular mass was observed in sample #4, which is most likely due to the sample not being fully denatured before loading. This would cause the sample to form dimers or multimers, causing a band at a higher molecular weight that still can bind to the antibody. A band at a lower molecular weight would have been indicative of protein degradation (perhaps due to protease inhibitors not being used during lysis).

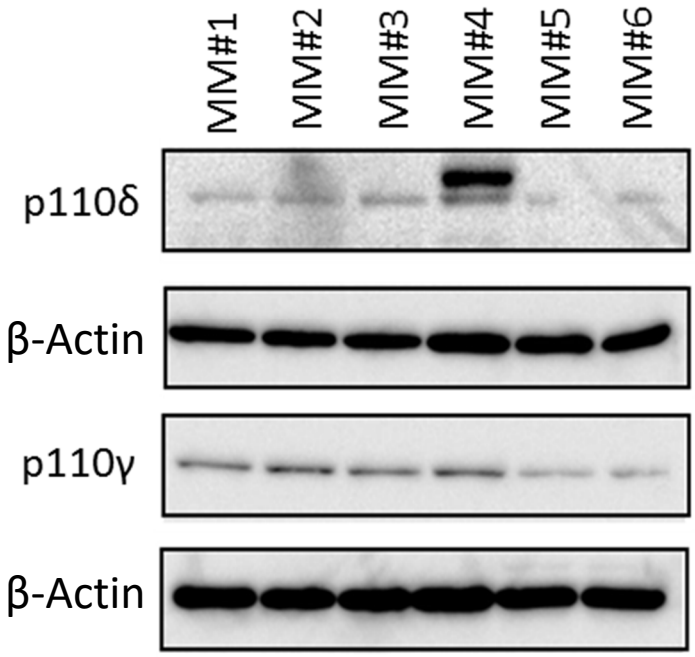

Figure 3.2.2 – MM primary cells show expression of both p110δ and p110γ subunits. p110δ/γ total protein was measured by Western Blot in 6 primary MM samples, blots were also probed with β-Actin to show sample loading.

3.2.2 – Pharmacological inhibition of p110δ and p110γ decreases cell viability and survival in MM cell lines

To investigate the significance of p110δ and p110γ expression in MM, I used a selection of PI3K isoform inhibitors and measured MM cell death. CAL-101 (a p110δ inhibitor), CZC24832 (a p110γ inhibitor) and IPI-145 (a p110δ and p110γ inhibitor) were used at a concentration of 1μM for 72h on MM cell lines MM.1s, RPMI-8226, LP-1 and U266 (n = 5 per cell line). This concentration was chosen based on preliminary experiments, previous literature [299] and concentrations that are achievable *in vivo*.

After this incubation, cells were assessed for viability using a CellTiter Glo assay (to measure levels of cellular ATP, see Section 2.4) and were normalised to a vehicle only control of 1% DMSO (results shown in Figure 3.2.3). IPI-145 (dual isotype inhibitor) significantly induced cell death in all of the cell lines tested ($p < 0.05$; Mann-Whitney test). Single isoform inhibition only significantly affected 2 out of 4 cell lines in each case, averaging 7% and 4.5% cell death respectively (compared to an average cell death of approximately 20% in dual inhibition assay).

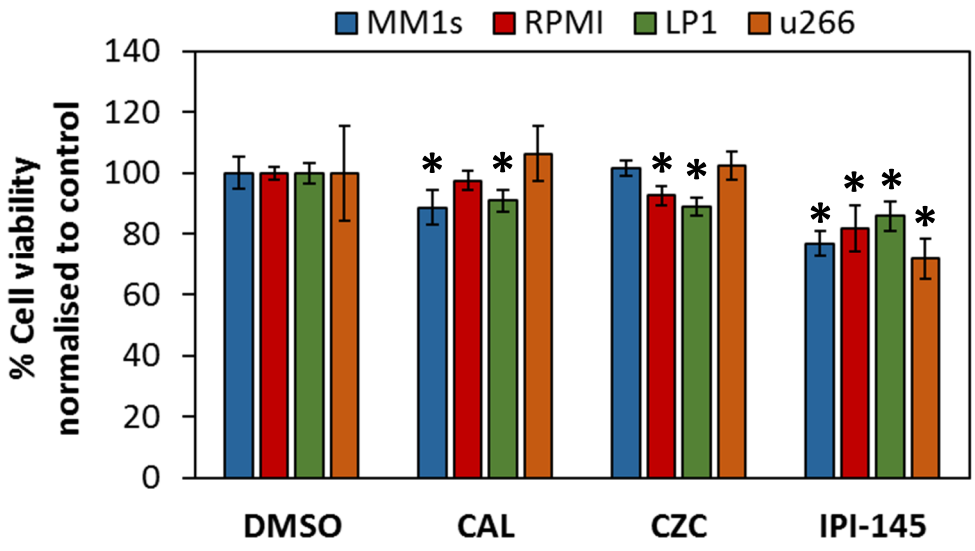

Figure 3.2.3 – MM cell viability decreases in response to p110δ/γ inhibitors.
MM cell lines were treated with 1μM of CAL-101 (p110δ inhibitor), CZC24832 (p110γ inhibitor) or IPI-145 (p110δ/γ inhibitor) for 72 hours and then assessed for cell viability using CellTiter Glo. *$p < 0.05$ when compared to DMSO only control (Mann-Whitney U), error bars show S.D of the mean (n = 5).

The CellTiter Glo assay was then repeated using 6 different patient derived samples (n = 5 per sample, and average reading was taken) at the same concentration of p110 isoform inhibitors described above (primary sample results shown in Figure 3.2.4). Statistically significant ($p < 0.01$, calculated using the Mann-Whitney test) cell death was achieved with dual p110δ / p110γ inhibition, at even greater levels than those seen in MM cell lines. No significant reduction in cell death was observed in either single inhibition groups (compared to the control) at the time points and concentrations used, although p110γ inhibition appeared to have a slightly more pronounced effect than p110δ inhibition.

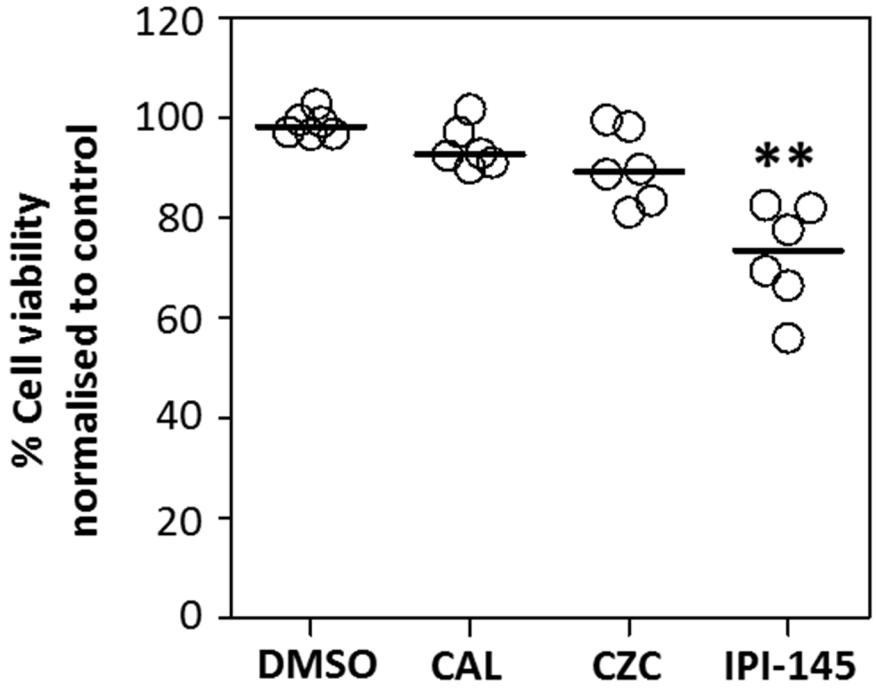

Figure 3.2.4 – MM cell viability decreases in response to combined p110δ/γ inhibition. MM primary cells were treated with 1μM of either CAL-101 (p110δ inhibitor), CZC24832 (p110γ inhibitor) or IPI-145 (p110δ/γ inhibitor) for 72 hours and then assessed for cell viability using CellTiter Glo. Significant reduction in cell viability seen in IPI-145 group in comparison to DMSO control group, **$p < 0.01$ (Mann-Whitney U test), bars show mean.

As a reduced cellular ATP concentration (and subsequent lower CellTiter Glo signal) could potentially be attributed to an inhibition of proliferation and lower cell number, a further four primary samples (n = 4) were assessed for apoptosis via flow cytometry using PI/Annexin V staining (see Section 2.5). In all samples tested, results showed an increase in PI/Annexin V positive cells (and therefore increased levels of cell death) which was in agreement with the results seen in the CellTitre Glo assay (representative result of MM primary sample shown in Figure 3.2.5, percentage of Annexin V positive cells shown in Figure 3.2.6).

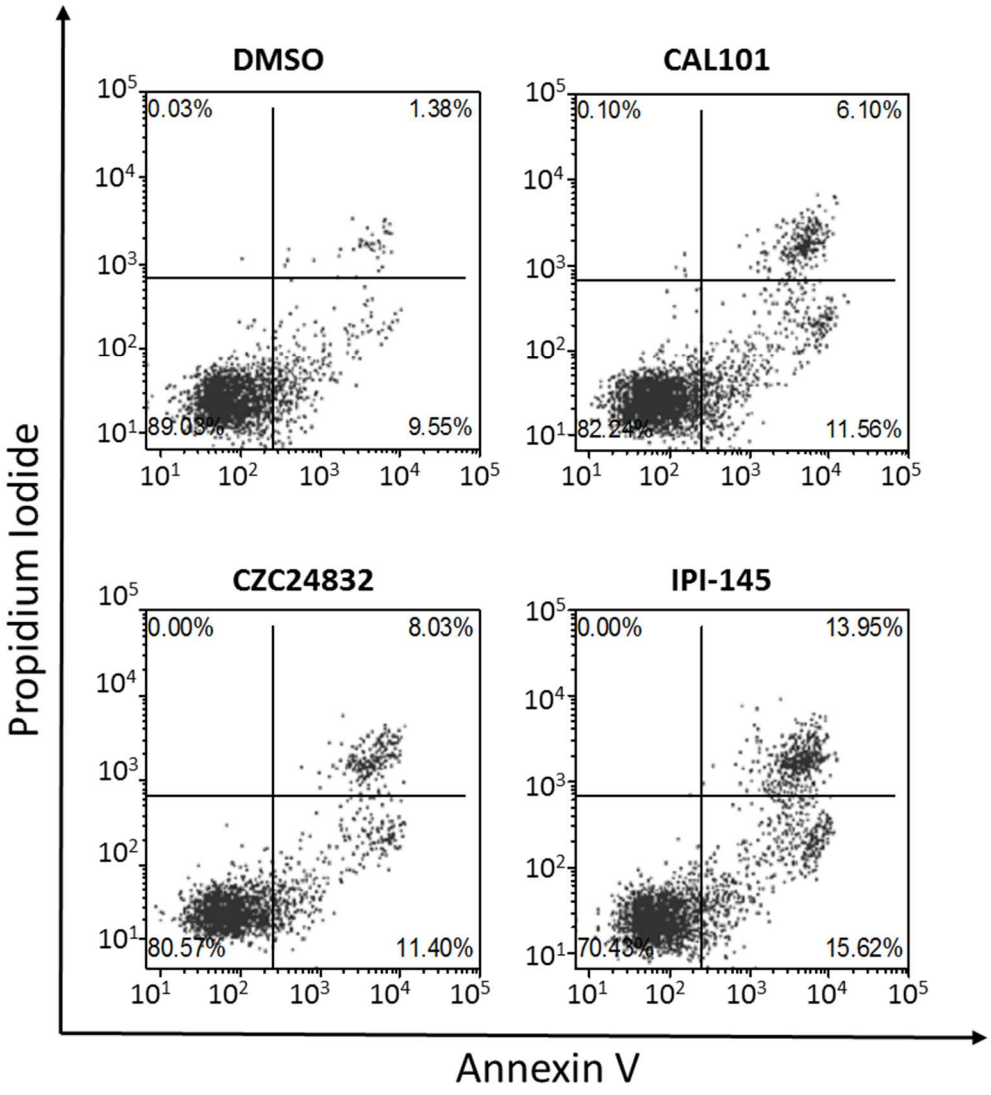

Figure 3.2.5 – Dual p110δ/γ inhibition increases levels of apoptosis in MM cells.
MM primary cells were treated with 1μM of either CAL-101 (p110δ inhibitor), CZC24832 (p110γ inhibitor) or IPI-145 (p110δ/γ inhibitor) for 72 hours and then assessed for apoptosis using PI/Annexin V staining (Representative analysis shown, n = 4). Results showed increased levels of cell death upon dual inhibition.

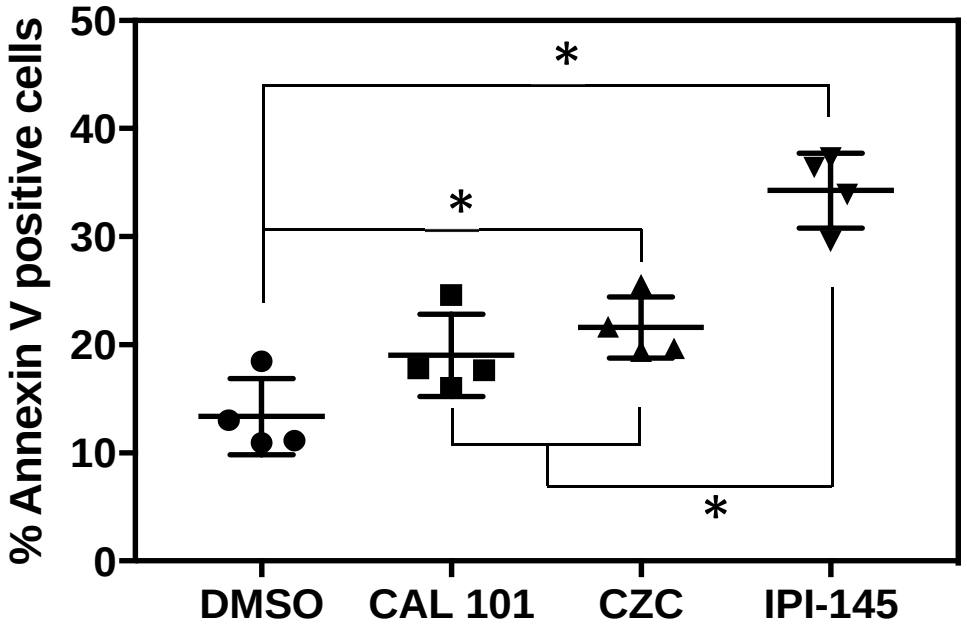

Figure 3.2.6 – Dual p110δ/γ inhibition significantly increases levels of apoptosis in comparison to single isoform inhibitors.
When compared to a DMSO only control, both CZC24832 and IPI-145 were shown to significantly increase the percentage of cells undergoing apoptosis (mean of 13.39% Annexin V positive cells in control vs 21.60% and 34.28% in CZC24832 and IPI-145 respectively). The increase seen in apoptosis with CAL101 was not significant in these samples. IPI-145 was also showed significantly higher cell apoptosis than both CAL101 and CZC24832 treatments. Error bars show mean and S.D; $p < 0.05$, Mann-Whitney U.

3.2.3 – Lentiviral knockdown of PI3Kδ and PI3Kγ genes reduces survival and initiates apoptosis in MM cell lines.

The MM cell lines MM.1s and RPMI-8226 were transduced with lentivirus (see Section 2.10 for methods) targeted to PI3Kδ (PIK3CD gene) or PI3Kγ (PIK3CG gene) for 96 hours (control used was an empty vector, ShE). These cells lines were selected due to their varying expression of p110δ and p110γ to represent the varying levels of these isoforms in primary samples (MM.1S low p110δ, high p110γ and RPMI-8226 high p110δ, low p110γ). Following lentiviral knockdown, RNA was extracted and gene expression was measured using RT-qPCR (see Section 2.9, gene expression is shown relative to housekeeping gene GAPDH) to confirm gene knockdown (Figure 3.2.7). Lentivirus showed high specificity, with PIK3CD targeting lentivirus achieving a mean knockdown of approximately 75% and 85% in MM.1S and RPMI-8226 cells respectively, but not significantly affecting PIK3CG expression. When PIK3CG was targeted similar levels of knockdown were seen in both cell lines (~75% in each case). Dual knockdown was more effective in the RPMI-8226 cell lines (> ~85% in both cases), with MM.1S achieving a ~65% reduction in PIK3CD expression and a ~70% reduction of PIK3CG.

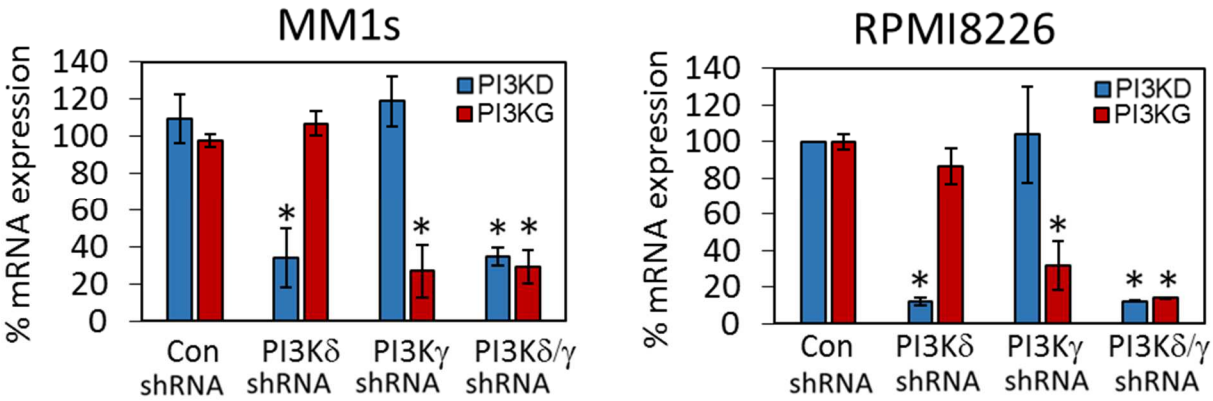

Figure 3.2.7 – Lentiviral Knockdown of p110δ/γ in MM cell lines.
MM.1s and RPMI-8226 cells were transduced with lentivirus targeted to PI3Kδ and/or PI3Kγ or control shRNA for 72h. RNA was then extracted and analysed for PI3Kδ/PI3Kγ mRNA expression by RT-qPCR. GAPDH was used as a housekeeping gene. *p < 0.05 Mann-Whitney U. Error bars show S.D of the mean (n = 3).

MM cell lines with isoform specific knockdown were then analysed for differences in cell viability. Following a 5 day monoculture incubation, cell survival was measured via CellTiter Glo and normalised to control (ShE) cells (Section 2.4). No significant difference in survival was found in the PIK3CD knockdown in either cell line ($p > 0.05$; Mann-Whitney U). PIK3CG knockdown resulted in a decrease in viability in both cell lines, but this was only shown to be significant for MM.1S cells (greater than 30% decrease in cell viability, $p < 0.05$; Mann-Whitney U). Dual knockdown caused a significant decrease in both cell lines ($p = 0.002$ and $p = 0.04$ in MM.1s and RPMI-8226 respectively), with MM.1S cell viability reduction >90% (Figure 3.2.8).

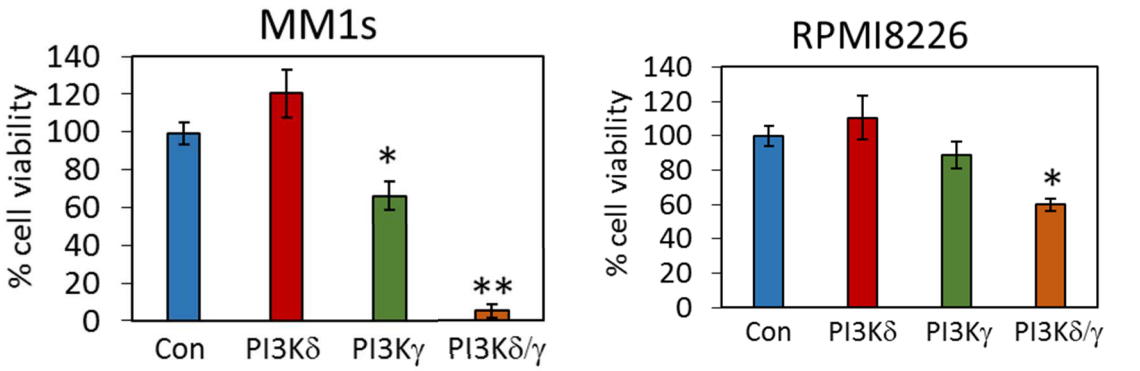

	Con	δ KD	γ KD	δ/γ KD
Mean % Survival	98.9	120.4	66.4	4.9
S.D	7.6	18.2	10.7	5.1
p-value (vs. control)	na	0.17	0.016	0.0020

	Con	δ KD	γ KD	δ/γ KD
Mean % Survival	98.9	110.5	88.7	59.8
S.D	8.22	18.4	10.6	5.1
p-value (vs. control)	na	0.43	0.23	0.0039

Figure 3.2.8 – Lentiviral Knockdown of PI3Kγ or PI3K δ/γ reduces cell viability.
MM.1s and RPMI-8226 cells were transduced with lentivirus targeted to PI3Kδ/PI3Kγ or control shRNA for 5 days, after which they were assessed for viability by Cell Titre Glo assay. *$p < 0.05$, **$p<0.01$ Mann-Whitney U. Error bars show S.D of the mean ($n = 5$).

To investigate if this decrease in cell viability was due to a reduction in cell proliferation or if it were due to an initiation of apoptosis, cells were stained with PI / Annexin V (see Section 2.5) and analysed via Flow Cytometry (Figure 3.2.9 – 3.2.10). I found that there was an increase in apoptotic markers in all knockdown cells (in comparison to the ShE control), and that this difference was in agreement with the results shown in Figure 3.2.8. PIK3CD knockdown once again caused the least difference in cell apoptosis frequency, with PIK3CG knockdown causing a more pronounced effect in the MM.1S cell line. Dual knockdown showed the greatest efficacy in both cell lines, with MM.1S cells affected the most.

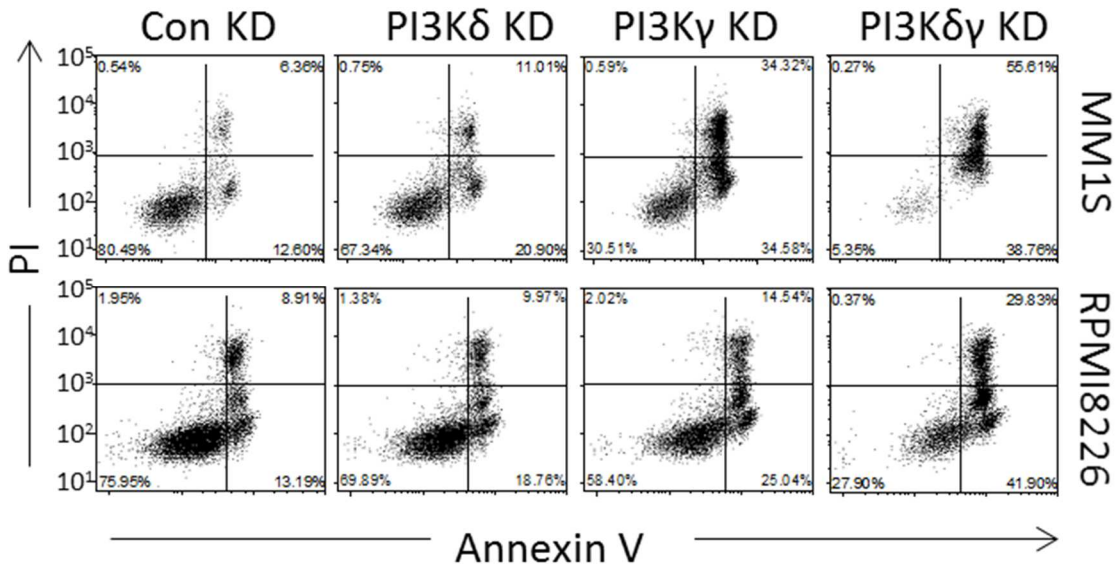

Figure 3.2.9 – Lentiviral Knockdown of PI3Kγ or PI3K δ/γ increases cell apoptosis.
MM.1s and RPMI-8226 cells were transduced with lentivirus targeted to PI3Kδ/γ or control shRNA for 5 days. Cell apoptosis was then assessed using PI/Annexin V staining (n = 3, representative image shown).

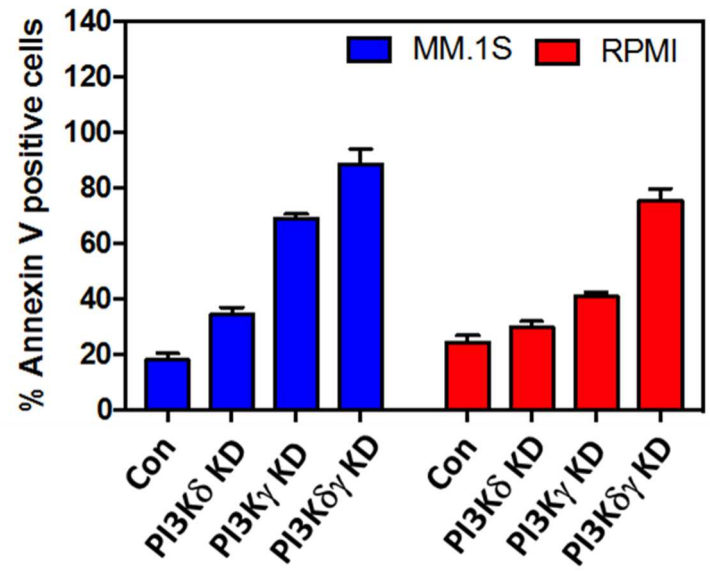

Figure 3.2.10 – Cell apoptosis increases in response to dual PI3K isoform inhibition. Full results from Figure 3.2.9. Dual PI3K isoform knockdown showed the greatest increase in cell apoptosis (represented by Annexin V positive cells), followed by PI3Kγ inhibition. No significant results were achieved from these results, likely due to low replicate number (n = 3, Mann-Whitney U test).

3.2.4 – Dual PI3Kδ/γ knockdown works synergistically to inhibit Akt

As the main target of the PI3K pathway is AKT, I analysed the phosphorylation of this protein (at the Serine 473 residue) in response to the PI3K isoform inhibitors previously used, at a concentration of 1μM (Figure 3.2.11) via Western Blot (Section 2.6). Both CAL101 and CZC24832 (p110δ and p110γ single isoform inhibitors respectively) failed to cause a noticeable change in the quantity of phosphorylated AKT available. Dual isoform inhibition using IPI-145 however, caused a visible decrease in both the U266 and MM1.S cell lines, almost completely blocking expression in the U266 cells (most likely due to its lower basal rate of expression). Total AKT was measured as a loading control and p44/42 MAPK (also known as ERK1/2) protein was analysed at each stage as an indicator of pathway specificity. Cell lines were chosen due to their approximately equal expression of both PI3K isoforms.

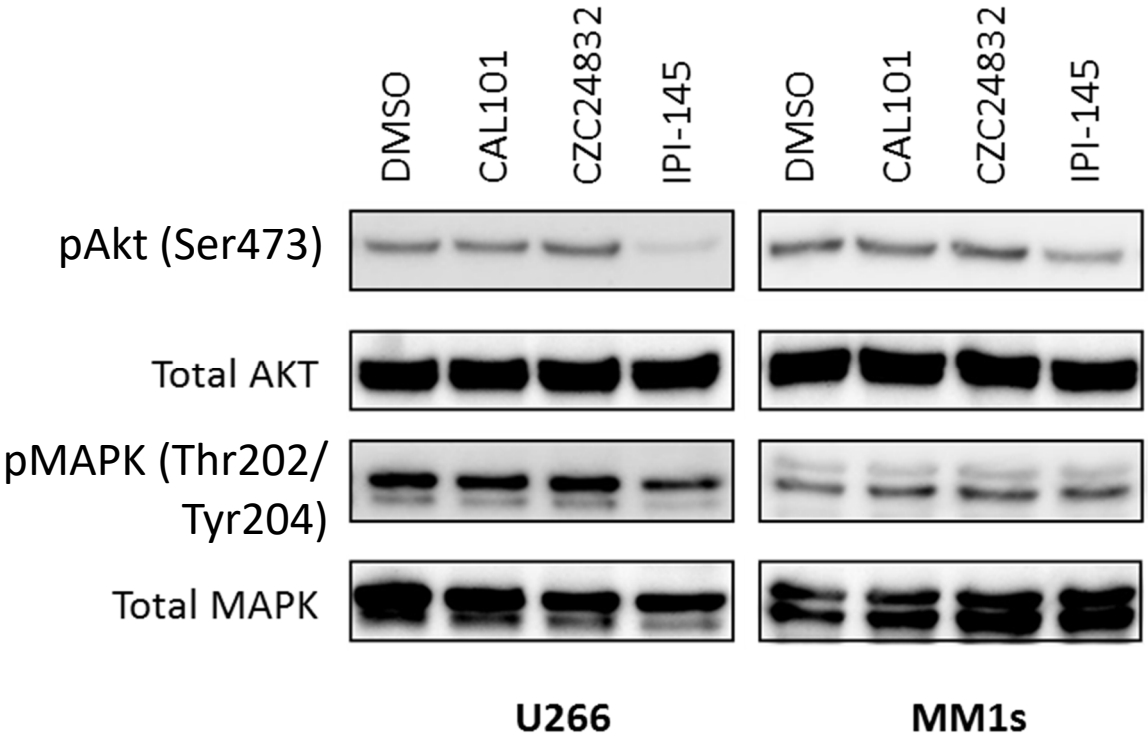

Figure 3.2.11 – Inhibition of PI3Kδ/γ inhibits AKT phosphorylation in MM cell lines. MM.1S and U266 cells were incubated with 1μM of either CAL-101 (p110δ inhibitor), CZC24832 (p110γ inhibitor) or IPI-145 (p110δ/γ inhibitor) for 4h. Total protein was then extracted and analysed for phospho-AKT (Ser473) and p44/42 phospho-p44/42 MAPK (Th202/Tyr204) levels via Western Blot. Image shown is representative of 3 independent experiments.

This experiment was repeated using primary MM cells obtained from two patient samples (Figure 3.2.12). IPI-145 was once again shown to be the most effective, with single isotype inhibition not sufficient to markedly inhibit AKT activation. In both cases the MAPK pathway was not affected. I then showed that the inhibition of activated AKT is dose dependent (Figure 3.2.13), with higher concentrations of IPI-145 correlating with the lowest pAKT activity.

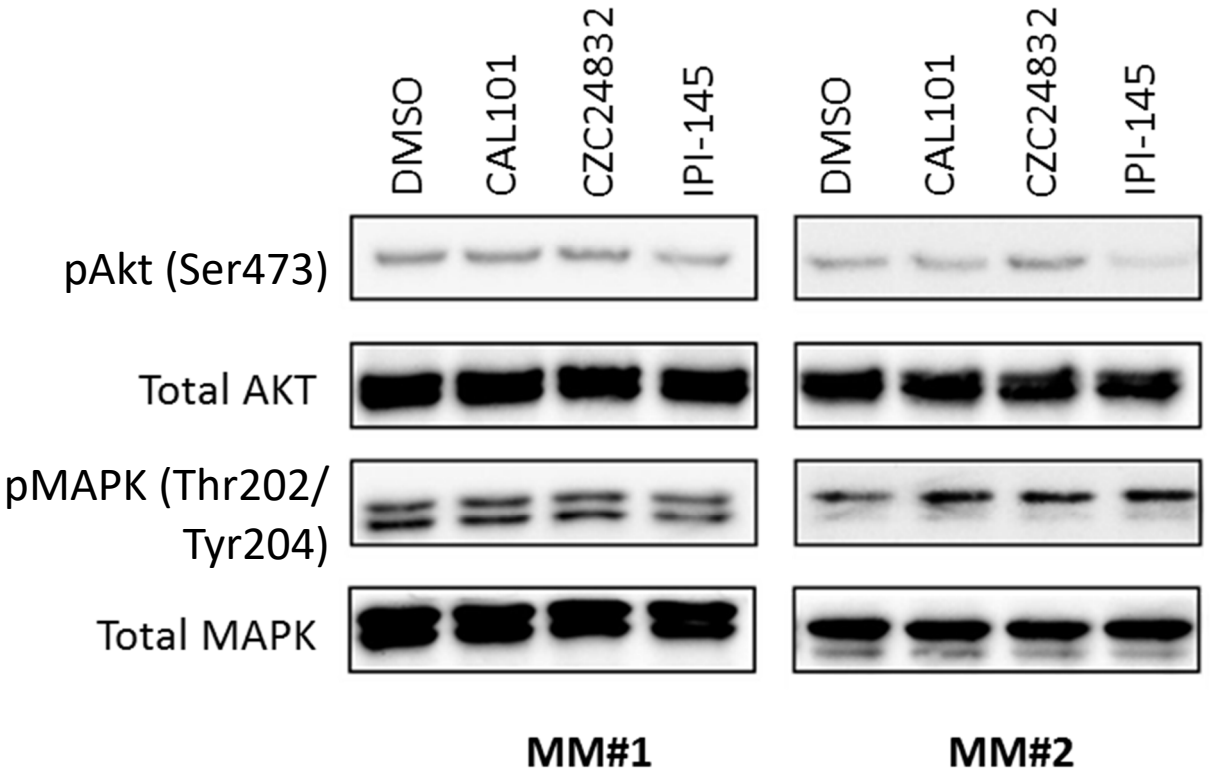

Figure 3.2.12 – Inhibition of PI3Kδ/γ inhibits AKT phosphorylation in MM primary cells. Primary cells were incubated with 1μM of either CAL-101 (p110δ inhibitor), CZC24832 (p110γ inhibitor) or IPI-145 (p110δ/γ inhibitor) for 4h. . Total protein was then extracted and analysed for phospho-AKT (Ser473) and p44/42 phospho-p44/42 MAPK (Th202/Tyr204) levels via Western Blot.

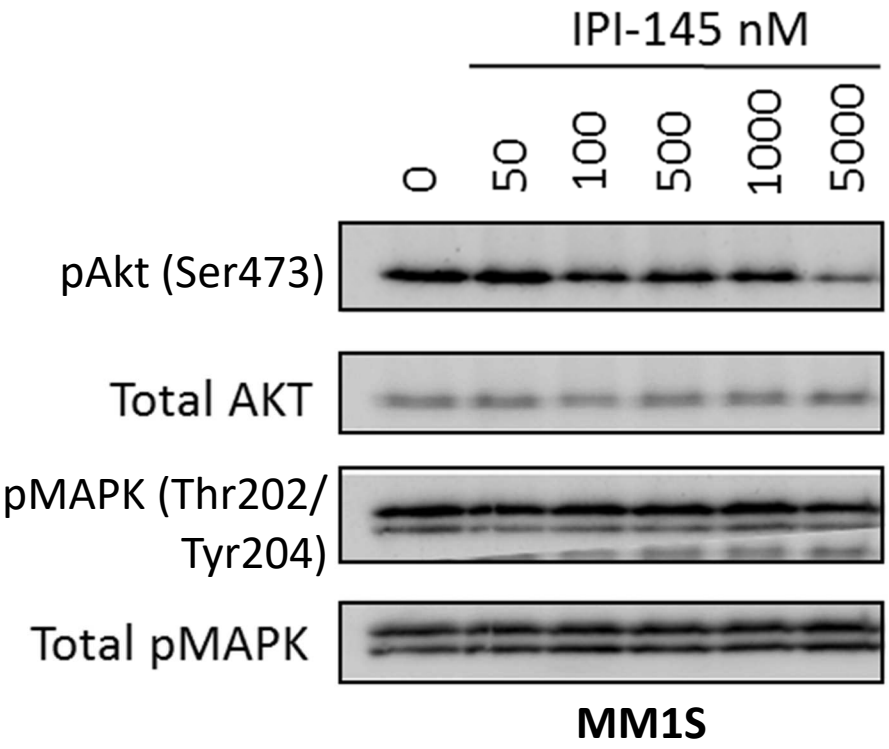

Figure 3.2.13 – IPI-145 inhibits pAKT in a dose-dependent manner.
MM.1S cells were incubated with increasing concentrations of IPI-145 for 4 hours. Total protein was then extracted and analysed for phospho-AKT (Ser473) and p44/42 phospho-p44/42 MAPK (Th202/Tyr204) levels via Western Blot. Image shown is representative of 3 independent experiments.

I then used lentivirus to knockdown the specific PI3K isoforms (both alone and in combination, see Section 2.10 for lentiviral methods). Figure 3.2.14 shows that, in agreement with previous results, dual inhibition is more effective at inhibiting AKT phosphorylation than either isoform in isolation. In this case the MAPK pathway was also affected, showing potential cross-talk between pathways.

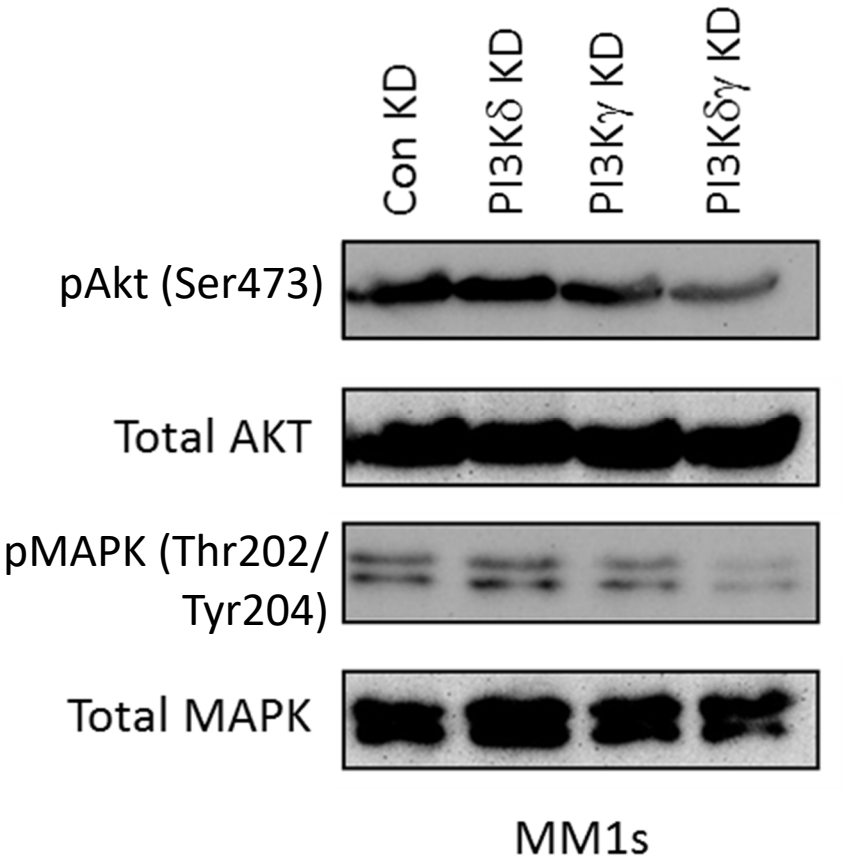

Figure 3.2.14 – PI3Kδ/γ lentiviral knockdown reduces pAKT in MM.1S cells.
MM.1S cells were transduced with lentivirus targeted to PI3Kδ/γ or control shRNA for 72h after which protein was extracted and probed for phospho-AKT and phospho-p44/42 MAPK via Western Blotting. Total AKT and p44/42 MAPK levels were used as loading controls. Image shown is representative of 3 independent experiments.

3.2.5 – Inhibition of both p110δ and p110γ isoforms decreases MM cell adhesion

The adhesion of MM to its microenvironment is critical in the regulation of MM disease progression, survival and drug resistance [219]. To this end, I wanted to investigate the roles of p110δ and p110γ on the MM cell's ability to adhere to primary BMSC, via the engagement of cell surface integrins. BMSC (seeded at 5 x 10^3 cells/ml) were co-cultured with MM cells for 4 hours. The MM cells used had been incubated with isoform specific inhibitors for 2h and stained with Calcein AM (see Section 2.7 for further details). Following supernatant removal, fluorescence was measured and normalised to a negative control (not shown).

Figure 3.2.15 shows that in both cell lines tested (Figure 3.2.15 A), only dual inhibition was sufficient to significantly reduce adhesion in comparison to a DMSO only control (approximately 30% and 25% reduction for RPMI-8226 and MM.1S cell lines respectively; $p < 0.05$, Mann-Whitney U). This result was mirrored when analysing primary patient samples (Figure 3.2.15 B), with single isoform inhibition not able to significantly reduce adhesion to BMSCs. Dual inhibition using IPI-145 resulted in up to a 40% reduction in adhesion, and was significantly reduced in the patient samples tested ($p < 0.05$; Mann-Whitney U) – suggesting a need for both isoforms in the regulation of MM cell adhesion.

MM has previously been shown to adhere to Fibronectin (Fn) by both VLA-4 and VLA-5 receptors and inhibition of this mechanism has been shown to cause increased tumour cell sensitivity to chemotherapy [219]. Because of this I next examined the effects of PI3K isoform inhibition on MM cell adhesion to Fn. Figure 3.2.16 (A) shows that the lentiviral knockdown of PIK3CG (but not PIK3CD) is sufficient to significantly inhibit the MM cell's ability to adhere to Fn. Dual inhibition caused an almost identical reduction in adherence, suggesting that p110δ does not play a role in this process.

As MM primary cells are not able to survive lentiviral knockdown (indeed MM primary cells start to die within days of culture with no interference at all [300]), PI3K isoforms were instead inhibited via pharmacological methods (Figure 3.2.16 B) at concentrations previously described. In this case single isoform inhibition was not sufficient to reduce MM cell adhesion to Fn, with only dual inhibition causing a significant reduction (approximately 20% and 30% in the samples tested; $p < 0.05$, Mann-Whitney U).

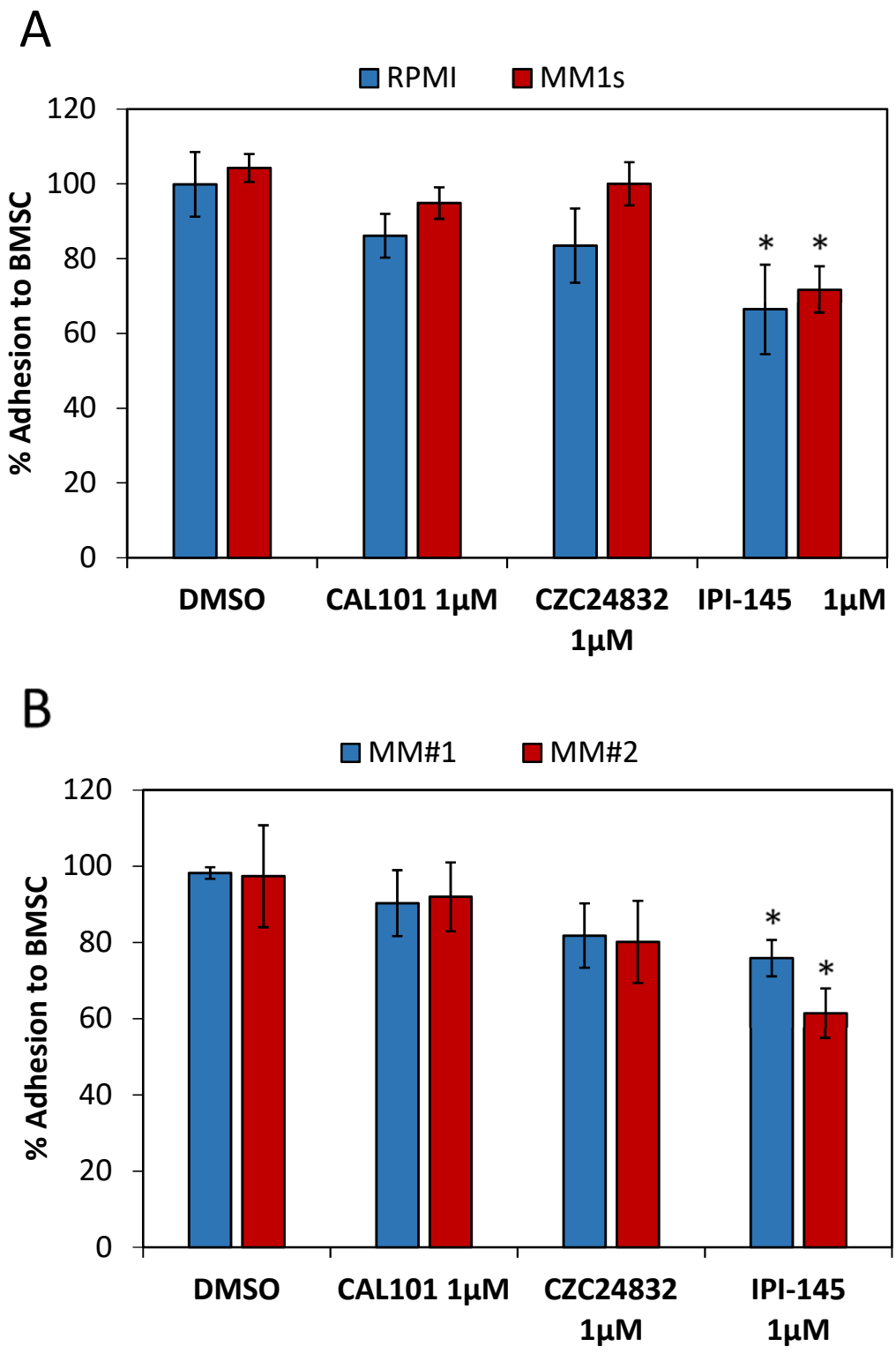

Figure 3.2.15 – MM cell adhesion to BMSC is reduced in response to IPI-145.
MM cell lines (A) or primary cells (B) were treated with 1µM of either CAL-101 (p110δ inhibitor), CZC24832 (p110γ inhibitor) or IPI-145 (p110δ/γ inhibitor) for 4 hours and stained with Calcein AM. Stained cells were co-cultured with BMSC on 96 well plates for a further 4 hours. Non-adherent cells were removed and fluorescence was measured. *p<0.05, **p<0.01, Mann-Whitney U. Error bars show S.D of the mean, n = 4.

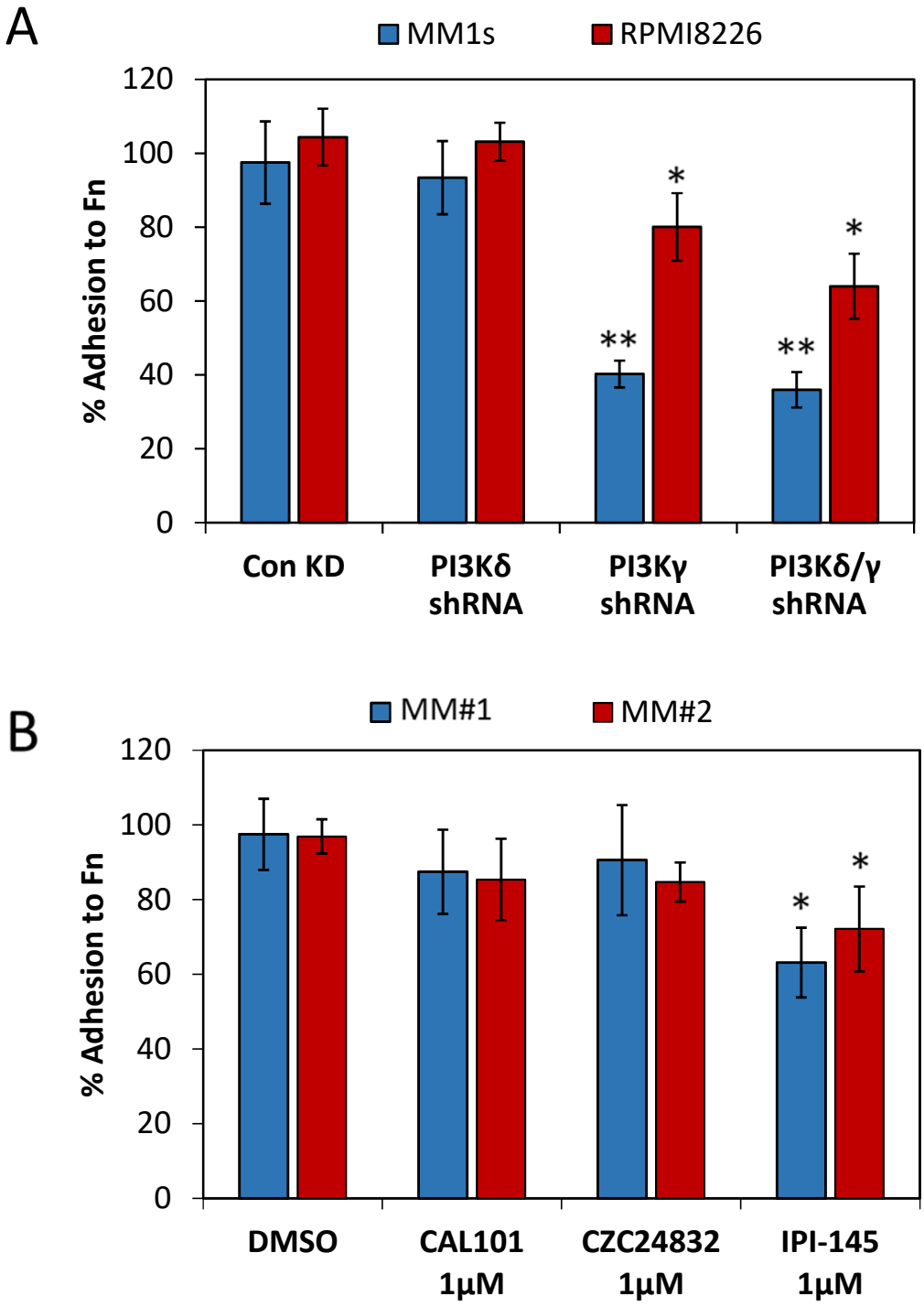

Figure 3.2.16 – Dual inhibition of p110δ/γ reduces MM cell adhesion to Fn.
(A) MM cell lines underwent lentiviral knockdown of PI3K isoforms, and ability for cells to adhere to Fn was measured. (B) Pharmacological inhibition of PI3K isoforms in MM primary cells. *p<0.05, **p<0.01, Mann-Whitney U. Error bars show S.D of the mean, n = 4.

3.2.6 – MM cell migration to SDF-1 is negated by p110δ and p110γ inhibition

The migration of immune cells to the BM has previously been shown to be regulated by PI3K [301, 302]. It would therefore be logical to conclude that inhibition of the p110δ and p110γ subunits (that are most prevalently expressed within the haematopoietic system) would result in the inhibition of MM cell migration. Figure 3.2.17 shows that MM cell migration increases by approximately 20% in response to SDF-1 supplemented media in all cases (when compared to non-supplemented media control), apart from the IPI-145 treated group. Dual inhibition of p110δ and p110γ isoforms was shown to negate this effect, returning to the base level of 20%. Individual isoform inhibition, once again, had no effect when compared to the vehicle control. Migration assay methods are shown in Section 2.8.

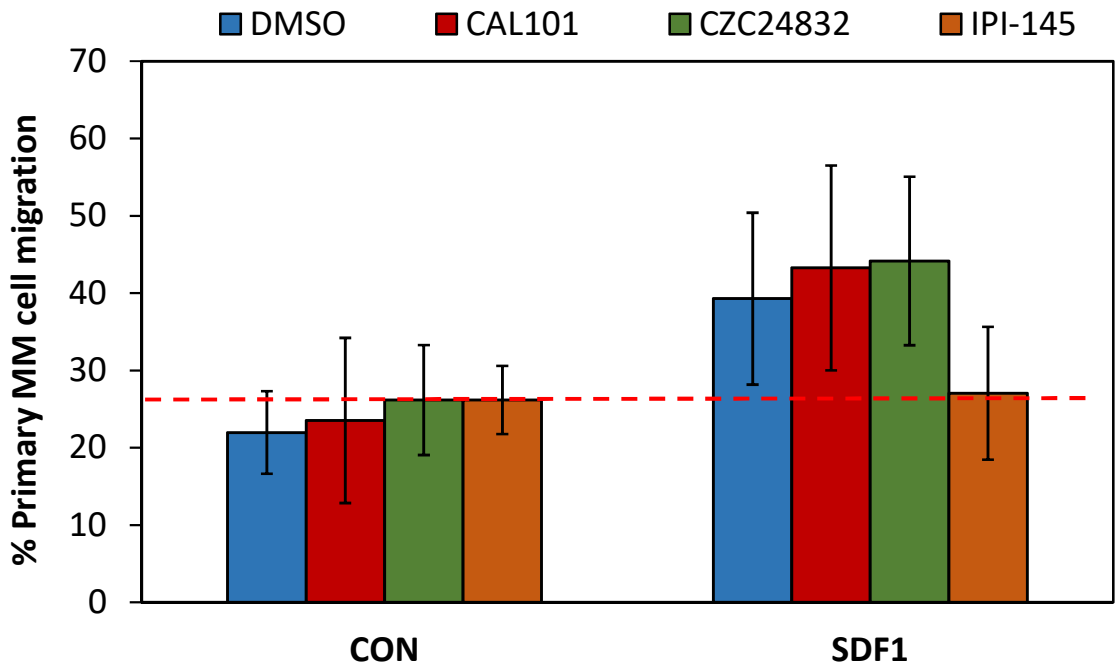

Figure 3.2.17 – Dual isoform inhibition counteracts SDF-1 induced MM migration. When migrating to control media (non-supplemented) approximately 22% of MM cells migrate into the bottom chamber of the transwell (control) and is not significantly increased upon treatment with PI3K inhibitors. SDF-1 supplemented media caused an increase in MM cell migration in all groups (approximately 20% increase), excluding cells treated with IPI-145 (which remained at approximately 25% migration. Error bars show S.D of the mean, n = 3.

3.3 – Summary

The activation of the PI3K pathway is known to aid in the progression of several tumour types, both solid and haematological. Although the PI3K isoforms p110α/β/γ/δ have all shown to be expressed in various MM cell lines [303], p110δ and p110γ are known to be preferentially expressed within leukocytes [304]. This provides the potential for a viable and specific therapeutic target, limiting side-effects and increasing tolerability in a typically elderly patient demographic.

In this section I have shown that both the p110δ and p110γ isoforms are expressed in all the MM cell lines used, as well as the six primary samples tested (albeit at lower levels than that seen in the MM cell lines). Data showed that both isoforms needed to be inhibited for significant reduction in PI3K pathway activation (shown via inhibition of Akt phosphorylation) and subsequent MM cell viability. Indeed, combined pharmacological inhibition of p110δ/γ acts synergistically – appearing to be more cytotoxic than the sum of single isoform inhibition.

Lentiviral inhibition of PIK3CG (the p110γ gene) caused a significant reduction in MM cell adhesion to fibronectin, suggesting an independent role for this isoform in this case. Adhesion was less affected in the RPMI-8226 cell line, potentially reflecting the lower expression of p110γ protein initially seen in these cells (see Figure 3.2.1). In primary cells, a significant reduction in adhesion was only achieved upon dual p110δ/γ inhibition. This could be due to either the lower expression of the PI3K isoforms themselves, or inferior efficacy of CZC24832 when compared to the ~80% PIK3CG knockdown that was achieved in the MM cell lines. Migration of MM cells towards SDF-1α was also shown to be affected in response to dual p110δ/γ inhibition, suggesting a role for these isoforms in MM cell homing to the BMM.

In summary, I have shown that both the p110δ/γ PI3K subunits are involved in the survival of MM cells and the suppression of these isoforms negatively impacts factors that are strongly associated with MM disease progression. The efficacy of this inhibition within the protective niche of the BMM, however, still needs to be investigated.

4 – PI3K activation in the BMM

4.1 – Introduction

The MM cell's critical dependence on its microenvironment has long been known [7, 219, 225, 305]. Once removed from the BM, the primary MM cell's capability for self-renewal and proliferation (that is not present in typical differentiated plasma cells) can only be extended via co-culture with other cells from the niche [306, 307] or supplementing the media with the necessary proteins. For example, in a study by Ludwig *et al.,* the proportion of primary MM cells in S-phase was able to be increased (by approximately 20%) via cytokine and interferon stimulation *in vitro* [308]. *In vivo*, the soluble factors continually secreted from BMSCs stimulate signalling cascades within the malignant cell – ensuring its longevity [309].

The PI3K pathway can be activated by RTKs (a class of enzyme-linked receptors), GPCRs, or by crosstalk with other signalling cascades [310] - with both the JAK/STAT and MAPK pathways having been shown to activate PI3K [311]. One such route of PI3K activation is via IL-6 cytokine stimulation [312], a cytokine that is highly prevalent in the MM BMM and critical for MM pathogenesis. IL-6 has been shown to directly trigger both the JAK/STAT [176, 313] and MAPK [314] pathways via its receptor IL-6R. Even in cell types where IL-6R is absent from the cellular membrane, IL-6 is capable of binding with soluble IL-6R and activating gp130 homodimers.

In this section I investigated the activity and targetability of the PI3K pathway in the context of the BMM. I then used an NSG mouse model with an MM-p110δ/γ knockdown xenoengraftment to determine the potential individualised roles for these isoforms *in vivo*.

4.2 – Results

4.2.1 – PI3K pathway inhibition is achievable in the MM microenvironment

4.2.1.1 – BMSC conditioned media

Many key BM-microenvironmental factors have been shown to cause the activation of the PI3K pathway in previous literature [312, 315, 316], and as such its potential for overcoming PI3K inhibition needed to be investigated. MM.1S and RPMI-8226 cells were incubated with IPI-145 for 6 hours, and subsequently activated with BMSC-conditioned media for 1 hour. Whole protein was then extracted and analysed via Western Blot (Figure 4.2.1, see Section 2.6 for methodology). As before, these cells lines were selected due to their varying expression of p110δ and p110γ to represent the varying levels of these isoforms in primary samples (MM.1S low p110δ, high p110γ and RPMI-8226 high p110δ, low p110γ).

As expected, BMSC-conditioned media activated the phosphorylation of AKT in both cell lines, however MM.1S showed much higher levels of baseline activity when compared to the RPMI-8226 cells. IPI-145 inhibited both cell lines AKT activation in a dose-dependent manner. Phosphorylated MAPK levels were also shown to increase in response to BMSC conditioned media, and was unresponsive to IPI-145 – indicating that this inhibitor does not have off target effects on this pathway.

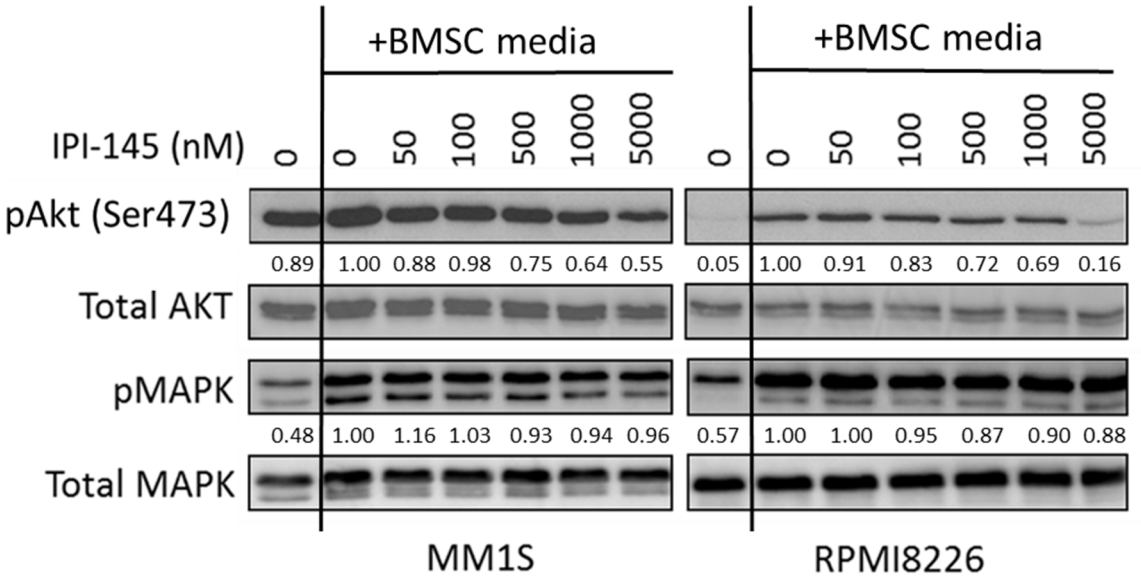

Figure 4.2.1 – The MM microenvironment PI3K pathway activation is inhibited by IPI-145 in a dose dependent manner.
MM cell lines were incubated with p110δ/γ inhibitor IPI-145 for 6h, and stimulated with BMSC-conditioned media (fresh media was incubated with confluent primary BMSC for 24 hours, normal media sample shown far left). Total protein was then extracted and analysed for phospho-AKT (Ser473) and p44/42 phospho-p44/42 MAPK (Th202/Tyr204) levels via Western Blot. Densitometry was performed using ImageJ software and is normalised to 0nM IPI-145 BMSC-conditioned media sample. Image shown is representative of 3 independent experiments.

Next, I wanted to determine if this inhibition in PI3K expression could increase MM cell death within the context of the BMM. MM primary cells (n=4) were co-cultured with BMSCs for 24 hours with and without PI3K isoform inhibitors. Whilst CAL101 (p110δ inhibitor) and CZC24832 (p110γ inhibitor) had little effect on cell apoptosis in comparison to a control, IPI-145 (dual isoform inhibitor) had significantly increased apoptotic and dead cells (Figure 4.2.2). Graphical representation of these results is shown in Figure 4.2.3, method in Section 2.5.

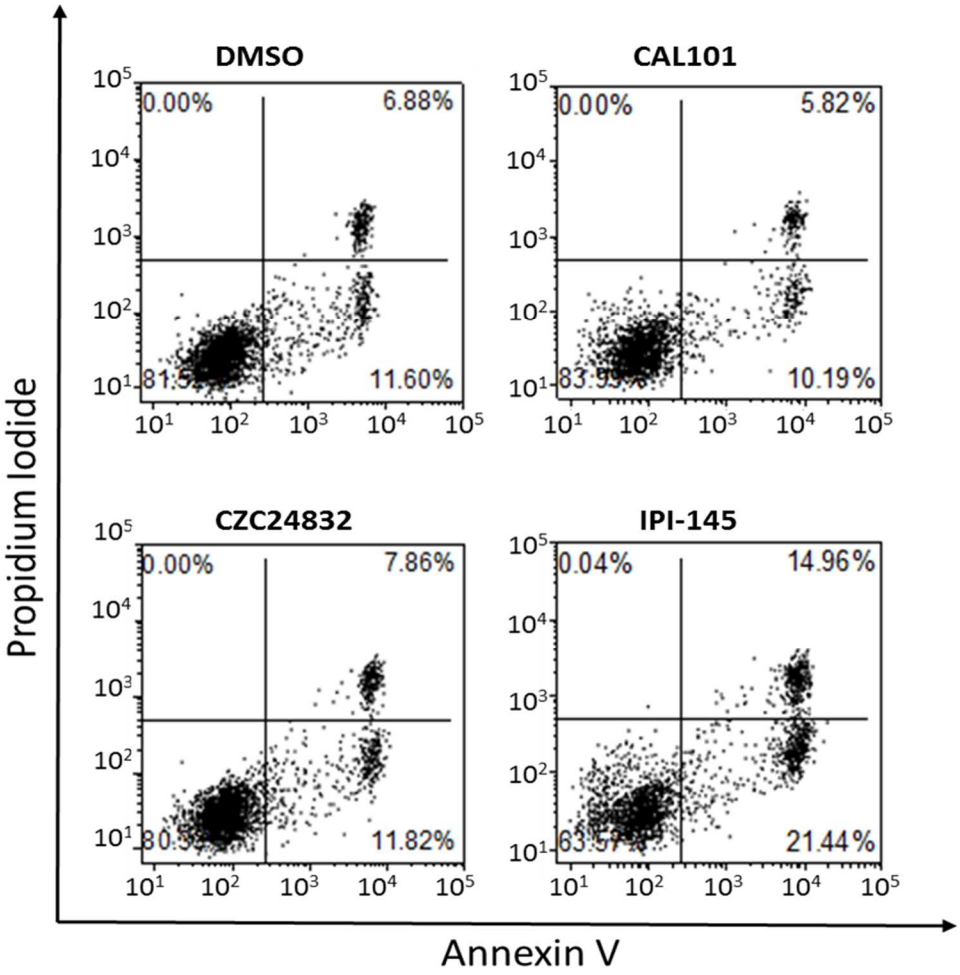

Figure 4.2.2 – Flow cytometry showing dual PI3K isoform inhibition can increase MM cell death in co-culture.
Following co-culture with BMSC and PI3K inhibitors, MM primary cells were analysed using PI-Annexin V Flow Cytometry. Representative image shown (n=4).

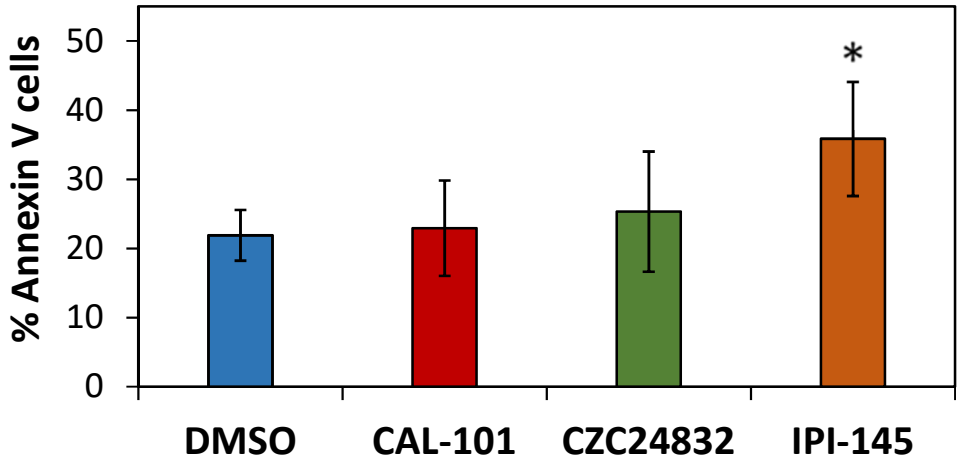

Figure 4.2.3 – Graphical representation of Figure 3.2.19.
Annexin V positive MM primary cells (n = 4) following PI3K isoform inhibition and co-culture with BMSC. *p < 0.05; Mann-Whitney U.

4.2.1.2 – IL-6 mediated protection

IL-6 activation of the PI3K pathway has previously been implicated in prostate cancer [317, 318] however its role in MM PI3K activation is less certain. In a paper by Pene *et al.* IL-6 was described as not phosphorylating Akt in MM cell lines (implying that it did not activate the PI3K pathway [319]), however these data were not shown. Instead, IGF-1 was proposed as the mechanism by which PI3K was activated and was shown to phosphorylate Akt at both the s473 and t308 residues – a result that has been confirmed in other studies [320, 321]. Conversely, other studies describe IL-6 activating the PI3K pathway in MM cell lines, alongside IGF-1 stimulation [312, 322].

I therefore decided to analyse if IL-6 on its own could stimulate Akt activation in MM cell lines and primary samples. MM cells were cultured with an increasing level of IPI-145 for 6 hours, and subsequently activated with 100ng/mL recombinant IL-6 for 30 minutes (control is untreated MM cells). Whole protein was extracted from samples and subject to Western Blot (Figure 4.2.4).

Results showed that IL-6 caused the phosphorylation of both MM cell lines tested, and that this stimulation was partially reversible with the use of IPI-145 (despite the high concentration of IL-6 used). Substantial inhibition of AKT phosphorylation can be seen upwards from 500nM IPI-145, and this drug showed minimal effect on MAPK activation.

To test if a single PI3K isoform inhibition was sufficient to reduce IL-6 PI3K stimulation, this MM cell lines and primary cells were cultured with CAL101, CZC24832 or IPI-145 (all at 1µM) and subsequently with 100ng/mL recombinant IL-6 for 30 minutes (control is untreated MM cells). Western blot analysis showed that IL-6 also induced PI3K activation in primary samples, and that the greatest reversal of this effect was with IPI-145 treatment (Figure 4.2.5). Single isoform inhibition did not appear to reduce the stimulatory effects of IL-6 (on either Akt or 44/42 MAPK, Figure 4.2.5), whereas dual inhibition either completely reversed these effects or visibly reduced the amount of activated protein.

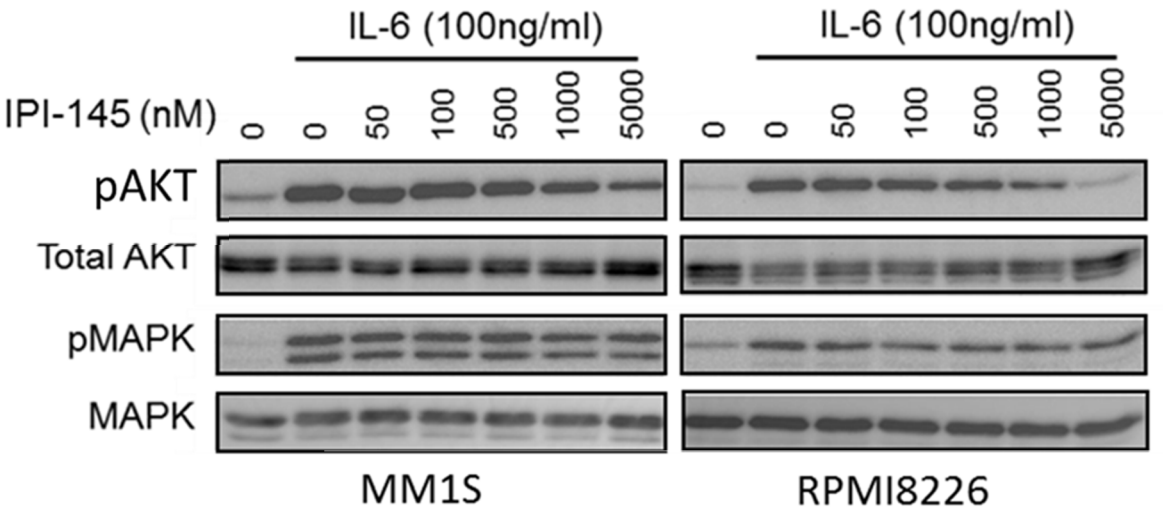

Figure 4.2.4 – IL-6 activation of the PI3K pathway can be inhibited by IPI-145 in a dose dependent manner.

MM cell lines were incubated with p110δ/γ inhibitor IPI-145 for 6 hours, and stimulated with increasing concentrations of IL-6. Image shown is representative of 3 independent experiments.

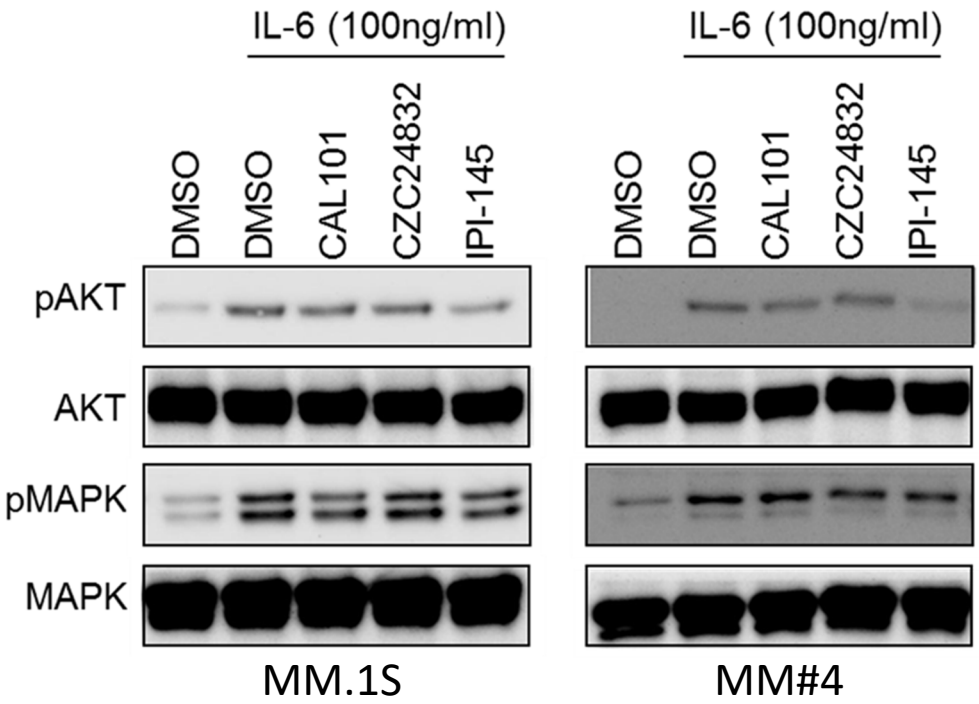

Figure 4.2.5 – IL-6 stimulation of PI3K pathway is reversible via p110δ/γ dual inhibition.

Representative (n = 3) Western blot showing the pAKT levels in IL-6 stimulated MM cells. CAL101 (p110δ inhibitor), CZC24832 (p110γ inhibitor) and IPI-145 (dual p110δ/p110γ) were used to assess PI3K isoform involvement. Cell line image shown is representative of 3 independent experiments.

Finally, I used shRNA specific to PIK3CD and PIK3CG (the genes for p110δ and p110γ respectively) to knockdown expression of these genes and investigate if this affected IL-6 stimulation of this pathway. MM.1S cells were transduced with gene specific lentivirus for 72hours (methods Section 2.10), after which knockdown was confirmed via RT-qPCR (see Section 2.9). Remaining cells were stimulated with 100ng/mL recombinant IL-6 for 10 minutes, whole protein was extracted and samples were subject to Western Blot analysis (Figure 4.2.6, methods Section 2.6). Results showed that the only case in which IL-6 could not induce AKT phosphorylation was when both isoforms had been knocked down. MAPK pathway activation was partially inhibited upon PIK3CG knockdown, potentially indicating a role for p110γ in MAPK signalling.

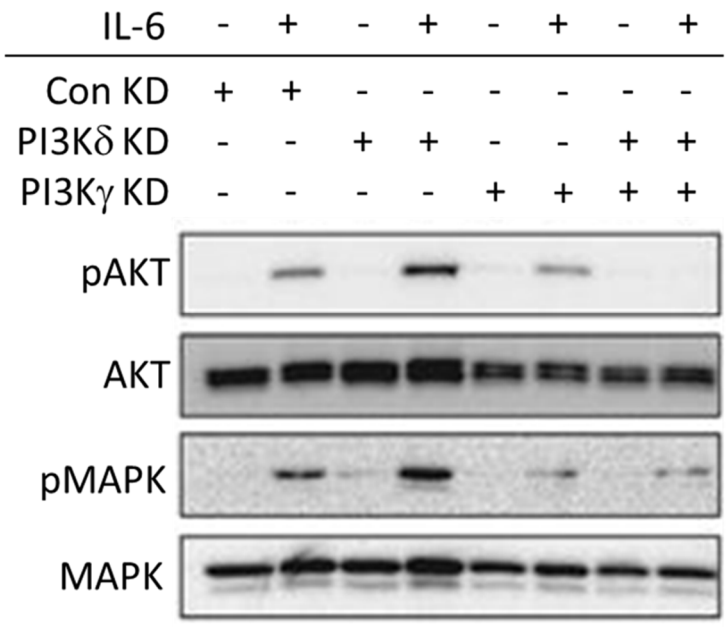

Figure 4.2.6 – Only inhibition of both PI3Kδ and PI3Kγ is sufficient for PI3K pathway inhibition in IL-6 stimulated cells.
Lentiviral knockdown of PI3Kδ and PI3Kγ isoforms negated the effects of IL-6 – PI3K pathway activation. Image shown is representative of 3 independent experiments.

4.2.2 – Inhibition of PI3Kδ/γ *in vivo*

In order to truly represent how PI3K knockdown affects MM disease progression, a MM *in vivo* model was needed. As a human MM xenograft model was required, NSG mice were selected for their highly compromised immune system (meaning that no radiation or chemotherapy would be needed to prevent graft versus host disease). U266 cells had previously been lentivirally transduced for 72 hours with a luciferase construct. This modification makes the cells detectable via bioluminescent imaging in live animals upon the introduction of a luciferin substrate (using the Bruker In-Vivo Xtreme II). Cells were subject to either PIK3CD or PIK3CG knockdown, which was confirmed with RT-qPCR prior to any animal experimentation. Mice were injected with 0.5 x 10^6 U266 cells (n = 4 in all groups) via the lateral tail vein and monitored with frequent visual checks and weekly bioluminescent imaging. U266 were selected due to successful preliminary *in vivo* engraftment experiments (data not shown). Female mice (n = 1 per group) were not imaged due to concerns over recovering these animals following anaesthesia due to their smaller size – however they were included in survival analysis. Further details on methodology can be found in Section 2.13.

4.2.2.1 – Isoform specific KD resulted in reduced tumour burden and increased overall survival (OS)

Figure 4.2.7 shows that by day 21, disease burden in all knockdown mice was considerably less in comparison to a knockdown control (ShE). Whereas multiple tumours are present in the control mice, tumours in knockdown mice (when present) tended to be more isolated. This was still true at day 28, with only one of the mice exhibiting a large tumour (group 2, PI3Kδ knockdown). Survival was shown using a Kaplan-Meier curve (see Figure 4.2.8) and statistically analysed using Mantel-Cox regression analysis (through GraphPad software). All PI3K isoform knockdown mouse groups were shown to have significantly increased survival in comparison to the control group ($p < 0.05$, Mantel-Cox regression), however specific isoform knockdowns did not statistically differ from each other.

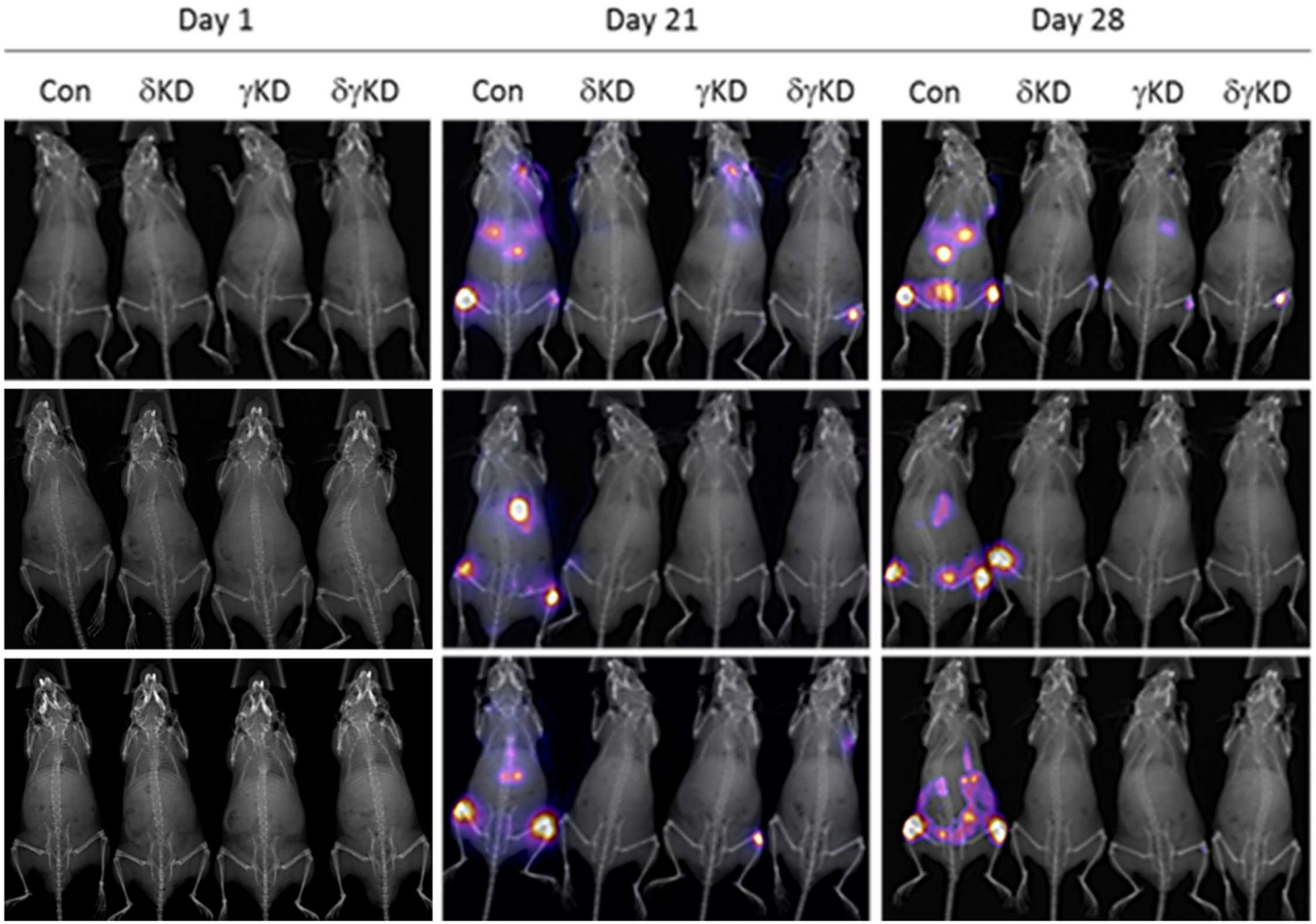

Figure 4.2.7 – *In vivo* bioluminescent imaging of MM cells.
U266-luciferase modified cells (1 x 10^6) were injected into NSG mice via the tail vein and monitored via BLI. Areas of high intensity indicates higher MM disease burden. Control mice (left) presented with advanced disease burden at day 21. MM cell burden was greatly reduced in all KD groups with luminescent cells only visible with a much longer exposure time (data not shown).

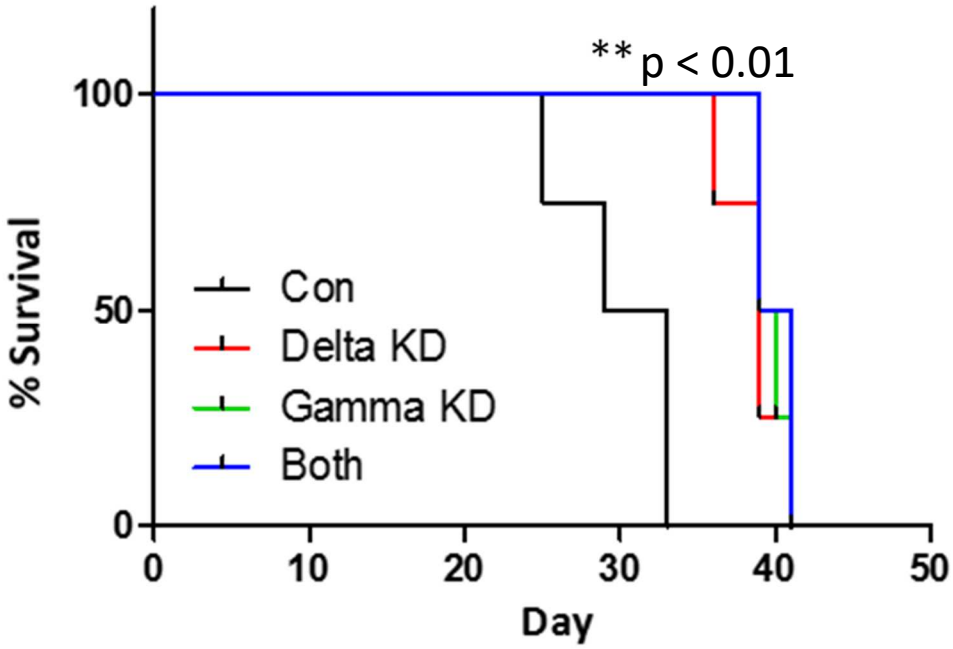

Figure 4.2.8 – Knockdown of PI3K isoforms results in increased survival in NSG mice.
Kaplan-Meier curve showing survival of NSG mice following PI3K isoform knockdown. Mantel-Cox regression was used for statistical analysis.

	Control	Delta KD	Gamma KD	Dual KD
Control	~	0.0091	0.0091	0.0091
Delta KD	0.0091	~	0.6446	0.0361
Gamma KD	0.0091	0.6446	~	0.5812
Dual KD	0.0091	0.0361	0.5812	~

Median Survival (Days)	
Control	31.0
Delta KD	39.0
Gamma KD	39.5
Dual KD	40.0

Table 4.2.1 – Table showing p-values and median survival.
p-values (left) and median survival (right) for data shown in Figures 4.2.7 and 4.2.8 was calculated using Mantel-Cox regression and Graphpad Prism 7 software.

4.2.2.2 – PIK3CG KD cells showed decreased levels of engraftment

Following disease endpoint, bone marrow was extracted from mice and stained for human CD45 and analysed by Flow Cytometry (see Section 2.13.6) to investigate the levels of MM cell engraftment. Figure 4.2.9 shows that PIK3CD knockdown had a highly variable effect on MM cell engraftment, but engraftment in PIK3CG knockdown cells was significantly reduced (p=0.029, Mann-Whitney U). Although dual knockdown also resulted in a reduction of MM cell engraftment (a mean value of 18.5%, compared to the control value of ~26%) this result was not statistically significant and a larger sample size may be needed to confirm results.

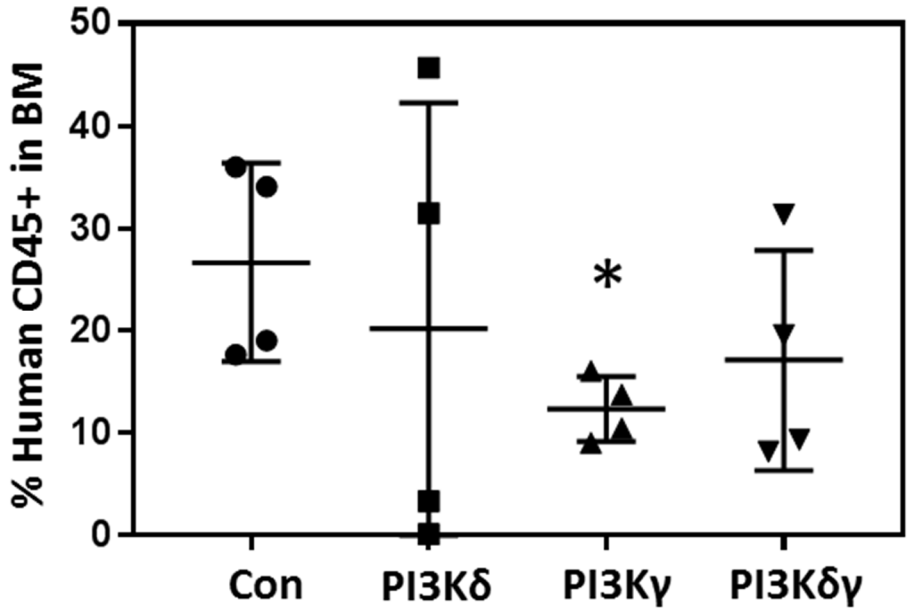

Figure 4.2.9 – PI3K p110γ knockdown correlates with a significant decrease in MM cell engraftment.
Following end-point, murine bone marrow was analysed for CD45+ cells via flow cytometry (n = 4). *p = 0.029 in comparison to control; Mann-Whitney U.

4.2.2.3 – IPI-145 decreased rate of tumour growth and increased OS

To ascertain if the effects of IPI-145 (dual PI3Kδ/γ inhibitor) seen *in vitro* were achievable *in vivo*, mice were injected with U266-luc cells as before (n = 12). MM cells were allowed a 5-day engraftment period before mice were randomly assigned into either control (n = 6) or IPI-145 (n = 6) treatment groups. Mice were treated every 24 hours from day 5-14 with 15mg/kg IPI-145 or the vehicle control (10% DMSO, 90% PBS) by IP injection and monitored via bioluminescent imaging (dose was selected based on previous literature and achievable plasma concentration of drug [323]).

Figure 4.2.10 shows that at day 11, mice showed similar levels of tumour burden, however by day 18 (4 days after the complement of IPI-145 treatment) tumour burden in treatment group had reduced when compared to the control ($p = 0.015$; Mann-Whitney U). Densitometry analysis (using ImageJ software) showed that tumour burden growth was significantly retarded in the treatment group, despite the short treatment time.

The reduced tumour burden seen in IPI-145 treated animals was reflected in animal survival, with treated animals surviving for a significantly longer period (27.5 days median survival vs 23.0 days control median survival - Figure 4.2.11, $p < 0.001$; Mantel-Cox regression).

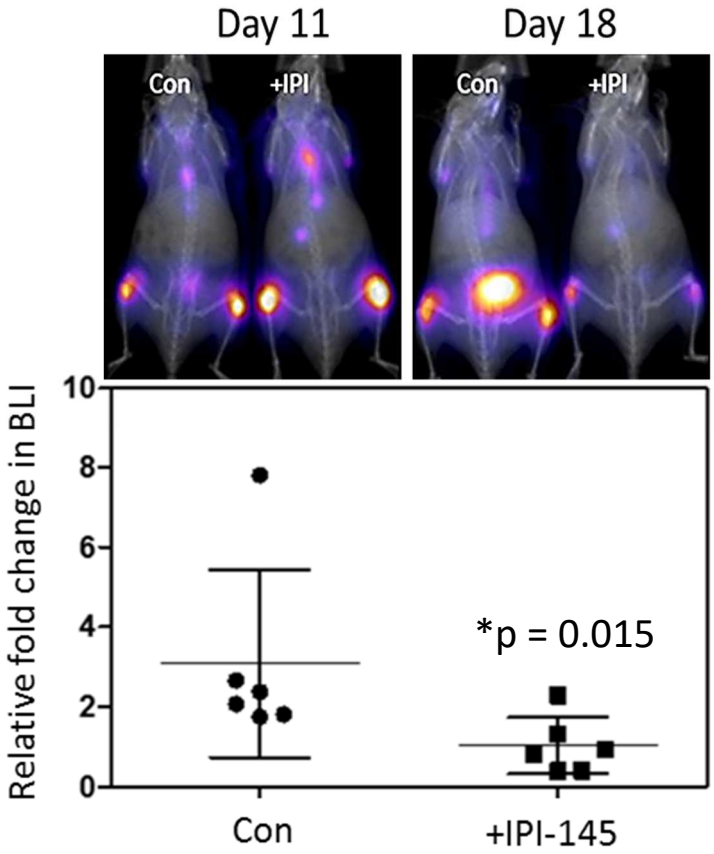

Figure 4.2.10 – Relative fold change in tumour burden over a 7 day period. Tumour progression was inhibited when treated with IPI-145 versus control. Mice were imaged at day 4 (following MM engraftment period, data not shown as signal too low), then weekly at days 11 and 18 using Bioluminescent Imaging, BLI. *p = 0.015, Mann-Whitney U.

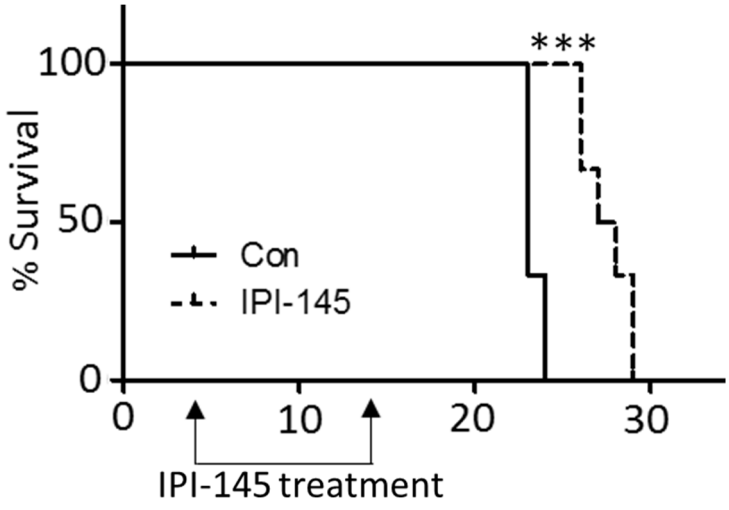

Figure 4.2.11 – IPI-145 inhibition of p110δ/γ caused an increase in OS. Kaplan-Meier curve showing survival of NSG mice following p110δ/γ isoform inhibition following a 5 day engraftment period. Mice were treated from day 5-14. Mantel-Cox regression was used for statistical analysis, ***p<0.001. Median survival control = 23.0 days, median survival treated = 27.5 days.

4.3 – Summary

When researching haematological malignancies, the importance of the BMM cannot be ignored [12, 307, 324]. Outside of this environment, MM cells are far more fragile and succumb to stressors far more easily [325, 326]. In this section I have shown how, even without adhesion to the structural components of the BM, cytokines secreted by the BMSCs can activate the PI3K pathway.

The PI3K pathway was shown to be stimulated by both BMSC conditioned media and IL-6 stimulation (a cytokine freely available in the MM-BMM). Inactivation of the PI3K pathway using isoform specific inhibitors was only achievable upon the inhibition of both p110δ and p110γ isoforms in both cases. This was reflected in MM-BMSC co-cultures, where only IPI-145 (p110δ and p110γ inhibitor) was able to significantly increase levels of MM cell apoptosis.

In vivo, knockdown of either isoform resulted in an increased survival time – however there was no observed difference in survival between isoforms in this case. I also showed that IPI-145 treatment resulted in retarded tumour growth, which also corresponded with an increase in survival duration. There are limitations to these *in vivo* studies however, not least the low subject number in each experiment (n = 16 and n = 12 respectively). The lack of a functional immune system too, although necessary for xenograft experiments, undoubtedly affects MM cell interactions with its microenvironment potentially skewing results.

5 – MM-remodelling of BMSCs to activate malignant PI3K

5.1 – Introduction

How MM cells influence their environment has been the focus of studies for decades, with early work by Uchiyama *et al.* [225] showing that MM cell adhesion can influence the transcriptional and translational profile of BMSCs. MM-BMSC adhesion has been shown to promote the survival of MM cells and increase drug resistance within the malignancy (CAM-DR), as well as causing the release of many soluble factors from the BMSCs that benefit disease progression such as IL-6 [327]. However, it has also been shown that MM cells can influence the BMSCs prior to any cellular contact. In a study by Zdzisińska *et al.*, the authors showed how direct binding of plasma cells to BMSCs was not required to induce BMSC cytokine secretion [328] (a finding that was in conflict with Uchiyama's earlier work).

In the previous section I showed how cytokines secreted from BMSCs could be responsible for the aberrant activation of the PI3K pathway in MM cells, however it is unclear if BMSCs consistently produce these cytokines or if MM cells adapt BMSCs for this purpose. In this section I investigate how BMSC cytokine production is influenced by MM cells and how MM cells could confer these changes prior to cellular adhesion.

5.2 – Results

5.2.1 – BMSC IL-6 and IL-8 secretion is increased in co-culture

To investigate what effect primary MM cells have on primary BMSCs, human XL cytokine arrays were used (cytokine arrays are capable of measuring 102 different cytokines simultaneously – see Section 2.12 for details). MM cells and/or BMSC were cultured for 24 hours, after which the supernatant was taken and used for this assay (representative result shown in Figure 5.2.1, n = 3).

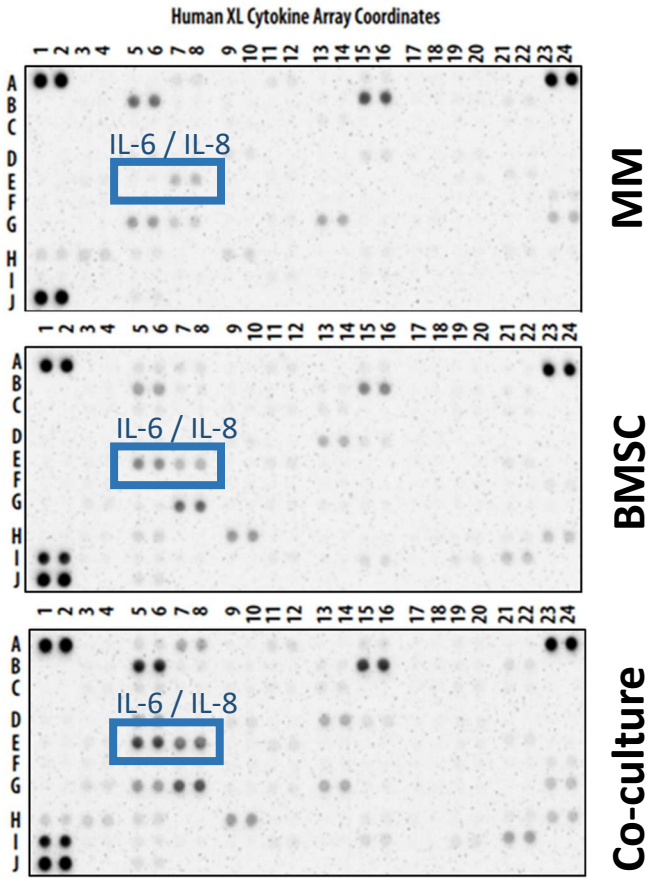

Figure 5.2.1 – IL-6/8 extracellular protein levels increase in BMSC in response to MM. Supernatant from primary MM only, BMSC only and MM-BMSC co-cultures were analysed for 102 different cytokines using human XL cytokine arrays (section 2.12), with each pair of dots representing a different cytokine (density is proportional to cytokine concentration). Results showed increased levels of IL-6 and IL-8 in co-culture membrane in comparison to the sum of signals from monocultures. Representative Cytokine array shown (n = 3).

Densitometry analysis of the cytokine arrays was performed using HLImage++ software (Figure 5.2.2). Output from this software is given as 'Mean Pixel Density (MPD)' and all cytokine results were first normalised against reference spots (shown at positions A1 and B1) for consistency between arrays.

Co-culture outputs (MPD) were then normalised to the sum of their corresponding BMSC only and MM only outputs (MPD). Results are displayed as relative fold changes in MPD that reflect net changes in protein levels (sum of monoculture intensities vs. co-culture intensity).

As well as increases in IL-6 and IL-8, analysis revealed increases in several other cytokines – including epidermal growth factor (EGF), myeloperoxidase (MPO) and vascular endothelial growth factor (VEFG). IL-6 and IL-8 increases were the only statistically significant changes detected however, most likely due to the high variability between the primary samples. An increased sample size would have been beneficial to identify other potential cytokine changes.

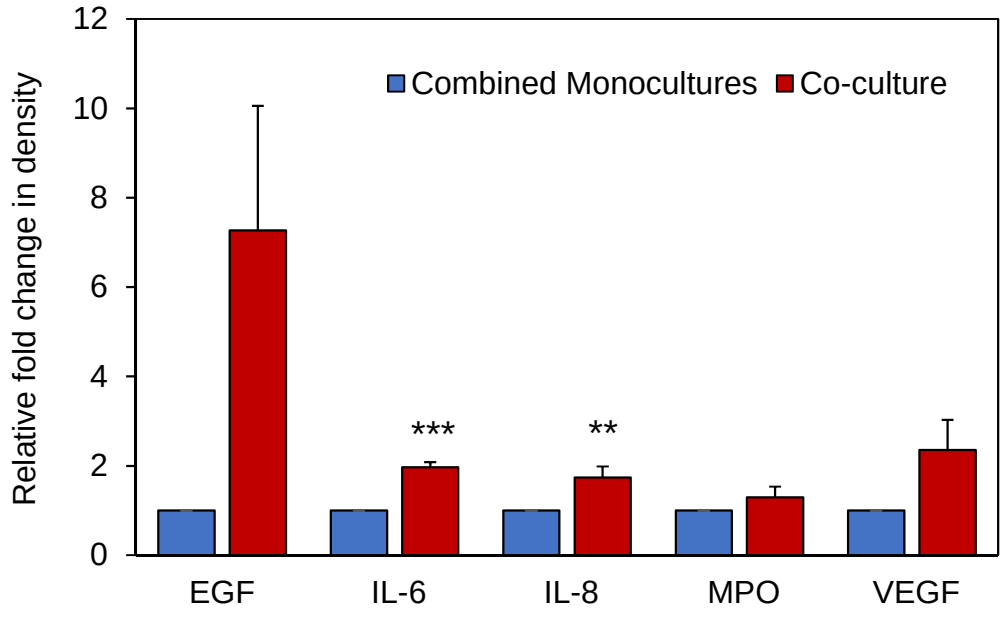

Figure 5.2.2 – Densitometry of co-culture cytokine array
Densitometry analysis using ImageJ (n = 3) of selected cytokines from arrays described in Figure 5.2.1. Blue bars shows combined intensities of the monocultures, red bars show intensity of co-culture array only. Error bars show SD from the mean, no error bars are present on monoculture bars due to normalisation of each sample. Statistical analyses performed using student's t-test, **p < 0.01, ***p < 0.001.

5.2.2 – MM cells have higher levels of MIF protein secretion and gene expression.

To determine the excretory cytokine profile of MM cells (and potential BMSC signallers), Human XL cytokine arrays were once again utilised (n = 3). Patient derived MM cells (1 x 10^6 cells per assay) were cultured in fresh media for 24 hours following $CD138^+$ purification. Cells were then pelleted and supernatant was used for assay. Analysis of densitometry revealed high levels of the cytokine Macrophage Migration Inhibitory Factor (MIF), detectable in all 3 cytokine arrays used (representative image shown in Figure 5.2.3). Other cytokines such as Chitinase 3-like 1 and MMP-9 were shown to have high levels, however the levels of these cytokines were far more variable in the samples tested, demonstrating the high levels of heterogeneity in MM disease.

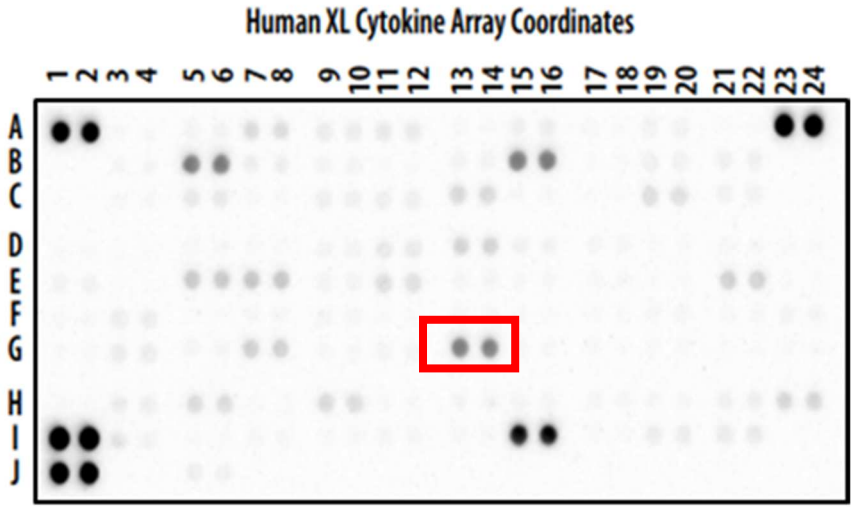

Figure 5.2.3 – High MIF levels detected in primary MM cell supernatants.
Representative cytokine array showing secreted protein from primary MM cells. High levels of MIF (red box) were detected in each array used (n = 3).

It has previously been shown that MIF is overexpressed in many different cancers, including MM [329-332]. To confirm these observations, I examined expression of MIF in MM at both mRNA (RT-qPCR analysis, Section 2.9) and protein level (via ELISA, Section 2.11). Figure 5.2.4 shows that in comparison to T cells, B cells and normal non-malignant plasma cells, primary MM cells (n = 5) had significantly increased MIF gene expression (approximately 1.8X higher than B-Cells) when analysed using RT-qPCR ($p < 0.01$; Mann-Whitney U test). MIF gene expression was normalised to the housekeeping gene, β-Actin.

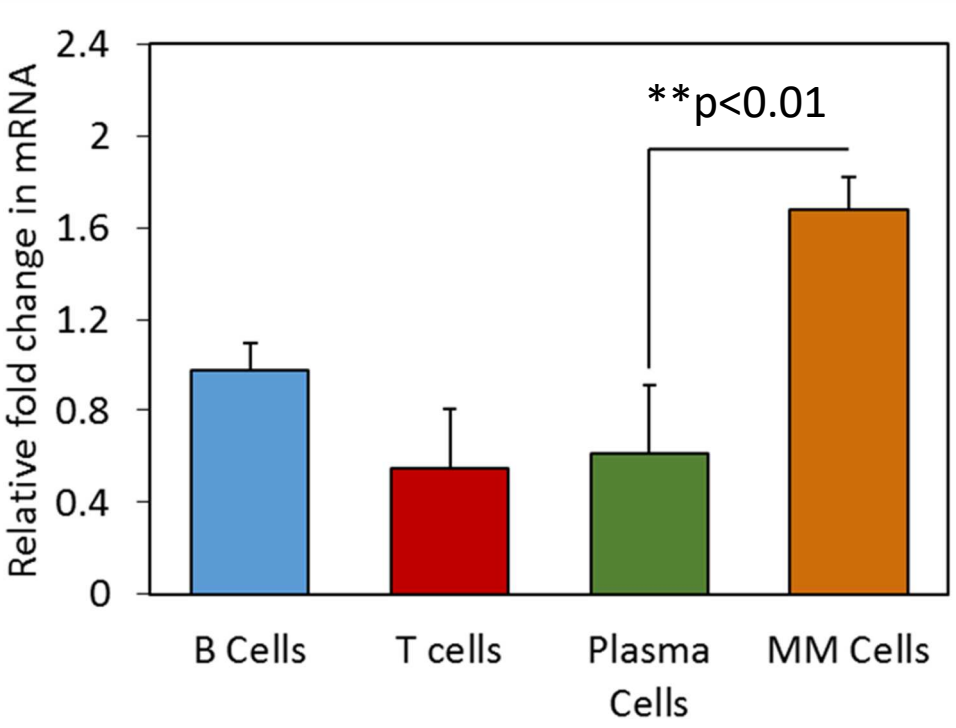

Figure 5.2.4 – MM primary cells have elevated levels of MIF gene expression.
RT-qPCR analysis of MIF expression, normalised to β-Actin housekeeping gene (n = 5 for each group). Error bars show S.D from the mean, **p < 0.01; Mann-Whitney U.

Extracellular protein levels of MIF were then measured in B-Cells, T-Cells, primary MM and MM cell lines (MM-CL consisting of RPMI-8226, MM.1S, MM.1R, U266 and H929 cells) by use of a cytokine specific ELISA (Figure 5.2.5). Results showed that both MM primary cells and MM-CL had elevated levels of MIF secretion, with MM cells lines showing the highest levels.

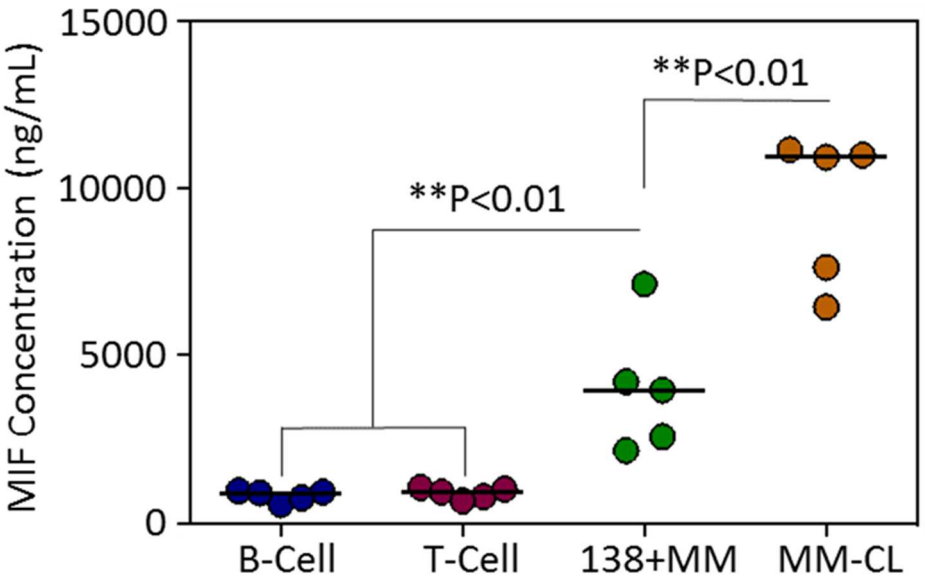

Figure 5.2.5 – MM cell lines and primary cells have increased levels of MIF secretion. MIF ELISA results of MM cells. Concentrations calculated using MIF standard curve. Mann-Whitney U analysis is of standard error mean (SEM), n = 5.

5.2.3 – MIF induces IL-6 and IL-8 production in BMSC

To determine if elevated MIF signalling was responsible for the elevated levels of IL-6 and IL-8 seen in MM-BMSC co-culture I used MIF to stimulate primary BMSCs and evaluate changes in the cytokine profiles (via Human XL cytokine array analysis, see Section 2.12 for details).

MIF (100ng/mL) was added to BMSC (n = 3) in culture for 24 hours, after which supernatant was analysed using cytokine arrays (representative array shown in Figure 5.2.6). As before, I saw an increase in IL-6 and IL-8 production (increasing approximately 3-fold in each case - $p < 0.05$ for both cytokines; Mann-Whitney), densitometry analysis is shown in Figure 5.2.7. Concentration of MIF chosen was based on previous literature, to conservatively reflect conditions in early MM [330].

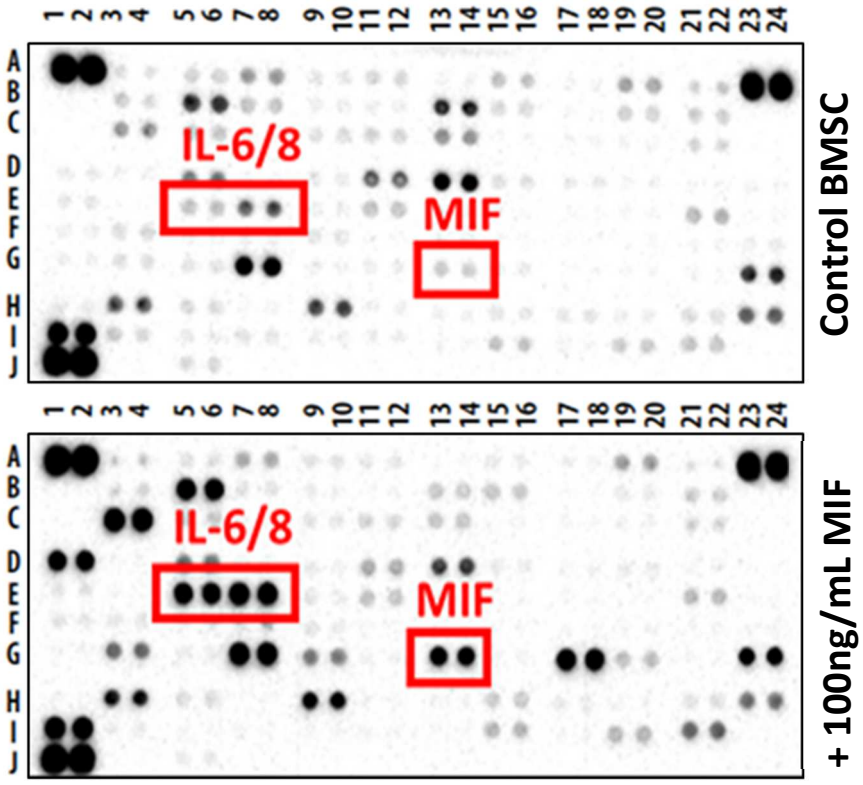

Figure 5.2.6 – Cytokine array showing increased levels of IL6/8 in response to MIF. Supernatant from primary MIF stimulated (100 ng/mL) BMSC showed increased levels of secreted IL-6 and IL-8. Representative Cytokine array shown (n = 3).

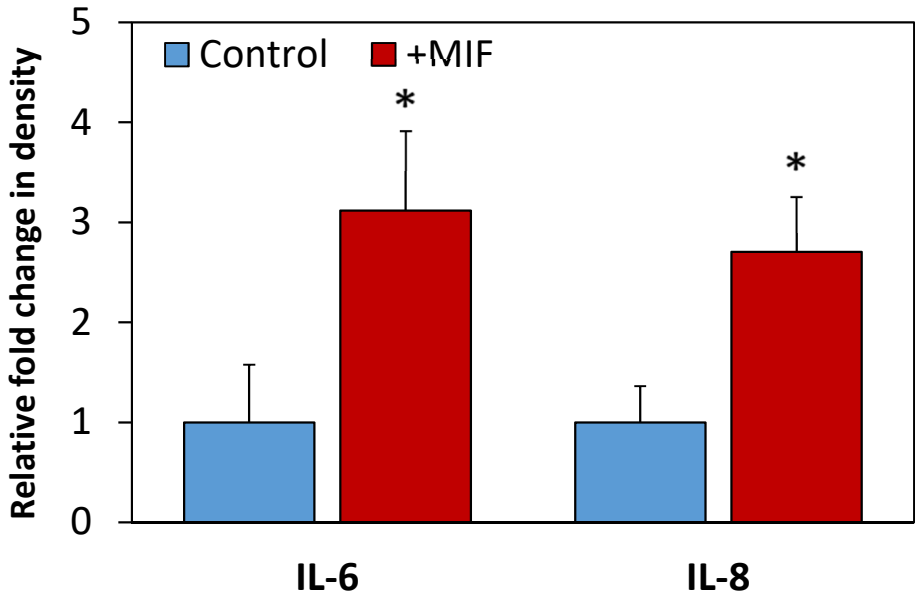

Figure 5.2.7 – Densitometry of MIF stimulated BMSC cytokine array.
Densitometry analysis using ImageJ (n=3) of IL-6 and IL-8 from arrays described in Figure 5.2.11. *p < 0.05 (Mann-Whitney U).

To quantify the increase in IL-6 and IL-8, I used cytokine specific ELISAs. Figure 5.2.8 shows that, in response to MIF stimulation, primary BMSCs (n = 4) secrete a significantly higher amount of both cytokines, in agreement with previous results.

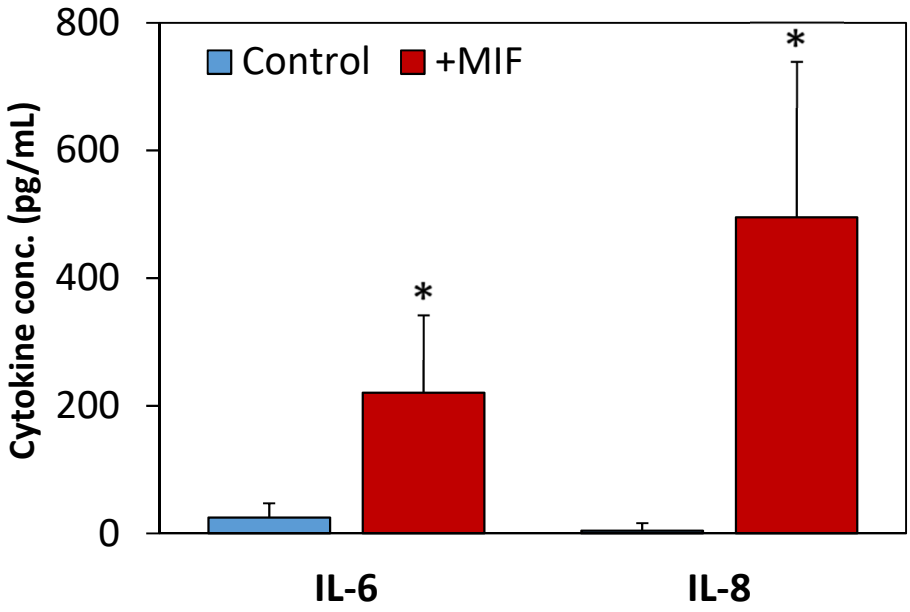

Figure 5.2.8 – Quantification of BMSC IL-6/8 secretion in response to MIF.
ELISA and standard curve were used to quantify cytokine concentration in BMSC supernatant following MIF (100ng/mL) stimulation. *p < 0.05 (Mann-Whitney U).

Furthermore, primary BMSC were pre-treated with the MIF antagonist ISO-1 at 10µg/mL (abcam, UK) and then were subject to MIF stimulation as before. ISO-1 inhibits MIF by binding to its tautomerase active site [333]. Figure 5.2.9 shows that MIF once again caused an increase in the transcriptional levels of IL-6 and IL-8 in BMSC (analysed by RT-qPCR; $p < 0.05$, Mann-Whitney U) and that this response was decreased in response to ISO-1 (n.s, Mann-Whitney U).

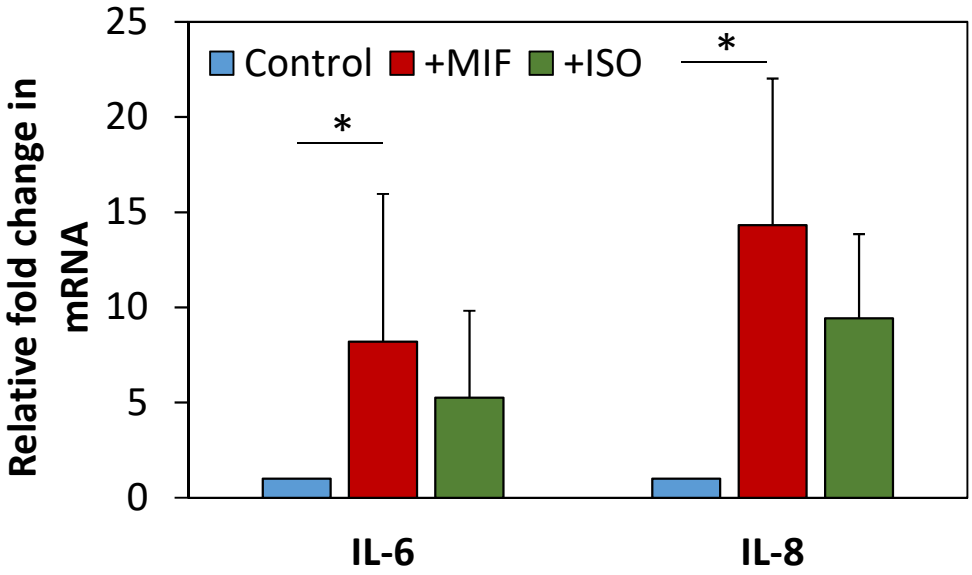

Figure 5.2.9 – Inhibition of MIF reverses transcriptional effects in BMSC.
Primary BMSC were incubated with/without ISO-1 (10µg/mL) for 1 hour, after which they were stimulated with MIF (100ng/mL) for 6 hours. RNA was extracted and transcriptional changes were analysed via RT-qPCR. Error bars are shown as the SD of the mean, *$p < 0.05$, $n = 4$, Mann-Whitney U.

To confirm that the increase seen in BMSC IL-6 and IL-8 production/secretion is achievable and comparable to the effect of primary MM cells, I cultured primary MM cells (n = 3) in a transwell insert with primary BMSC for 6 hours. The same BMSC samples were also stimulated with 100ng/mL MIF in parallel. After this time, conditioned media from the lower chamber was taken and subject to a cytokine specific ELISA.

Results showed that IL-6 levels (shown in Figure 5.2.10 A) significantly increased in both MM contact (where the MM cells were allowed to adhere to the BMSCs) and MM secretory (transwell) profiles. These increases were not significantly different from each other, showing that adhesion is not required for IL-6 secretion. IL-8 secretion also

increased in response to MM in both cases (Figure 5.2.10 B) – however this cytokine was shown to have more variability in response to adhesion (with one primary sample showing extremely high levels of IL-8).

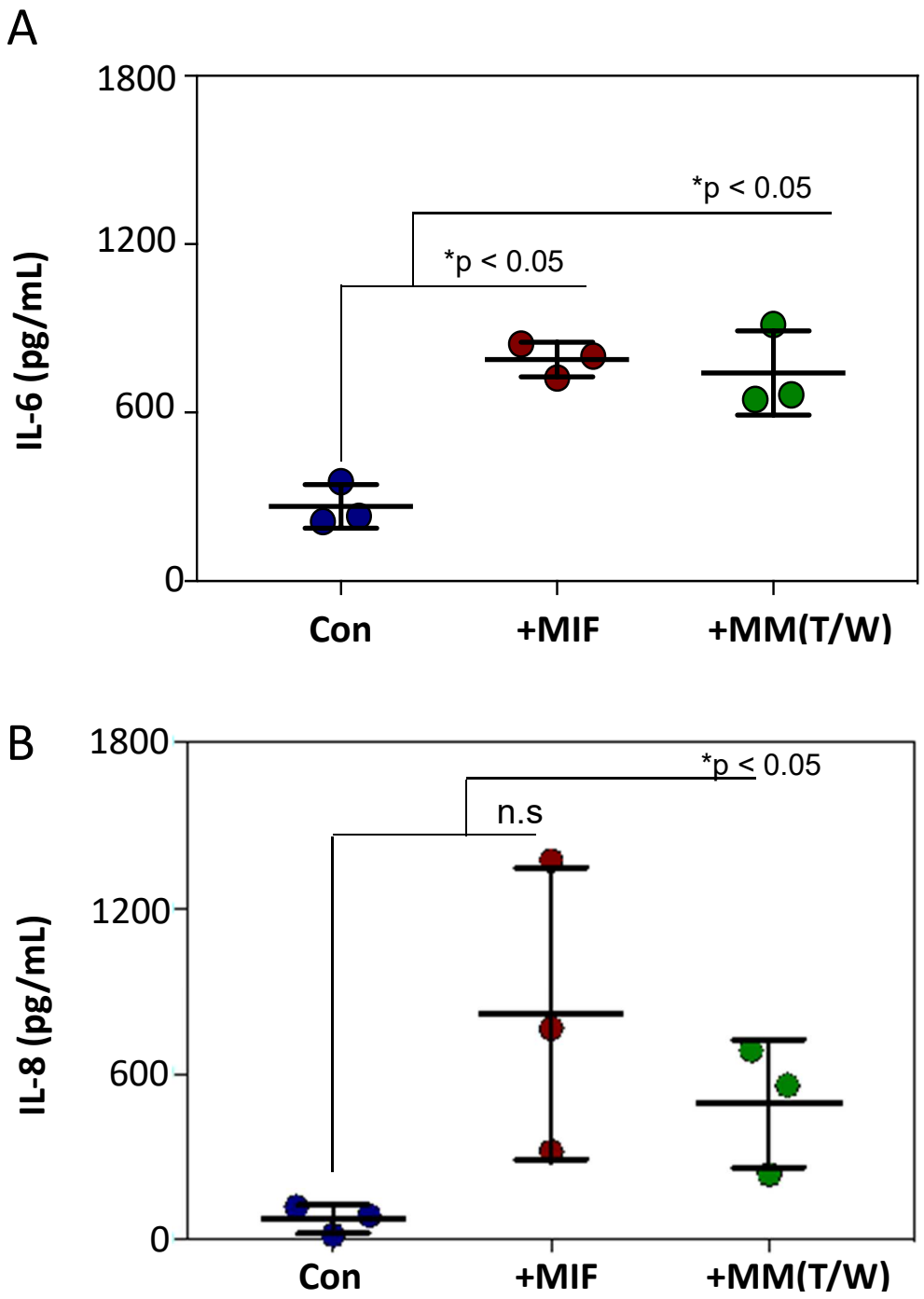

Figure 5.2.10 – BMSC IL-6 and IL-8 secretion is not dependent on MM cell adhesion. BMSC were cultured with MIF (100ng/mL) or co-cultured with MM cells suspended in a transwell system for 6 hours, after which media was collected and analysed for IL-6 (A) and IL-8 (B) using ELISAs. Mann-Whitney U test used for statistical analysis, error bars show the S.D of the mean.

5.2.4 – MIF knockdown reduces MM cell survival in MM-BMSC co-culture.

To determine the role of MIF in MM proliferation and metastasis within the BMM I used targeted shRNA KD of MIF mRNA. 96 hours after MM cell line transduction, cells were analysed for MIF expression using RT-qPCR normalised to β-Actin (see Sections 2.10 and 2.9 for details on lentiviral and gene expression analysis methodology). Figure 5.2.11 shows that significant knockdown of MIF was achieved in both MM.1S and RPMI-8226 cell lines (approximately 80% and 95% respectively). MM.1S and RPMI-8226 knockdown cells were incubated for 24 hours in fresh media, after which media was subject to ELISA analysis (Section 2.11). Results showed that this knockdown does indeed correspond with a reduction in IL-6 and IL-8 protein secretion (Figure 5.2.12).

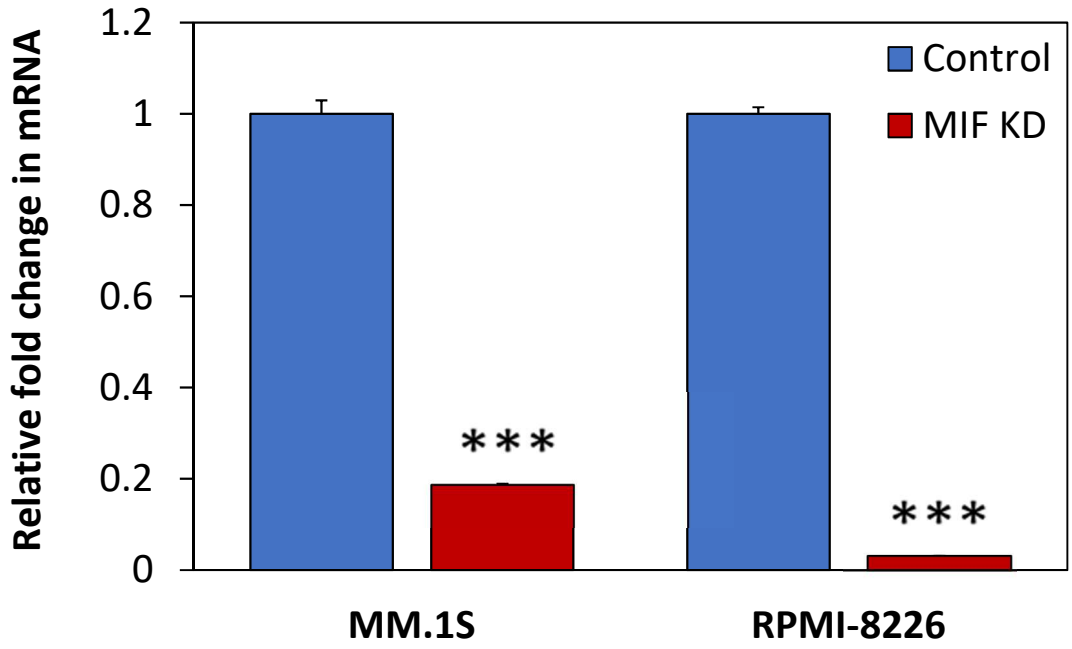

Figure 5.2.11 – Effective MIF knockdown achieved in MM cell lines.
MM.1s and RPMI-8226 cells were transduced with lentivirus targeted MIF or control shRNA for 96h. RNA was then extracted and analysed for MIF mRNA expression by RT-qPCR. β-Actin was used as a housekeeping gene. ***$p < 0.001$, Mann-Whitney U test.

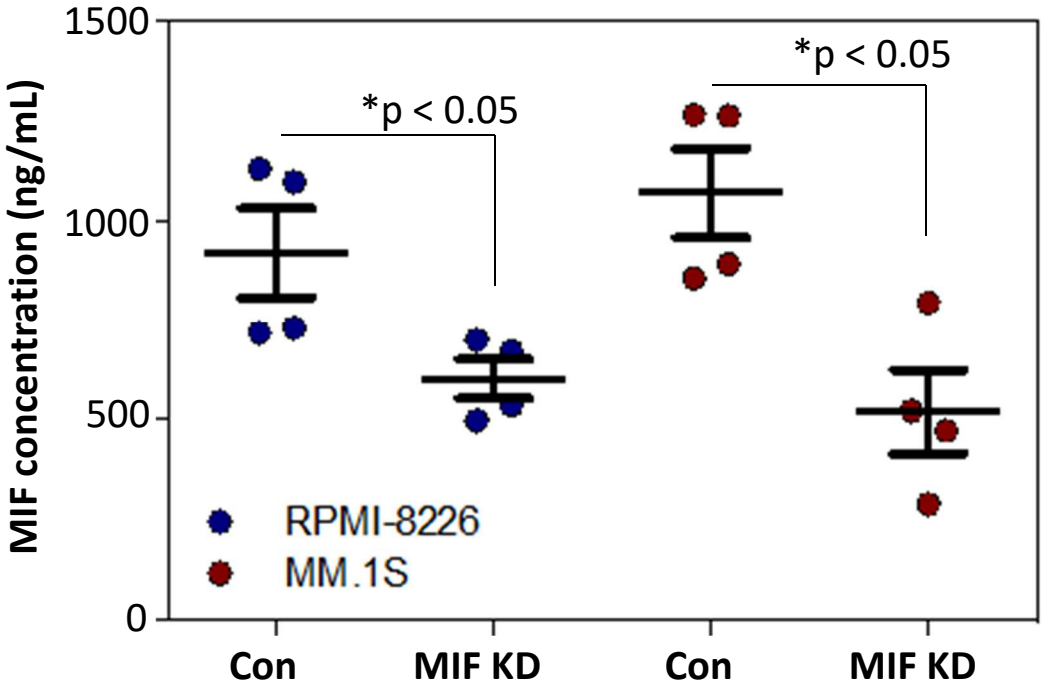

Figure 5.2.12 – MIF knockdown causes a reduction in MIF secretion in MM cell lines. MIF secretion in MM.1S and RPMI-8226 control and MIF knockdown cells was measured using a cytokine specific ELISA. Mean values were subject to Mann-Whitney U test, *p < 0.05, error bars show the S.D of the mean.

To determine the effect of this knockdown on MM cell growth rates, MM control and knockdown cells were co-cultured with primary BMSC for 72 hours. After this time, MM cells were removed and measured for cell proliferation using a Cell-Titre Glo assay (Figure 5.2.13, see section 2.4 for methodology). Proliferation of MM cells was shown to be significantly lower in MIF-knockdown MM cells when compared to the control.

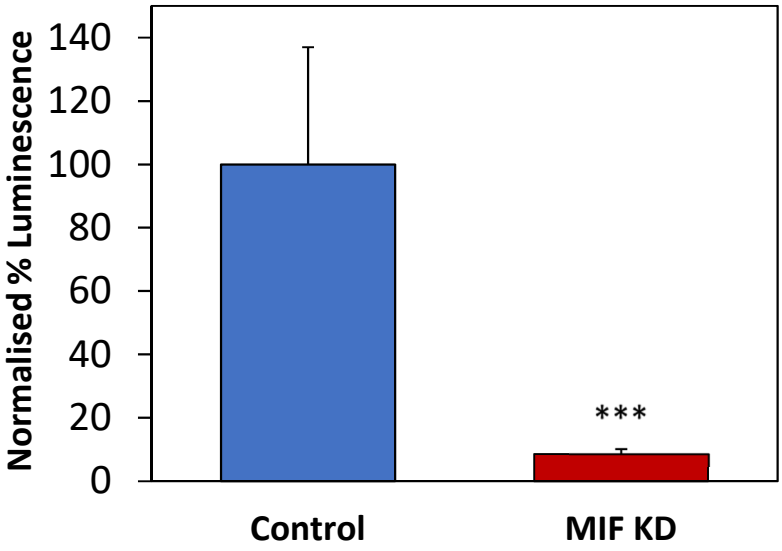

Figure 5.2.13 – MIF knockdown reduces MM cell survival in co-culture with BMSC. MM.1S control and MIF knockdown cells were co-cultured with primary BMSC for 72 hours after which they underwent CellTitre Glo analysis to determine levels of proliferation. Mean values (n = 5) were subject to Mann-Whitney U test, *p < 0.001, error bars show the S.D of the mean.

5.2.5 – MIF is critical for MM disease progression *in vivo*.

To analyse how MIF knockdown would affect MM disease progression, an NSG xenograft model was used. 1 x 10^6 MM.1S control or MIF knockdown cells (all containing the pCDH-luciferase-T2A-mCherry and luciferin constructs) were injected into the tail vein of 6-8 week old NSG mice (control knockdown n = 10, MIF knockdown n = 8) . Disease was monitored via bioluminescent imaging. Figure 5.2.14 shows that disease burden was highly reduced in the MIF knockdown group, most noticeable at day 28. This decrease in disease burden correlated with an increase in animal survival (Figure 5.2.15, p = 0.0005; Mantel-Cox regression test). Mice receiving MM control knockdown cells had a mean survival of 28.1 days, whereas the MIF knockdown group has a mean survival of 35.8 days.

Although the rate of disease progression was comparable between both male and female mice, the initial disease burden in males was higher (seen one to two weeks after initial MM cell engraftment). This result highlights a difference in MM disease development between the sexes, and could potentially indicate one of the reasons why there is a higher incidence of MM in men. Unfortunately, the majority of murine studies use only male mice (to remove sex as a variable), and could therefore miss important

and relevant results in the female animals. Sex differences in disease development (seen in many diseases such as liver cancer[334] and autoimmune diseases [335]), as well as the differences in male and female drug metabolism [336], further shows the need to study both sexes both *in vivo* and in clinical trials.

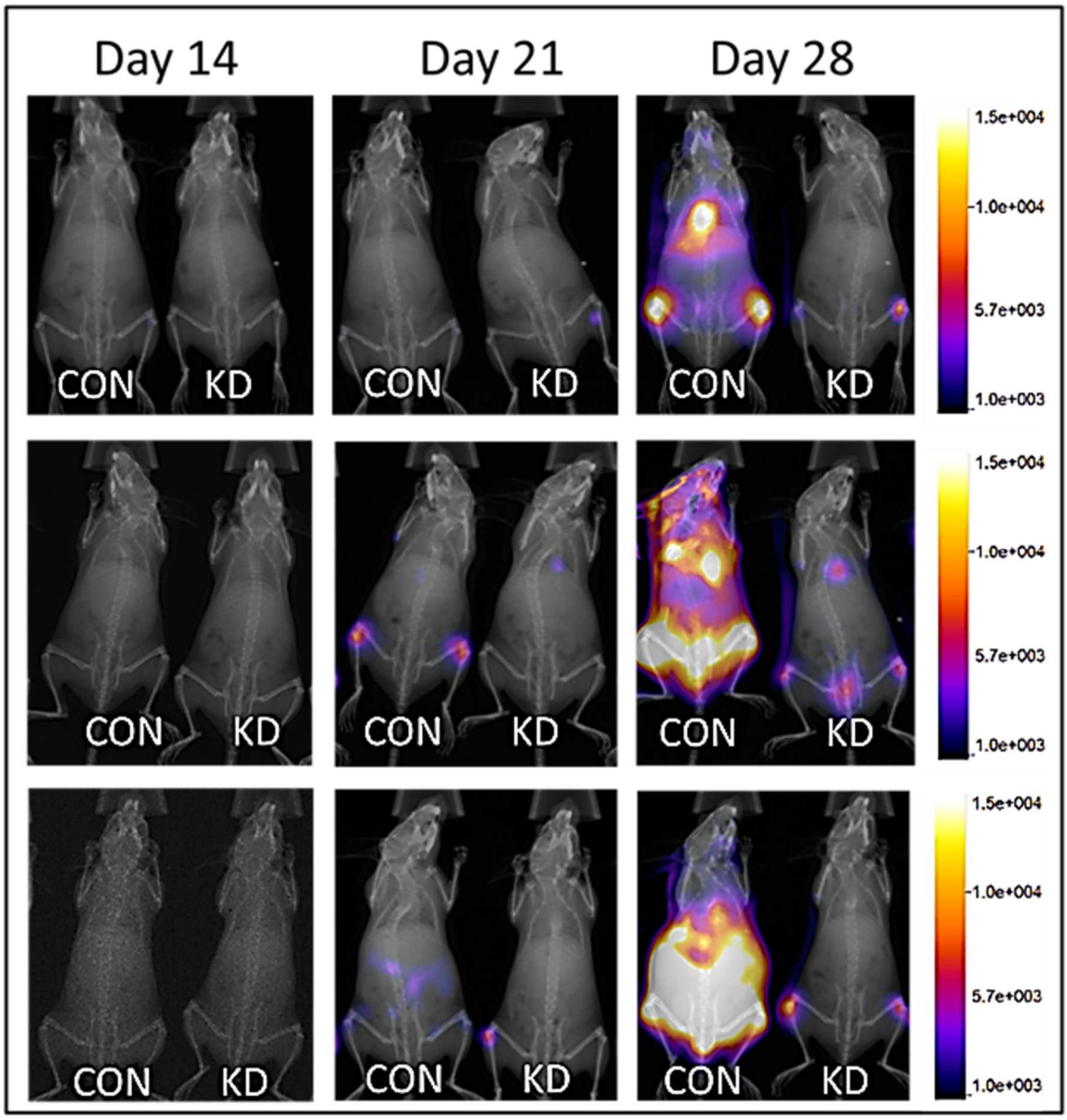

Figure 5.2.14 – MIF knockdown decreases MM disease burden *in vivo*.
NSG mice were injected with 1 x 10^6 MM.1S ShE control or MIF KD cells via lateral tail vein IV injection. MIF KD animals showed decreased disease burden when compared to the control KD. Control group: n = 10, MIF knockdown group: n = 8. Disease burden was monitored weekly via bioluminescent imaging. Images from 6 representative mice displayed (3 per condition) to show progression of disease.

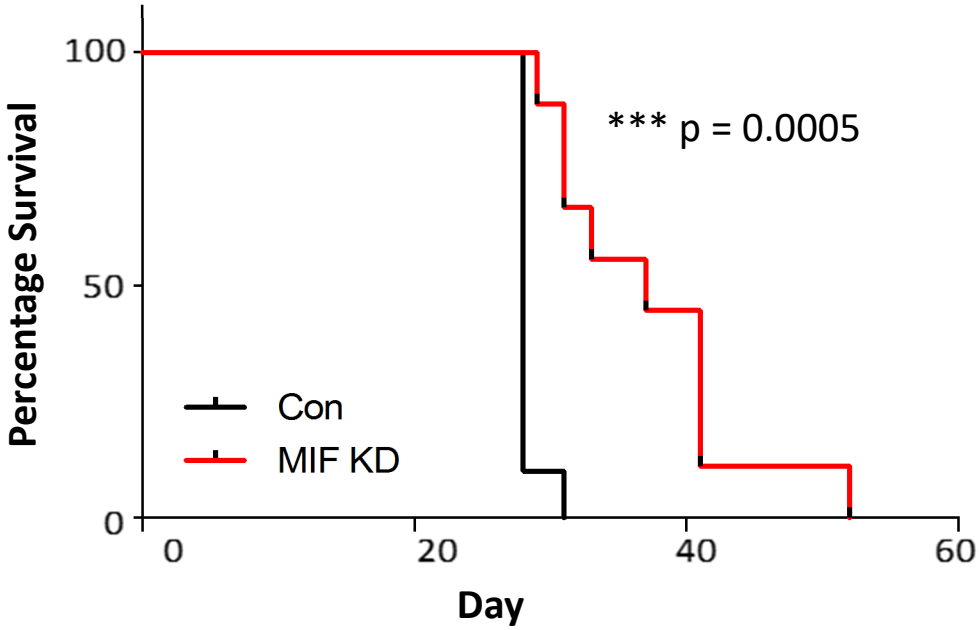

Figure 5.2.15 – MM MIF knockdown increases animal survival.
Kaplan-Meier curve showing increased survival in MIF knockdown group. Mantel-Cox regression (Graphpad Prism software) was used for statistical analysis, n = 18.

To confirm human MM cell engraftment, at endpoint mouse bone marrow was harvested and stained for human CD38 and CD45 and analysed using flow cytometry (see Figures 5.2.16 – 5.2.17). Two MIF KD samples were not available for analysis.

As expected, no differences in MM BM engraftment was seen in the two groups at end-point, suggesting mice humanely sacrificed at comparable disease burden. MM cell presence in the spleen was also analysed, as a marker for disease metastasis. In the control group, average presence of $CD38/45^{+}$ cells in the spleen was approximately 70% (although in one case a very low proportion of malignant cells was observed). However, two thirds of the MIF knockdown group showed a much reduced engraftment to the spleen, with the whole group only achieving approximately 35% malignant cells – suggesting a role for MIF in the establishment of secondary tumour sites.

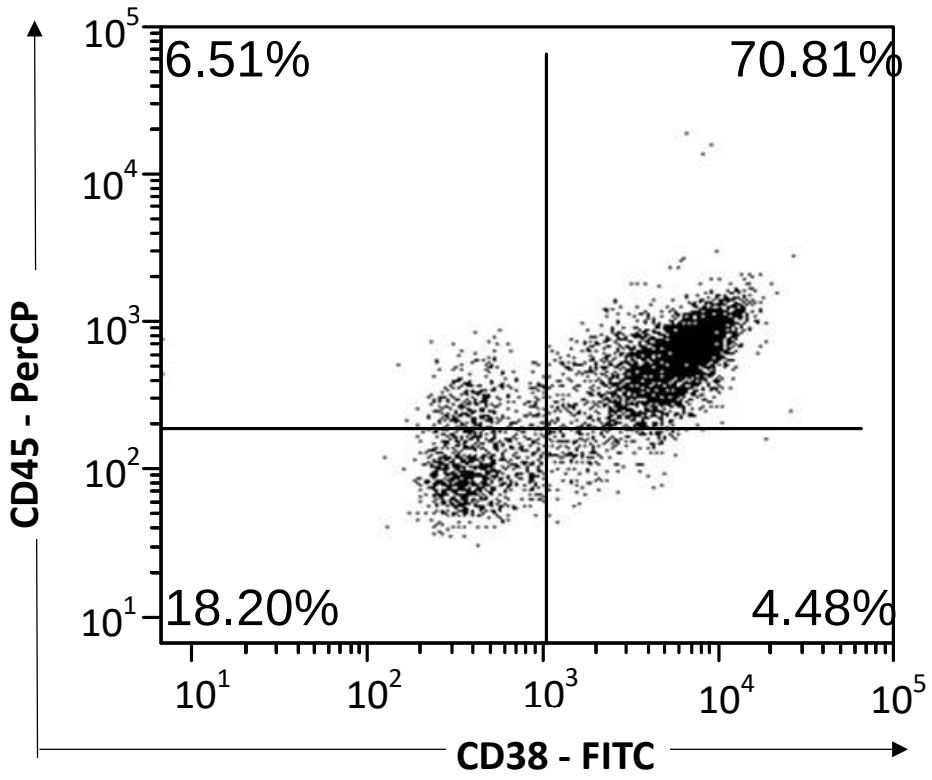

Figure 5.2.16 – Representative flow cytometry analysis of mouse BM showing levels of engraftment.

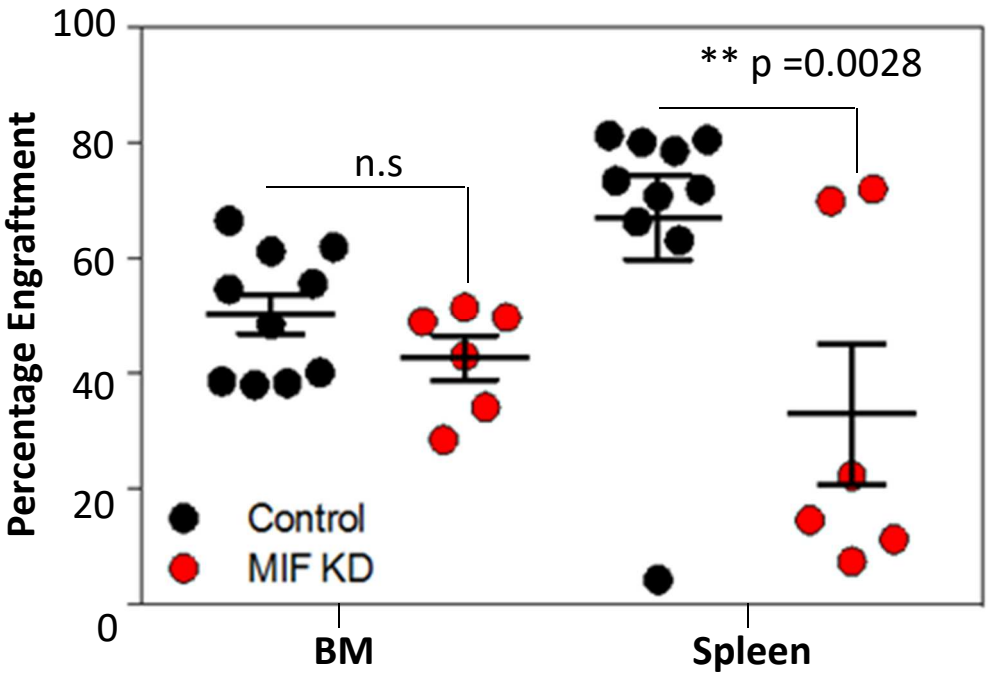

Figure 5.2.17 – MIF knockdown inhibits secondary site metastasis in NSG mice.
Percentage of CD38/45^{+} cells engrafted in mouse, as analysed by flow cytometry. BM engraftment does not vary between groups, but metastasis to the spleen is reduced with MIF knockdown. Error bars show S.D of mean, **p = 0.0028; Mann-Whitney U test.

5.2.6 – Mechanism of IL-6/IL-8 activation in BMSCs

To identify the potential mechanism of action by which MIF causes IL-6 and IL-8 activation in BMSCs a panel of common pathway inhibitors was used. Primary BMSC were pre-treated for 30 minutes with either a vehicle control, Bortezomib at 10nM (a proteasome inhibitor), PS1445 at 100nM (a NF-κB inhibitor), Lenalidomide at 500nM (inhibits various pathways, including the PI3K pathway), SP600125 at 10μM (JNK pathway inhibitor), or JQ1 at 500nM (shown to inhibit cMyc [337]). Following this, the BMSC were stimulated with 100ng/mL MIF for 2 hours (with the control group subject to vehicle control). RNA was extracted and transcriptional levels of IL-6 and IL-8 were analysed via RT-qPCR (Section 2.9, ΔΔCt method used for analysis with a β-Actin control). Results from experiment (performed by S. Rushworth, UEA) are shown in Figure 5.2.18.

When compared to the unstimulated control, BMSC IL-6 was shown to be highly upregulated in response to SP600125 (approximately 15X higher expression). This result was unexpected as inhibition of JNK has previously been shown to an increase in IL-6 synthesis [338], however this result was shown in osteoclasts and no data was shown in BMSC. In response to Bortezomib, IL-8 levels were also dramatically increased. This effect has been shown previously in prostate cancer [339], and has been attributed to an increased IKKα-dependent p65 recruitment to the IL-8 promoter (as no other NF-κB genes appear to be affected).

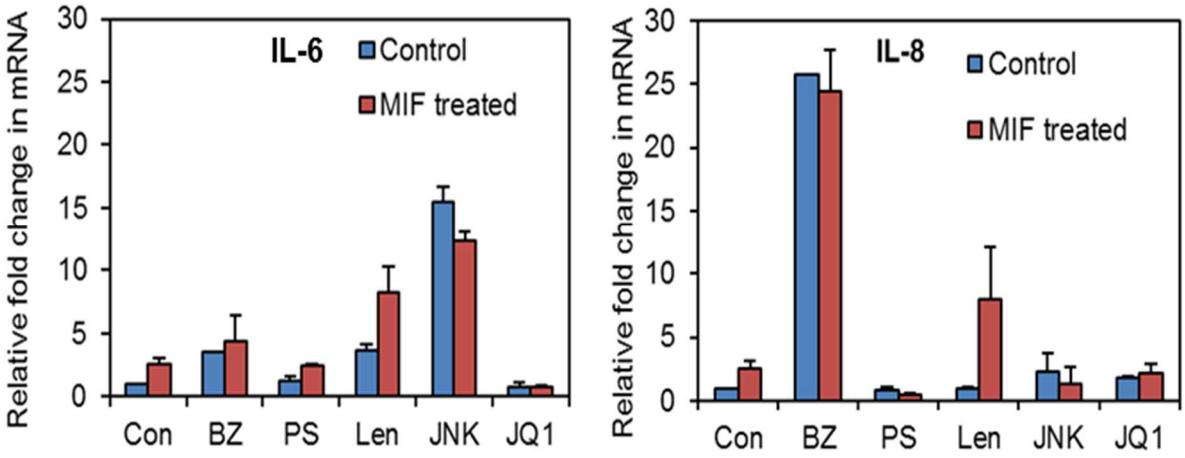

Figure 5.2.18 – Common MM therapeutics used to identify possible MIF-stimulated pathways indicated a role for cMYC.
MIF induces the transcription of both IL-6 and IL-8. Negation of this increase is only seen when using the c-Myc inhibitor JQ1. Bortezomib (BZ), PS1445 (PS) and Lenalidomide (Len), SP600125 (JNK) all show IL6/8 increase or decrease. Experiment performed by S. Rushworth (Norwich Medical School, UEA, UK).

In terms of MIF stimulation, the control group IL-6 and IL-8 levels were once again shown to be increased when incubated with MIF. IL-6 levels were shown to further increase in the Bortezomib, PS1445 and Lenalidomide (which also showed a large transcriptional increase in IL-8) treated groups, showing that these pathways are unlikely to be involved in MIF stimulated BMSC IL-6 production. In regard to IL-8 transcription, MIF stimulated effects appeared to be negated in several of the drugs tested, including Bortezomib, PS1445 and JQ1.

From all of the inhibitors tested, only JQ1 showed negligible changes in IL-6/IL-8 between control and MIF stimulated groups. This indicated a potential role for the transcription factor c-Myc in the regulation of IL-6 / IL-8 in the MIF stimulated BMSC.

5.2.7 – cMYC inhibition in primary BMSC reverses MIF stimulated IL-6 and IL-8 transcription

Primary BMSC samples (n = 3) were stimulated with 100 ng/mL of MIF and subsequently treated with a vehicle control or the cMyc inhibitor JQ1 (at 1µM or 5µM) for 2 hours. Following this incubation, RNA was extracted from the BMSC and analysed using RT-qPCR (Figure 5.2.19). At both JQ1 concentrations used (1µM and 5µM), IL-6 (A) and IL-8 (B) inhibition was achieved, indicating a role for cMyc in the regulation of these cytokines.

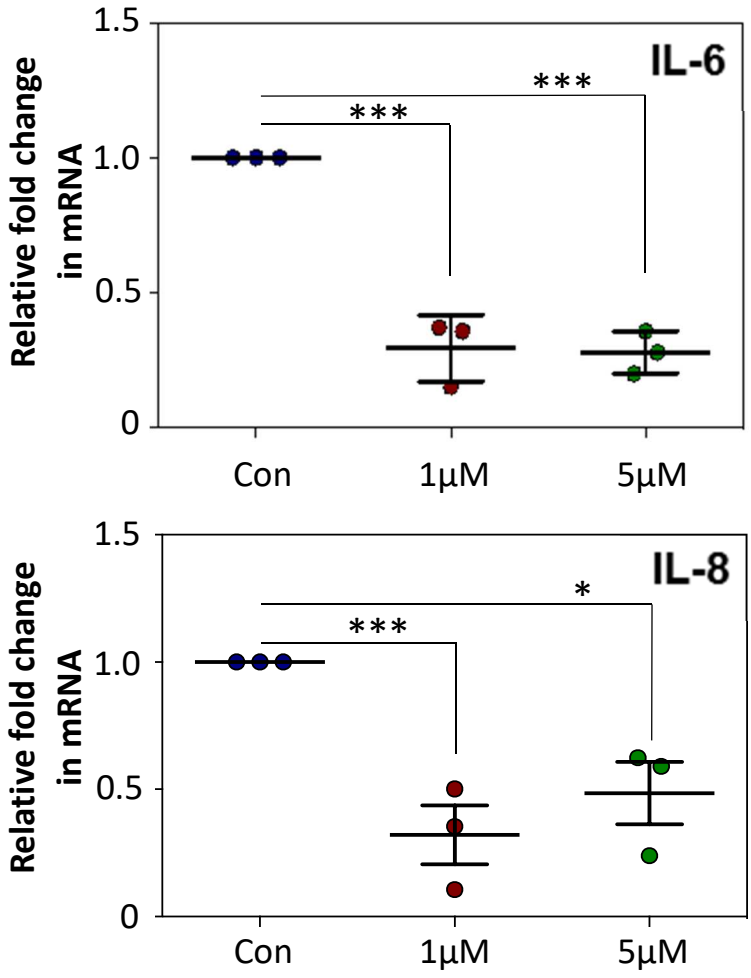

Figure 5.2.19 – Pharmacological inhibition of cMyc results in the reversal of MIF-induced IL-6/8 transcription in BMSC.
MIF stimulated primary BMSCs (n = 3) were incubated with JQ1 and analysed for relative IL-8 and IL-8 gene expression. Expression was normalised to β-Actin. Error bars show S.D of the mean; Mann-Whitney U test, *p<0.05, ***p<0.001.

5.2.8 – Lentiviral cMYC inhibition in BMSC

To confirm results achieved using JQ1, lentiviral particles to target cMYC were generated and used to transduce primary BMSCs (see Section 2.10). BMSCs were seeded onto 12 well plates and grown until approximately 50-60% confluent after which media was replaced and cells were subject to transduction at MOIX10. Despite many attempts, only a 20-30% knockdown of cMYC was achieved in the 7 primary BMSC samples that were transduced (with one sample not showing any significant reduction in expression at all). Even with this modest reduction in cMYC expression, both IL-6 and IL-8 transcriptional levels were shown to be affected. However, there is much variation between each sample and sample MM#1116 (which had no detectable change in cMYC expression) still showed a reduction in both IL-6 and IL-8 expression. All results are shown in Figure 5.2.20.

As c-Myc play such an essential role in the growth and proliferation of cells (including its essential role in DNA replication [222]) there is a possibility that cells which experience a more substantial knockdown cannot survive. When trialling other MOIs, I found that higher MOIs actually resulted in a less effective knockdown of cMYC – further adding weight to this theory (preliminary MOI data shown in Table 5.2.1).

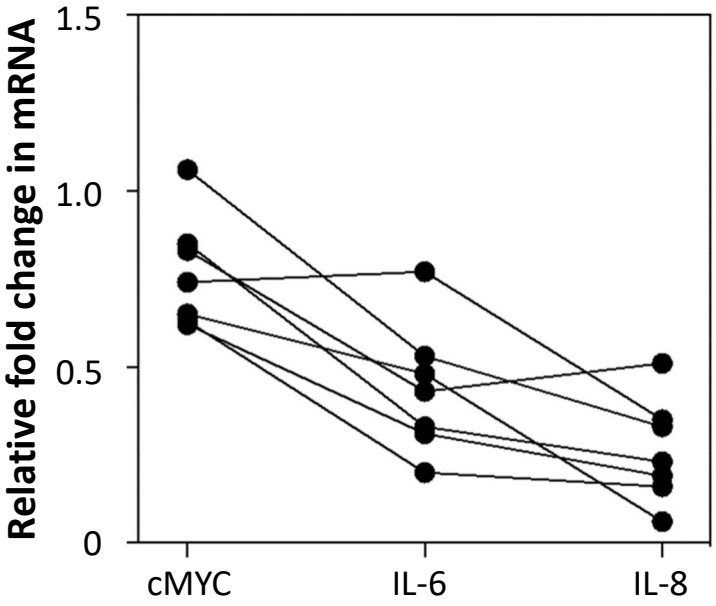

	cMyc	IL-6	IL-8
MM #1109	0.62	0.31	0.19
MM #1112	0.83	0.43	0.51
MM #1114	0.74	0.77	0.35
MM #1113	0.63	0.2	0.16
MM# 1116	1.06	0.53	0.33
MM# 1091	0.85	0.33	0.23
MM #1103	0.65	0.48	0.06
Av. expression	0.77	0.44	0.26
S.D	0.16	0.18	0.15

Figure 5.2.20 – cMYC lentiviral knockdown in primary BMSC was highly variable between samples.
Relative to a ShE control, cMYC knockdown was 20-30% over all primary BMSC samples tested (n = 7). IL-6 and IL-8 transcriptional levels were also reduced overall, however reduction was not proportional to cMYC knockdown.

		MOIX		
		5	10	20
MM Sample	#1113	0.77	0.63	1.14
	#1116	0.75	1.06	0.98
	#1091	0.56	0.85	0.94
	#1103	0.66	0.65	0.93

Table 5.2.1 – Lower MOIs resulted in an improved knockdown in BMSCs.

5.2.9 – *In vivo* cMYC inhibition reduces BMSC IL-6 secretion

Although only a modest knockdown of cMYC was achieved in primary BMSCs, a trend in IL-6 / IL-8 reduction was observed. To investigate this further, I decided to use the cMYC inhibitor JQ1 in the treatment of MM xenograft NSG mice and to measure murine IL-6 (mIL-6) serum levels (IL-6 produced by the BMSC and not by the human disease). As IL-8 is unfortunately not present in the murine genome, the effect of cMYC inhibition on the production of this cytokine from the BMSCs could not be tested.

1 x 10^6 U266 luciferase modified cells were injected into the tail vein of 6-8 week old NSG mice and an engraftment period of 2 weeks was allowed. Mice were imaged to ensure equal disease burden and split into two groups, control and treatment (JQ1 at 50mg/kg). Blood samples were taken from all mice at days 0, 14 (prior to any treatment) and 18. Blood serum was analysed using a mIL-6 specific ELISA. A schematic of the experimental design is shown in Figure 5.2.21.

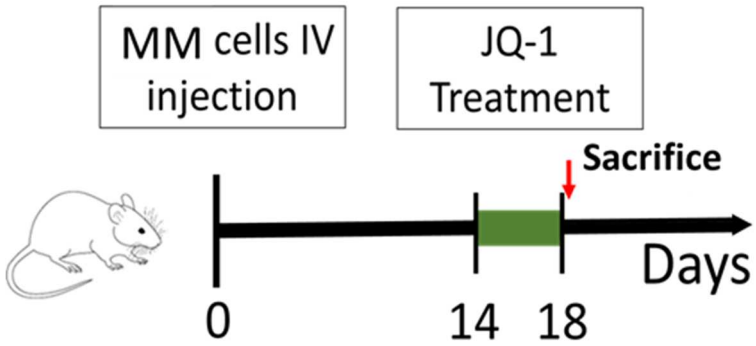

Figure 5.2.21 – Schematic detailing JQ1 *in vivo* experiment.
U266 cells were injected into mouse lateral tail vein (n = 8). At day 14, treatment group received 50mg/kg of JQ1 once daily via IP injection. Bloods were taken at day 0, 14 and 18.

ELISA results (Figure 5.2.22, see Section 2.11 for methodology) showed that prior to MM injection, no measureable level of mIL-6 was detected. Levels were shown to have increased slightly by day 14, as expected with MM disease. By day 18, the control group showed varying increases in mIL-6 – however JQ1 treated mice had levels similar to those seen at day 14. Control mIL-6 levels were shown to be significantly higher than those seen in the treated group.

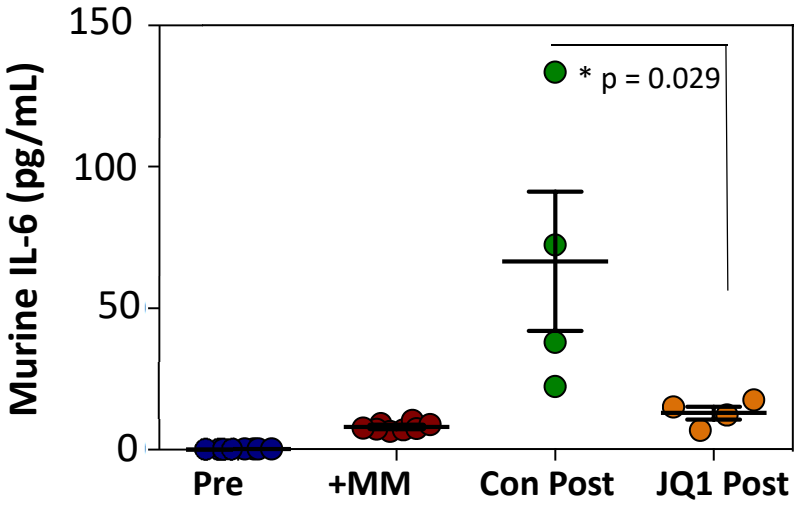

Figure 5.2.22 – Murine IL-6 serum levels significantly lower in the JQ1 treated group. Sera from blood samples (n = 8) was analysed for murine IL-6 content via ELISA, concentration was determined using a standard curve. Error bars show S.D of the mean, *p = 0.029; Mann-Whitney U.

Mice were imaged prior to experiment end point, with no obvious difference identified between control and treatment group's disease burden. 5 days of treatment with JQ1 (at 50 mg/kg/day) was predicted to have no measurable effect on tumour burden (based on the work of Delmore *et al.* [337]), and was chosen to remove tumour burden as an experimental variable (as differences in tumour burden is likely to cause variations in MIF secretion and subsequent BMSC IL-6 expression). Figure 5.2.23 shows that tumour burden between control and treatment groups remains comparable over this time point.

Following end point, mouse bone marrow was removed and BMSCs were sorted ($CD105^{+}$) using a BD FACS Aria II cell sorter (courtesy of Dr Zhigang Zhou, Norwich Medical School, UEA, UK) to test for cMYC and IL6 transcriptional levels. Unfortunately sample volume did not yield large enough quantities of RNA following extraction, and C_t values for tested genes were too high to rule out the possibility of non-specific artefacts.

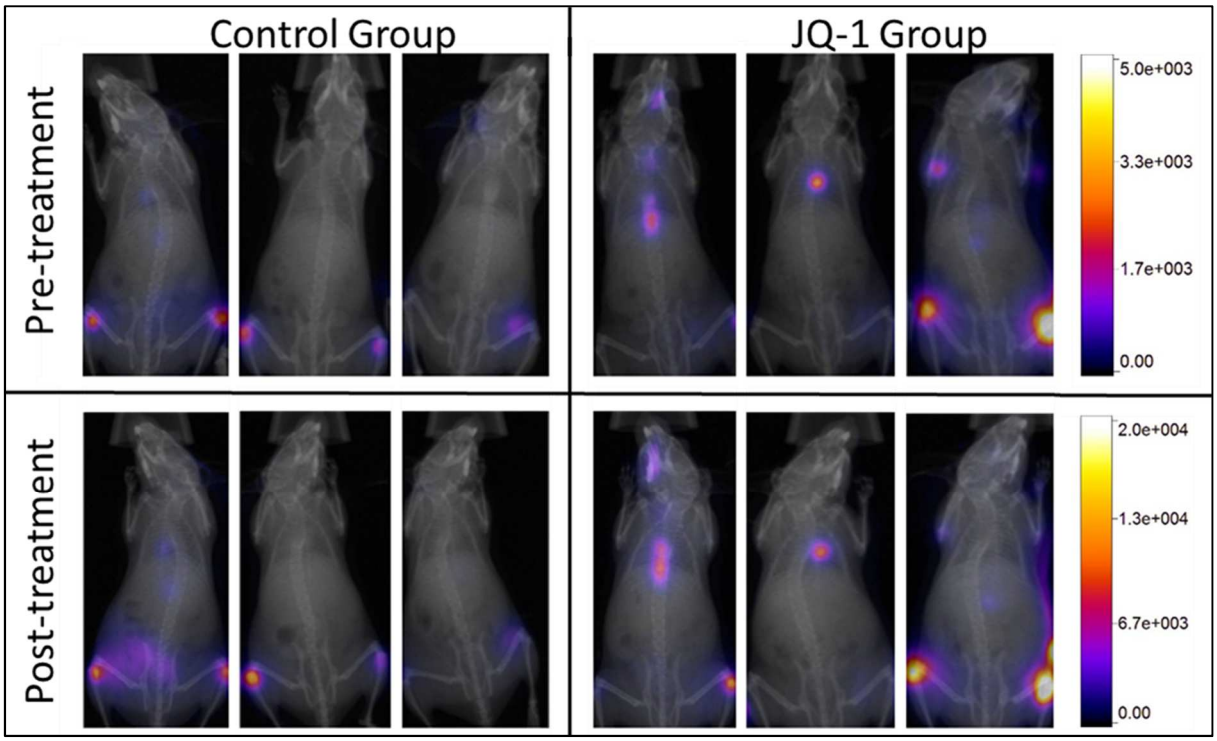

Figure 5.2.23 – MM Disease burden was unaffected by JQ1 treatment
Mice were injected with 1 x 10^6 U266 luciferase modified cells via the lateral tail vein. Following a 2 week engraftment period mice were imaged to ensure equal tumour burden and split into control and JQ1 treatment groups (50mg/kg via IP injection daily, for 5 days). Following treatment, tumour burden between groups was comparable. Changes in serum IL-6 levels can therefore only be attributed to cMYC inhibition. Only males were imaged following treatment.

5.3 – Summary

Despite MIF's prior association with cancers, previous work has investigated the effects of MIF on the malignant cell itself and not its effect on the BMSCs [330]. In this section I have shown how MIF expression and excretion is upregulated in primary MM cells (and further elevated in MM cell lines). I showed that this over-expression is pro-tumoural by its ability to induce both IL-6 and IL-8 secretion from the BMSCs.

cMYC was identified as a potential regulator of this expression within these non-malignant BMSCs with the cMYC inhibitor JQ1 shown to reverse MIF stimulated IL-6 and IL-8 secretion. *In vivo* use of JQ1 led to significantly reduced levels of mIL-6 in the serum, indicating that c-Myc regulates IL-6 level via BMSCs - the primary source of IL-6 production in MM.

In conclusion, the data shown in this section identifies a novel pro-tumoural mechanism that exists between malignant plasma cells and BMSCs, prior to any cell-cell contact. MM derived MIF stimulates the production of IL-6 from the BMSCs which in turn can cause PI3K pathway activation in the MM cell (shown in Section 4, figures 4.2.4-4.2.5). The data presented here provides evidence for a new potential therapeutic target - MIF.

6 – Discussion

6.1 – Overview

Targeting the malignant cells in patients with Multiple Myeloma with the aim of eradicating the disease is not working. Current therapies are highly effective at removing the bulk of disease burden, however a small subset of MM cells will survive within the bone marrow microenvironment and continue to proliferate and grow, resulting in patient relapse. Within this environment, MM is protected by multiple mechanisms including protective cytokines provided by other cells within the milieu and via cell adhesion mediated drug resistance (CAM-DR) or by adhesion to the structural components of its surroundings. A deeper understanding of the MM cell's interactions with its microenvironment is desperately needed to reduce, and ultimately negate, these protective effects.

One of the major pathways that is known to contribute to MM cell proliferation is the PI3K/Akt pathway. This pathway has been implicated in a plethora of solid and haematological malignancies, including MM [303, 340]. Unlike many other cancers, however, MM PI3K activation is most likely caused by the continual signalling from the microenvironment, as the disease typically lacks PI3K pathway associated mutations. Isoform specific inhibition of PI3K (i.e. targeting of the p110α, p110β, p110δ or p110γ catalytic subunits) could provide a more tissue specific approach to treatment, reducing secondary effects. This is critical in MM as it is primarily a disease of the elderly and as such patients can lack tolerability and/or the general fitness needed to endure the adverse effects of some drug regimens. With the p110δ and p110γ isoforms known to be highly enriched in leukocytes, a novel opportunity is provided for the successful inhibition of this pathway in MM disease. The stimulation of PI3K signalling by the microenvironment, however, still remains a problem. It is therefore necessary to not only target the malignancy itself, but also the tumorous microenvironment – targeting the soil as well as the seed.

BMSCs within the BM niche are known to produce cytokines that can activate PI3K signalling. One such cytokine, IL-6, is not secreted in high levels under typical conditions, however the levels of IL-6 have been shown to increase alongside MM disease burden and is marker of poor prognosis. The adhesion of MM cells to the BMSCs has been shown to induce the production of BMSC IL-6 [12]. However, it is possible that MM cells can modify BMSCs even prior to cell-cell contact via cytokine signalling, re-modelling the niche to benefit MM disease progression.

6.2 – Key Findings

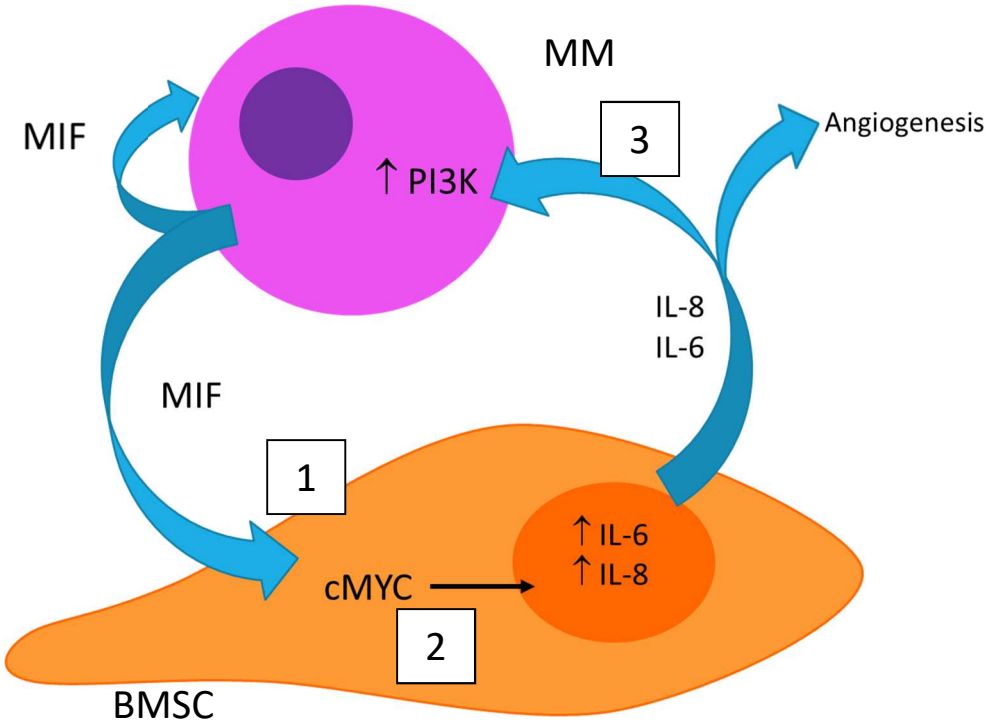

Figure 6.2.1 – Schematic of key findings.
1 – MIF is overexpressed in MM, causing the upregulation of IL-6 and IL-8 in BMSCs. 2 – cMYC is involved in the regulation of IL-6 and IL-8 expression, and inhibition of cMYC results in lower levels of these cytokines. 3 – The PI3K pathway is critical in MM disease and is upregulated by IL-6. Inhibition of PI3K p110δ/γ isoforms results in increased overall survival (OS) *in vivo* and less invasive disease type.

1. MM derived MIF re-modelling of the microenvironment

One of the primary objectives of this study was to determine if MM could influence its microenvironment, to benefit disease progression. The cytokine arrays I initially utilised to detect variations in primary MM-BMSC co-culture indicated a large net increase in several different cytokines, and of these both the IL-6 and IL-8 increase was shown to be statistically significant in the three primary MM samples tested. Macrophage migratory Inhibitory Factor (MIF) was identified as a possible mechanism by which MM cells could signal the BMSCs to initiate these changes, due to the aberrantly high levels found in MM monoculture and lack of production from primary BMSCs. Other proteins were also identified as potential BMSC signallers (such as MMP-9 and Chitinase-3-like-1), however expression of these proteins varied widely between the patient samples tested – unlike the consistently high secretion of MIF. Recombinant MIF was used to stimulate primary BMSCs and I observed an increase in both the transcriptional level and extracellular protein concentration of both IL-6 and IL-8 (confirming the results seen in co-culture cytokine array experiments). This increase was shown to be proportional to the stimulatory effects induced in a non-contact (transwell) MM-BMSC co-culture.

MIF is a cytokine associated with various roles - including pro-inflammatory signalling, lymphocytic immunity, and endocrine functions [341]. It is a homo-trimer (see Figure 6.2.2) and all mammalian MIFs (including human, mouse, rat and cow) have approximately 90% homology and it has been shown to promote B-cell chemotaxis via the co-operative efforts of its receptors [342]. MIF was one of the first cytokines characterised, during experiments investigating delayed type hypersensitivity reaction in the 1960s [343, 344], and over the following decades was described to be involved in a range of macrophage functions. Elevated levels of MIF have previously been detected in a selection of other cancers with high levels of MIF frequently associated with a poor patient prognosis [345-347]. However, the relationship between MIF and tumour progression is potentially more complicated than first realised, with MIF shown to work in both a paracrine and an autocrine fashion [348-350]. Furthermore, in a study by Verjans *et al*. extracellular MIF was shown to be pro-oncogenic (as found in other studies), however patients who had high levels of cytosolic MIF were actually shown to have a significantly improved OS [351].

Unravelling the relationship of this cytokine with the BMM and tumorigenesis could provide a novel target for the treatment of haematological cancers, including MM.

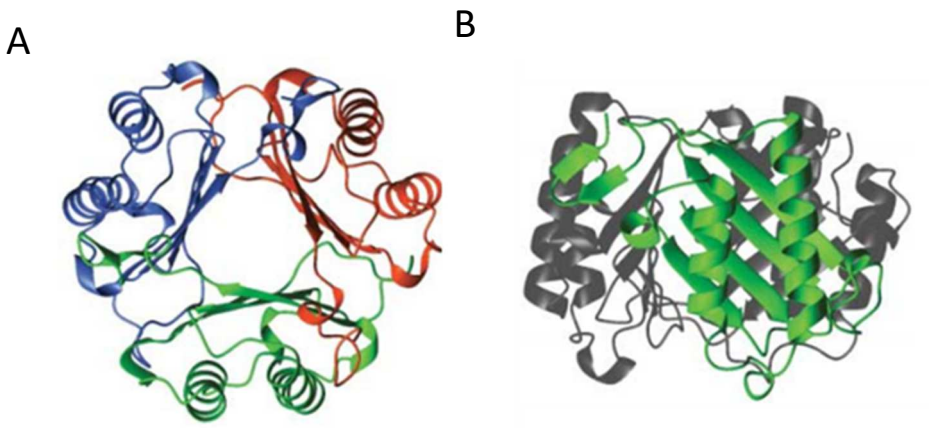

Figure 6.2.2 – Three dimensional structure of MIF.
(A) Top view (B) Side view. Image adapted from Calandra and Roger, 2003 [352].

My results showed that, *in vivo*, MIF KD in MM cells resulted in a reduced tumour burden and increased survival time in NSG mice. Moreover, engraftment of malignant cells to the spleen (used as an example of secondary site metastasis) was significantly reduced upon MIF KD – identifying a potential role for MIF in MM cell migration. MIF has previously been identified as an activator of CXCR4 [353], and MIF produced by colon carcinoma cell lines has been shown to stimulate this GPCR on the colon cell itself, causing an increase in malignant cell invasion and metastasis [354]. With both MM cells and BMSCs known to express CXCR4, it is likely that MIF is working in both an autocrine and paracrine manner in MM disease – activating signalling cascades within the MM cell, whilst at the same time playing an active role in MM cell mobilisation and invasion (alongside CXCR4/SDF-1 signalling). In hindsight, testing the role of MIF in the migration of MM cells *in vitro* would have been of interest.

Whilst the elevated MIF levels that I measured in Section 5 were in agreement with data collected by Zheng and colleagues [330], the decreased rate of tumour growth I observed was not. Zheng *et al*. observed that MM MIF KD cells had reduced levels of BM engraftment and retention with no real effect on MM cell proliferation, instead

forming large solid tumours within the abdomen. Despite my results also showing a difference in initial BM engraftment, I found (using the same cell line) that the growth of the tumour burden was retarded with no solid tumours located within the abdomen at end point. Although my findings differ to those in the study mentioned above, they are in fact in agreement with the trends observed in other cancer types, where MIF deficiency was associated with a decreased tumour burden [355, 356]. This potentially gives a more consistent description for the role of MIF in disease progression.

MIF has previously been implicated in the regulation of IL-6 in severe inflammatory responses [357] as well as having been shown to induce IL-6 and IL-12 production in macrophages [358]. Therefore the association of these cytokines with MIF is not a new concept [359]. Despite this, the MIF stimulated production of IL-6 that I observed has not previously been described in BMSCs in any haematological malignancy. Given the importance of IL-6 in MM disease progression as well as its role in the production of osteoclasts (and subsequent osteolytic lesions), this result alone warrants further investigation into MIF's role in the MM microenvironment. Chauhan *et al.* has previously shown that adhesion of MM cells to the BMSCs stimulates the secretion of IL-6, however no detectable increase was shown when measuring IL-8 [12]. Despite this, the production of IL-8 from MM patient BMSCs has been shown to be higher than that of BMSCs from healthy donors and increased serum levels of IL-8 have been reported in MM patients [360, 361]. IL-8 if most frequently associated with elevated levels of angiogenesis, and has also been shown to increase with MM disease [361], however the exact mechanism by which BMSCs IL-8 increase occurs is not clearly defined. My results showed that alongside IL-6, IL-8 was also stimulated by MM derived MIF, a result that is in agreement with a recent study by Abdul-Aziz *et al.* who showed that AML derived MIF was responsible for the increase in IL-8 from AML patient BMSCs [362].

Since my data has shown that MIF induces both IL-6 and IL-8 in the MM BMM, I believe that it provides the rationale for the investigation of MIF inhibitors for MM in a clinical setting, potentially removing the need for separate anti-IL6/IL8 therapies. Furthermore, MIF has been shown to inhibit the cell cycle checkpoint protein p53 by directly stimulating the PI3K/Akt pathway in several different cell types [363, 364].

Assuming that this is also true for plasma cells, targeting MIF is potentially a multi-pronged attack; preventing MIF from stimulating PI3K directly in the malignant cell and also by reducing BMSC IL-6 secretion (and subsequent PI3K activation). In retrospect it would have been of interest to test the expression of p53 in both MM control and MIF kd cells. However, despite the established association of MIF and tumorigenesis and the MIF antagonist ISO-1 being highly utilised in pre-clinical studies, I found no record of this compound (or other MIF inhibitors) being tested in clinical trials. Anti-MIF monoclonal antibodies, however, have proven highly effective pre-clinically and clinical trials of these antibodies are currently underway with Phase I studies completed in 2016 [345]. Although in their infancy, these studies seem to be targeting solid tumours in patients (such as rectal adenocarcinoma and prostate cancer) and no current investigations into the benefits of anti-MIF antibodies for the treatment of haematological malignancies are being performed.

Targeting the MIF receptor CD74 is another potential way in which the effects of MIF could be limited, and has shown promising results in pre-clinical investigations [365, 366]. Phase I/II clinical trials of the anti-CD74 antibody milatuzamab (also known as hLL1) have already been completed in a variety of B-cell malignancies and has shown to have high tolerability [367]. However, it remains to be seen if these antibodies result in a reduced disease burden as MIF is known to have a variety of other receptors (including CD44 and the co-receptors CXCR2 and CXCR4 [368]). Considering the elevated MIF levels displayed in MM (as well as the benefits of MIF knockdown myself and others have shown) it would be pertinent to see if this treatment would benefit MM patients alongside current treatment regimens.

MIF was not the only cytokine shown to be elevated in my cytokine array analysis of MM and therefore there is scope for other potential BMM effectors. Chitinase-3-like-1 (CHI3L1, also known as YKL-40), monocyte chemoattractant protein 1 (MCP-1, also known as CCL2), MMP-9, osteopontin and Serpin-e1 were all shown to be highly expressed by MM cells at varying levels. All of these cytokines have previously been implicated in angiogenesis [242, 369, 370] and have also been associated with a variety of other disease beneficial mechanisms. For example, MM cells are known to secrete MCP-1 when stimulated by IL-6 [371], and MCP-1 has been shown to play an

important role in the recruitment of macrophages into the tumour microenvironment, contributing to MM drug resistance [372].

MMP-9 has previously been shown to degrade collagens and fibronectin [373] and the high levels of MM derived MMP-9 shown in this study potentially highlights the ability of these cells to invade both the stroma and the sub-endothelial basement membrane. Further to this, a study by Barillé *et al.* revealed that MMP-9 was produced consistently by MM cells (with no measurable levels detected from BMSCs), and this secretion was not effected by any cytokine or hormone tested [240], although it was slightly elevated in co-culture. Elevated levels of osteopontin have previously been reported in MM patients in a study by Standal *et al.* [374]. They found that not only was osteopontin produced by both MM cells and BMSCs but that MM cell lines actually adhered to osteopontin, implicating a role for this cytokine in the retention of MM cells to the bone marrow.

Serpin-e1 (also known as plasminogen activation inhibitor-1, PAI-1) is a serine protease inhibitor, and the elevated levels found in my work are in agreement with previous studies in MM [375]. These increased levels of serpin-e1 may be due to genetic variants in the SERPINE gene, which have been associated with an increase in risk of MM [376], however no correlation was found in the cited study. Indeed, despite the known pro-cancerous effects of these cytokines, little has been done to investigate their interactions with the BMSCs. Perhaps of greater interest to myself and others are the cytokines that are upregulated in response to MM-BMSC co-culture.

In Section 5, I showed how co-culture of primary BMSC and MM cells changes the cytokine profile to increase the availability of both IL-6 and IL-8 in comparison to BMSC and MM cell monocultures – however these were not the only cytokines which were upregulated. EGF and VEGF were both shown to increase upon co-culture (however these results were not statistically significant with the sample size used). Increased VEGF has been synonymous with cancer for decades, upregulated by either oncogene expression, cytokine signalling, or hypoxia - and as such its increased level in co-culture was not unexpected. VEGF plays a crucial role in tumour vascularisation, with high levels of angiogenesis needed to maintain malignant cell growth. This remains true in Myeloma, where it is produced by the MM cell and has been shown

to not only increase levels of angiogenesis, but also stimulates microvascular endothelial cells to secrete IL-6 [377].

EGF showed a drastic increase in concentration (approximately a 7 fold increase), but this elevation was highly variable between patient samples. The EGF family have previously been implicated in MM disease progression, with heparin-binding EGF (HB-EGF) a known growth factor for malignant plasma cells [378]. Interestingly, HB-EGF is not expressed by mesenchymal BMSCs however its receptor, EGFR-1, is expressed (receptor is also known as HER-1 or Erb-B1). Upon EFGR-1 stimulation, BMSCs have been shown to proliferate more rapidly without differentiating [379], in a dose dependent manner. The BMSCs inability to differentiate could also mean that the MM cell is effectively preventing the formation of osteoblasts and subsequently preventing bone repair (further exacerbating MM symptoms). As EGF also binds to the same receptor as HB-EGF, it would be logical to conclude that the increased production of EGF from either the MM cell or BMSC (as both were shown to have similar levels in co-culture), could also cause this increased arrest in BMSC differentiation and increase in proliferation. On reflection, it would have been of interest to see if there were similar increases in other members of the EGF family, unfortunately the cytokine arrays used only measure EGF from this particular group of proteins.

2. cMYC regulation of MIF induced IL-6 and IL-8

To determine the potential mechanism by which MIF acts to increase IL-6 and IL-8 within the BMSCs, a panel of common pathway inhibitors were used (a proteasome, NF-κB, PI3K/AKT, JNK and c-Myc inhibitor were all tested). In these experiments, cMYC was identified as a potential instigator for these increases. Use of the cMYC inhibitor JQ1 resulted in the reversal of both IL-6 and IL-8 increased transcriptional levels seen in MIF stimulated BMSCs and this reduction was confirmed in 3 other primary BMSC samples. To confirm the role of cMYC, I attempted to KD cMYC RNA in primary BMSCs, however the KD achieved was too modest to be considered for experimentation. I believe that the lack of successful KD in these samples may have been due to the critical role that cMYC plays in the growth of the majority of cells. As

only a modest KD of cMYC was achieved in primary BMSCs, I instead chose to use an *in vivo* model to assess cMYC inhibitory effect on IL-6 levels. *In vivo* testing of JQ1 was unfortunately limited to IL-6 only analysis, due to the lack of IL-8 gene (and its receptor CXCR1) present in the murine genome [380]. cMYC inhibition via treatment with JQ1 was shown to significantly decrease murine IL-6 serum levels in established disease. Overall, I showed that MM derived MIF can stimulate IL-6 and IL-8 production in BMSCs via cMYC, both *in vitro* and *in vivo*.

Others have shown that JQ1 treatment reduces tumour burden and survival of NSG mice transplanted with MM cells [381]. Although BMSC are often cyto-protective in the context of anti-MM therapy, in this study the authors observed that the sensitivity of MM cell lines to JQ1 is largely unchanged by the presence of HS-5 cells (a BMSCs cell line). Furthermore, the authors show that less than 7 days of JQ1 treatment (at 50 mg/kg IP daily) was predicted to have no measurable effect on tumour burden [381]. In my study, I designed the experiment so that this dosage was used to control for the effects that reduced tumour burden may have on MM MIF secretion and subsequent BMSC IL-6 expression. NSG mice were IV injected with U266 MM cells, and the treatment group was administered with JQ1 for 5 days. As expected, 5 days of JQ1 treatment showed little difference in MM disease burden (as measured by BLI) between the two groups of animals. However, despite similar tumour burden, murine IL-6 was significantly reduced in the JQ1 treated animals (carrying human MM) compared to vehicle control treated animals. This result shows that not only is the fall in murine IL-6 levels independent of the effects of tumour burden, but that the JQ1 c-Myc inhibition is exerting it's anti MM activity by inhibiting BMSC IL-6 transcription. This result may also help to explain why BMSCs do not appear to offer MM protection from JQ1 therapy.

Unfortunately, due to the non-elevated expression of cMYC coupled with its ubiquitous nature, targeting this transcription factor for therapeutic purposes would not be a simple option. This is perhaps why clinical studies investigating c-Myc inhibition are either very much in their infancy (with NCT02157636, NCT02757326 and NCT01943851 only now recruiting for Phase I studies), or have been terminated prematurely (NCT02110563). Interestingly, there may already be a MM drug that helps to combat BMSC c-Myc. Bortezomib (BZ) is a highly effective drug in the

treatment of haematological malignancies, including MM. Until lately, the exact mechanism by which this drug works was poorly understood, although previous studies have shown that BZ can induce apoptosis by blocking of the NF-κB pathway (detailed in Section 1.1.5). As well as this, a recent study by *Suk et al*. showed that another way by which BZ can inhibit malignant cell proliferation is by the downregulation of c-Myc expression, and this was shown in Burkitt's lymphoma cells [382]. It is therefore possible that BZ's efficacy in MM is not only due to its effect on the malignant cell, but via the reduction of extracellular IL-6. Unfortunately, the effect of BZ on other cells within the microenvironment was not considered in this study and without the benefit of determining where the serum IL-6 originates in clinical trials (as I was able to do in a murine-human xenograft model) it will be difficult to determine which cell population cMYC inhibition is affecting.

3. PI3K p110δ and p110γ isoforms are targetable in MM

In Section 5 I showed how MIF stimulation of BMSCs significantly increased the levels of BMSC IL-6 production, which is pivotal in MM disease. In Section 4, I showed how both BMSC conditioned media and IL-6 on its own can stimulate previously low levels of activity in the PI3K pathway within MM cells. In the bone marrow microenvironment, MM cells will be continuously subjected to this stimulation, accounting for the increased levels of PI3K activity reported in other studies [303] (even when genetic abnormality in PI3K related genes is lacking). Aberrant PI3K signalling has long been a hallmark of cancer, however pharmacological attempts to reverse this oncogenic pathway have the potential to effect multiple tissue types, due to the ubiquitous nature of PI3K signalling. Recently, there has been significant progress made in the production of PI3K inhibitors that can differentiate between the four class I PI3K isoforms (which have been frequently linked with cancer). As the p110δ and p110γ PI3K isoforms are preferentially expressed by leukocytes, this provides the opportunity for a more targeted treatment which could have the potential to be highly effective in several blood cancers, including Multiple Myeloma [288, 290].

IPI-145 (brand name Duvelisib) is one such drug that has shown high affinity for the treatment of haematological malignancies, as it targets both the p110δ and p110γ PI3K subunits. At present it is not used clinically, however Phase III trials are currently underway for the use of this drug in the treatment of diseases such as CLL and follicular lymphoma (NCT02004522, NCT02049515). It is currently unclear how effective IPI-145 will be in any form of advanced disease, as the only clinical trial that was specifically focused on this was prematurely terminated to 'focus resources on studies which can potentially enable the registration of duvelisib' (NCT01476657). The use of this drug for the treatment of MM patients is not currently being investigated.

My data showed that not only are p110δ and p110γ expressed in patient derived MM samples, but that use of the dual inhibitor IPI-145 was more beneficial than single isoform inhibition *in vitro*. Single isoform inhibition was achieved using the drugs CAL-101 and CZC24832. CAL-101 (also known as Idelalisib) is a selective p110δ inhibitor that has been shown to be highly effective at reducing downstream Akt activation in both CLL and Mantle Cell Lymphoma (MCL) at as little as 0.1μM concentration [211] and is already in clinical use for the treatment of CLL (according to current NICE guidelines). In MM, despite showing preclinical potential by Ikeda and colleagues [290, 303], the use of CAL-101 has not been taken forward to clinical trials – possibly as the prior *in vivo* experiments failed to take into account the effects of the BMM (with authors instead investigating sub-cutaneous tumours). Indeed, the concentrations of CAL-101 needed to produce a similar levels of inhibition in MM cells is far higher than that needed in CLL cells (greater than 10 fold increase).

CZC24832 was the first p110γ inhibitor developed and shows great selectivity (greater than 10 fold over other isoforms), however the authors describe that further optimisation of the drug would be needed to take it to clinical trials. Since conducting my study, a new p110γ inhibitor has been developed [383] that is highly specific (with greater than 100-fold selectivity over the other p110 isoforms). This drug could have proven useful in clarifying the role of p110γ in primary MM cells, as lentiviral modification of these cells is not possible.

My results showed that in MM, the use of IPI-145 (in comparison to both a control and single isoform inhibition) resulted in significant reduction in cell viability as well as an increased level of cell apoptosis in both monoculture and when co-cultured with BMSCs. I also found that for the reduction of MM cell adhesion to BMSCs, both isoforms needed to be inhibited to produce a significant result. MM is not the only condition in which dual inhibition of these isoforms has been shown to be the most effective, with it also being shown in an antibody-induced arthritis model [384].

Interestingly, lentiviral knockdown of p110γ was sufficient to significantly reduce MM-Fn adhesion in both of the MM cell lines tested. Although this result was not mirrored when measuring primary MM cell adhesion to Fn, this may be due to pharmacological inhibition not being as effective as lentiviral suppression of p110γ expression. Despite this, the data shows a potentially unique role for p110γ in MM cell adhesion and as such provides further evidence for the use of dual inhibitors over p110δ only inhibitors (such as CAL-101 or TGR-1202). Whereas MM cell adhesion results suggested a prominent role for p110γ, MM cell migration towards media containing SDF-1 was only reduced with dual inhibition showing that both of these isoforms play a critical role in this process. Although a role for p110α has previously been identified in ovarian cancer cell and endothelial cell migration [385, 386], this is the first time that the p110δ and p110γ isoforms have been implicated in the migration of MM cells.

The expression of the differing PI3K isoforms in both MM cell lines and primary cells has been a contentious issue, with varying expression seen in the same cell lines between different studies [278, 340]. As such, I measured the expression of both p110δ and p110γ in all the MM cell lines and primary samples that I used and found that both isoforms are expressed in all cells tested at slightly varying levels. To test the roles of the isoforms *in vivo*, both p110δ and p110γ knockdown was performed on U266 cells (via the PIK3CD and PIK3CG genes respectively). This cell line was selected due to the similar levels of expression seen in both subunits, mirroring what was observed in the primary MM samples tested. At end point, results showed similar levels of reduction in tumour burden and increase in OS, in comparison to an ShE control. No extra benefit was seen with a double knockdown in terms of OS during this time frame. The increase in OS observed is in agreement with a recent study by

Sahin *et al.*, who showed that only p110α knockdown had no effect on survival *in vivo* [278]. However, the highly reduced tumour burden I saw in my PIK3CG knockdown had not been observed before, and perhaps is instead indicative of its role in MM cell adhesion (seen *in vitro*) which would correlate with the reduced levels of MM cells engrafting to the bone marrow. Although the efficacy of IPI-145 in the treatment of CLL and AML [387, 388] has previously been shown, preclinical investigations for the use of this drug in MM have not been performed. Here, my data shows that with only 7 days of IPI-145 treatment (at 15mg/kg via IP injection) the increase in MM tumour burden can be significantly reduced in established disease. This in turn led to a significant increase in overall survival, which could potentially be amplified further with an increase in treatment duration.

Throughout my study, IL-6 has played a key role in MM disease and it would be reasonable to suggest that therapeutic targeting of this cytokine could prove highly effective. Unfortunately, all attempts to negate the effects of IL-6 in Myeloma have thus far proven ineffective with current clinical trials showing no difference in patient OS when an IL-6 inhibitor is used alongside the standard treatment regimen [389, 390]. It may therefore be necessary to target the source of the IL-6 upregulation (using an anti-MIF antibody for example), as well as using the anti-IL-6 antibody that proved to be so effective *in vitro* [391].

6.3 – Limitations

This study had a number of limitations, one of which is undoubtedly the rarity of primary MM samples. Larger sample numbers would have been invaluable not only to aid with statistical analysis, but also to provide a more accurate representation of MM disease. Also with each primary sample obtained and purified, on average less than 0.5 x 10^6 $CD138^+$ cells were isolated, limiting the number of assays that could be performed. Lack of patient history due to confidentiality agreements also meant that the treatment provided and the severity of disease of a patient was unknown, and it unclear how these factors could potentially influence MM's dependency on its microenvironment.

As no global gene expression profiling was undertaken during this work, the significance of the transcriptional changes that I observed throughout this thesis is limited. DNA microarray data or transcriptome sequencing of both the BMSCs and MM cells I used would have been of great benefit in this study.

Cell lines are not ideal for investigations into the BMM, as they are ultimately independent from this system and can only be used as an indicator on how a highly advanced MM would progress. Unfortunately, attempts at engrafting primary MM cells into NSG mice were unsuccessful. This is most likely due to the MM cell's dependency on its microenvironment making the cells highly susceptible to apoptosis. I do however believe that it is possible to get primary MM cells to engraft in NSG mice, but the procedure will be highly time dependent and will have better success rates with a more aggressive disease phenotype (due to secondary mutations causing the cells to be more independent of their microenvironment).

In vivo work was subject to several limitations, not least the mouse model used. NSG mice are severely immunocompromised which allows for the engraftment of human cells without risk of rejection, which is why they were selected for this research. However, the lack of immune system for which they were selected undoubtedly has an impact on disease progression. To circumnavigate this issue a C57BL/KaLwRij mouse model in combination with the 5TGM1 cell line could be used (C57 background which is predisposed to MM, 5TGM1 cells were originally isolated from a symptomatic KaLwRij mouse [392]), however this would lose the human disease

aspect from the model and, regrettably, neither of the models described allows for the direct manipulation of the BMM (instead we are limited to using pharmacological influence).

The lack of IL-8 expression in particular has proved to be highly limiting in my research, however with no mice expressing this gene (or its receptor CXCR1) there is little that can be done to overcome this issue. There are functional homologues of IL-8 (such as macrophage inflammatory protein 2 and liposaccharide-induced CXC chemokine) which could potentially work in the same manner however this would require further investigation [393]. The limitations of mouse models will continue to be an issue in all areas of medical research. However good a xenograft model is, it is a human MM cell interacting with a murine BMM. The continuing optimisation of 3D tissue culture models could in the future more accurately reflect human MM's interactions with its microenvironment, as well as providing the cytokines (including IL-8) which are lacking from the murine system.

6.4 – Conclusions and Future Work

The work described in this thesis not only aids in the current understanding of MM's relationship with its microenvironment, but also poses more questions and paves the way for future investigations. I have shown that MIF signalling from MM cells causes transcriptional changes in the BMSC (via cMYC) that are beneficial to disease progression. MIF stimulated BMSCs had significantly increased production and secretion of IL-6/IL-8 into the BMM, which in turn can cause the activation of the PI3K pathway. This pathway was shown to be targetable via the p110δ and p110γ inhibitor, IPI-145 which retarded tumour growth and increased overall survival *in vivo*. However, the question of if the inhibition of MIF or indeed PI3K could increase the efficacy of current therapeutics still remains. Further work is needed to see if targeting PI3K with IPI-145 is beneficial for MM patients, and I would recommend the clinical trialling of this compound alongside the current treatment regimens. In regards to MIF, we are only beginning to discover the potential of this cytokine in the re-modelling of its environment. If phase I studies of anti-MIF antibodies prove it to

be well tolerated, its use in the treatment of MM should be of great interest in the coming years.

In conclusion, my thesis objectives were as follows:

1. **Investigate if PI3K p110δ and p110γ signalling within the malignant cell benefits MM disease progression.**

   The combination of p110δ and p110γ activity was shown to benefit MM cell survival, adhesion and migration – in both cell lines and primary patient samples.

2. **Determine if these PI3K isoforms are activated by the BMM and if they can be inhibited within this environment.**

   The PI3K pathway was shown to be stimulated in response to both BMSC-conditioned media and recombinant IL-6. Inhibition of this pathway with the drug IPI-145 was shown to be possible both *in vitro* (even when co-cultured with BMSCs) and increased survival time significantly *in vivo*.

3. **Explore if MM cell signalling can re-model the BMM to benefit its survival.**

   The cytokine MIF was shown to be secreted at high levels from MM cells (but not BMSCs). Recombinant MIF was shown to stimulate the production of both IL-6 and IL-8 from the BMSCs – contributing to a MM beneficial environment. Inhibition of cMyc in the BMSCs was shown to aid in negating these effects, indicating a role for cMYC in the regulation of MIF stimulated IL-6/8 expression.

7 – References

1. Durie BG, Salmon SE. A clinical staging system for multiple myeloma. Correlation of measured myeloma cell mass with presenting clinical features, response to treatment, and survival. Cancer. 1975;36(3):842-541182674.
2. Walker R, Barlogie B, Haessler J, Tricot G, Anaissie E, Shaughnessy JD, Jr., et al. Magnetic resonance imaging in multiple myeloma: diagnostic and clinical implications. J Clin Oncol. 2007;25(9):1121-817296972.
3. Melton LJ, Kyle RA, Achenbach SJ, Oberg AL, Rajkumar SV. Fracture Risk With Multiple Myeloma: A Population-Based Study. Journal of Bone and Mineral Research. 2005;20(3):487-93
4. Eleutherakis-Papaiakovou V, Bamias A, Gika D, Simeonidis A, Pouli A, Anagnostopoulos A, et al. Renal failure in multiple myeloma: Incidence, correlations, and prognostic significance. Leukemia & Lymphoma. 2007;48(2):337-41
5. Oshima K, Kanda Y, Nannya Y, Kaneko M, Hamaki T, Suguro M, et al. Clinical and pathologic findings in 52 consecutively autopsied cases with multiple myeloma. American Journal of Hematology. 2001;67(1):1-5
6. Howlader N NA, Krapcho M, Miller D, Bishop K, Kosary CL, Yu M, Ruhl J, Tatalovich Z, Mariotto A, Lewis DR, Chen HS, Feuer EJ, Cronin KA (eds). SEER Cancer Statistics Review, 1975-2014, National Cancer Institute. https://seer.cancer.gov/csr/1975_2014/: SEER; 2016 [cited 2017 April].
7. Lichtenstein A, Berenson J, Norman D, Chang M-P, Carlile A. Production of cytokines by bone marrow cells obtained from patients with multiple myeloma. Blood. 1989;74(4):1266-73
8. Vacca A, Ribatti D, Presta M, Minischetti M, Iurlaro M, Ria R, et al. Bone marrow neovascularization, plasma cell angiogenic potential, and matrix metalloproteinase-2 secretion parallel progression of human multiple myeloma. Blood. 1999;93(9):3064-73
9. Pearse RN, Sordillo EM, Yaccoby S, Wong BR, Liau DF, Colman N, et al. Multiple myeloma disrupts the TRANCE/osteoprotegerin cytokine axis to trigger bone destruction and promote tumor progression. Proceedings of the National Academy of Sciences. 2001;98(20):11581-6
10. Lokhorst HM, Lamme T, De Smet M, Klein S, De Weger R, Van Oers R, et al. Primary tumor cells of myeloma patients induce interleukin-6 secretion in long-term bone marrow cultures. Blood. 1994;84(7):2269-77
11. Wallace SR, Oken MM, Lunetta KL, Panoskaltsis-Mortari A, Masellis AM. Abnormalities of bone marrow mesenchymal cells in multiple myeloma patients. Cancer. 2001;91(7):1219-30
12. Chauhan D, Uchiyama H, Akbarali Y, Urashima M, Yamamoto K-l, Libermann TA, et al. Multiple myeloma cell adhesion-induced interleukin-6 expression in bone marrow stromal cells involves activation of NF-kappa B. Blood. 1996;87(3):1104-12
13. Kyle RA, Gertz MA, Witzig TE, Lust JA, Lacy MQ, Dispenzieri A, et al., editors. Review of 1027 patients with newly diagnosed multiple myeloma. Mayo Clinic Proceedings; 2003: Elsevier.
14. Bladé J, Lust JA, Kyle RA. Immunoglobulin D multiple myeloma: presenting features, response to therapy, and survival in a series of 53 cases. Journal of Clinical Oncology. 1994;12(11):2398-4047964956.
15. Owen RG, Treon SP, Al-Katib A, Fonseca R, Greipp PR, McMaster ML, et al., editors. Clinicopathological definition of Waldenstrom's macroglobulinemia: consensus panel recommendations from the Second International Workshop on Waldenstrom's Macroglobulinemia. Seminars in oncology; 2003: Elsevier.
16. R. SS, Vincent RS, Angela D, William M, Moreno AA, Stephen A, et al. IgM multiple myeloma: Disease definition, prognosis, and differentiation from Waldenstrom's macroglobulinemia. American Journal of Hematology. 2010;85(11):853-5

17. Avet-Loiseau H, Garand R, Lodé L, Harousseau J-L, Bataille R. Translocation t(11;14)(q13;q32) is the hallmark of IgM, IgE, and nonsecretory multiple myeloma variants. Blood. 2003;101(4):1570-1
18. Johansson SGO, Bennich H. Immunological studies of an atypical (myeloma) immunoglobulin. Immunology. 1967;13(4):381-94PMC1409218.
19. Lonial S, Kaufman JL. Non-secretory myeloma: a clinician's guide. Oncology (Williston Park). 2013;27(9):924-8, 3024282993.
20. Landgren O, Kyle RA, Pfeiffer RM, Katzmann JA, Caporaso NE, Hayes RB, et al. Monoclonal gammopathy of undetermined significance (MGUS) consistently precedes multiple myeloma: a prospective study. Blood. 2009;113(22):5412-7
21. Weiss BM, Abadie J, Verma P, Howard RS, Kuehl WM. A monoclonal gammopathy precedes multiple myeloma in most patients. Blood. 2009;113(22):5418-22
22. Chapman MA, Lawrence MS, Keats JJ, Cibulskis K, Sougnez C, Schinzel AC, et al. Initial genome sequencing and analysis of multiple myeloma. Nature. 2011;471(7339):467-7221430775.
23. Fonseca R, Blood EA, Oken MM, Kyle RA, Dewald GW, Bailey RJ, et al. Myeloma and the t(11;14)(q13;q32); evidence for a biologically defined unique subset of patients. Blood. 2002;99(10):3735-41
24. Ocqueteau M, Orfao A, Almeida J, Blade J, Gonzalez M, Garcia-Sanz R, et al. Immunophenotypic characterization of plasma cells from monoclonal gammopathy of undetermined significance patients. Implications for the differential diagnosis between MGUS and multiple myeloma. Am J Pathol. 1998;152(6):1655-659626070.
25. Sezer O, Heider U, Zavrski I, Possinger K. Differentiation of monoclonal gammopathy of undetermined significance and multiple myeloma using flow cytometric characteristics of plasma cells. Haematologica. 2001;86(8):837-4311522540.
26. Kyle RA, Therneau TM, Rajkumar SV, Larson DR, Plevak MF, Offord JR, et al. Prevalence of monoclonal gammopathy of undetermined significance. N Engl J Med. 2006;354(13):1362-916571879.
27. Hällén J. Frequency of “Abnormal” Serum Globulins (M-Components) in the Aged. Acta Medica Scandinavica. 1963;173(6):737-44
28. Weinhold N, Johnson DC, Rawstron AC, Försti A, Doughty C, Vijayakrishnan J, et al. Inherited genetic susceptibility to monoclonal gammopathy of unknown significance. Blood. 2014;123(16):2513-7
29. Vachon CM, Kyle RA, Therneau TM, Foreman BJ, Larson DR, Colby CL, et al. Increased risk of monoclonal gammopathy in first-degree relatives of patients with multiple myeloma or monoclonal gammopathy of undetermined significance. Blood. 2009;114(4):785-90
30. Landgren O, Kyle RA, Hoppin JA, Beane Freeman LE, Cerhan JR, Katzmann JA, et al. Pesticide exposure and risk of monoclonal gammopathy of undetermined significance in the Agricultural Health Study. Blood. 2009;113(25):6386-91
31. Saleun JP, Vicariot M, Deroff P, Morin JF. Monoclonal gammopathies in the adult population of Finistère, France. Journal of Clinical Pathology. 1982;35(1):63-8
32. Kyle RA, Durie BG, Rajkumar SV, Landgren O, Blade J, Merlini G, et al. Monoclonal gammopathy of undetermined significance (MGUS) and smoldering (asymptomatic) multiple myeloma: IMWG consensus perspectives risk factors for progression and guidelines for monitoring and management. Leukemia. 2010;24(6):1121-720410922.
33. Kyle RA, Therneau TM, Rajkumar SV, Offord JR, Larson DR, Plevak MF, et al. A Long-Term Study of Prognosis in Monoclonal Gammopathy of Undetermined Significance. New England Journal of Medicine. 2002;346(8):564-911856795.
34. Landgren O, Graubard BI, Katzmann JA, Kyle RA, Ahmadizadeh I, Clark R, et al. Racial Disparities in the Prevalence of Monoclonal Gammopathies: A population-based study of 12,482 persons from the National Health and Nutritional Examination Survey. Leukemia. 2014;28(7):1537-42PMC4090286.

35. Blade J, Lopez-Guillermo A, Rozman C, Cervantes F, Salgado C, Aguilar JL, et al. Malignant transformation and life expectancy in monoclonal gammopathy of undetermined significance. British journal of haematology. 1992;81(3):391-4
36. Gregersen H, Mellemkjaer L, Ibsen J, Dahlerup J, Thomassen L, Sorensen H. The impact of M-component type and immunoglobulin concentration on the risk of malignant transformation in patients with monoclonal gammopathy of undetermined significance. Haematologica. 2001;86(11):1172-9
37. Cesana C, Klersy C, Barbarano L, Nosari AM, Crugnola M, Pungolino E, et al. Prognostic factors for malignant transformation in monoclonal gammopathy of undetermined significance and smoldering multiple myeloma. Journal of Clinical Oncology. 2002;20(6):1625-34
38. Ghobrial IM, Landgren O. How I treat smoldering multiple myeloma. Blood. 2014;124(23):3380-8
39. Mateos M-V, Hernández M-T, Giraldo P, de la Rubia J, de Arriba F, Corral LL, et al. Lenalidomide plus Dexamethasone for High-Risk Smoldering Multiple Myeloma. New England Journal of Medicine. 2013;369(5):438-4723902483.
40. Benovus Bio I. Phase I Study of an Oncofetal Antigen Multi-Peptide Immunotherapy in Subjects With Hematologic Cancer. 2016.NCT02240537 Available from: https://ClinicalTrials.gov/show/NCT02240537.
41. Center MDAC, Merck S, Dohme C. Pembrolizumab for Smoldering Multiple Myeloma (SMM). 2019.NCT02603887 Available from: https://ClinicalTrials.gov/show/NCT02603887.
42. City of Hope Medical C. Melphalan and Radiation Therapy Followed By Lenalidomide in Treating Patients Who Are Undergoing Autologous Stem Cell Transplant for Stage I, Stage II, or Stage III Multiple Myeloma. 2017.NCT00112827 Available from: https://ClinicalTrials.gov/show/NCT00112827.
43. Dana-Farber Cancer I, Bristol-Myers S, Celgene. Trial of Combination of Elotuzumab Lenalidomide and Dexamethasone in High-Risk Smoldering Multiple Myeloma. 2020.NCT02279394 Available from: https://ClinicalTrials.gov/show/NCT02279394.
44. Janssen R, Development LLC. A Study to Evaluate 3 Dose Schedules of Daratumumab in Participants With Smoldering Multiple Myeloma. 2017.NCT02316106 Available from: https://ClinicalTrials.gov/show/NCT02316106.
45. Janssen R, Development LLC. A Study of Siltuximab (Anti- IL 6 Monoclonal Antibody) in Patients With High-risk Smoldering Multiple Myeloma. 2019.NCT01484275 Available from: https://ClinicalTrials.gov/show/NCT01484275.
46. Mayo C, National Cancer I. Lenalidomide and Dexamethasone With or Without Anakinra in Treating Patients With Early Stage Multiple Myeloma. 2020.NCT02492750 Available from: https://ClinicalTrials.gov/show/NCT02492750.
47. National Cancer I. Lenalidomide in Treating Patients With Multiple Myeloma Undergoing Autologous Stem Cell Transplant. 2012.NCT00114101 Available from: https://ClinicalTrials.gov/show/NCT00114101.
48. National Cancer I. Lenalidomide or Observation in Treating Patients With Asymptomatic High-Risk Smoldering Multiple Myeloma. 2026.NCT01169337 Available from: https://ClinicalTrials.gov/show/NCT01169337.
49. Rennes University H, Intergroupe Francophone du M. Study of DNA Copy Numbers Variations and Gene Expression Profile of Bone Marrow Plasma Cells From MGUS and SMM. 2018.NCT01079429 Available from: https://ClinicalTrials.gov/show/NCT01079429.
50. Mills KHG, Cawley JC. Abnormal monoclonal antibody-defined helper/suppressor T-cell subpopulations in multiple myeloma: relationship to treatment and clinical stage. British Journal of Haematology. 1983;53(2):271-5
51. Blimark C, Holmberg E, Mellqvist U-H, Landgren O, Björkholm M, Hultcrantz M, et al. Multiple myeloma and infections: a population-based study on 9253 multiple myeloma patients. Haematologica. 2015;100(1):107-13
52. Coleman RE. Skeletal complications of malignancy. Cancer. 1997;80(S8):1588-94

53. Giuliani N, Colla S, Morandi F, Lazzaretti M, Sala R, Bonomini S, et al. Myeloma cells block RUNX2/CBFA1 activity in human bone marrow osteoblast progenitors and inhibit osteoblast formation and differentiation. Blood. 2005;106(7):2472-83
54. Yaccoby S, Wezeman MJ, Zangari M, Walker R, Cottler-Fox M, Gaddy D, et al. Inhibitory effects of osteoblasts and increased bone formation on myeloma in novel culture systems and a myelomatous mouse model. Haematologica. 2006;91(2):192-9
55. Mundy GR, Raisz LG, Cooper RA, Schechter GP, Salmon SE. Evidence for the secretion of an osteoclast stimulating factor in myeloma. New England Journal of Medicine. 1974;291(20):1041-6
56. Yaccoby S, Pearse RN, Johnson CL, Barlogie B, Choi Y, Epstein J. Myeloma interacts with the bone marrow microenvironment to induce osteoclastogenesis and is dependent on osteoclast activity. British journal of haematology. 2002;116(2):278-90
57. Abe M, Hiura K, Wilde J, Shioyasono A, Moriyama K, Hashimoto T, et al. Osteoclasts enhance myeloma cell growth and survival via cell-cell contact: a vicious cycle between bone destruction and myeloma expansion. Blood. 2004;104(8):2484-91
58. Knudsen LM, Hippe E, Hjorth M, Holmberg E, Westin J. Renal function in newly diagnosed multiple myeloma—a demographic study of 1353 patients. European journal of haematology. 1994;53(4):207-12
59. Granell M, Calvo X, Garcia-Guinon A, Escoda L, Abella E, Martinez CM, et al. Prognostic impact of circulating plasma cells in patients with multiple myeloma: implications for plasma cell leukemia definition. Haematologica. 2017;102(6):1099-10428255016.
60. Kyle RA, Child JA, Anderson K, Barlogie B, Bataille R, Bensinger W, et al. Criteria for the classification of monoclonal gammopathies, multiple myeloma and related disorders: a report of the International Myeloma Working Group. British journal of haematology. 2003;121(5):749-57
61. Smith A, Howell D, Patmore R, Jack A, Roman E. Incidence of haematological malignancy by sub-type: a report from the Haematological Malignancy Research Network. British Journal of Cancer. 2011;105(11):1684-92PMC3242607.
62. Health AIo. Cancer Survival and Prevalence in Australia: Period Estimates from 1982 to 2010: AIHW; 2012.
63. Boyd KD, Ross FM, Chiecchio L, Dagrada G, Konn ZJ, Tapper WJ, et al. Gender Disparities in the Tumor Genetics and Clinical Outcome of Multiple Myeloma. Cancer epidemiology, biomarkers & prevention : a publication of the American Association for Cancer Research, cosponsored by the American Society of Preventive Oncology. 2011;20(8):1703-7PMC4545514.
64. Whitacre CC. Sex differences in autoimmune disease. Nat Immunol. 2001;2(9):777-80
65. Juutilainen A, Kortelainen S, Lehto S, Rönnemaa T, Pyörälä K, Laakso M. Gender Difference in the Impact of Type 2 Diabetes on Coronary Heart Disease Risk. Diabetes Care. 2004;27(12):2898-904
66. Van Den Eeden SK, Tanner CM, Bernstein AL, Fross RD, Leimpeter A, Bloch DA, et al. Incidence of Parkinson's disease: variation by age, gender, and race/ethnicity. American journal of epidemiology. 2003;157(11):1015-22
67. Geller SE, Koch A, Pellettieri B, Carnes M. Inclusion, analysis, and reporting of sex and race/ethnicity in clinical trials: have we made progress? Journal of Women's Health. 2011;20(3):315-20
68. Waxman AJ, Mink PJ, Devesa SS, Anderson WF, Weiss BM, Kristinsson SY, et al. Racial disparities in incidence and outcome in multiple myeloma: a population-based study. Blood. 2010;116(25):5501-6PMC3031400.
69. Ferlay J, Soerjomataram I, Dikshit R, Eser S, Mathers C, Rebelo M, et al. Cancer incidence and mortality worldwide: sources, methods and major patterns in GLOBOCAN 2012. Int J Cancer. 2015;136(5):E359-8625220842.

70. Huang SY, Yao M, Tang JL, Lee WC, Tsay W, Cheng AL, et al. Epidemiology of multiple myeloma in Taiwan: increasing incidence for the past 25 years and higher prevalence of extramedullary myeloma in patients younger than 55 years. Cancer. 2007;110(4):896-90517594697.
71. Lee JH, Lee DS, Lee JJ, Chang YH, Jin JY, Jo D-Y, et al. Multiple myeloma in Korea: past, present, and future perspectives. Experience of the Korean Multiple Myeloma Working Party. International Journal of Hematology. 2010;92(1):52-7
72. Virani S, Sriplung H, Rozek LS, Meza R. Escalating burden of breast cancer in southern Thailand: analysis of 1990–2010 incidence and prediction of future trends. Cancer epidemiology. 2014;38(3):235-43
73. Baker A, Braggio E, Jacobus S, Jung S, Larson D, Therneau T, et al. Uncovering the biology of multiple myeloma among African Americans: a comprehensive genomics approach. Blood. 2013;121(16):3147-52
74. Greenberg AJ, Philip S, Paner A, Velinova S, Badros A, Catchatourian R, et al. Racial differences in primary cytogenetic abnormalities in multiple myeloma: a multi-center study. Blood Cancer Journal. 2015;5:e271
75. Stewart JH, Bertoni AG, Staten JL, Levine EA, Gross CP. Participation in surgical oncology clinical trials: gender-, race/ethnicity-, and age-based disparities. Annals of surgical oncology. 2007;14(12):3328-34
76. Murthy VH, Krumholz HM, Gross CP. Participation in cancer clinical trials: race-, sex-, and age-based disparities. Jama. 2004;291(22):2720-6
77. Stringhini S, Carmeli C, Jokela M, Avendaño M, Muennig P, Guida F, et al. Socioeconomic status and the 25 x 25 risk factors as determinants of premature mortality: a multicohort study and meta-analysis of 1.7 million men and women. The Lancet.389(10075):1229-37
78. Wilper AP, Woolhandler S, Lasser KE, McCormick D, Bor DH, Himmelstein DU. Health Insurance and Mortality in US Adults. American Journal of Public Health. 2009;99(12):2289-95PMC2775760.
79. Franks P, Clancy CM, Gold MR. Health insurance and mortality. Evidence from a national cohort. Jama. 1993;270(6):737-418336376.
80. Costa LJ, Brill IK, Brown EE. Impact of marital status, insurance status, income, and race/ethnicity on the survival of younger patients diagnosed with multiple myeloma in the United States. Cancer. 2016;122(20):3183-9027548407.
81. Kristinsson SY, Björkholm M, Goldin LR, Blimark C, Mellqvist UH, Wahlin A, et al. Patterns of hematologic malignancies and solid tumors among 37,838 first-degree relatives of 13,896 patients with multiple myeloma in Sweden. International journal of cancer. 2009;125(9):2147-50
82. Lynch HT, Ferrara K, Barlogie B, Coleman EA, Lynch JF, Weisenburger D, et al. Familial myeloma. New England Journal of Medicine. 2008;359(2):152-7
83. Struewing JP, Hartge P, Wacholder S, Baker SM, Berlin M, McAdams M, et al. The Risk of Cancer Associated with Specific Mutations of BRCA1 and BRCA2 among Ashkenazi Jews. New England Journal of Medicine. 1997;336(20):1401-89145676.
84. Broderick P, Chubb D, Johnson DC, Weinhold N, Försti A, Lloyd A, et al. Common variation at 3p22. 1 and 7p15. 3 influences multiple myeloma risk. Nature genetics. 2012;44(1):58
85. Dang CV. MYC on the Path to Cancer. Cell. 2012;149(1):22-35PMC3345192.
86. Li N, Johnson DC, Weinhold N, Studd JB, Orlando G, Mirabella F, et al. Multiple myeloma risk variant at 7p15. 3 creates an IRF4-binding site and interferes with CDCA7L expression. Nature communications. 2016;7:13656
87. Chubb D, Weinhold N, Broderick P, Chen B, Johnson DC, Försti A, et al. Common variation at 3q26. 2, 6p21. 33, 17p11. 2 and 22q13. 1 influences multiple myeloma risk. Nature genetics. 2013;45(10):1221

88. Ogden CL, Carroll MD, Curtin LR, McDowell MA, Tabak CJ, Flegal KM. Prevalence of overweight and obesity in the United States, 1999-2004. Jama. 2006;295(13):1549-55
89. Solly S. Remarks on the pathology of mollities ossium; with cases. Med Chir Trans. 1844;27:435-98 820895811.
90. Macintyre W. Case of Mollities and Fragilitas Ossium, accompanied with urine strongly charged with animal matter. Medico-chirurgical transactions. 1850;33:211-32PMC2104246.
91. Bergel F, Stock J. Cyto-active amino-acid and peptide derivatives. Part I. Substituted phenylalanines. Journal of the Chemical Society (Resumed). 1954:2409-17
92. Blokhin N, Larionov L, Perevodchikova N, Chebotareva L, Merkulova N. [Clinical experiences with sarcolysin in neoplastic diseases]. Ann N Y Acad Sci. 1958;68(3):1128-3213627766.
93. Bergsagel DE, Sprague CC, Austin C, Griffith KM. Evaluation of new chemotherapeutic agents in the treatment of multiple myeloma. IV. L-Phenylalanine mustard (NSC-8806). Cancer Chemother Rep. 1962;21:87-9913867794.
94. Hoogstraten B, Sheehe PR, Cuttner J, Cooper T, Kyle RA, Oberfield RA, et al. Melphalan in multiple myeloma. Blood. 1967;30(1):74-836028709.
95. ALEXANIAN R, BERGSAGEL DE, MIGLIORE PJ, VAUGHN WK, HOWE CD. Melphalan therapy for plasma cell myeloma. Blood. 1968;31(1):1-10
96. Bergsagel DE, Migliore PJ, Griffith KM. Myeloma Proteins and the Clinical Response to Melphalan Therapy. Science. 1965;148(3668):376-7
97. Mass RE. A comparison of the effect of prednisone and a placebo in the treatment of multiple myeloma. Cancer Chemother Rep. 1962;16:257-914470881.
98. Salmon SE, Shadduck RK, Schilling A. Intermittent high-dose prednisone (NSC-10023) therapy for multiple myeloma. Cancer Chemother Rep. 1967;51(3):179-876043738.
99. Alexanian R, Haut A, Khan AU, Lane M, McKelvey EM, Migliore PJ, et al. Treatment for multiple myeloma. Combination chemotherapy with different melphalan dose regimens. JAMA. 1969;208(9):1680-55818682.
100. Lee BJ, Sahakian G, Clarkson BD, Krakoff IH. Proceedings: Combination chemotherapy of multiple myeloma with alkeran, cytoxan, vincristine, prednisone, and BCNU. Cancer. 1974;33(2):533-84812771.
101. Combination chemotherapy versus melphalan plus prednisone as treatment for multiple myeloma: an overview of 6,633 patients from 27 randomized trials. Myeloma Trialists' Collaborative Group. J Clin Oncol. 1998;16(12):3832-429850028.
102. Lenz W, Pfeiffer RA, Kosenow W, Hayman D. Thalidomide and congenital abnormalities. The Lancet. 1962;279(7219):45-6
103. Sheskin J. Thalidomide in the treatment of lepra reactions. Clinical Pharmacology & Therapeutics. 1965;6(3):303-6
104. Sheskin J. The treatment of lepra reaction in lepromatous leprosy. International journal of dermatology. 1980;19(6):318-22
105. Saylan T, Saltik I. Thalidomide in the treatment of Behcet's syndrome. Archives of Dermatology. 1982;118(8):536-
106. Youle M, Clarbour J, Farthing C, Connolly M, Hawkins D, Staughton R, et al. Treatment of resistant aphthous ulceration with thalidomide in patients positive for HIV antibody. BMJ: British Medical Journal. 1989;298(6671):432
107. D'Amato RJ, Loughnan MS, Flynn E, Folkman J. Thalidomide is an inhibitor of angiogenesis. Proc Natl Acad Sci U S A. 1994;91(9):4082-57513432.
108. Singhal S, Mehta J, Desikan R, Ayers D, Roberson P, Eddlemon P, et al. Antitumor activity of thalidomide in refractory multiple myeloma. N Engl J Med. 1999;341(21):1565-7110564685.
109. Rock KL, Gramm C, Rothstein L, Clark K, Stein R, Dick L, et al. Inhibitors of the proteasome block the degradation of most cell proteins and the generation of peptides presented on MHC class I molecules. Cell. 1994;78(5):761-71

110. Palombella VJ, Rando OJ, Goldberg AL, Maniatis T. The ubiquitin-proteasome pathway is required for processing the NF-kappa B1 precursor protein and the activation of NF-kappa B. Cell. 1994;78(5):773-858087845.
111. Beg AA, Baltimore D. An essential role for NF-kB in preventing TNF-a-induced cell death. Science-AAAS-Weekly Paper Edition. 1996;274(5288):782-3
112. Read MA, Neish AS, Luscinskas FW, Palombella VJ, Maniatis T, Collins T. The proteasome pathway is required for cytokine-induced endothelial-leukocyte adhesion molecule expression. Immunity. 1995;2(5):493-5067538441.
113. Huang S, Pettaway CA, Uehara H, Bucana CD, Fidler IJ. Blockade of NF-kB activity in human prostate cancer cells is associated with suppression of angiogenesis, invasion, and metastasis. invasion, and metastasis. 2001;20(4188):4197
114. Richardson PG, Barlogie B, Berenson J, Singhal S, Jagannath S, Irwin D, et al. A Phase 2 Study of Bortezomib in Relapsed, Refractory Myeloma. New England Journal of Medicine. 2003;348(26):2609-1712826635.
115. San Miguel JF, Schlag R, Khuageva NK, Dimopoulos MA, Shpilberg O, Kropff M, et al. Bortezomib plus Melphalan and Prednisone for Initial Treatment of Multiple Myeloma. New England Journal of Medicine. 2008;359(9):906-1718753647.
116. Moreau P, Masszi T, Grzasko N, Bahlis NJ, Hansson M, Pour L, et al. Oral Ixazomib, Lenalidomide, and Dexamethasone for Multiple Myeloma. N Engl J Med. 2016;374(17):1621-3427119237.
117. Richardson PG, Zimmerman TM, Hofmeister CC, Talpaz M, Chanan-Khan AA, Kaufman JL, et al. Phase 1 study of marizomib in relapsed or relapsed and refractory multiple myeloma: NPI-0052-101 Part 1. Blood. 2016;127(22):2693-70027009059.
118. NICE. Multiple Myeloma https://www.nice.org.uk/guidance/ng35: National Institute for Health and Care Excellence; 2017 [updated Feb 2016; cited 2017 25.10.17]. Available from: https://www.nice.org.uk/guidance/ng35.
119. Calvi LM, Adams GB, Weibrecht KW, Weber JM, Olson DP, Knight MC, et al. Osteoblastic cells regulate the haematopoietic stem cell niche. Nature. 2003;425(6960):841-6
120. Bianco P, Robey PG. Skeletal stem cells. Development. 2015;142(6):1023-7
121. Jacobson L, Marks E, Robson M. Effect of spleen protection on mortality following x-irradiation. 1949
122. Lorenz E, Congdon C, Uphoff D. Modification of acute irradiation injury in mice and guinea-pigs by bone marrow injections. Radiology. 1952;58(6):863-77
123. Nowell PC, Cole LJ, Habermeyer JG, Roan PL. Growth and continued function of rat marrow cells in X-irradiated mice: US Naval Radiological Defense Laboratory; 1955.
124. Gengozian N, Urso I, Congdon C, Conger A, Makinodan T. Thymus specificity in lethally irradiated mice treated with rat bone marrow. Proceedings of the Society for Experimental Biology and Medicine. 1957;96(3):714-20
125. Till JE, McCulloch EA. A Direct Measurement of the Radiation Sensitivity of Normal Mouse Bone Marrow Cells. Radiation Research. 1961;14(2):213-22
126. Cheshier SH, Morrison SJ, Liao X, Weissman IL. In vivo proliferation and cell cycle kinetics of long-term self-renewing hematopoietic stem cells. Proceedings of the National Academy of Sciences. 1999;96(6):3120-5
127. Sugiyama T, Kohara H, Noda M, Nagasawa T. Maintenance of the Hematopoietic Stem Cell Pool by CXCL12-CXCR4 Chemokine Signaling in Bone Marrow Stromal Cell Niches. Immunity. 2006;25(6):977-88
128. Morrison SJ, Wright DE, Weissman IL. Cyclophosphamide/granulocyte colony-stimulating factor induces hematopoietic stem cells to proliferate prior to mobilization. Proceedings of the National Academy of Sciences. 1997;94(5):1908-13
129. Uchida N, Friera AM, He D, Reitsma MJ, Tsukamoto AS, Weissman IL. Hydroxyurea Can Be Used to Increase Mouse c-kit⁺Thy-

1.1^{lo}Lin^{−/lo}Sca-1⁺ Hematopoietic Cell Number and Frequency in Cell Cycle In Vivo. Blood. 1997;90(11):4354-62
130. Szilvassy SJ, Humphries RK, Lansdorp PM, Eaves AC, Eaves CJ. Quantitative assay for totipotent reconstituting hematopoietic stem cells by a competitive repopulation strategy. Proceedings of the National Academy of Sciences. 1990;87(22):8736-40
131. Baum CM, Weissman IL, Tsukamoto AS, Buckle A-M, Peault B. Isolation of a candidate human hematopoietic stem-cell population. Proceedings of the National Academy of Sciences. 1992;89(7):2804-8
132. Gunji Y, Nakamura M, Osawa H, Nagayoshi K, Nakauchi H, Miura Y, et al. Human primitive hematopoietic progenitor cells are more enriched in KITlow cells than in KIThigh cells. Blood. 1993;82(11):3283-9
133. Terstappen L, Huang S, Safford M, Lansdorp PM, Loken MR. Sequential generations of hematopoietic colonies derived from single nonlineage-committed CD34+ CD38- progenitor cells. Blood. 1991;77(6):1218-27
134. Friedenstein AJ, Piatetzky S, II, Petrakova KV. Osteogenesis in transplants of bone marrow cells. J Embryol Exp Morphol. 1966;16(3):381-905336210.
135. Tavassoli M, Crosby WH. Transplantation of Marrow to Extramedullary Sites. Science. 1968;161(3836):54-6
136. Friedenstein AJ, Chailakhjan RK, Lalykina KS. The development of fibroblast colonies in monolayer cultures of guinea-pig bone marrow and spleen cells. Cell Tissue Kinet. 1970;3(4):393-4035523063.
137. Friedenstein AJ, Petrakova KV, Kurolesova AI, Frolova GP. Heterotopic of bone marrow. Analysis of precursor cells for osteogenic and hematopoietic tissues. Transplantation. 1968;6(2):230-475654088.
138. Sacchetti B, Funari A, Michienzi S, Di Cesare S, Piersanti S, Saggio I, et al. Self-renewing osteoprogenitors in bone marrow sinusoids can organize a hematopoietic microenvironment. Cell. 2007;131(2):324-36
139. Zhou BO, Yue R, Murphy MM, Peyer JG, Morrison SJ. Leptin-receptor-expressing mesenchymal stromal cells represent the main source of bone formed by adult bone marrow. Cell stem cell. 2014;15(2):154-68
140. Orlic D, Kajstura J, Chimenti S, Jakoniuk I, Anderson SM, Li B, et al. Bone marrow cells regenerate infarcted myocardium. Nature. 2001;410(6829):701-5
141. Woodbury D, Schwarz EJ, Prockop DJ, Black IB. Adult rat and human bone marrow stromal cells differentiate into neurons. Journal of neuroscience research. 2000;61(4):364-70
142. Sanchez-Ramos J, Song S, Cardozo-Pelaez F, Hazzi C, Stedeford T, Willing A, et al. Adult bone marrow stromal cells differentiate into neural cells in vitro. Experimental neurology. 2000;164(2):247-56
143. Chopp M, Zhang XH, Li Y, Wang L, Chen J, Lu D, et al. Spinal cord injury in rat: treatment with bone marrow stromal cell transplantation. Neuroreport. 2000;11(13):3001-5
144. Firth AL, Yuan JX-J. Identification of functional progenitor cells in the pulmonary vasculature. Pulmonary circulation. 2012;2(1):84-100
145. Vaananen HK, Laitala-Leinonen T. Osteoclast lineage and function. Arch Biochem Biophys. 2008;473(2):132-818424258.
146. Meunier P, Aaron J, Edouard C, Vignon G. Osteoporosis and the replacement of cell populations of the marrow by adipose tissue. A quantitative study of 84 iliac bone biopsies. Clin Orthop Relat Res. 1971;80:147-545133320.
147. Zhou BO, Yu H, Yue R, Zhao Z, Rios JJ, Naveiras O, et al. Bone marrow adipocytes promote the regeneration of stem cells and haematopoiesis by secreting SCF. Nat Cell Biol. 2017;19(8):891-903
148. Ross SE, Hemati N, Longo KA, Bennett CN, Lucas PC, Erickson RL, et al. Inhibition of adipogenesis by Wnt signaling. Science. 2000;289(5481):950-3

149. Bennett CN, Ross SE, Longo KA, Bajnok L, Hemati N, Johnson KW, et al. Regulation of Wnt signaling during adipogenesis. Journal of Biological Chemistry. 2002;277(34):30998-1004
150. Rawadi G, Vayssiere B, Dunn F, Baron R, Roman-Roman S. BMP-2 controls alkaline phosphatase expression and osteoblast mineralization by a Wnt autocrine loop. J Bone Miner Res. 2003;18(10):1842-5314584895.
151. Tang QQ, Otto TC, Lane MD. Commitment of C3H10T1/2 pluripotent stem cells to the adipocyte lineage. Proc Natl Acad Sci U S A. 2004;101(26):9607-1115210946.
152. Sottile V, Seuwen K. Bone morphogenetic protein-2 stimulates adipogenic differentiation of mesenchymal precursor cells in synergy with BRL 49653 (rosiglitazone). FEBS Letters. 2000;475(3):201-4
153. zur Nieden NI, Kempka G, Rancourt DE, Ahr HJ. Induction of chondro-, osteo- and adipogenesis in embryonic stem cells by bone morphogenetic protein-2: effect of cofactors on differentiating lineages. BMC Dev Biol. 2005;5:115673475.
154. Zanotti S, Smerdel-Ramoya A, Stadmeyer L, Durant D, Radtke F, Canalis E. Notch inhibits osteoblast differentiation and causes osteopenia. Endocrinology. 2008;149(8):3890-9
155. Kurpinski K, Lam H, Chu J, Wang A, Kim A, Tsay E, et al. Transforming Growth Factor-β and Notch Signaling Mediate Stem Cell Differentiation into Smooth Muscle Cells. STEM CELLS. 2010;28(4):734-42
156. Takada I, Kato S. A new PPAR-[gamma] function in bone. IBMS BoneKEy. 2008;5(7):258-61
157. Huey DJ, Hu JC, Athanasiou KA. Unlike Bone, Cartilage Regeneration Remains Elusive. Science. 2012;338(6109):917-21
158. Bhosale AM, Richardson JB. Articular cartilage: structure, injuries and review of management. British medical bulletin. 2008;87:77-9518676397.
159. Johnstone B, Hering TM, Caplan AI, Goldberg VM, Yoo JU. In vitro chondrogenesis of bone marrow-derived mesenchymal progenitor cells. Exp Cell Res. 1998;238(1):265-729457080.
160. Worster AA, Brower-Toland BD, Fortier LA, Bent SJ, Williams J, Nixon AJ. Chondrocytic differentiation of mesenchymal stem cells sequentially exposed to transforming growth factor-β1 in monolayer and insulin-like growth factor-I in a three-dimensional matrix. Journal of Orthopaedic Research. 2001;19(4):738-49
161. Bi W, Huang W, Whitworth DJ, Deng JM, Zhang Z, Behringer RR, et al. Haploinsufficiency of Sox9 results in defective cartilage primordia and premature skeletal mineralization. Proceedings of the National Academy of Sciences. 2001;98(12):6698-703
162. Luo X-H, Guo L-J, Yuan L-Q, Xie H, Zhou H-D, Wu X-P, et al. Adiponectin stimulates human osteoblasts proliferation and differentiation via the MAPK signaling pathway. Experimental cell research. 2005;309(1):99-109
163. Zhang W, Liu HT. MAPK signal pathways in the regulation of cell proliferation in mammalian cells. Cell research. 2002;12(1):9-18
164. Bragado P, Armesilla A, Silva A, Porras A. Apoptosis by cisplatin requires p53 mediated p38α MAPK activation through ROS generation. Apoptosis. 2007;12(9):1733-42
165. Barault L, Veyrie N, Jooste V, Lecorre D, Chapusot C, Ferraz JM, et al. Mutations in the RAS-MAPK, PI (3) K (phosphatidylinositol-3-OH kinase) signaling network correlate with poor survival in a population-based series of colon cancers. International journal of cancer. 2008;122(10):2255-9
166. Ciampi R, Knauf JA, Kerler R, Gandhi M, Zhu Z, Nikiforova MN, et al. Oncogenic AKAP9-BRAF fusion is a novel mechanism of MAPK pathway activation in thyroid cancer. Journal of Clinical Investigation. 2005;115(1):94
167. Namba H, Nakashima M, Hayashi T, Hayashida N, Maeda S, Rogounovitch TI, et al. Clinical implication of hot spot BRAF mutation, V599E, in papillary thyroid cancers. The Journal of Clinical Endocrinology & Metabolism. 2003;88(9):4393-7

168. Biankin AV, Waddell N, Kassahn KS, Gingras MC, Muthuswamy LB, Johns AL, et al. Pancreatic cancer genomes reveal aberrations in axon guidance pathway genes. Nature. 2012;491(7424):399-40523103869.
169. Fernández-Medarde A, Santos E. Ras in Cancer and Developmental Diseases. Genes & Cancer. 2011;2(3):344-58PMC3128640.
170. Prior IA, Lewis PD, Mattos C. A comprehensive survey of Ras mutations in cancer. Cancer Research. 2012;72(10):2457-67PMC3354961.
171. Zhu J, Blenis J, Yuan J. Activation of PI3K/Akt and MAPK pathways regulates Myc-mediated transcription by phosphorylating and promoting the degradation of Mad1. Proceedings of the National Academy of Sciences. 2008;105(18):6584-9
172. Lionetti M, Barbieri M, Todoerti K, Agnelli L, Marzorati S, Fabris S, et al. Molecular spectrum of BRAF, NRAS and KRAS gene mutations in plasma cell dyscrasias: implication for MEK-ERK pathway activation. Oncotarget. 2015;6(27):24205
173. Bezieau S, Devilder MC, Avet-Loiseau H, Mellerin MP, Puthier D, Pennarun E, et al. High incidence of N and K-Ras activating mutations in multiple myeloma and primary plasma cell leukemia at diagnosis. Human mutation. 2001;18(3):212-24
174. Navas T, Nguyen A, Hideshima T, Reddy M, Ma J, Haghnazari E, et al. Inhibition of p38α MAPK enhances proteasome inhibitor-induced apoptosis of myeloma cells by modulating Hsp27, Bcl-XL, Mcl-1 and p53 levels in vitro and inhibits tumor growth in vivo. Leukemia. 2006;20(6):1017-27
175. Chatterjee M, Stühmer T, Herrmann P, Bommert K, Dörken B, Bargou RC. Combined disruption of both the MEK/ERK and the IL-6R/STAT3 pathways is required to induce apoptosis of multiple myeloma cells in the presence of bone marrow stromal cells. Blood. 2004;104(12):3712-21
176. Puthier D, Bataille R, Amiot M. IL-6 up-regulates mcl-1 in human myeloma cells through JAK/STAT rather than ras/MAP kinase pathway. European journal of immunology. 1999;29(12):3945-50
177. Riley JK, Takeda K, Akira S, Schreiber RD. Interleukin-10 Receptor Signaling through the JAK-STAT Pathway requirement for two distinct receptor-derived signals for anti-inflammatory action. Journal of Biological Chemistry. 1999;274(23):16513-21
178. Finbloom DS, Winestock KD. IL-10 induces the tyrosine phosphorylation of tyk2 and Jak1 and the differential assembly of STAT1 alpha and STAT3 complexes in human T cells and monocytes. The Journal of Immunology. 1995;155(3):1079-90
179. Bacon CM, McVicar DW, Ortaldo JR, Rees RC, O'Shea J, Johnston JA. Interleukin 12 (IL-12) induces tyrosine phosphorylation of JAK2 and TYK2: differential use of Janus family tyrosine kinases by IL-2 and IL-12. Journal of Experimental Medicine. 1995;181(1):399-404
180. Darnell Jr JE, Kerr IM, Stark GR. Jak-STAT pathways and transcriptional activation in response to IFNs and other extracellular signaling proteins. Science-AAAS-weekly paper edition-including guide to scientific information. 1994;264(5164):1415-20
181. Bowman T, Broome MA, Sinibaldi D, Wharton W, Pledger W, Sedivy JM, et al. Stat3-mediated Myc expression is required for Src transformation and PDGF-induced mitogenesis. Proceedings of the National Academy of Sciences. 2001;98(13):7319-24
182. Shirogane T, Fukada T, Muller JM, Shima DT, Hibi M, Hirano T. Synergistic roles for Pim-1 and c-Myc in STAT3-mediated cell cycle progression and antiapoptosis. Immunity. 1999;11(6):709-19
183. Bromberg JF, Wrzeszczynska MH, Devgan G, Zhao Y, Pestell RG, Albanese C, et al. Stat3 as an oncogene. Cell. 1999;98(3):295-303
184. Fukada T, Ohtani T, Yoshida Y, Shirogane T, Nishida K, Nakajima K, et al. STAT3 orchestrates contradictory signals in cytokine-induced G 1 to S cell-cycle transition. The EMBO Journal. 1998;17(22):6670-7
185. Matsumura I, Kitamura T, Wakao H, Tanaka H, Hashimoto K, Albanese C, et al. Transcriptional regulation of the cyclin D1 promoter by STAT5: its involvement in cytokine-dependent growth of hematopoietic cells. The EMBO journal. 1999;18(5):1367-77

186. Nosaka T, Kawashima T, Misawa K, Ikuta K, Mui ALF, Kitamura T. STAT5 as a molecular regulator of proliferation, differentiation and apoptosis in hematopoietic cells. The EMBO Journal. 1999;18(17):4754-65
187. Wolf MJ, Hoos A, Bauer J, Boettcher S, Knust M, Weber A, et al. Endothelial CCR2 signaling induced by colon carcinoma cells enables extravasation via the JAK2-Stat5 and p38MAPK pathway. Cancer cell. 2012;22(1):91-105
188. Murata T, Noguchi PD, Puri RK. IL-13 induces phosphorylation and activation of JAK2 Janus kinase in human colon carcinoma cell lines: similarities between IL-4 and IL-13 signaling. The Journal of Immunology. 1996;156(8):2972-8
189. Gao B, Shen X, Kunos G, Meng Q, Goldberg ID, Rosen EM, et al. Constitutive activation of JAK–STAT3 signaling by BRCA1 in human prostate cancer cells. FEBS letters. 2001;488(3):179-84
190. To K, Chan M, Leung W, Ng E, Yu J, Bai A, et al. Constitutional activation of IL-6-mediated JAK/STAT pathway through hypermethylation of SOCS-1 in human gastric cancer cell line. British Journal of Cancer. 2004;91(7):1335-41
191. Witthuhn BA, Quelle FW, Silvennoinen O, Yi T, Tang B, Miura O, et al. JAK2 associates with the erythropoietin receptor and is tyrosine phosphorylated and activated following stimulation with erythropoietin. Cell. 1993;74(2):227-36
192. Green MR, Monti S, Rodig SJ, Juszczynski P, Currie T, O'Donnell E, et al. Integrative analysis reveals selective 9p24. 1 amplification, increased PD-1 ligand expression, and further induction via JAK2 in nodular sclerosing Hodgkin lymphoma and primary mediastinal large B-cell lymphoma. Blood. 2010;116(17):3268-77
193. Joos S, Küpper M, Ohl S, von Bonin F, Mechtersheimer G, Bentz M, et al. Genomic imbalances including amplification of the tyrosine kinase gene JAK2 in CD30+ Hodgkin cells. Cancer research. 2000;60(3):549-52
194. Lee JW, Kim YG, Soung YH, Han KJ, Kim SY, Rhim HS, et al. The JAK2 V617F mutation in de novo acute myelogenous leukemias. Oncogene. 2005;25:1434
195. Shi L, Wang S, Zangari M, Xu H, Cao TM, Xu C, et al. Over-expression of CKS1B activates both MEK/ERK and JAK/STAT3 signaling pathways and promotes myeloma cell drug-resistance. Oncotarget. 2010;1(1):22
196. Scuto A, Krejci P, Popplewell L, Wu J, Wang Y, Kujawski M, et al. The novel JAK inhibitor AZD1480 blocks STAT3 and FGFR3 signaling, resulting in suppression of human myeloma cell growth and survival. Leukemia. 2011;25(3):538-50
197. Houldsworth J, Mathew S, Rao PH, Dyomina K, Louie DC, Parsa N, et al. REL proto-oncogene is frequently amplified in extranodal diffuse large cell lymphoma. Blood. 1996;87(1):25-9
198. Rao PH, Houldsworth J, Dyomina K, Parsa NZ, Cigudosa JC, Louie DC, et al. Chromosomal and gene amplification in diffuse large B-cell lymphoma. Blood. 1998;92(1):234-40
199. Migliazza A, Lombardi L, Rocchi M, Trecca D, Chang C-C, Antonacci R, et al. Heterogeneous chromosomal aberrations generate 39 truncations of the NFKB2/lyt-10 gene in lymphoid malignancies. Blood. 1994;84(11):3850-60
200. Neri A, Chang C-C, Lombardi L, Salina M, Corradini P, Maiolo AT, et al. B cell lymphoma-associated chromosomal translocation involves candidate oncogene lyt-10, homologous to NF-κB p50. Cell. 1991;67(6):1075-87
201. Neri A, Fracchiolla NS, Roscetti E, Garatti S, Trecca D, Boletini A, et al. Molecular analysis of cutaneous B-and T-cell lymphomas. Blood. 1995;86(8):3160-72
202. Annunziata CM, Davis RE, Demchenko Y, Bellamy W, Gabrea A, Zhan F, et al. Frequent engagement of the classical and alternative NF-kappaB pathways by diverse genetic abnormalities in multiple myeloma. Cancer Cell. 2007;12(2):115-3017692804.
203. Keats JJ, Fonseca R, Chesi M, Schop R, Baker A, Chng WJ, et al. Promiscuous mutations activate the noncanonical NF-kappaB pathway in multiple myeloma. Cancer Cell. 2007;12(2):131-4417692805.

204. Nakano H, Shindo M, Sakon S, Nishinaka S, Mihara M, Yagita H, et al. Differential regulation of IkappaB kinase alpha and beta by two upstream kinases, NF-kappaB-inducing kinase and mitogen-activated protein kinase/ERK kinase kinase-1. Proc Natl Acad Sci U S A. 1998;95(7):3537-429520401.
205. Ahmad A, Biersack B, Li Y, Kong D, Bao B, Schobert R, et al. Targeted Regulation of PI3K/Akt/mTOR/NF-κB Signaling by Indole Compounds and their Derivatives: Mechanistic Details and Biological Implications for Cancer Therapy. Anti-cancer agents in medicinal chemistry. 2013;13(7):1002-13PMC3901097.
206. Kloster MM, Naderi EH, Carlsen H, Blomhoff HK, Naderi S. Hyperactivation of NF-κB via the MEK signaling is indispensable for the inhibitory effect of cAMP on DNA damage-induced cell death. Molecular cancer. 2011;10(1):45
207. Villanueva J, Vultur A, Lee JT, Somasundaram R, Fukunaga-Kalabis M, Cipolla AK, et al. Acquired resistance to BRAF inhibitors mediated by a RAF kinase switch in melanoma can be overcome by cotargeting MEK and IGF-1R/PI3K. Cancer cell. 2010;18(6):683-95
208. Lui VW, Hedberg ML, Li H, Vangara BS, Pendleton K, Zeng Y, et al. Frequent mutation of the PI3K pathway in head and neck cancer defines predictive biomarkers. Cancer discovery. 2013;3(7):761-9
209. Johnson SM, Gulhati P, Rampy BA, Han Y, Rychahou PG, Doan HQ, et al. Novel expression patterns of PI3K/Akt/mTOR signaling pathway components in colorectal cancer. Journal of the American College of Surgeons. 2010;210(5):767-76
210. Kubota Y, Ohnishi H, Kitanaka A, Ishida T, Tanaka T. Constitutive activation of PI3K is involved in the spontaneous proliferation of primary acute myeloid leukemia cells: direct evidence of PI3K activation. Leukemia. 2004;18(8):1438-
211. Lannutti BJ, Meadows SA, Herman SE, Kashishian A, Steiner B, Johnson AJ, et al. CAL-101, a p110δ selective phosphatidylinositol-3-kinase inhibitor for the treatment of B-cell malignancies, inhibits PI3K signaling and cellular viability. Blood. 2011;117(2):591-4
212. Samuels Y, Wang Z, Bardelli A, Silliman N, Ptak J, Szabo S, et al. High frequency of mutations of the PIK3CA gene in human cancers. Science. 2004;304(5670):554-
213. Campbell IG, Russell SE, Choong DY, Montgomery KG, Ciavarella ML, Hooi CS, et al. Mutation of the PIK3CA gene in ovarian and breast cancer. Cancer research. 2004;64(21):7678-81
214. Li J, Yen C, Liaw D, Podsypanina K, Bose S, Wang SI, et al. PTEN, a putative protein tyrosine phosphatase gene mutated in human brain, breast, and prostate cancer. science. 1997;275(5308):1943-7
215. Wang S, Gao J, Lei Q, Rozengurt N, Pritchard C, Jiao J, et al. Prostate-specific deletion of the murine Pten tumor suppressor gene leads to metastatic prostate cancer. Cancer cell. 2003;4(3):209-21
216. Ho F, Lortan JE, MaClennan I, Khan M. Distinct short-lived and long-lived antibody-producing cell populations. European journal of immunology. 1986;16(10):1297-301
217. Rawstron AC, Owen RG, Davies FE, Johnson RJ, Jones RA, Richards SJ, et al. Circulating plasma cells in multiple myeloma: characterization and correlation with disease stage. British journal of haematology. 1997;97(1):46-55
218. Paiva B, Paino T, Sayagues J-M, Garayoa M, San-Segundo L, Martín M, et al. Detailed characterization of multiple myeloma circulating tumor cells shows unique phenotypic, cytogenetic, functional, and circadian distribution profile. Blood. 2013;122(22):3591-8
219. Damiano JS, Cress AE, Hazlehurst LA, Shtil AA, Dalton WS. Cell adhesion mediated drug resistance (CAM-DR): role of integrins and resistance to apoptosis in human myeloma cell lines. Blood. 1999;93(5):1658-67
220. Green SK, Frankel A, Kerbel RS. Adhesion-dependent multicellular drug resistance. Anticancer Drug Des. 1999;14(2):153-6810405642.
221. Schey SA, Yong KL, Marcus R, Anderson KC. Myeloma: Pathology, Diagnosis, and Treatment: Cambridge University Press; 2013.

222. Tatsumi T, Shimazaki C, Goto H, Araki S, Sudo Y, Yamagata N, et al. Expression of adhesion molecules on myeloma cells. Japanese journal of cancer research : Gann. 1996;87(8):837-428797890.
223. Hideshima T, Mitsiades C, Tonon G, Richardson PG, Anderson KC. Understanding multiple myeloma pathogenesis in the bone marrow to identify new therapeutic targets. Nature Reviews Cancer. 2007;7(8):585-98
224. Hatano K, Kikuchi J, Takatoku M, Shimizu R, Wada T, Ueda M, et al. Bortezomib overcomes cell adhesion-mediated drug resistance through downregulation of VLA-4 expression in multiple myeloma. Oncogene. 2009;28(2):231-42
225. Uchiyama H, Barut BA, Mohrbacher AF, Chauhan D, Anderson KC. Adhesion of human myeloma-derived cell lines to bone marrow stromal cells stimulates interleukin-6 secretion. Blood. 1993;82(12):3712-20
226. Ogata A, Chauhan D, Teoh G, Treon SP, Urashima M, Schlossman RL, et al. IL-6 triggers cell growth via the Ras-dependent mitogen-activated protein kinase cascade. The Journal of Immunology. 1997;159(5):2212-21
227. Catlett-Falcone R, Landowski TH, Oshiro MM, Turkson J, Levitzki A, Savino R, et al. Constitutive activation of Stat3 signaling confers resistance to apoptosis in human U266 myeloma cells. Immunity. 1999;10(1):105-15
228. Jourdan M, Veyrune J-L, De Vos J, Redal N, Couderc G, Klein B. A major role for Mcl-1 antiapoptotic protein in the IL-6-induced survival of human myeloma cells. Oncogene. 2003;22(19):2950-9
229. Vacca A, Loreto MD, Ribatti D, Stefano RD, Gadaleta-Caldarola G, Iodice G, et al. Bone marrow of patients with active multiple myeloma: Angiogenesis and plasma cell adhesion molecules LFA-1, VLA-4, LAM-1, and CD44. American journal of hematology. 1995;50(1):9-14
230. Ribatti D, Vacca A, Nico B, Quondamatteo F, Ria R, Minischetti M, et al. Bone marrow angiogenesis and mast cell density increase simultaneously with progression of human multiple myeloma. British Journal of Cancer. 1999;79(3-4):451
231. Nakagawa N, Kinosaki M, Yamaguchi K, Shima N, Yasuda H, Yano K, et al. RANK is the essential signaling receptor for osteoclast differentiation factor in osteoclastogenesis. Biochemical and biophysical research communications. 1998;253(2):395-400
232. Dougall WC, Glaccum M, Charrier K, Rohrbach K, Brasel K, De Smedt T, et al. RANK is essential for osteoclast and lymph node development. Genes & development. 1999;13(18):2412-24
233. Kudo O, Sabokbar A, Pocock A, Itonaga I, Fujikawa Y, Athanasou NA. Interleukin-6 and interleukin-11 support human osteoclast formation by a RANKL-independent mechanism. Bone. 2003;32(1):1-712584029.
234. Tamura T, Udagawa N, Takahashi N, Miyaura C, Tanaka S, Yamada Y, et al. Soluble interleukin-6 receptor triggers osteoclast formation by interleukin 6. Proceedings of the National Academy of Sciences. 1993;90(24):11924-8
235. DuVillard L, Guiguet M, Casasnovas RO, Caillot D, Monnier-Zeller V, Bernard A, et al. Diagnostic value of serum IL-6 level in monoclonal gammopathies. Br J Haematol. 1995;89(2):243-97873373.
236. Walker RC, Brown TL, Jones-Jackson LB, De Blanche L, Bartel T. Imaging of multiple myeloma and related plasma cell dyscrasias. Journal of Nuclear Medicine. 2012;53(7):1091-101
237. Holmgren L, O'Reilly MS, Folkman J. Dormancy of micrometastases: balanced proliferation and apoptosis in the presence of angiogenesis suppression. Nature medicine. 1995;1(2):149-53
238. Hashizume H, Baluk P, Morikawa S, McLean JW, Thurston G, Roberge S, et al. Openings between defective endothelial cells explain tumor vessel leakiness. The American journal of pathology. 2000;156(4):1363-80

239. Vacca A, Ribatti D, Roncali L, Ranieri G, Serio G, Silvestris F, et al. Bone marrow angiogenesis and progression in multiple myeloma. British journal of haematology. 1994;87(3):503-8
240. Barillé S, Akhoundi C, Collette M, Mellerin M-P, Rapp M-J, Harousseau J-L, et al. Metalloproteinases in multiple myeloma: production of matrix metalloproteinase-9 (MMP-9), activation of proMMP-2, and induction of MMP-1 by myeloma cells. Blood. 1997;90(4):1649-55
241. Kumar S, Witzig TE, Timm M, Haug J, Wellik L, Fonseca R, et al. Expression of VEGF and its receptors by myeloma cells. Leukemia. 2003;17(10):2025-31
242. Colla S, Morandi F, Lazzaretti M, Rizzato R, Lunghi P, Bonomini S, et al. Human myeloma cells express the bone regulating gene Runx2/Cbfa1 and produce osteopontin that is involved in angiogenesis in multiple myeloma patients. Leukemia. 2005;19(12):2166-76
243. Gao X, Neufeld TP, Pan D. Drosophila PTEN regulates cell growth and proliferation through PI3K-dependent and-independent pathways. Developmental biology. 2000;221(2):404-18
244. Kozma SC, Thomas G. Regulation of cell size in growth, development and human disease: PI3K, PKB and S6K. Bioessays. 2002;24(1):65-71
245. Brunet A, Bonni A, Zigmond MJ, Lin MZ, Juo P, Hu LS, et al. Akt promotes cell survival by phosphorylating and inhibiting a Forkhead transcription factor. cell. 1999;96(6):857-68
246. Brunet A, Datta SR, Greenberg ME. Transcription-dependent and-independent control of neuronal survival by the PI3K–Akt signaling pathway. Current opinion in neurobiology. 2001;11(3):297-305
247. Carnero A, Paramio JM. The PTEN/PI3K/AKT Pathway in vivo, Cancer Mouse Models. Frontiers in Oncology. 2014;4(252)
248. Datta SR, Dudek H, Tao X, Masters S, Fu H, Gotoh Y, et al. Akt Phosphorylation of BAD Couples Survival Signals to the Cell-Intrinsic Death Machinery. Cell. 1997;91(2):231-41
249. Rosenquist M. 14-3-3 proteins in apoptosis. Brazilian Journal of Medical and Biological Research. 2003;36(4):403-8
250. Cardone MH, Roy N, Stennicke HR, Salvesen GS, Franke TF, Stanbridge E, et al. Regulation of Cell Death Protease Caspase-9 by Phosphorylation. Science. 1998;282(5392):1318-21
251. Medema RH, Kops GJ, Bos JL, Burgering BM. AFX-like Forkhead transcription factors mediate cell-cycle regulation by Ras and PKB through p27kip1. Nature. 2000;404(6779):782-710783894.
252. Dijkers PF, Medema RH, Pals C, Banerji L, Thomas NS, Lam EW, et al. Forkhead transcription factor FKHR-L1 modulates cytokine-dependent transcriptional regulation of p27(KIP1). Mol Cell Biol. 2000;20(24):9138-4811094066.
253. Seoane J, Le HV, Shen L, Anderson SA, Massague J. Integration of Smad and forkhead pathways in the control of neuroepithelial and glioblastoma cell proliferation. Cell. 2004;117(2):211-2315084259.
254. Essafi A, Fernandez de Mattos S, Hassen YA, Soeiro I, Mufti GJ, Thomas NS, et al. Direct transcriptional regulation of Bim by FoxO3a mediates STI571-induced apoptosis in Bcr-Abl-expressing cells. Oncogene. 2005;24(14):2317-2915688014.
255. Goto T, Takano M, Hirata J, Tsuda H. The involvement of FOXO1 in cytotoxic stress and drug-resistance induced by paclitaxel in ovarian cancers. British journal of cancer. 2008;98(6):1068-75
256. Piddock RE, Bowles KM, Rushworth SA. The Role of PI3K Isoforms in Regulating Bone Marrow Microenvironment Signaling Focusing on Acute Myeloid Leukemia and Multiple Myeloma. Cancers (Basel). 2017;9(4)28350342.
257. Bodine SC, Stitt TN, Gonzalez M, Kline WO, Stover GL, Bauerlein R, et al. Akt/mTOR pathway is a crucial regulator of skeletal muscle hypertrophy and can prevent muscle atrophy in vivo. Nature cell biology. 2001;3(11):1014-9

258. Zhu H, Shyh-Chang N, Segrè Ayellet V, Shinoda G, Shah Samar P, Einhorn William S, et al. The Lin28/let-7 Axis Regulates Glucose Metabolism. Cell. 2011;147(1):81-94
259. Kim D-H, Sarbassov DD, Ali SM, King JE, Latek RR, Erdjument-Bromage H, et al. mTOR Interacts with Raptor to Form a Nutrient-Sensitive Complex that Signals to the Cell Growth Machinery. Cell. 2002;110(2):163-75
260. Kim J, Kundu M, Viollet B, Guan K-L. AMPK and mTOR regulate autophagy through direct phosphorylation of Ulk1. Nature cell biology. 2011;13(2):132-41
261. Weisberg E, Banerji L, Wright RD, Barrett R, Ray A, Moreno D, et al. Potentiation of antileukemic therapies by the dual PI3K/PDK-1 inhibitor, BAG956: effects on BCR-ABL– and mutant FLT3-expressing cells. Blood. 2008;111(7):3723-34
262. Schwindinger WF, Robishaw JD. Heterotrimeric G-protein betagamma-dimers in growth and differentiation. Oncogene. 2001;20(13):1653-6011313913.
263. Guillermet-Guibert J, Bjorklof K, Salpekar A, Gonella C, Ramadani F, Bilancio A, et al. The p110beta isoform of phosphoinositide 3-kinase signals downstream of G protein-coupled receptors and is functionally redundant with p110gamma. Proc Natl Acad Sci U S A. 2008;105(24):8292-718544649.
264. Bachman KE, Argani P, Samuels Y, Silliman N, Ptak J, Szabo S, et al. The PIK3CA gene is mutated with high frequency in human breast cancers. Cancer Biol Ther. 2004;3(8):772-515254419.
265. Lai Y-L, Mau B-L, Cheng W-H, Chen H-M, Chiu H-H, Tzen C-Y. PIK3CA exon 20 mutation is independently associated with a poor prognosis in breast cancer patients. Annals of surgical oncology. 2008;15(4):1064-9
266. Barbareschi M, Cuorvo LV, Girlando S, Bragantini E, Eccher C, Leonardi E, et al. PI3KCA mutations and/or PTEN loss in Her2-positive breast carcinomas treated with trastuzumab are not related to resistance to anti-Her2 therapy. Virchows Archiv. 2012;461(2):129-39
267. Oda K, Stokoe D, Taketani Y, McCormick F. High frequency of coexistent mutations of PIK3CA and PTEN genes in endometrial carcinoma. Cancer research. 2005;65(23):10669-73
268. Catasus L, Gallardo A, Cuatrecasas M, Prat J. PIK3CA mutations in the kinase domain (exon 20) of uterine endometrial adenocarcinomas are associated with adverse prognostic parameters. Modern pathology. 2008;21(2):131-9
269. Ogino S, Nosho K, Kirkner GJ, Shima K, Irahara N, Kure S, et al. PIK3CA mutation is associated with poor prognosis among patients with curatively resected colon cancer. Journal of clinical oncology. 2009;27(9):1477-84
270. Ikenoue T, Kanai F, Hikiba Y, Obata T, Tanaka Y, Imamura J, et al. Functional analysis of PIK3CA gene mutations in human colorectal cancer. Cancer research. 2005;65(11):4562-7
271. Costa C, Ebi H, Martini M, Beausoleil SA, Faber AC, Jakubik CT, et al. Measurement of PIP3 levels reveals an unexpected role for p110beta in early adaptive responses to p110alpha-specific inhibitors in luminal breast cancer. Cancer Cell. 2015;27(1):97-10825544637.
272. Hummerdal P, Andersson P, Willander K, Linderholm M, Söderkvist P, Jönsson JI. Absence of hot spot mutations of the PIK3CA gene in acute myeloid leukaemia. European journal of haematology. 2006;77(1):86-7
273. Müller CI, Miller CW, Hofmann W-K, Gross ME, Walsh CS, Kawamata N, et al. Rare mutations of the PIK3CA gene in malignancies of the hematopoietic system as well as endometrium, ovary, prostate and osteosarcomas, and discovery of a PIK3CA pseudogene. Leukemia research. 2007;31(1):27-32
274. Jackson SP, Schoenwaelder SM, Goncalves I, Nesbitt WS, Yap CL, Wright CE, et al. PI 3-kinase p110beta: a new target for antithrombotic therapy. Nat Med. 2005;11(5):507-1415834429.
275. Zhu Q, Youn H, Tang J, Tawfik O, Dennis K, Terranova P, et al. Phosphoinositide 3-OH kinase p85α and p110β are essential for androgen receptor transactivation and tumor progression in prostate cancers. Oncogene. 2008;27(33):4569-79

276. Wee S, Wiederschain D, Maira SM, Loo A, Miller C, deBeaumont R, et al. PTEN-deficient cancers depend on PIK3CB. Proc Natl Acad Sci U S A. 2008;105(35):13057-6218755892.
277. Thorpe LM, Yuzugullu H, Zhao JJ. PI3K in cancer: divergent roles of isoforms, modes of activation and therapeutic targeting. Nature Reviews Cancer. 2015;15(1):7
278. Sahin I, Moschetta M, Mishima Y, Glavey S, Tsang B, Azab F, et al. Distinct roles of class I PI3K isoforms in multiple myeloma cell survival and dissemination. Blood cancer journal. 2014;4(4):e204
279. Fruman DA. Regulatory subunits of class IA PI3K. Phosphoinositide 3-kinase in Health and Disease: Springer; 2010. p. 225-44.
280. Hirsch E, Katanaev VL, Garlanda C, Azzolino O, Pirola L, Silengo L, et al. Central Role for G Protein-Coupled Phosphoinositide 3-Kinase γ in Inflammation. Science. 2000;287(5455):1049-53
281. Camps M, Rückle T, Ji H, Ardissone V, Rintelen F, Shaw J, et al. Blockade of PI3Kγ suppresses joint inflammation and damage in mouse models of rheumatoid arthritis. Nature medicine. 2005;11(9):936-43
282. Belloni E, Veronesi G, Rotta L, Volorio S, Sardella D, Bernard L, et al. Whole exome sequencing identifies driver mutations in asymptomatic computed tomography-detected lung cancers with normal karyotype. Cancer Genet. 2015;208(4):152-525850996.
283. Conte E, Gili E, Fruciano M, Korfei M, Fagone E, Iemmolo M, et al. PI3K p110gamma overexpression in idiopathic pulmonary fibrosis lung tissue and fibroblast cells: in vitro effects of its inhibition. Lab Invest. 2013;93(5):566-7623439433.
284. Vanhaesebroeck B, Welham MJ, Kotani K, Stein R, Warne PH, Zvelebil MJ, et al. P110δ, a novel phosphoinositide 3-kinase in leukocytes. Proceedings of the National Academy of Sciences. 1997;94(9):4330-5
285. Ramadani F, Bolland DJ, Garcon F, Emery JL, Vanhaesebroeck B, Corcoran AE, et al. The PI3K isoforms p110alpha and p110delta are essential for pre-B cell receptor signaling and B cell development. Sci Signal. 2010;3(134):ra6020699475.
286. Sujobert P, Bardet V, Cornillet-Lefebvre P, Hayflick JS, Prie N, Verdier F, et al. Essential role for the p110delta isoform in phosphoinositide 3-kinase activation and cell proliferation in acute myeloid leukemia. Blood. 2005;106(3):1063-615840695.
287. Hoellenriegel J, Meadows SA, Sivina M, Wierda WG, Kantarjian H, Keating MJ, et al. The phosphoinositide 3'-kinase delta inhibitor, CAL-101, inhibits B-cell receptor signaling and chemokine networks in chronic lymphocytic leukemia. Blood. 2011;118(13):3603-12
288. Flinn IW, Byrd JC, Furman RR, Brown JR, Lin TS, Bello C, et al. Preliminary evidence of clinical activity in a phase I study of CAL-101, a selective inhibitor of the p1108 isoform of phosphatidylinositol 3-kinase (P13K), in patients with select hematologic malignancies. Journal of Clinical Oncology. 2009;27(15_suppl):3543-27961357.
289. Zhang Q, Xia B, Qu F, Yuan T, Guo S, Zhao W, et al. [Effect of PI3Kdelta inhibitor CAL-101 on myeloma cell lines and preliminary study of synergistic effects with other new drugs]. Zhonghua Xue Ye Xue Za Zhi. 2014;35(10):926-3025339332.
290. Ikeda H, Hideshima T, Okawa Y, Vallet S, Pozzi S, Santo L, et al. CAL-101, a Specific Inhibitor of the p110δ Isoform of Phosphatidylinositide 3-Kinase Induces Cytotoxicity in Multiple Myeloma (MM). Blood. 2008;112(11):2753-
291. Bataille R, Jego G, Robillard N, Barille-Nion S, Harousseau JL, Moreau P, et al. The phenotype of normal, reactive and malignant plasma cells. Identification of "many and multiple myelomas" and of new targets for myeloma therapy. Haematologica. 2006;91(9):1234-4016956823.
292. Strober W. Trypan blue exclusion test of cell viability. Curr Protoc Immunol. 2001;Appendix 3:Appendix 3B18432654.
293. Crouch SP, Kozlowski R, Slater KJ, Fletcher J. The use of ATP bioluminescence as a measure of cell proliferation and cytotoxicity. J Immunol Methods. 1993;160(1):81-87680699.

294. Livak KJ, Schmittgen TD. Analysis of relative gene expression data using real-time quantitative PCR and the 2− ΔΔCT method. methods. 2001;25(4):402-8
295. Sahin I, Azab F, Mishima Y, Moschetta M, Tsang B, Glavey SV, et al. Targeting survival and cell trafficking in multiple myeloma and Waldenstrom macroglobulinemia using pan-class I PI3K inhibitor, buparlisib. American journal of hematology. 2014;89(11):1030-6
296. Sujobert P, Bardet V, Cornillet-Lefebvre P, Hayflick JS, Prie N, Verdier F, et al. Essential role for the p110δ isoform in phosphoinositide 3-kinase activation and cell proliferation in acute myeloid leukemia. Blood. 2005;106(3):1063-6
297. Brown JR, Byrd JC, Coutre SE, Benson DM, Flinn IW, Wagner-Johnston ND, et al. Idelalisib, an inhibitor of phosphatidylinositol 3-kinase p110δ, for relapsed/refractory chronic lymphocytic leukemia. Blood. 2014;123(22):3390-7
298. Hickey FB, Cotter TG. BCR-ABL regulates phosphatidylinositol 3-kinase-p110γ transcription and activation and is required for proliferation and drug resistance. Journal of Biological Chemistry. 2006;281(5):2441-50
299. Dong S, Guinn D, Dubovsky JA, Zhong Y, Lehman A, Kutok J, et al. IPI-145 antagonizes intrinsic and extrinsic survival signals in chronic lymphocytic leukemia cells. Blood. 2014;124(24):3583-6
300. Zlei M, Egert S, Wider D, Ihorst G, Wäsch R, Engelhardt M. Characterization of in vitro growth of multiple myeloma cells. Experimental Hematology. 2007;35(10):1550-61
301. Sasaki T, Irie-Sasaki J, Jones RG, Oliveira-dos-Santos AJ, Stanford WL, Bolon B, et al. Function of PI3Kgamma in thymocyte development, T cell activation, and neutrophil migration. Science. 2000;287(5455):1040-610669416.
302. Ma P, Vemula S, Munugalavadla V, Chen J, Sims E, Borneo J, et al. Balanced interactions between Lyn, the p85alpha regulatory subunit of class I(A) phosphatidylinositol-3-kinase, and SHIP are essential for mast cell growth and maturation. Mol Cell Biol. 2011;31(19):4052-6221791602.
303. Ikeda H, Hideshima T, Fulciniti M, Perrone G, Miura N, Yasui H, et al. PI3K/p110{delta} is a novel therapeutic target in multiple myeloma. Blood. 2010;116(9):1460-820505158.
304. Koyasu S. The role of PI3K in immune cells. Nature immunology. 2003;4(4):313-9
305. Klein B, Zhang XG, Jourdan M, Content J, Houssiau F, Aarden L, et al. Paracrine rather than autocrine regulation of myeloma-cell growth and differentiation by interleukin-6. Blood. 1989;73(2):517-262783861.
306. Bloem AC, Lamme T, de Smet M, Kok H, Vooijs W, Wijdenes J, et al. Long-term bone marrow cultured stromal cells regulate myeloma tumour growth in vitro: studies with primary tumour cells and LTBMC-dependent cell lines. Br J Haematol. 1998;100(1):166-759450806.
307. Yaccoby S, Wezeman MJ, Henderson A, Cottler-Fox M, Yi Q, Barlogie B, et al. Cancer and the microenvironment: myeloma-osteoclast interactions as a model. Cancer Res. 2004;64(6):2016-2315026338.
308. Ludwig CU, Durie BG, Salmon SE, Moon TE. Tumor growth stimulation in vitro by interferons. European Journal of Cancer and Clinical Oncology. 1983;19(11):1625-32
309. Nefedova Y, Landowski T, Dalton W. Bone marrow stromal-derived soluble factors and direct cell contact contribute to de novo drug resistance of myeloma cells by distinct mechanisms. Leukemia. 2003;17(6):1175
310. Mendoza MC, Er EE, Blenis J. The Ras-ERK and PI3K-mTOR pathways: cross-talk and compensation. Trends in biochemical sciences. 2011;36(6):320-8
311. Rodriguez-Viciana P, Warne PH, Dhand R, Vanhaesebroeck B, Gout I, Fry MJ, et al. Phosphatidylinositol-3-OH kinase direct target of Ras. Nature. 1994;370(6490):527-32
312. Hideshima T, Nakamura N, Chauhan D, Anderson KC. Biologic sequelae of interleukin-6 induced PI3-K/Akt signaling in multiple myeloma. Oncogene. 2001;20(42):5991-6000
313. Chang Q, Bournazou E, Sansone P, Berishaj M, Gao SP, Daly L, et al. The IL-6/JAK/Stat3 feed-forward loop drives tumorigenesis and metastasis. Neoplasia. 2013;15(7):848IN40-62IN45

314. Heinrich PC, Behrmann I, Serge H, Hermanns HM, Müller-Newen G, Schaper F. Principles of interleukin (IL)-6-type cytokine signalling and its regulation. Biochemical journal. 2003;374(1):1-20
315. Moreaux J, Legouffe E, Jourdan E, Quittet P, Rème T, Lugagne C, et al. BAFF and APRIL protect myeloma cells from apoptosis induced by interleukin 6 deprivation and dexamethasone. Blood. 2004;103(8):3148-57
316. Tai Y-T, Podar K, Mitsiades N, Lin B, Mitsiades C, Gupta D, et al. CD40 induces human multiple myeloma cell migration via phosphatidylinositol 3–kinase/AKT/NF-κB signaling. Blood. 2003;101(7):2762-9
317. Yang L, Wang L, Lin H-K, Kan P-Y, Xie S, Tsai M-Y, et al. Interleukin-6 differentially regulates androgen receptor transactivation via PI3K-Akt, STAT3, and MAPK, three distinct signal pathways in prostate cancer cells. Biochemical and biophysical research communications. 2003;305(3):462-9
318. Wegiel B, Bjartell A, Culig Z, Persson JL. Interleukin-6 activates PI3K/Akt pathway and regulates cyclin A1 to promote prostate cancer cell survival. International journal of cancer. 2008;122(7):1521-9
319. Pene F, Claessens YE, Muller O, Viguie F, Mayeux P, Dreyfus F, et al. Role of the phosphatidylinositol 3-kinase/Akt and mTOR/P70S6-kinase pathways in the proliferation and apoptosis in multiple myeloma. Oncogene. 2002;21(43):6587-9712242656.
320. Descamps G, Pellat-Deceunynck C, Szpak Y, Bataille R, Robillard N, Amiot M. The Magnitude of Akt/Phosphatidylinositol 3'-Kinase Proliferating Signaling Is Related to CD45 Expression in Human Myeloma Cells. The Journal of Immunology. 2004;173(8):4953-9
321. Stitt TN, Drujan D, Clarke BA, Panaro F, Timofeyva Y, Kline WO, et al. The IGF-1/PI3K/Akt pathway prevents expression of muscle atrophy-induced ubiquitin ligases by inhibiting FOXO transcription factors. Molecular cell. 2004;14(3):395-403
322. Choi Y, Zhang J, Murga C, Yu H, Koller E, Monia BP, et al. PTEN, but not SHIP and SHIP2, suppresses the PI3K/Akt pathway and induces growth inhibition and apoptosis of myeloma cells. Oncogene. 2002;21(34):5289
323. Winkler DG, Faia KL, DiNitto JP, Ali JA, White KF, Brophy EE, et al. PI3K-δ and PI3K-γ inhibition by IPI-145 abrogates immune responses and suppresses activity in autoimmune and inflammatory disease models. Chemistry & biology. 2013;20(11):1364-74
324. Görgün GT, Whitehill G, Anderson JL, Hideshima T, Maguire C, Laubach J, et al. Tumor-promoting immune-suppressive myeloid-derived suppressor cells in the multiple myeloma microenvironment in humans. Blood. 2013;121(15):2975-87
325. Meads MB, Hazlehurst LA, Dalton WS. The bone marrow microenvironment as a tumor sanctuary and contributor to drug resistance. Clinical Cancer Research. 2008;14(9):2519-26
326. Tai Y-T, Li X-F, Breitkreutz I, Song W, Neri P, Catley L, et al. Role of B-cell–activating factor in adhesion and growth of human multiple myeloma cells in the bone marrow microenvironment. Cancer research. 2006;66(13):6675-82
327. Chauhan D, Uchiyama H, Urashima M, Yamamoto K, Anderson KC. Regulation of interleukin 6 in multiple myeloma and bone marrow stromal cells. Stem Cells. 1995;13 Suppl 2:35-98520509.
328. Zdzisinska B, Bojarska-Junak A, Dmoszynska A, Kandefer-Szerszen M. Abnormal cytokine production by bone marrow stromal cells of multiple myeloma patients in response to RPMI8226 myeloma cells. Archivum immunologiae et therapiae experimentalis. 2008;56(3):207-2118512025.
329. Xu X, Wang B, Ye C, Yao C, Lin Y, Huang X, et al. Overexpression of macrophage migration inhibitory factor induces angiogenesis in human breast cancer. Cancer Letters. 2008;261(2):147-57
330. Zheng Y, Wang Q, Li T, Qian J, Lu Y, Li Y, et al. Role of myeloma-derived MIF in myeloma cell adhesion to bone marrow and chemotherapy response. JNCI: Journal of the National Cancer Institute. 2016;108(11)

331. Abdul-Aziz AM, Shafat MS, Mehta TK, Di Palma F, Lawes MJ, Rushworth SA, et al. MIF-induced stromal PKCβ/IL8 is essential in human acute myeloid leukemia. Cancer research. 2017;77(2):303-11
332. Takahashi N, Nishihira J, Sato Y, Kondo M, Ogawa H, Ohshima T, et al. Involvement of macrophage migration inhibitory factor (MIF) in the mechanism of tumor cell growth. Molecular medicine. 1998;4(11):707
333. Lubetsky JB, Dios A, Han J, Aljabari B, Ruzsicska B, Mitchell R, et al. The tautomerase active site of macrophage migration inhibitory factor is a potential target for discovery of novel anti-inflammatory agents. Journal of Biological Chemistry. 2002;277(28):24976-82
334. Naugler WE, Sakurai T, Kim S, Maeda S, Kim K, Elsharkawy AM, et al. Gender Disparity in Liver Cancer Due to Sex Differences in MyD88-Dependent IL-6 Production. Science. 2007;317(5834):121-4
335. Whitacre CC. Sex differences in autoimmune disease. Nature immunology. 2001;2(9):777
336. O'Malley K, Crooks J, Duke E, Stevenson IH. Effect of Age and Sex on Human Drug Metabolism. British Medical Journal. 1971;3(5775):607-9
337. Delmore Jake E, Issa Ghayas C, Lemieux Madeleine E, Rahl Peter B, Shi J, Jacobs Hannah M, et al. BET Bromodomain Inhibition as a Therapeutic Strategy to Target c-Myc. Cell. 2011;146(6):904-17
338. Kondo A, Otsuka T, Matsushima-Nishiwaki R, Kuroyanagi G, Mizutani J, Wada I, et al. Inhibition of SAPK/JNK leads to enhanced IL-1-induced IL-6 synthesis in osteoblasts. Arch Biochem Biophys. 2013;535(2):227-3323624146.
339. Manna S, Singha B, Phyo SA, Gatla HR, Chang T-P, Sanacora S, et al. Proteasome inhibition by bortezomib increases IL-8 expression in androgen-independent prostate cancer cells: the role of IKKα. The Journal of Immunology. 2013;191(5):2837-46
340. Hofmann C, Stühmer T, Schmiedl N, Wetzker R, Mottok A, Rosenwald A, et al. PI3K-dependent multiple myeloma cell survival is mediated by the PIK3CA isoform. British Journal of Haematology. 2014;166(4):529-39
341. Lue H, Kleemann R, Calandra T, Roger T, Bernhagen J. Macrophage migration inhibitory factor (MIF): mechanisms of action and role in disease. Microbes and Infection. 2002;4(4):449-60
342. Klasen C, Ohl K, Sternkopf M, Shachar I, Schmitz C, Heussen N, et al. MIF Promotes B Cell Chemotaxis through the Receptors CXCR4 and CD74 and ZAP-70 Signaling. The Journal of Immunology. 2014;192(11):5273-84
343. Bloom BR, Bennett B. Mechanism of a reaction in vitro associated with delayed-type hypersensitivity. Science. 1966;153(3731):80-2
344. David JR. Delayed hypersensitivity in vitro: its mediation by cell-free substances formed by lymphoid cell-antigen interaction. Proceedings of the National Academy of Sciences. 1966;56(1):72-7
345. Shi X, Leng L, Wang T, Wang W, Du X, Li J, et al. CD44 is the signaling component of the macrophage migration inhibitory factor-CD74 receptor complex. Immunity. 2006;25(4):595-60617045821.
346. Krockenberger M, Kranke P, Hausler S, Engel JB, Horn E, Nurnberger K, et al. Macrophage migration-inhibitory factor levels in serum of patients with ovarian cancer correlates with poor prognosis. Anticancer Res. 2012;32(12):5233-823225421.
347. Legendre H, Decaestecker C, Nagy N, Hendlisz A, Schüring M-P, Salmon I, et al. Prognostic values of galectin-3 and the macrophage migration inhibitory factor (MIF) in human colorectal cancers. Modern pathology. 2003;16(5):491
348. Liao H, Bucala R, Mitchell RA. Adhesion-dependent signaling by macrophage migration inhibitory factor (MIF). Journal of Biological Chemistry. 2003;278(1):76-81
349. Onodera S, Suzuki K, Matsuno T, Kaneda K, Takagi M, Nishihira J. Macrophage migration inhibitory factor induces phagocytosis of foreign particles by macrophages in autocrine and paracrine fashion. Immunology. 1997;92(1):131-7

350. Meinhardt A, Bacher M, Wennemuth G, Eickhoff R, Hedger M. Macrophage migration inhibitory factor (MIF) as a paracrine mediator in the interaction of testicular somatic cells. Andrologia. 2000;32(1):46-8
351. Verjans E, Noetzel E, Bektas N, Schütz AK, Lue H, Lennartz B, et al. Dual role of macrophage migration inhibitory factor (MIF) in human breast cancer. BMC Cancer. 2009;9(1):230
352. Calandra T, Roger T. Macrophage migration inhibitory factor: a regulator of innate immunity. Nature Reviews Immunology. 2003;3:791
353. Bernhagen J, Krohn R, Lue H, Gregory JL, Zernecke A, Koenen RR, et al. MIF is a noncognate ligand of CXC chemokine receptors in inflammatory and atherogenic cell recruitment. Nat Med. 2007;13(5):587-9617435771.
354. Dessein A-F, Stechly L, Jonckheere N, Dumont P, Monté D, Leteurtre E, et al. Autocrine induction of invasive and metastatic phenotypes by the MIF-CXCR4 axis in drug-resistant human colon cancer cells. Cancer research. 2010;70(11):4644-54
355. Meyer-Siegler KL, Iczkowski KA, Leng L, Bucala R, Vera PL. Inhibition of macrophage migration inhibitory factor or its receptor (CD74) attenuates growth and invasion of DU-145 prostate cancer cells. The Journal of Immunology. 2006;177(12):8730-9
356. Ren Y, Chan H, Fan J, Xie Y, Chen Y, Li W, et al. Inhibition of tumor growth and metastasis in vitro and in vivo by targeting macrophage migration inhibitory factor in human neuroblastoma. Oncogene. 2006;25(25):3501
357. Chuang C-C, Chuang Y-C, Chang W-T, Chen C-C, Hor L-I, Huang AM, et al. Macrophage migration inhibitory factor regulates interleukin-6 production by facilitating nuclear factor-kappa B activation during Vibrio vulnificus infection. BMC Immunology. 2010;11:50-PMC2965133.
358. P. de Jong Y, Abadía-Molina A, Satoskar A, Clarke K, T. Rietdijk S, A. Faubion W, et al. Development of chronic colitis is dependent on the cytokine MIF2001. 1061-6 p.
359. Rougier F, Cornu E, Praloran V, Denizot Y. IL-6 and IL-8 production by human bone marrow stromal cells. Cytokine. 1998;10(2):93-79512898.
360. Herrero AB, García-Gómez A, Garayoa M, Corchete LA, Hernández JM, San Miguel J, et al. Effects of IL-8 Up-Regulation on Cell Survival and Osteoclastogenesis in Multiple Myeloma. The American Journal of Pathology. 2016;186(8):2171-82
361. Kline M, Donovan K, Wellik L, Lust C, Jin W, Moon-Tasson L, et al. Cytokine and chemokine profiles in multiple myeloma; significance of stromal interaction and correlation of IL-8 production with disease progression. Leukemia Research.31(5):591-8
362. Abdul-Aziz AM, Shafat MS, Zaitseva L, Lawes MJ, Rushworth SA, Bowles KM. Hypoxia Drives AML Proliferation in the Bone Marrow Microenvironment Via Macrophage Inhibitory Factor. Am Soc Hematology; 2016.
363. Amin MA, Volpert OV, Woods JM, Kumar P, Harlow LA, Koch AE. Migration inhibitory factor mediates angiogenesis via mitogen-activated protein kinase and phosphatidylinositol kinase. Circulation research. 2003;93(4):321-9
364. Lue H, Thiele M, Franz J, Dahl E, Speckgens S, Leng L, et al. Macrophage migration inhibitory factor (MIF) promotes cell survival by activation of the Akt pathway and role for CSN5/JAB1 in the control of autocrine MIF activity. Oncogene. 2007;26(35):5046-5917310986.
365. Stein R, Qu Z, Cardillo TM, Chen S, Rosario A, Horak ID, et al. Antiproliferative activity of a humanized anti-CD74 monoclonal antibody, hLL1, on B-cell malignancies. Blood. 2004;104(12):3705-1115297317.
366. Binsky I, Haran M, Starlets D, Gore Y, Lantner F, Harpaz N, et al. IL-8 secreted in a macrophage migration-inhibitory factor- and CD74-dependent manner regulates B cell chronic lymphocytic leukemia survival. Proceedings of the National Academy of Sciences. 2007;104(33):13408-13
367. Kaufman JL, Niesvizky R, Stadtmauer EA, Chanan-Khan A, Siegel D, Horne H, et al. Phase I, multicentre, dose-escalation trial of monotherapy with milatuzumab (humanized

anti-CD74 monoclonal antibody) in relapsed or refractory multiple myeloma. Br J Haematol. 2013;163(4):478-8624112026.
368. Al-Abed Y, VanPatten S. MIF as a disease target: ISO-1 as a proof-of-concept therapeutic. Future medicinal chemistry. 2011;3(1):45-63
369. Mylin AK, Rasmussen T, Johansen JS, Knudsen LM, Norgaard PH, Lenhoff S, et al. Serum YKL-40 concentrations in newly diagnosed multiple myeloma patients and YKL-40 expression in malignant plasma cells. Eur J Haematol. 2006;77(5):416-2416930142.
370. Giraudo E, Inoue M, Hanahan D. An amino-bisphosphonate targets MMP-9–expressing macrophages and angiogenesis to impair cervical carcinogenesis. The Journal of clinical investigation. 2004;114(5):623-33
371. Arendt B, Velazquez-Dones A, Tschumper R, Howell K, Ansell SM, Witzig TE, et al. Interleukin 6 induces monocyte chemoattractant protein-1 expression in myeloma cells. Leukemia. 2002;16(10):2142
372. Li Y, Zheng Y, Li T, Wang Q, Qian J, Lu Y, et al. Chemokines CCL2, 3, 14 stimulate macrophage bone marrow homing, proliferation, and polarization in multiple myeloma. Oncotarget. 2015;6(27):24218
373. Ray JM, Stetler-Stevenson W. Gelatinase A activity directly modulates melanoma cell adhesion and spreading. The EMBO journal. 1995;14(5):908-17
374. Standal T, Hjorth-Hansen H, Rasmussen T, Dahl I, Lenhoff S, Brenne A-T, et al. Osteopontin is an adhesive factor for myeloma cells and is found in increased levels in plasma from patients with multiple myeloma. haematologica. 2004;89(2):174-82
375. Yagci M, Sucak GT, Haznedar R. Fibrinolytic activity in multiple myeloma. Am J Hematol. 2003;74(4):231-714635202.
376. Purdue MP, Lan Q, Menashe I, Zheng T, Zhang Y, Yeager M, et al. Variation in innate immunity genes and risk of multiple myeloma. Hematological oncology. 2011;29(1):42-6PMC2980579.
377. Dankbar B, Padró T, Leo R, Feldmann B, Kropff M, Mesters RM, et al. Vascular endothelial growth factor and interleukin-6 in paracrine tumor-stromal cell interactions in multiple myeloma. Blood. 2000;95(8):2630-6
378. Mahtouk K, Jourdan M, De Vos J, Hertogh C, Fiol G, Jourdan E, et al. An inhibitor of the EGF receptor family blocks myeloma cell growth factor activity of HB-EGF and potentiates dexamethasone or anti–IL-6 antibody-induced apoptosis. Blood. 2004;103(5):1829-37
379. Krampera M, Pasini A, Rigo A, Scupoli MT, Tecchio C, Malpeli G, et al. HB-EGF/HER-1 signaling in bone marrow mesenchymal stem cells: inducing cell expansion and reversibly preventing multilineage differentiation. Blood. 2005;106(1):59-66
380. Singer M, Sansonetti PJ. IL-8 is a key chemokine regulating neutrophil recruitment in a new mouse model of Shigella-induced colitis. Journal of immunology (Baltimore, Md : 1950). 2004;173(6):4197-20615356171.
381. Delmore JE, Issa GC, Lemieux ME, Rahl PB, Shi J, Jacobs HM, et al. BET bromodomain inhibition as a therapeutic strategy to target c-Myc. Cell. 2011;146(6):904-17PMC3187920.
382. Suk FM, Lin SY, Lin RJ, Hsine YH, Liao YJ, Fang SU, et al. Bortezomib inhibits Burkitt's lymphoma cell proliferation by downregulating sumoylated hnRNP K and c-Myc expression. Oncotarget. 2015;6(28):25988-600126317903.
383. Evans CA, Liu T, Lescarbeau A, Nair SJ, Grenier L, Pradeilles JA, et al. Discovery of a Selective Phosphoinositide-3-Kinase (PI3K)-gamma Inhibitor (IPI-549) as an Immuno-Oncology Clinical Candidate. ACS medicinal chemistry letters. 2016;7(9):862-727660692.
384. Randis TM, Puri KD, Zhou H, Diacovo TG. Role of PI3Kδ and PI3Kγ in inflammatory arthritis and tissue localization of neutrophils. European journal of immunology. 2008;38(5):1215-24PMC2972192.
385. Meng Q, Xia C, Fang J, Rojanasakul Y, Jiang B-H. Role of PI3K and AKT specific isoforms in ovarian cancer cell migration, invasion and proliferation through the p70S6K1 pathway. Cellular Signalling. 2006;18(12):2262-71

386. Graupera M, Guillermet-Guibert J, Foukas LC, Phng L-K, Cain RJ, Salpekar A, et al. Angiogenesis selectively requires the p110α isoform of PI3K to control endothelial cell migration. Nature. 2008;453(7195):662
387. Pillinger G, Loughran NV, Piddock RE, Shafat MS, Zaitseva L, Abdul-Aziz A, et al. Targeting PI3Kdelta and PI3Kgamma signalling disrupts human AML survival and bone marrow stromal cell mediated protection. Oncotarget. 2016;7(26):39784-9527174919.
388. O'Brien S, Patel M, Kahl BS, Horwitz SM, Foss FM, Porcu P, et al. Duvelisib (IPI-145), a PI3K-δ, γ inhibitor, is clinically active in patients with relapsed/refractory chronic lymphocytic leukemia. Am Soc Hematology; 2014.
389. Orlowski RZ, Gercheva L, Williams C, Sutherland H, Robak T, Masszi T, et al. A phase 2, randomized, double-blind, placebo-controlled study of siltuximab (anti-IL-6 mAb) and bortezomib versus bortezomib alone in patients with relapsed or refractory multiple myeloma. Am J Hematol. 2015;90(1):42-925294016.
390. San-Miguel J, Bladé J, Shpilberg O, Grosicki S, Maloisel F, Min C-K, et al. Phase 2 randomized study of bortezomib-melphalan-prednisone with or without siltuximab (anti–IL-6) in multiple myeloma. Blood. 2014;123(26):4136-42PMC4123433.
391. Hunsucker SA, Magarotto V, Kuhn DJ, Kornblau SM, Wang M, Weber DM, et al. Blockade of interleukin-6 signalling with siltuximab enhances melphalan cytotoxicity in preclinical models of multiple myeloma. Br J Haematol. 2011;152(5):579-9221241278.
392. Radl J, Hollander C, Van den Berg P, De Glopper E. Idiopathic paraproteinaemia. I. Studies in an animal model--the ageing C57BL/KaLwRij mouse. Clinical and experimental immunology. 1978;33(3):395
393. Hol J, Wilhelmsen L, Haraldsen G. The murine IL-8 homologues KC, MIP-2, and LIX are found in endothelial cytoplasmic granules but not in Weibel-Palade bodies. Journal of leukocyte biology. 2010;87(3):501-820007247.

8 – Appendices

8.1 – Appendix A – MM cytokine array results

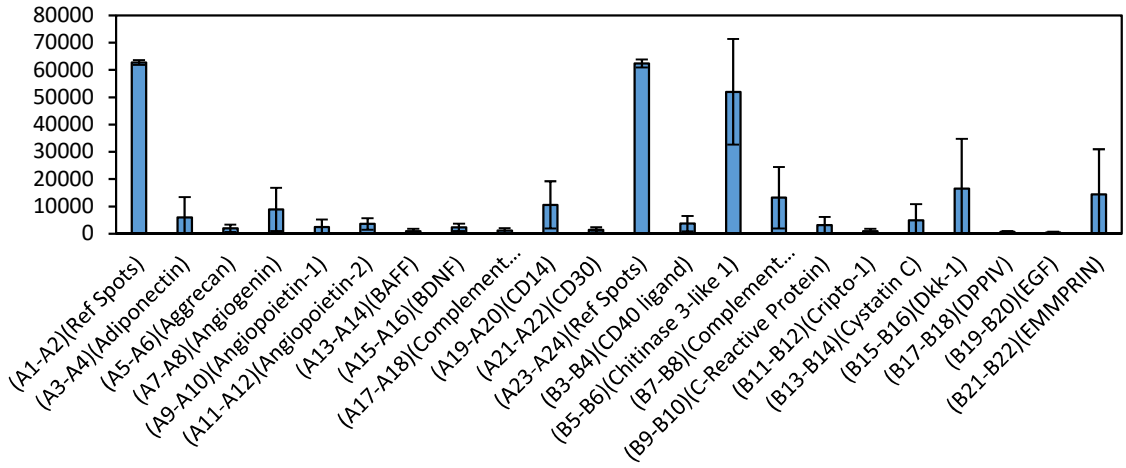

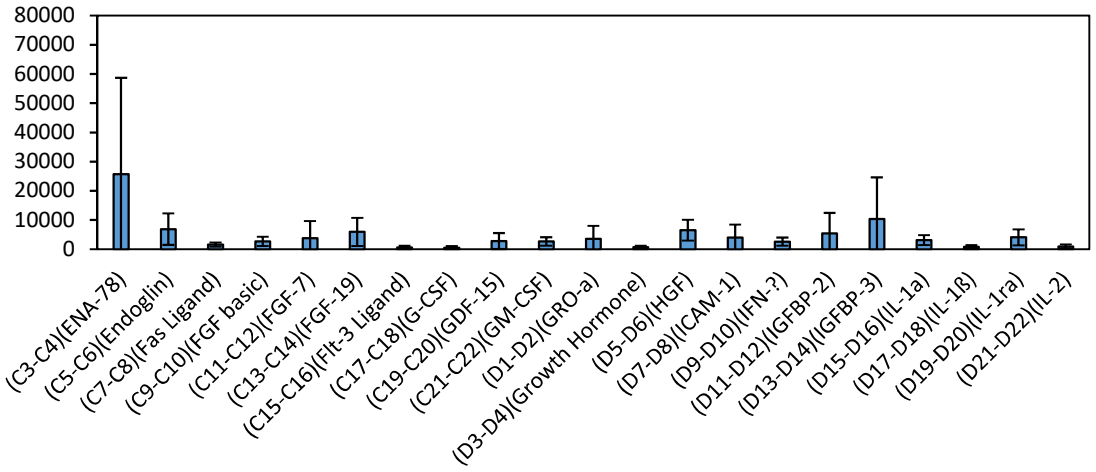

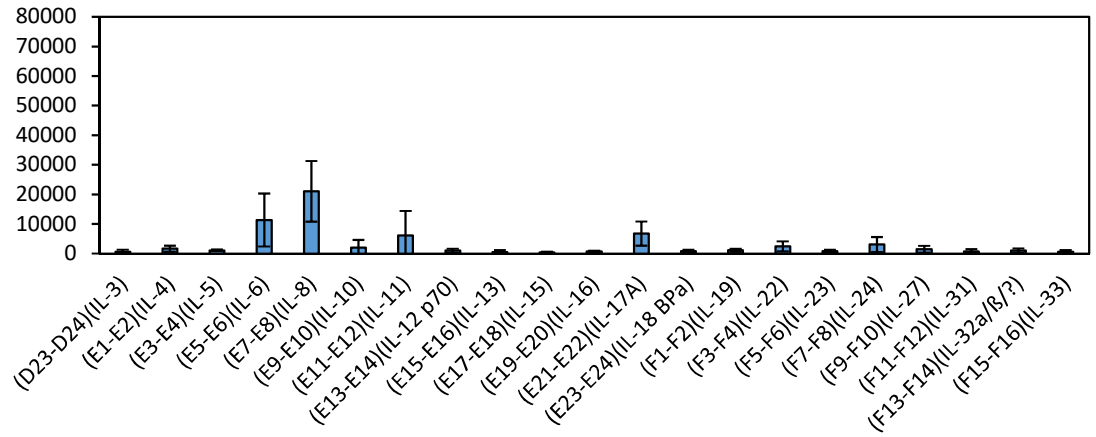

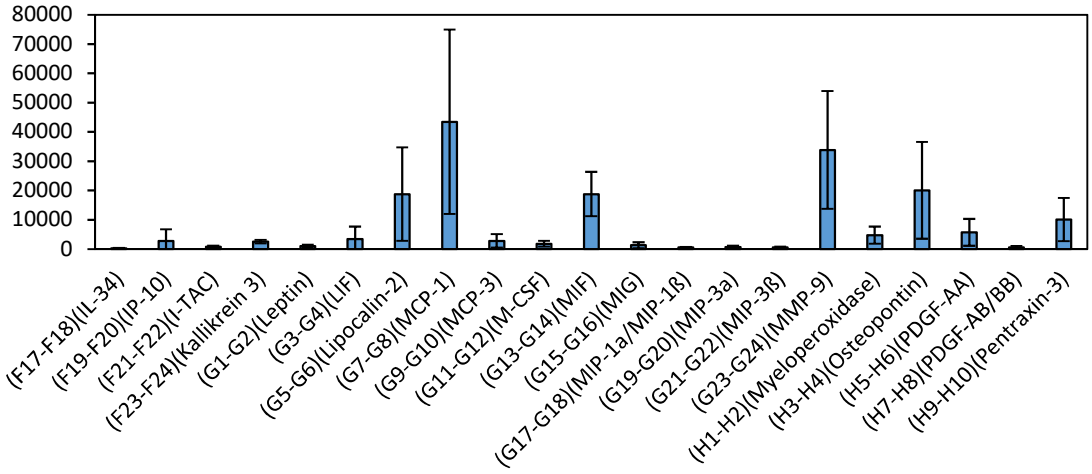
80000
70000
60000
50000
40000
30000
20000
10000
0
(F17-F18)(IL-34)
(F19-F20)(IP-10)
(F21-F22)(I-TAC)
(F23-F24)(Kallikrein 3)
(G1-G2)(Leptin)
(G3-G4)(LIF)
(G5-G6)(Lipocalin-2)
(G7-G8)(MCP-1)
(G9-G10)(MCP-3)
(G11-G12)(M-CSF)
(G13-G14)(MIF)
(G15-G16)(MIG)
(G17-G18)(MIP-1a/MIP-1ß)
(G19-G20)(MIP-3a)
(G21-G22)(MIP-3ß)
(G23-G24)(MMP-9)
(H1-H2)(Myeloperoxidase)
(H3-H4)(Osteopontin)
(H5-H6)(PDGF-AA)
(H7-H8)(PDGF-AB/BB)
(H9-H10)(Pentraxin-3)

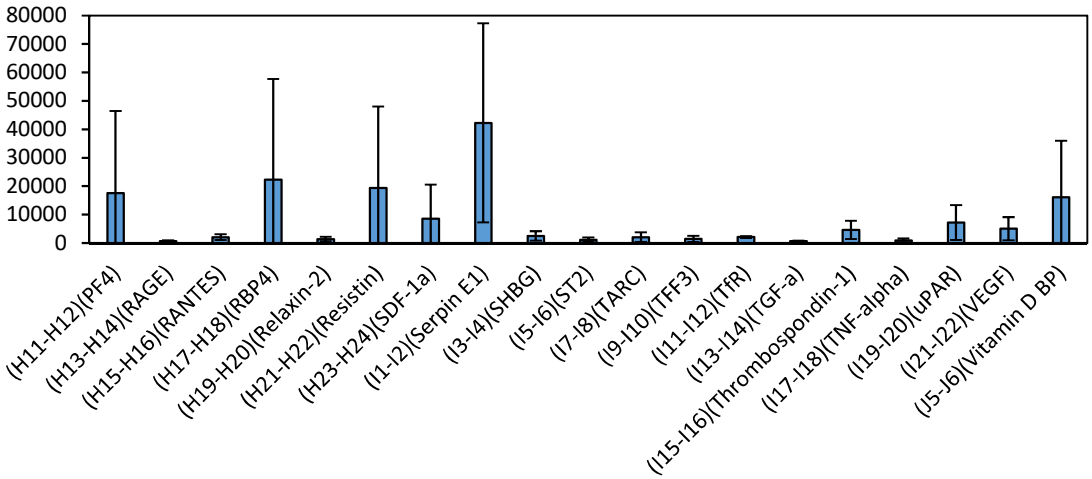
80000
70000
60000
50000
40000
30000
20000
10000
0
(H11-H12)(PF4)
(H13-H14)(RAGE)
(H15-H16)(RANTES)
(H17-H18)(RBP4)
(H19-H20)(Relaxin-2)
(H21-H22)(Resistin)
(H23-H24)(SDF-1a)
(I1-I2)(Serpin E1)
(I3-I4)(SHBG)
(I5-I6)(ST2)
(I7-I8)(TARC)
(I9-I10)(TFF3)
(I11-I12)(TfR)
(I13-I14)(TGF-a)
(I15-I16)(Thrombospondin-1)
(I17-I18)(TNF-alpha)
(I19-I20)(uPAR)
(I21-I22)(VEGF)
(J5-J6)(Vitamin D BP)

8.2 – Appendix B – Relative density co-culture cytokine array results

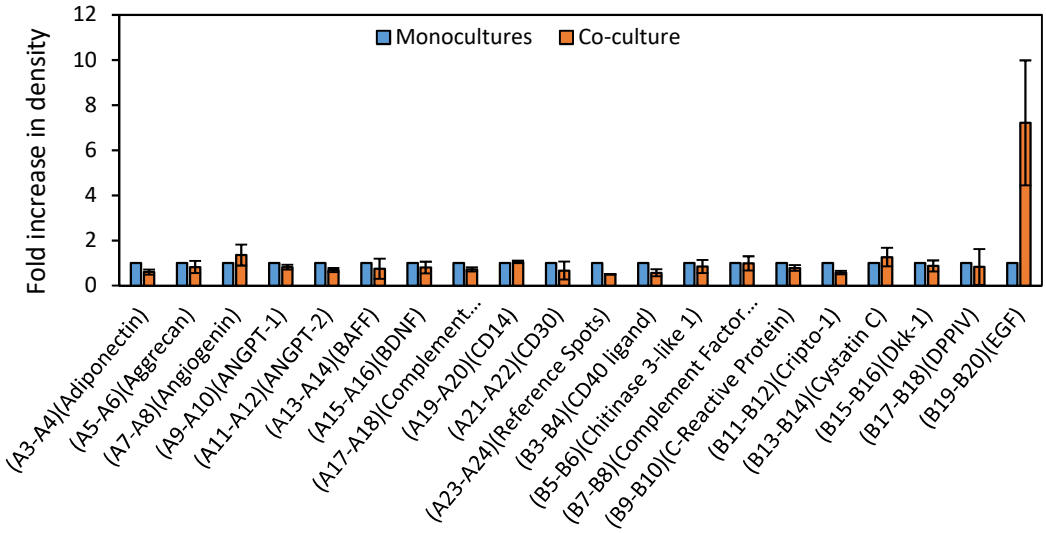

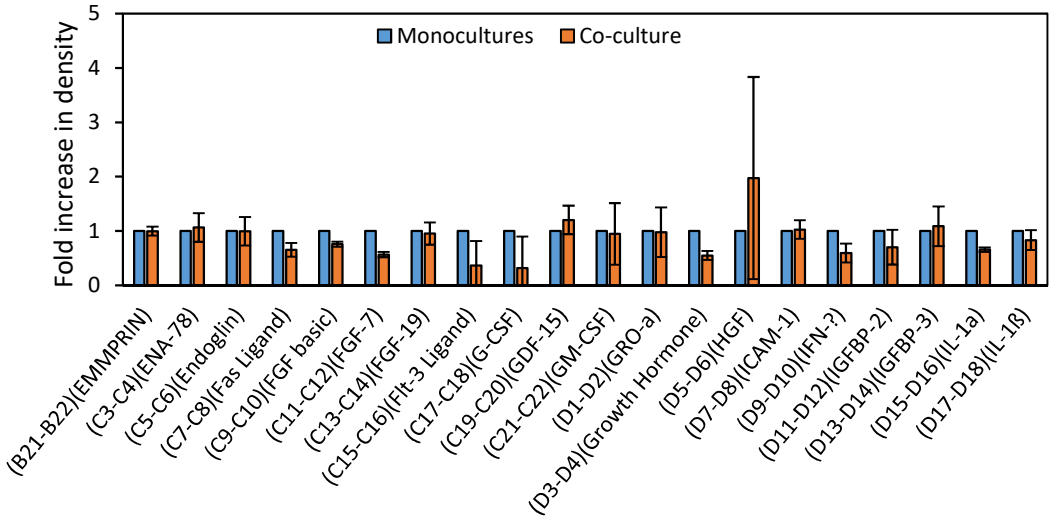

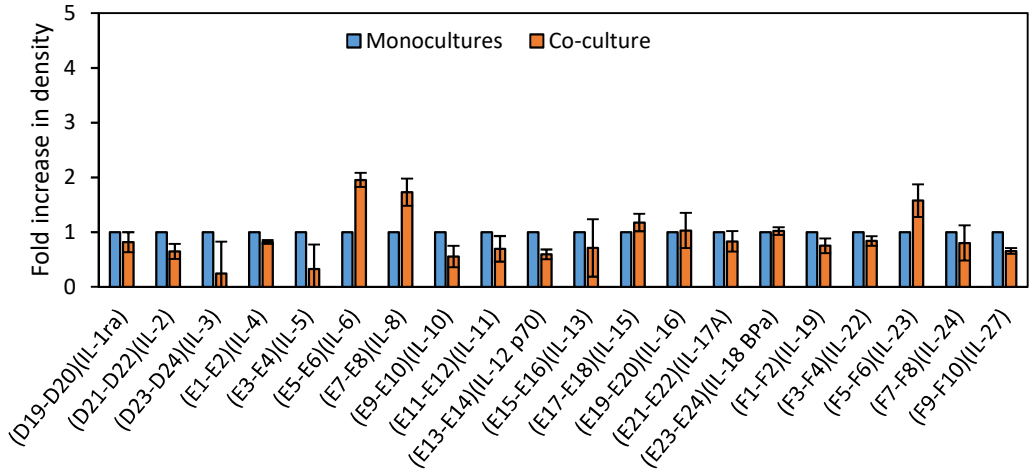

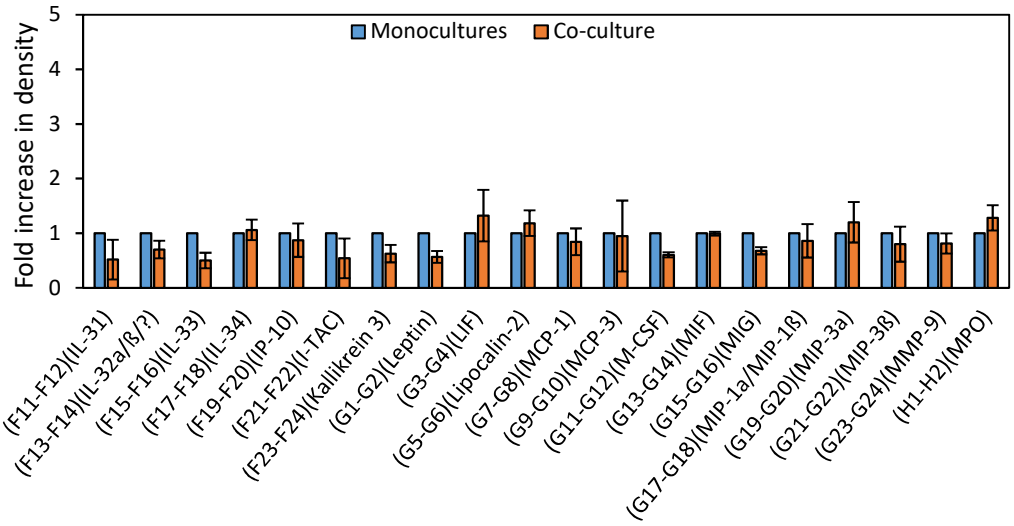
Monocultures
Co-culture
Fold increase in density
0
1
2
3
4
5
(F11-F12)(IL-31)
(F13-F14)(IL-32a/ß/?)
(F15-F16)(IL-33)
(F17-F18)(IL-34)
(F19-F20)(IP-10)
(F21-F22)(I-TAC)
(F23-F24)(Kallikrein 3)
(G1-G2)(Leptin)
(G3-G4)(LIF)
(G5-G6)(Lipocalin-2)
(G7-G8)(MCP-1)
(G9-G10)(MCP-3)
(G11-G12)(M-CSF)
(G13-G14)(MIF)
(G15-G16)(MIG)
(G17-G18)(MIP-1a/MIP-1ß)
(G19-G20)(MIP-3a)
(G21-G22)(MIP-3ß)
(G23-G24)(MMP-9)
(H1-H2)(MPO)

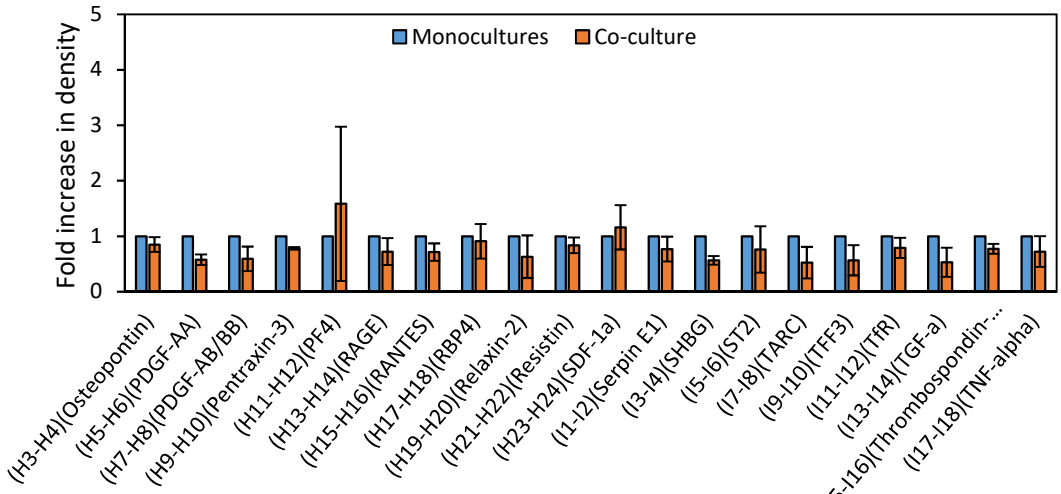
Monocultures
Co-culture
Fold increase in density
0
1
2
3
4
5
(H3-H4)(Osteopontin)
(H5-H6)(PDGF-AA)
(H7-H8)(PDGF-AB/BB)
(H9-H10)(Pentraxin-3)
(H11-H12)(PF4)
(H13-H14)(RAGE)
(H15-H16)(RANTES)
(H17-H18)(RBP4)
(H19-H20)(Relaxin-2)
(H21-H22)(Resistin)
(H23-H24)(SDF-1a)
(I1-I2)(Serpin E1)
(I3-I4)(SHBG)
(I5-I6)(ST2)
(I7-I8)(TARC)
(I9-I10)(TFF3)
(I11-I12)(TfR)
(I13-I14)(TGF-a)
(I15-I16)(Thrombospondin-...
(I17-I18)(TNF-alpha)

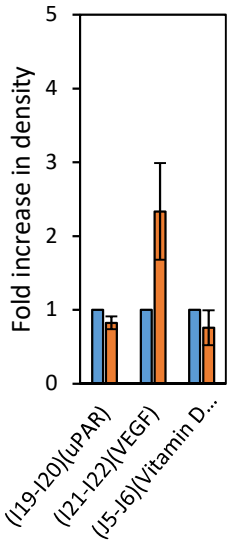
Fold increase in density
0
1
2
3
4
5
(I19-I20)(uPAR)
(I21-I22)(VEGF)
(J5-J6)(Vitamin D...

8.3 – Appendix C – Publications

1. **Piddock RE**, Marlein CR, Abdul-Aziz A, Shafat MS, Auger MJ, Bowles KM, et al. Myeloma-derived macrophage inhibitory factor regulates bone marrow stromal cell-derived IL-6 via c-MYC. J Hematol Oncol. 2018;11(1):66.

2. Abdul-Aziz AM, Shafat MS, Marlein CR, **Piddock RE**, Robinson SD, et al. HIF1alpha drives chemokine factor pro-tumoral signaling pathways in acute myeloid leukemia. Oncogene. 2018.

3. Marlein CR, Zaitseva L, **Piddock RE**, Robinson SD, Edwards DR, Shafat MS, et al. NADPH oxidase-2 derived superoxide drives mitochondrial transfer from bone marrow stromal cells to leukemic blasts. Blood. 2017;130(14):1649-60.

4. **Piddock RE**, Bowles KM, Rushworth SA. The Role of PI3K Isoforms in Regulating Bone Marrow Microenvironment Signaling Focusing on Acute Myeloid Leukemia and Multiple Myeloma. Cancers (Basel). 2017;9(4).

5. **Piddock RE**, Loughran N, Marlein CR, Robinson SD, Edwards DR, Yu S, et al. PI3Kdelta and PI3Kgamma isoforms have distinct functions in regulating pro-tumoural signalling in the multiple myeloma microenvironment. Blood Cancer J. 2017;7(3):e539.

6. Pillinger G, Loughran NV, **Piddock RE**, Shafat MS, Zaitseva L, Abdul-Aziz A, et al. Targeting PI3Kdelta and PI3Kgamma signalling disrupts human AML survival and bone marrow stromal cell mediated protection. Oncotarget. 2016;7(26):39784-95.

7. Shafat MS, Oellerich T, Mohr S, Robinson SD, Edwards DR, **Piddock RE**, et al. Leukemic blasts program bone marrow adipocytes to generate a protumoral microenvironment. Blood. 2017;129(10):1320-32.

8. Rushworth SA, Pillinger G, Abdul-Aziz A, **Piddock R**, Shafat MS, Murray MY, et al. Activity of Bruton's tyrosine-kinase inhibitor ibrutinib in patients with CD117-positive acute myeloid leukaemia: a mechanistic study using patient-derived blast cells. The Lancet Haematology. 2015;2(5):e204-11.